INVESTIGATION OF THE AMORPHOUS PROPERTIES OF LACTOSE AND INDOMETACIN

A thesis submitted in partial fulfillment of the requirements for the degree of Doctor of Philosophy

Rita Coelho Ramos

Department of Pharmaceutics
The School of Pharmacy
University of London
2006

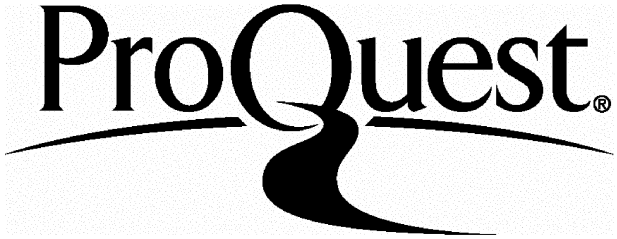

PLAGIARISM STATEMENT

This thesis describes research conducted in the School of Pharmacy, University of London between 2003 and 2006 under supervision of Prof. Graham Buckton and Dr. Simon Gaisford. I confirm that the research described is original and that any parts of work that have been conducted by collaboration are clearly indicated. I also certify that I have written the text herein and have clearly indicated by suitable citation any part of this dissertation that has already appeared in publication.

Signature

Date

ABSTRACT

Amorphous material can either be introduced in a formulation to aid bioavailability or induced accidentally during processing, which may have a detrimental effect on product performance, which means that its characterisation, detection and quantification are essential. My project aimed to characterise the amorphous material in order to better understand. This project aimed to investigate the influence of the variability of the amorphous and crystalline forms of a material on the quantification of amorphous content. A further aim of this project was to investigate the effect of the structural relaxation of amorphous material on its enthalpy of solution and dispersive surface energy and to develop a new methodology to characterise molecular mobility from enthalpy of solution and dispersive surface energy data.

Two principal methods were employed to quantify amorphous content; isothermal calorimetry (IC) and solution (ampoule-breaking) calorimetry (SC) and lactose was used as a model substance. IC allowed the quantification of amorphous content of lactose samples and a non-linear calibration curve could be plotted. This was ascribed to the fact that lactose exists as two anomers, each of which has a different enthalpy of crystallisation and amorphous lactose recrystallised to a final lactose with different anomeric composition, according to the initial amorphous content and anomeric composition of the initial crystalline portion.

Isothermal Perfusion Calorimetry and SC were employed to investigate the impact of the previous findings on the quantification of small amounts of amorphous material in low amorphous content samples with different anomeric composition. The quantification of amorphous content of a material with different initial anomeric composition, whose anomers exhibit different enthalpy crystallisation, is impossible unless the amorphous samples are prepared under the same conditions as those used to construct the calibration curves. Hence, unless the initial anomeric composition of the sample is known, one cannot have confidence in the amorphous content derived from the data. This observation had not previously been noted. A similar effect was noted for the SC data, because the anomers also had different enthalpies of solution.

SC and Inverse Phase Gas Chromatography (iGC) were used to investigate the effect of aging of amorphous lactose on its enthalpy of solution and dispersive surface energy, respectively. As aging time and temperature increase, enthalpy of solution and dispersive surface energies approach those of the crystalline state. Aging of amorphous material clearly affects its enthalpy of solution, which has a detrimental effect on the quantification of amorphous material using SC. The use of SC and iGC for the determination of the relaxation of an amorphous material was also investigated and compared to StepScanDSC. The relaxation of amorphous indometacin was also characterised using SSDSC, SC and iGC. The use of SC and iGC to follow the relaxation of amorphous materials is entirely novel and offers great promise.

ACKNOWLEDGMENTS

I would like to express my sincere gratitude to my supervisors Prof. Graham Buckton and Dr. Simon Gaisford for their supervision, guidance and support throughout my PhD.

I would like to thank the technical staff of the Department of Pharmaceutics for their help, especially Keith Barnes for all his help during my first year.

All the Pharmaceutics posgrads and postdocs helped make the three years really enjoyable. I would like to especially thank Richard, Matt, Ameet, Laurent, Paulo, Lara, Mike, Ravi, Ding, Meena, Gabriela, Lara, Karolina.

I would like to thank my family and friend and my dear Manuel for their support and encouragement.

TABLE OF CONTENTS

CHAPTER ONE

CHAPTER TWO

CHAPTER THREE

CHAPTER FIVE

LIST OF TABLES

CHAPTER ONE

CHAPTER TWO

CHAPTER THREE

CHAPTER FOUR

A	Peak area (DSC)
a_i	A weighing factor for each decaying state
AM	Amorphous
$AM_{\alpha:\beta}/CX_{\alpha\beta}$	Partially amorphous sample
B	Material parameter related to its fragility
b	Heating rate (DSC)
C	Constant that takes into account the weigh, surface area and vapour pressure of probes in the gaseous state (iGC)
CX	Crystalline
D	Flow rate of the eluting carrier gas (iGC)
DSC	Differential Scanning Calorimetry
E^0	Sum of the lattice and vibration al energies
FID	Flame ionisation detector
G	Gibb´s free energy
H	Enthalpy
H_{exc}	Excess enthalpy
H^s	Enthalpy of solution
Hyper-DSC	High speed differential scanning calormimetry
I	Current supplied to the heater (DSC)
iGC	Inverse Phase Gas Chromatography
J	Correction factor that considers the compressibility of the gas as the pressure drops across the column (iGC)
K	Calorimetric sensitivity (DSC)
K	a constant of the measure of the free volume to the mixture by each of its constituents at any temperature (Gordon-Taylor Equation)
KWW	Kohlrausch-Williams-Watts
L	Ligand (SolCal)
m	Mass of sample (DSC)
n	The total number of independent decaying microstates
P	Pressure (Thermodynamics)
P	Power supplied in order to maintain the reference and sample pans at the same temperature (DSC)
P_i	Pressure at the inlet of the column (iGC)
P_0	Pressure at the outlet of the column (iGC)

Q	Heat absorbed/evolved by the system
R	The ideal gas constant (iGC)
R	Resistance of the heater (DSC)
RH	Relative humidity
S	Entropy
S	Substrate (SolCal)
SolCal	Thermometric 2225 Precision Solution Calorimeter
T	Temperature
T_a	Annealing temperature
T_c	Crystallisation temperature
T_g	Glass transition temperature
T_{gmix}	Glass transition temperature of a two component mixture
T_{g1}	Glass transition temperature of component 1
T_{g2}	Glass transition temperature of component 2
T_k	Kauzmann temperature
T_m	Melting temperature
T_∞	The temperature of the maximum possible relaxation time
t	Time
t_r	Retention time of the liquid probe (iGC)
t_0	Retention time of methane (iGC)
TAM	Thermal Activity Monitor
TCD	Thermal conductivity detector
TGA	Thermal gravimetric analysis
U	Internal Energy
V	Volume
V_N	Retention volume (iGC)
VTF	Vogel-Tammann-Fulcher
W	Watt
w	Work
w_{adh}	Work of adhesion (iGC)
w_1	Weigh fraction of component 1
w_2	Weigh fraction of component 2
X_a and X_b	Weigh fractions of two non-interacting substances (SolCal)
XRPD	x-Ray powder diffraction
β	The stretch power, distribution of relaxation states
γ^d_s	Dispersive component of the solid (iGC)
γ^d_l	Dispersive component of the solid (iGC)

ΔC_p	Heat capacity change at the glass transition temperature
ΔG^0_{ads}	Free energy of adsorption (IGC)
ΔG^D_{ads}	Non-polar dispersive surface energy
ΔG^{Spec}_{ads}	Acid/base or specific free energy of adsorption
ΔH	Enthalpy change
ΔH	Heats of solution of two non-interacting substances
$\Delta H_{(\infty)}$	Maximum possible enthalpy relaxation
ΔS	Entropy change
ΔT	Temperature Steps on StepScan DSC
ΔU	Change in internal energy
ΔY	Difference in baseline (DSC)
$\varphi(t)$	Extent of relaxation
τ	Average molecular relaxation time at temperature T
τ^β	Relaxation time constant on the stretched time scale
τ_0	The shortest possible relaxation time
τ_i	Exponential decay time constant
$^\circ C$	Degree Celsius
$\sum E^i$	Sum of the internal energy

CHAPTER ONE

INTRODUCTION

1. INTRODUCTION

Solid dosage forms are the most commonly used form of drug delivery. These include tablets, capsules, and dry powder inhalers, for example.

The active ingredient in the solid dosage form can exist in the amorphous or crystalline form. It is important that the most stable form of the active is used; this is normally the most stable polymorph of the drug. The use of the amorphous or a metastable polymorph form can be a choice because of advantages over the most stable form.

The amorphous state in pharmaceutical systems may arise as a result of three sets of circumstances. Firstly, the drug, excipient or delivery system may be deliberately produced in an amorphous form to enhance the performance of the final product; pharmaceutical excipients can be rendered amorphous to aid processing, drugs can be used in the amorphous state to improve their dissolution rate and bioavailability, and delivery systems can be produced in the amorphous state to enhance stability (for example, freeze dried protein formulations). Secondly, pharmaceutical materials might be at least partially amorphous at room or body temperature. Thirdly, amorphous material might also be unintentionally introduced during processing, which can be problematic during subsequent processing stages and affect product performace.

Consequently, the study of the crystalline and amorphous states is of great importance in pharmaceutics. This thesis aims better to understand the amorphous state from the pharmaceutical point of view. As such, a few theoretical considerations related to the amorphous and crystalline states should first be introduced.

1.1. THE CRYSTALLINE STATE

The crystalline state is defined as that of long range order. A crystalline substance exhibits a three-dimensional ordered structure, which is formed by highly ordered arrays of structural motifs (atoms, groups of atoms, molecules and ions) held together by non-covalent interactions (Byrn et al., 1999). The imaginary parallelepiped that contains one unit of a repeated pattern of structural motifs is called a unit cell (Byrn et al., 1999). Within a specific crystal, each unit cell is the same size and contains the same number of structural motifs arranged in the same way. All structural motifs are equivalent with respect to their binding energy (Byrn et al., 1999). This results in the breakdown of the crystal occurring at a fixed, unique level (i.e. temperature) and endows the crystal with specific chemical, thermal, optical and mechanical properties (Byrn et al., 1999). The three-dimensional array of structural motifs is referred to as a crystal lattice.

1.1.1. POLYMORPHISM

Unit cells, and thus the crystals, are classified into seven crystal systems, according to the symmetry elements they possess. Inorganic compounds tend to crystallise in one specific system (Carstensen, 1993). However, organic compounds often crystallise in different crystal systems, depending on the crystallisation or precipitation conditions to which they were exposed (Byrn et al., 1999). This phenomenon is known as polymorphism, whereby the same organic molecules will have a different packing arrangement, forming different polymorphs (Byrn et al., 1999). Polymorphs are thus different crystal forms of the same compound and may exist in either an enantiotropic state (transitions between two equally stable forms) or monotropic state (transitions from the metastable to the stable form) (Byrn et al., 1999). Polymorphs can be interconverted by heat, mechanical activation or by a solvent mediated process (Guillory, 1999). This is very important pharmaceutically, as polymorphs of the same substance may exhibit different melting points, chemical and physical stability, dissolution rates, different bioavailability, and compression properties (Byrn et al., 1999; Guillory, 1999).

When a molecule of solvent is incorporated into the crystal structure, a change in the physical properties of the material can also be observed and this phenomenon is known as pseudopolymorphism or solvation (Byrn et al., 1999). The solvent incorporation can be stoichiometric or non-stoichiometric. If water is the solvent of

crystallisation, the solvates are called hydrates. When no solvent is incorporated, the crystals are known as anhydrates.

1.1.2. CRYSTAL HABIT

The external shape of a crystal, termed crystal habit, is altered by the crystal growth rate at the different faces of the crystal. Changes in the internal packing can originate distinguishable crystal habits. For the same crystal packing, it is possible to change the crystal habit by changing the crystallisation conditions (Byrn et al., 1999). The hydrophobicity of the environment in which the crystal grows will affect the growth rate and the direction in which the crystal grows (Buckton, 1995b).

The same compound can crystallise into different crystal habits. This is very important pharmaceutically as different crystal habits of the same substance may exhibit different mixing and flow properties, dissolution rate and suspension stability, for example.

1.2. THE AMORPHOUS STATE

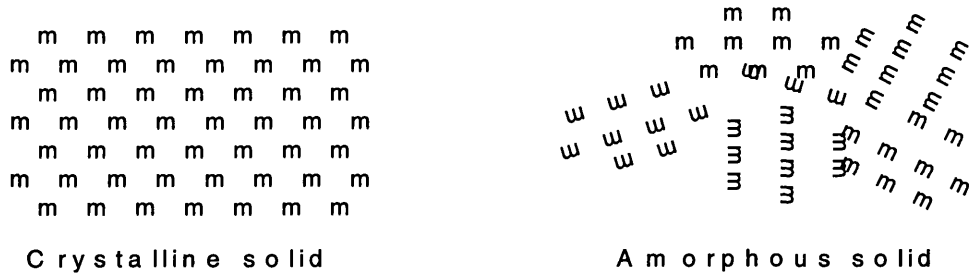

Figure 1.1 *Schematic representation of the structure of an amorphous solid (Adapted from Yu, 2001).*

In the amorphous state the position of the molecules relatively to one another is more random as in the liquid state (Hancock and Zografi, 1997). Amorphous materials might exhibit a molecular arrangement that is not totally random but possess some crystal like short-range order (over a few Angstroms), which may include, for example, the same type of hydrogen bonding found in its crystalline counterpart. However, unlike crystals, an amorphous solid does not exhibit any long-range translational-rotational symmetry that characterises a crystalline solid.

Amorphous materials have different properties from those of their corresponding crystalline state, including the fact that they do not have a distinct melting point, more readily absorb water, can exhibit a faster dissolution rate, tendency towards crystallisation, enhanced chemical reactivity, and have no (or very broad) X-ray powder diffraction pattern (Hancock and Zografi, 1997).

1.3. PHARMACEUTICAL PROCESSES INFLUENCED BY THE PHYSICAL FORM.

Each polymorphic form normally exhibits different physicochemical properties. These include density, hardness, optical properties, water uptake, thermodynamic properties such as melting point and enthalpy, and chemical/physical stability (Byrn et al. 1999). This can ultimately affect pharmaceutically important processes such as tabletting, flowability, drying, filtration, dissolution, freeze drying, granulation, mixing, suspension, and milling (Byrn et al., 1999).

1.4. PHARMACEUTICAL IMPLICATIONS OF THE PHYSICAL FORM

Table 1.1 *Applications of various physical forms of pharmaceutical ingredients. (Byrn et al., 1999).*

Purpose	Subtance	Physical form
Stable	Beclomethasone	Chlorofluorocarbon solvate
Non-hygroscopic	Amoxicilin	Anhydrous sodium salt
	Azithromicin	Dihydrate
High bioavailability	Mefloquine HCl	Polymorph
High activity	Cefuroxime axetil	Amorphous
Improved flow	Piroxicam	β-form
Improved tabletting	Sorbitol	γ-form

As the physical forms of pharmaceuticals exhibit different properties and processing attributes, the selection of the appropriate physical form is essential. A particular physical form is selected over another for one or more of the following reasons: improved stability, non-hygroscopic, release profile, improved flow, improved tabletting, etc (Byrn et al., 1999), as summarised in Table 1.1.

1.5. BASIC CONCEPTS OF THERMODYNAMICS RELATING TO THE CRYSTALLINE AND AMORPHOUS STATES

Thermodynamics is the study of the transformation of energy, and can be used to investigate the heat changes that occur during a chemical or physical process. In thermodynamics the world is considered as two parts: the system and its surroundings, which are separated by a boundary. While the system is the part of interest, such as a reaction vessel, the surroundings are everything outside. When energy, but no matter, can be transferred between the system and its surroundings, the system is known as a closed system. An isolated system does not allow transfer of energy or matter between the system and its surroundings.

Thermodynamic properties include temperature (T), pressure (P), volume (V), internal energy (U), enthalpy (H), Gibb's free energy (G) and entropy (S). These properties are related by the following equations:

$$H = U + PV \qquad \textit{Equation 1.1}$$

$$G = H - TS \qquad \textit{Equation 1.2}$$

According to the first law of thermodynamics, energy cannot be created or destroyed; it can only be transformed from one form to another. The energy change for a system can be described as:

$$\Delta U = Q - W \qquad \textit{Equation 1.3}$$

where:

- ΔU is the change in internal energy
- Q represents the heat absorbed by the system
- W represents the work done by the system.

Equation 1.3 shows that the internal energy of a system (U) can be changed through changes in heat (Q) and work (W). At constant volume no work is done by/on to the system and measured heat is equal to the internal energy. At constant pressure, work can be done by/on to the system and the heat that is absorbed or evolved

when a system changes its thermodynamic state under constant pressure corresponds to the enthalpy change (ΔH). If the temperature (T) of the surroundings is higher than that of the system, then heat will flow into the system. Considering a substance as the system, if heat (energy) flows into it, the motions of its atoms and molecules will increase. As a result of their increased motion, the atoms and molecules occupy more space and the substance expands. This motion gives every object its internal energy (U). As heat raises the internal energy of a system, its atoms and molecules gain motion and become increasingly disordered. Entropy (S) is a measure of the degree of disorder in a system.

The entropy of a system increases whenever the energy available to do work decreases. Heat, when flowing into a system, will always increase its internal energy and disorder and increase its temperature. Consequently, heat will disrupt the arrangement of atoms and molecules. Substances with a highly organised structure and strong inter-atomic bonding tend to have low entropy. However, gases and substances made of large, flexible molecules tend to have larger entropy values.

The second law of thermodynamics states that all the spontaneous changes in an isolated system are accompanied by an overall increase in disorder (entropy). This law deals with heat efficiency and is also related to the definition of energy as the stored capacity to do work. Therefore, according to this law, a consequence of a spontaneous process is that there is an increase in disorder or decrease in ΔG, according to the Equation 1.2. Processes do not usually occur in isolation, and therefore we have to consider the entropy change of the surroundings as well as the system. The overall change in entropy (ΔS_{total}) is the sum of two terms, the entropy of the system (ΔS_{syst}) and the surroundings (ΔS_{surr}), as shown in the following equation:

$$\Delta S_{total} = \Delta S_{syst} + \Delta S_{surr} \qquad \textit{Equation 1.4}$$

For processes such as crystallisation (which is known to be spontaneous) order is being introduced into the system causing the entropy to decrease, which is not the favoured direction of ΔS. This discrepancy can be explained by considering the original statement for the second law, where the overall entropy change (ΔS_{total}) must be positive. Since crystallisation is a highly exothermic process, heat energy is

released into the surroundings. This causes a large increase in the entropy of the surroundings so that the overall entropy change is positive.

1.6. THERMODYNAMICS OF THE GENERATION OF THE AMORPHOUS STATE

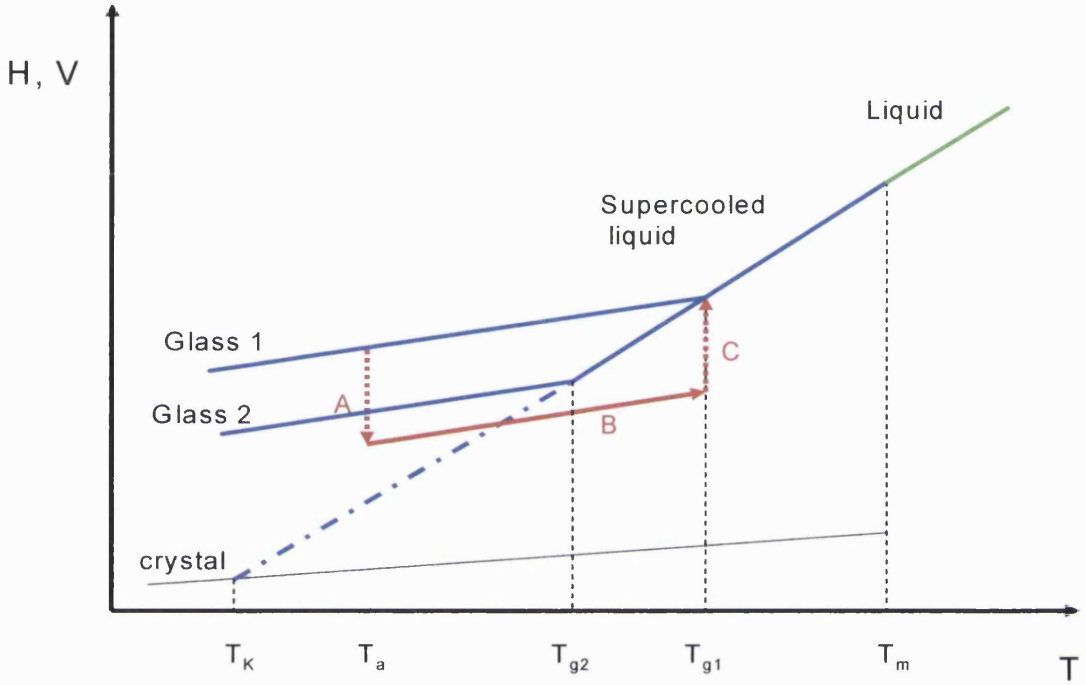

Figure 1.2 *Schematic representation of the variation of enthalpy and volume of a solid material according to its temperature. T_m is the melting point, T_g is the glass transition temperature, T_a is the annealing temperature and T_K is the Kauzmann (the lower value for the glass transition temperature, also known as the zero mobility temperature) temperature. A corresponds to the structural relaxation, B the heating during a DSC scan and C the enthalpy recovery at T_g.*

Figure 1.2 represents the variation of enthalpy (H) and volume (V) of a solid according to its temperature. A crystalline material exhibits a small increase in V and H with respect to temperature. At its melting temperature (T_m), a discontinuity in both H and V can be seen, which is indicative of a phase transition to the liquid state. Cooling of the melt can cause the material to attain a supercooled liquid state, provided that crystallisation is avoided. At this point the material is said to be a supercooled liquid or a rubbery amorphous material, and is characterised by a high temperature-dependence of its H and V (and other properties such as viscosity and molecular mobility). Further cooling of the supercooled liquid causes a decrease in

H and V over a certain temperature range, after which, a break point in temperature dependence of H and V is seen. This break point occurs at a characteristic temperature and is known as the glass transition. The temperature at which the break occurs is known as the glass transition temperature (Section 1.7). At this point, the material's H and V deviate from those of the equilibrium supercooled liquid. The glass transition is also accompanied by a rise in viscosity from a liquid like viscosity, characteristic of the supercooled liquid, to a solid like viscosity (Section 1.8). Below the glass transition temperature the amorphous material is normally said to be in the glassy state, whose H and V continue to decrease as temperature is lowered, but with lower temperature dependence.

1.7. THE GLASS TRANSITION TEMPERATURE

The glass transition temperature may be defined as the temperature at which a change from a glassy mechanical solid to a rubbery liquid occurs or vice-versa (Ferry, 1980).

When an amorphous solid is produced, a system is created which is unstable and of a higher free energy than the corresponding crystalline state. At temperatures just below the crystalline melting temperature the molecular motions of the amorphous material (a few seconds) are very rapid compared to the timescale of normal experimental measurements (minutes or hours). Both energy and entropy terms adjust to changing temperature so that volume vs Gibbs energy is minimum and the system is at equilibrium. The molecules' movements are such that they overlap and thus free volume exists throughout the system; free volume is the volume unoccupied by the solid matter of the molecules and represents the volume available for molecular movement. As long as free volume exists throughout the system, the molecules are able to move, and molecular motion leading to crystal formation is possible. If that amorphous material is cooled, there is a temperature at which the free volume no longer extends throughout all the solid and its molecular motions are slowed down. At this temperature the viscosity of the system becomes too high for molecular motions to follow the temperature lowering (Hancock et al., 1995). This temperature is the glass transition temperature (T_g) (Flink, 1983). Re-heating causes the molecules to absorb some thermal energy and molecular mobility increases. When the range of movements extends throughout the material, T_g is passed and the solid is said to be in the rubbery phase, which exhibits the properties of a liquid. The glass transition temperature is therefore a reversible event

and corresponds to the change between the solid, glassy phase and the rubbery, liquid-like phase.

The T_g of an amorphous material can be determined by several methods, the most common being differential scanning calorimetry (DSC) (Ford and Timmons, 1989). It is seen as a change in the heat capacity of a sample, and seen as a discontinuity between the specific heat of the sample and its temperature. The position of the T_g can vary with experimental heating and cooling rates, sample molecular mass, sample thermal history, sample geometry, sample purity and water content (Ford and Timmins, 1989; Höhne et al., 2003).

1.8. PROPERTIES OF THE AMORPHOUS STATE

The amorphous state has a higher G than its corresponding crystalline state. Its U and S are also larger. In the amorphous material, the molecules are positioned further apart from each other than in the crystalline state. This accounts for a greater specific volume, lower density and greater free volume than in the crystalline state (Hancock and Zografi, 1997). As a consequence of its higher U and V, not only is the amorphous state expected to have an enhanced dissolution and bioavailability relative to the crystalline state, but also exhibit greater chemical reactivity and a tendency to crystallise spontaneously.

The amorphous state includes the glassy state (below the glass transition temperature) and the supercooled liquid or rubbery state. The glass transition distinguishes between these (Figure 1.2). The transition from a supercooled liquid and a glass and vice versa is accompanied by changes in many properties.

Above the glass transition, the amorphous material is characterised by a high temperature dependence of molecular motions and viscosity. The viscosity of the supercooled liquid can be compared to that of water or benzene at room temperature (10^{-2} P) (Ediger et al., 1996). Supercooled liquids exhibit different temperature dependence of viscosity. The viscosity of SiO_2 exhibits almost Arrhenius dependence (linear relationship between log of viscosity and the inverse of temperature), while the viscosity and rotation times of *o*-terphenyl are extreme non-Arrhenius behaviour. Most of the supercooled liquids would fall in between these two examples. The temperature dependence of viscosity and other properties of supercooled liquids have been classified as strong and fragile (Angell, 1991). The

strong liquids exhibit Arrhenius relationship for temperature dependence of viscosity and relaxation process and typically are characterised by three dimensional network structures of covalent bonds, as the example of SiO_2. Fragile liquids follow a non-Arrhenius relationship and consist of molecules interacting through nondirectional, noncovalent interactions such as dispersion forces (e.g. *o*-terphenyl).

The temperature dependence of molecular mobility (or viscosity) can be described by the Vogel-Tammann-Fulcher (VTF) equation (Equation 1.5);

$$\tau = \tau_0 \exp\left(\frac{B}{T - T_\infty}\right) \qquad \textit{Equation 1.5}$$

where

- τ is the mean molecular relaxation time and could be replaced by viscosity
- T is the temperature
- τ_0 is the shortest possible relaxation time
- T_∞ is the temperature of longest relaxation time
- B is a material parameter related to its fragility

In the glass transition region, the properties of the amorphous material are dependent on both temperature and time. In this region the viscosity of the amorphous material increases to about 10^{13} (P), increasing further below the glass transition (Ediger et al., 1996). The time scale for molecular motions increases as a supercooled liquid approaches the vicinity of the glass transition; near the glass transition the molecular relaxation time reaches a high value (from second to year, depending on the material) as compared to pico and nanoseconds observed in the supercooled liquid. These long relaxation times originate time dependent properties such as structural relaxation or aging and annealing of the glass.

The temperature dependence of the molecular motions below T_g is less extreme than above T_g. Furthermore, in the glassy amorphous state below T_g, the molecular mobility is generally considered to be much reduced (in normal experimental time scales) in relation to the molecular motions above T_g in the rubbery amorphous region (Hancock et al., 1995; Hancock and Zografi, 1997). Although molecular motions (rotational and translational) occur below T_g over longer time scales, which

are relatively slow in normal experimental terms (minutes to hours), they can however still have a significant effect over the shelf life of pharmaceutical product (years) (Hancock et al., 1995).

Figure 1.1 shows two glassy forms of the same material, namely glass 1 and 2. Glasses 1 and 2 are obtained with different cooling rates and have different apparent glass transitions ($T_{g1}$and T_{g2}) (Ediger et al., 1996). Glass 1 is the result of a faster cooling rate than that used to produce glass 2. The molecular mobility at temperatures below T_g greatly depends upon the conditions under which the glass was formed. Thus, it can be considered the existence of various metastable glasses depending on the conditions they were formed.

1.9. MOLECULAR MOBILITY AND RELAXATION OF THE AMORPHOUS MATERIAL

As an amorphous solid is held below its T_g, the material has the tendency to transform into a stable state. The glassy material may crystallise, or even if crystallisation does not occur on the experimental time scales, glassy solids will 'relax' toward the equilibrium supercooled liquid state, as shown by arrow A in Figure 1.2. This spontaneous process is known as relaxation and is a consequence of the significant molecular mobility of the glassy material. Relaxation may be caused, among others, by structural relaxation (α-relaxation) and Johari-Goldstein relaxation (β-relaxation) (Kawakami and Pikal, 2005). Structural relaxation corresponds to the motion of the whole molecule. β-relaxation is believed to be caused by intramolecular motion, such as rotation of a side chain of a polymer or motion of a small group of atoms that is not coupled with the motion of the entire molecule.

A decrease in energy, entropy, and free volume is observed during such relaxation. The structural relaxation depends on the time and temperature at which the material is held below T_g. Thus, the difference between the temperature T and T_g can have a significant effect on the solid-state molecular mobility of drugs and excipients, which in turn affects their chemical degradation, solid state phase transformation and mechanical strength (Alnheck and Zografi, 1990). This will have implications in process control, product quality, safety and shelf life of an amorphous product (Levine and Slade, 1989). Because structural relaxation is an indicator of molecular mobility, physical/chemical stability and structural relaxation may well be closely

related and a full characterisation and understanding of the relaxation process is necessary in order to ameliorate those problems in the amorphous state.

The structural relaxation is a multiexponential decay from the initial state, where the configurations were frozen in during processing, towards the equilibrium state at a storage temperature T_a. The decay function can be described as follows:

$$\phi(t) = \sum_n a_i . \exp\left(\frac{t}{\tau_i}\right) \qquad \textit{Equation 1.6}$$

where

- φ(t) is the decay function
- t is time
- n is total number of independent decaying microstates
- a_i is a weighting factor for each given state *i*
- τ_i is an exponential decay time constant.

This multiexponential decay can be approximated by the Kohlrausch-Williams-Watts (KWW) equation (Williams and Watts, 1970),

$$\phi_{KWW}(t,T) = \exp\left[-\left(\frac{t}{\tau(T)}\right)^{\beta}\right] \qquad \textit{Equation 1.7}$$

where

- τ is the average molecular relaxation time at temperature T
- β is known as the stretch power
- *t* is the time the material was kept at T
- T is the temperature.

Both τ and β are necessary to describe the structural relaxation in an amorphous glass. τ is the average time taken for a particular motion to take place. An increase in τ means a decrease in molecular mobility. The parameter β, which may take on values between 0 and 1, is considered to reflect the distribution of independently relaxing states. A small β represents a board distribution of states, while a β near the unity represents a narrow distribution of states.

DSC is the most used method for the determination of the enthalpy lost during relaxation (Kawakami and Pikal, 2005). Briefly, a sample is allowed to relax for a given time at temperature T_a, and the energy decreases as indicated by arrow A on Figure 1.2. On a DSC experiment, the sample is heated along line B on Figure 1.2 and when the temperature is near T_g and molecular mobility is again high, the enthalpy recovers to the supercooled liquid state as shown by arrow C on Figure 1.2. This recovery event is seen as an endotherm in a DSC trace and is termed enthalpy recovery. Assuming that enthalpy relaxation and enthalpy recovery are the same, the enthalpy relaxation value is obtained. The process is repeated for a number of annealing times. The extent of relaxation ($\Phi_{kww}(t)$) is calculated from the enthalpy relaxation $\Delta H_{(t)}$ at time t using the following equation:

$$\phi_{kww(t)} = 1 - \left(\frac{\Delta H_{(t)}}{\Delta H_{(\infty)}} \right) \qquad \textit{Equation 1.8}$$

where $\Delta H_{(\infty)}$ is the maximum possible enthalpy relaxation, which can be calculated using Equation 1.9.

$$\Delta H_{(\infty)} = \Delta C_p (T_g - T) \qquad \textit{Equation 1.9}$$

where,

- ΔC_p is the heat capacity change at T_g
- T_g is the glass transition temperature
- T is the annealing temperature.

Relaxation time (τ) and stretched exponential parameter (β) can be obtained by fitting Equation 1.7 to the data using nonlinear regression analysis. The experimental conditions (i.e. annealing time) have a significant effect on the τ and β parameters, but the relaxation time constant on the stretched time scale, τ^{β}, remains largely invariant to annealing times (Kawakami and Pikal, 2005). Use of τ^{β} for the comparison of data is a more powerful methodology than τ.

Using "ageing" experiments, Hancock et al (1995) found that for the studied materials (sucrose, PVP and indometacin) it was necessary to cool the temperature down to 50K below T_g in order for the molecular motion to be slowed to a point

where they were insignificant over a lifetime of a pharmaceutical product. This temperature, 50K below T_g, appears to be the Kauzmann temperature (T_K), which is where equilibrium supercooled line would cross the crystal line. For a glassy material the T_K represents a temperature below which the time scale for molecular motions is of the order of years (Shamblin et al., 1999).

1.10. THE INTERACTION OF WATER WITH THE AMORPHOUS AND CRYSTALLINE STATES

Crystalline materials can interact with water in a number of ways. Water can be adsorbed to the crystalline surface, in a process called adsorption and that is limited by the surface area of the material (Buckton, 1995b). The first layer of water molecules is bonded to the surface and then two or three more layers can form at high relative humidity. The adsorption of water is reversible by increasing the temperature or by decreasing the relative humidity to which the crystal is exposed (Ahlneck and Zografi, 1990). Water can also undergo capillary condensation within the crystal structure and deliquescence constituting the bulk water. Water can also penetrate the crystal lattice to form hydrates; normally by forming hydrogen bonds in a well defined molecular position within the unit-cells (Ahlneck and Zografi, 1990; Cartensen, 1993). Water that is hydrogen-bonded to the surface or that is forming hydrates is unavailable to dissolve the solid, while more nonspecific surface water in excess of one layer and bulk water are available to dissolve the solid (Ahlneck and Zografi, 1990).

As the amorphous material has a disorganised structure, water can easily dissolve within it. The uptake of water into an amorphous solid is termed absorption and is determined by the total mass of the amorphous content (Ahlneck and Zografi, 1990). Amorphous materials take up considerably more water then the corresponding crystalline form (Pikal et al., 1978). In this situation, if a small amount of amorphous material is present in a mainly crystalline bulk, only a small amount of water is absorbed. However, this absorbed water is a high water content when localised in the amorphous region and can increase the molecular mobility of these amorphous regions and therefore influence the physical and chemical stability of the material. The effect of water on the solid-state properties of a material is then dependent on the amount of amorphous portion of the material.

The term sorption is used to refer to both adsorption and absorption.

1.10.1. PLASTICISER

When an additive lowers the T_g it is said to have a plasticising effect and is referred to as a plasticiser, whereas one that raises T_g it is said to have an antiplasticising effect (Hancock and Zografi, 1994).

1.10.2. WATER AS A PLASTICISER

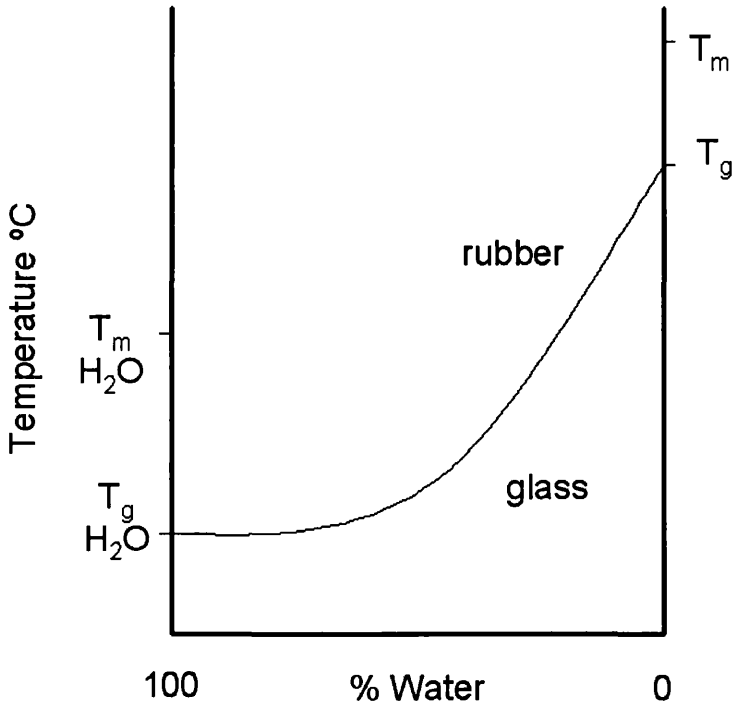

Figure 1.3 *Schematic representation of the plasticizing effect of water on the T_g of an amorphous solid having a high water solubility and very high T_g in the dry state (Adapted from Ahlneck and Zografi, 1990).*

Water has been recognised as a potent plasticiser for a wide range of amorphous and partially amorphous pharmaceutical solids (Hancock and Zografi, 1994). Due to its high hydrogen bonding capacity, when water molecules dissolve into a solid, they can disrupt the hydrogen bonds between the solid molecules, increasing the molecular mobility and free volume of the solid. In addition, water has a very small molecular size and a low T_g (135 K) (Sugisaki et al., 1968), which renders it capable of reducing the T_g of a solid system as its concentration in the solid increases (Hancock and Zografi, 1994). A schematic representation of this effect is shown in

Figure 1.3. The line connecting the T_g of the solid and the T_g of water represents the T_g of the solid/water mixture for each water content.

An important effect of water plasticisation, as it decreases T_g below the operating temperature (which is equivalent of increasing the temperature above T_g), is the change in the viscoelastic properties of the material above and below the operating temperature. An amorphous glassy solid heated to just 20 °C above T_g will have its viscosity decreased. This is accompanied by a significant increase in the molecular mobility of the solid and water. Thus, if the mixture of the two amorphous components is kept below the T_g line (Figure 1.3), it will remain as an extremely viscous glassy material where the water molecules will be as if they were in a tightly bound state. However, if the temperature of the solid-water system goes above the T_g line, a less viscous rubbery state is formed, which will exhibit a greater molecular mobility of both the solid and water.

The effect of water on the physicochemical properties of an amorphous material is conditioned by the T_g of the dry solid with respect to the operating temperature, the density of the amorphous material and its ability to take up and interact with water from its surroundings (Hancock and Zografi, 1994). Therefore, in addition to the effect of temperature on T_g, this can also be lowered to below the operating temperature by increasing the water content of the amorphous system. The material may then change from the glassy to the rubbery form.

Using a mixing rule and assuming no interaction between the components and that volume additivity occurs, an equation has been developed whereby an estimate of the effect of adding a given amount of one substance to another may be made. It is known as the Gordon-Taylor equation (Gordon and Taylor, 1952) and for a two component mixture is as follows:

$$T_{gmix} = \frac{w_1 T_{g1} + K w_2 T_{g2}}{w_1 + K w_2} \qquad \textit{Equation 1.10}$$

where:

- T_{gmix} is the T_g of a two component mixture
- T_{g1} is the T_g of component 1

- T_{g2} is the T_g of component 2
- w_1 is the weight fraction of component 1
- w_2 is the weight fraction of component 2
- K is a constant and a measure of the free volume to the mixture by each of its constituents at any temperature.

It has been observed that at each temperature, a critical water content exists at which a glassy material is sufficiently plasticised that it transforms to a rubbery material (Oksaken and Zografi, 1990). Using the Gordon-Taylor equation (Equation 1.10) it is possible to calculate the quantity of water required to lower T_g to T, and from the T_{gmix} value, an indication of the stability of the mixture under certain storage condition can be inferred. For example, using isothermal microcalorimetry and gravimetric vapour sorption methods to study the crystallisation of amorphous lactose (Briggner et al., 1994; Buckton and Darcy, 1996) an area of critical relative humidity (ca. 45% RH at 25 °C) has been identified below which amorphous lactose does not recrystallise spontaneously. Around this critical RH is the point below which the water content is not, and above which the water content in the amorphous material is sufficiently high to plasticise it such that T_g drops to 25 °C. Using Gordon-Taylor equation (Equation 1.9) it was possible to calculate that a water content of 7.25% of the mass of lactose is needed to make T_g drop to 25 °C. Thus, sorption experiments at 40% RH and 25 °C would result in water absorption amounting to less than 7.25% weight gain of lactose, whilst at 50% RH and 25 °C the water absorbed should be above this value.

1.11. THE COLLAPSE PHENOMENON

The collapse phenomenon is a characteristic of amorphous materials and occurs at a certain temperature, the collapse temperature, which is characteristic of the amorphous material. When above their T_g, amorphous materials can collapse, due to the fact that a rubbery material is unable to support its own weight under gravity. However, not all amorphous materials collapse; for example a brittle amorphous material (e.g. amorphous indometacin) does not collapse, while a free flowing porous amorphous material (e.g. spray dried amorphous lactose) can collapse.

Levine and Slade (1986 and 1988) proposed a mechanism for collapse. This mechanism considers that collapse is a consequence of a structural relaxation process characteristic of the material. According to these authors, as T rises above

T_g (or T_g drops below T due to plasticising water) free volume increases and consequently molecular mobility also increases and viscosity falls below the characteristic η_g at T_g. As a result the glass-to-rubber transition occurs and allows viscous liquid flow. At this point, viscous liquid flow can happen freely and diffusion-controlled relaxations (including structural collapse) are free to proceed with rates that increase exponentially with increasing ΔT above T_g. The T_g is the boundary between physical states in which collapse can ($T>T_g$) and cannot ($T<T_g$) happen over realistic times.

The collapse phenomenon has been ascribed to the presence of plasticising water, low solute concentration, high residual moisture and high storage temperature, all of which induce collapse by decreasing viscosity (White and Cakebread, 1966). The collapse temperature decreased as the sample moisture content increased and mixtures of materials exhibited a collapse temperature intermediate to that of the individual components (Tsourouflis et al., 1976). In order to prevent collapse, the material can be stored below its T_g or, in case of a formulation, formulated to increase its T_g (Tsourouflis et al., 1976; Flink, 1983; Levine and Slade, 1989).

Buckton and Darcy (1996) showed that longer exposures to elevated humidities may increase the degree of collapse of a sample. Prior to collapse, the water within the amorphous material may be easily absorbed or desorbed from a sample. The rate of desorption of water from an amorphous uncollapsed sample is related to the external relative humidity and the concentration gradient at the surface of the solid. However, there is a point at which the molecular motion of the material increases sufficiently to prevent the material from being able to support its own weight under gravity and it collapses. As collapse takes place, the material entraps water within the particle. After this point, removal of water from the collapsed structure is governed by diffusion within the sample and not by the external relative humidity. Therefore, collapsed materials are associated with large quantities of water, which may have a detrimental effect on the behaviour of the material.

1.12. THE AMORPHOUS TO CRYSTALLINE TRANSITION

As mentioned before, amorphous solids are thermodynamically unstable. Kauzmann (1948) has suggested that the existence of a metastable amorphous form indicates that free energy barriers exist which hinder the attainment of the stable crystalline state. The barrier that prevents a system from attaining its equilibrium state is called

the activation step (or activation energy) (Buckton, 1995b). It might then be necessary to supply sufficient energy to an amorphous material so that it overcomes the activation energy barrier and reaches the crystalline state (equilibrium state). The activation energy barrier that separates the amorphous material from the crystalline form can continuously be lowered by exposure to water and/or heat (Oksaken and Zografi, 1990; Hancock and Zografi, 1994; Hancock et al., 1995; Hancock and Zografi, 1997), presumably due to an increase in molecular mobility and greater free volume within the amorphous state. Transition from the amorphous state to the crystalline state can occur when the temperature of the material is increased above T_g (or when its T_g is lowered to T by absorption of a plasticiser).

Crystallisation from the amorphous state has been studied in detail in order to provide an understanding how it could be enhanced (e.g. if a small amount of amorphous material was inadvertently introduced during processing) or inhibited (e.g. when a material is wanted in the amorphous state). Crystallisation from the amorphous state is known to be governed by the same factors as crystallisation from the melt; nucleation (or seeding) and crystal growth (Kauzmann, 1948). Depending on the temperature or the material, either of these steps might control crystallisation. According to Kauzmann (1948) there are at least two energy barriers for crystallisation, one for nucleation (or seeding) and one for crystal growth.

1.12.1. NUCLEATION

Nucleation is the process by which individual molecules come together to form solid state nuclei from which crystals can grow. Primary nucleation can either involve molecules coming together to form a cluster (homogeneous nucleation) or molecules can cluster around a foreign body within the system (heterogeneous nucleation). Secondary nucleation occurs when new nuclei form from existing crystals (Byrn et al., 1999). In both situations it is necessary to form an amorphous (or liquid)–crystal interface that is favourable to the deposition of molecules from the amorphous material for crystallisation to occur (Franks, 1992).

If the nucleation and growth rates are functions of temperature only (not of position or time), there are three possible mechanisms for nucleation; continuous nucleation when nuclei continue to form and grow throughout the transformation, fixed number nucleation when growth proceeds from a fixed number of nuclei and is independent of experimental conditions and site-saturated nucleation when all the nuclei are

present in the beginning of the transformation but the number of nuclei depends on the temperature (Woldt, 1992).

Figure 1.4 shows the relationship between the rates of nucleation, molecular motion and crystallisation that occurs in the temperature range between T_g and T_m. It can be seen that for any amorphous system, the temperature at which optimal nucleation and crystallisation occurs, depends on the degree of supercooling below T_m and where the temperature lies in relation to T_g. The closer to T_g the higher the degree of supercooling and the higher the nucleation rate. However, this is accompanied by an increase in viscosity, which reduces the molecular motion and impedes crystal growth.

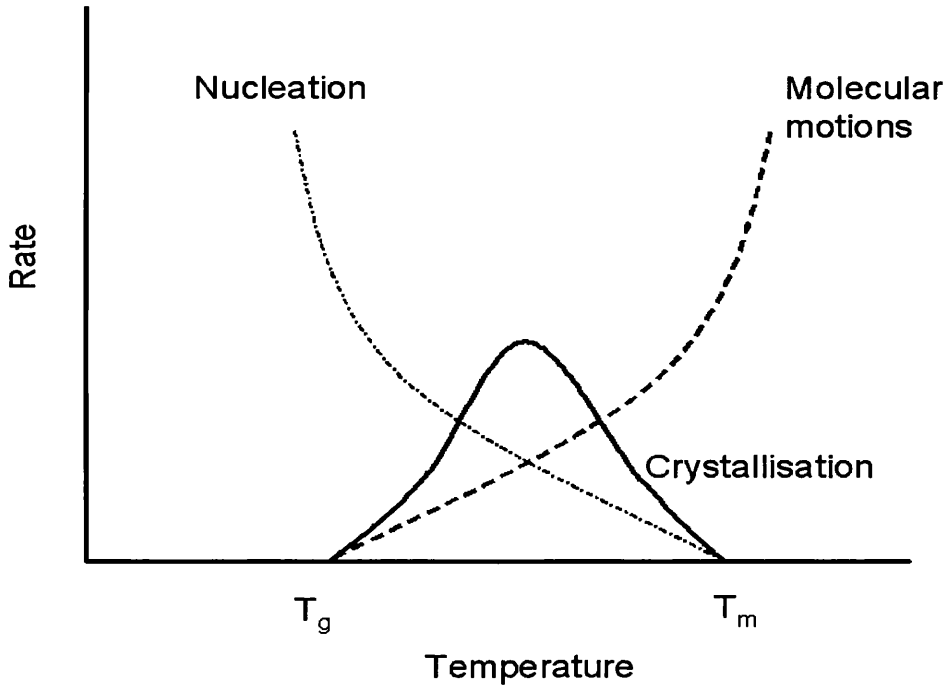

Figure 1.4 *The rates of nucleation and molecular motion associated with the crystallisation from the amorphous state between T_g and T_m. (Adapted from Hancock and Zografi, 1997).*

Thus at some temperature between T_g and T_m there is a temperature at which the rate of nucleation equals the rate of molecular motion, giving rise to a maximum crystallisation rate (Saleki-Gerhardt and Zografi, 1994a); this is the crystallisation temperature (T_c). In Figure 1.3 the rates of nucleation and molecular motion are symmetric, which if true, would lead to a T_c at the midpoint between T_g and T_m. Since the nucleation and molecular motion very likely have different temperature

dependencies, this assumption is not exactly true (Saleki-Gerhardt and Zografi, 1994a).

The T_c of amorphous sugars can be reduced by the presence of water, in the same way as the plasticising effect of water on T_g, which demonstrates the importance of molecular mobility in the crystallisation process. Crystallisation from the amorphous system can then be prevented by keeping the material below its T_g, by reducing the water content or by raising the T_g of the system (Hancock and Zografi, 1997). Since nucleation has to precede crystallisation, preventing or retarding nucleation can therefore avoid crystallisation (Van Scoik and Carstensen, 1990).

1.12.2. SEEDING

Seeding is the process of adding an additive, the desired crystal or any other material, to the system in order to stimulate nucleation and growth to produce crystals of a particular form (Byrn et al., 1999). It is a form of secondary nucleation.

If considering seeding in a partially amorphous system, in the presence of a seed material, the molecular motion of the amorphous state needs only to be sufficient for molecular reordering for secondary nucleation and growth. The presence of a seed material would be expected to reduce the activation energy for nucleation and growth, as seen for the isothermal and non-isothermal crystallisation of lactose (Schmitt et al., 1999). However, the interface between the seed and the amorphous (or liquid) material has to be favourable to nucleation and growth (Franks, 1992).

The number of particles and the crystal form resulting from a crystallisation are determined by the nucleation process. Furthermore, different conditions for crystallisation, such as temperature and/or presence of seed material might favour the nucleation and growth to one or more crystal forms. The crystallisation of amorphous indometacin at temperatures close to or below T_g was seen to favour the formation of the stable γ polymorphic form, while crystallisation above T_g favoured the metastable α-crystal form (Andronis and Zografi, 2000).

1.12.3. CRYSTALLISATION AND FLEXIBILITY OF MOLECULES

Conformational flexibility of molecules can introduce two potential difficulties to the crystallisation process (Yu et al., 2000). First, a number of structural options are

available for crystallisation, giving rise to polymorphs that differ not only in the type of packing but also in the molecular conformation. This phenomenon is described in Figure 1.5 for a system with two competing pathways originating from two different conformers and leading to two different mature crystals. Second, the tendency of crystallisation may be significantly reduced by conformational flexibility. This is because flexible molecules exist in solution or melts as mixtures of energetically similar conformers, the process of crystallisation must select the "right" conformers from among the "wrong" ones. In other words, the process of crystallisation from a solution or a melt proceeds with the selection of a particular conformer, a difficulty not encountered by rigid molecules. The same can be observed for the crystallisation of materials, such as carbohydrates, that exist in solution as a mixture of anomers (configurational isomers).

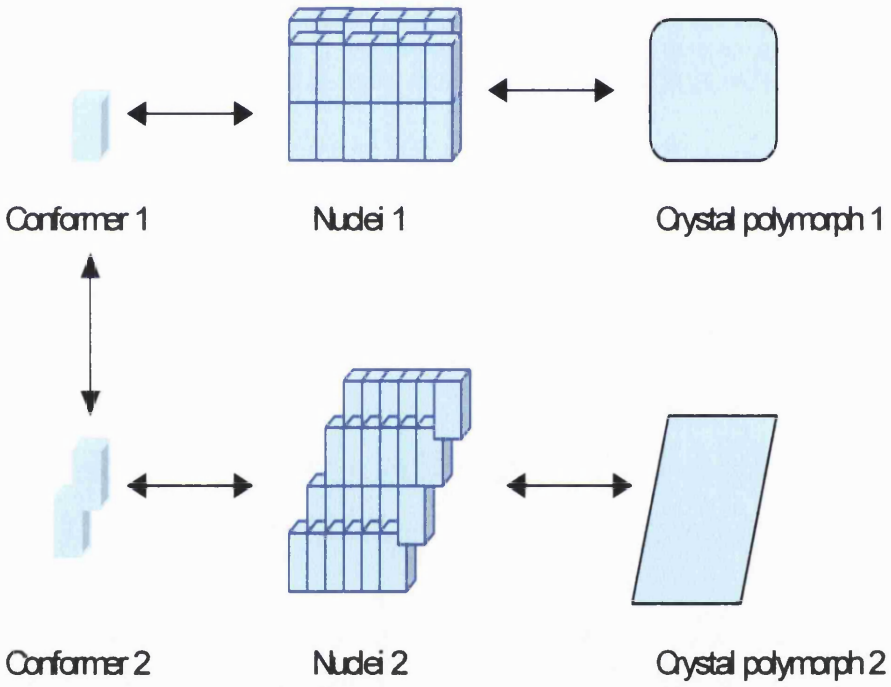

Figure 1.5 **A schematic representation of the crystallisation of flexible molecules (Adapted from Yu et al., 2000).**

1.13. DISORDER IN CRYSTALLINE MATERIAL

Pharmaceutical solids rarely exist as totally crystalline or totally amorphous solids. The well organised structure of the crystalline state is most often altered by the presence of defects, imperfections and regions of amorphous structure. These can be inadvertently or intentionally originated during pharmaceutical processing of

powders. For example, it is often desirable to increase the rate of dissolution of a drug by reducing its particle size through communition (Florence and Salole, 1976). Particle size reduction is also a commonly used method to obtain dose uniformity in inhalation formulations. In the above cases, processing will certainly induce disorder on the surface of the particles (Newell, et al., 2001) originating a partially amorphous particle with a crystalline core and an amorphous corona. Due to its location on the surface, the amorphous portion is capable of having a greater effect on the material behaviour than its proportions to the total mass would indicate, as materials are known to interact through their surfaces (Buckton, 1995a). In order to aid processing, many excipients come to the formulation stages in a fully amorphous state (e.g. spray dried lactose) (Bolhuis and Chowan, 1996). Biological products and injectable drugs are normally rendered amorphous by freeze-drying to enhance stability (Manning et al., 1989; Pikal, 1990). Processes like spray-drying and freeze-drying can be controlled to render fully or partially amorphous materials.

Not all materials can form the amorphous state readily or they may not form the amorphous state at all. The formation of the amorphous state can be very straightforward for some materials (good glass formers) but difficult for other materials (poor glass formers). The process of formation of the amorphous state is governed by thermodynamic and kinetic properties of the molecules. Thermodynamically, the ability to form a glass originates from a crystalline state that is not substantially more stable than the correspondent amorphous state. In kinetic terms, a slow crystallisation rate might allow the material to freeze into a glassy state (Yu, 2001)

1.13.1. SPRAY- AND FREEZE-DRYING

Spray drying converts a liquid into a powder in a one step process; it involves the production of small droplets of a solution or suspension, which will be exposed to temperatures high enough to evaporate the solvent. Depending upon the material and the process conditions, spray drying can be used to produce fully or partially amorphous particles (Chidavaenzi et al., 1997, 2001 and 2002; Harjunen, 2002). The spray dried material has an increased solubility (dissolution rate) (Corrigan, 1995) and compactability (Vromans et al., 1986; Sebhatu et al., 1994b). Spray dried lactose was the first excipient specially designed for direct compaction (Bolhuis and Chowan, 1996). According to Corrigan (1995) the spray drying conditions may result in the formation of amorphous material with different T_g values and physical

properties. For example, amorphous furosemide prepared using two spray drying protocols showed distinct T_g (Matsuda et al., 1992). Spray drying is further discussed in Chapter 2.

Freeze-drying, or lyophilisation, involves the desiccation of a substance by crystallisation of ice, followed by sublimation of water vapour from the solid state at reduced pressure. This process avoids the drying at high temperatures, which prevents chemical degradation. Freeze drying is normally used for the production of amorphous materials, often with the objective to ease reconstitution of the final product. The freeze dried material tends to have a porous structure, which facilitates the reconstitution process. Freeze drying has been investigated for stabilisation of gene delivery systems (Talsma et al., 1997; Miyata et al., 2005) and proteins (Manning et al., 1989; Österberg and Wadsten, 1999; Passot et al., 2005).

1.13.2. HEAT DRYING

Heat drying is a process by which the material is rendered amorphous by manipulation of temperature and pressure conditions. In the 1970's it was found that the progressive drying of α-lactose monohydrate under vacuum resulted in a continuous decrease in the degree of order of the material (Hüttenrauch and Keiner, 1979). Through progressive drying, progressive water is lost from the crystal lattice what results in lattice defects. This method of preparation of amorphous material has been reported for α,α-trehalose dihydrate (Ding et al., 1996), and raffinose pentahydrate (Saleki-Gerhardt et al., 1995).

1.13.3. COMMUNITION

Communition involves the reduction of particle size by a process of crack propagation. The applied stress produces strains in the particles which are large enough to cause breaking of bonds and crack propagation. These cracks are propagated through regions of the material with more flaws or discontinuities; where least resistance to cracking exists. A high amount of energy is involved in the process, of which only a small amount is involved in the reduction of the particle size, the remaining is lost many ways, including elastic deformation of particles without fracture, deformation to initiate cracks, deformation of the metal components of the machine, interparticulate friction, particle-machine friction, heat, sound and vibration. Communition introduced cracks and deformation at the surface of the

particles, decreasing the degree of crystallinity (Suryanarayanan and Mitchell, 1985), creating local "hot spots" which store energy at the surface of the particle, causing large changes in the surface energetics (Buckton et al., 1988; Newell et al., 2001), and, consequently in the performance of the product. Communition has proved to increase the dissolution rate of the material (Florence and Salole, 1976; Elamin et al., 1994). Both the dissolution rate and bioavailability of phenytoin were greatly improved when this drug was ground in presence of microcrystalline cellulose (Yamamoto et al., 1976). Tablet compression was also improved when milled materials were used (Hüttenrauch, 1983). On the other hand, communition can affect the chemical stability of a material (Otsuka and Kaneniwa, 1990). The physical stability of a ground material can also be affected; for example amorphous lactose formed by grinding underwent mutarotation which was induced by the mechanical activation of grinding (Otsuka et al., 1991) and, in addition, agglomeration can occur during crystallisation of the amorphous material (Ward and Schultz, 1995). Communition is normally used in pharmaceutics to reduce particle size in inhalation products.

1.13.4. MIXING

Disruption of the crystalline order can also be caused by mixing. Reduced pressure mixing was employed to mix an organic crystalline drug with an adsorbent and produced an amorphous system (Konno, 1990). Pressure, temperature and rotating speed all affected the degree of crystallinity of the final product.

1.13.5. SUPERCOOLING OF THE MELT

Amorphous material can also be prepared by melting the material and rapidly cooled it by immersion into liquid nitrogen, for example. The rapid cooling prevents the crystallisation of the amorphous material. However, this procedure is limited by the possibility of the material undergo degradation at a temperature very close to the melting temperature.

1.13.6. VARIATION IN AMORPHOUS MATERIAL FORMED BY DIFFERENT ROUTES

All the methods of preparation of amorphous material described above aim to reduce the long range order of the crystalline state into a state of short range or no order at all, which is characteristic of the amorphous state. However, it is clear that

they vary in their efficiency. Consequently, amorphous material formed by different routes could exhibit different characteristics such as glass transition temperature, water uptake profile, relaxation profile, surface characteristics, crystallisation tendency, morphology and, obviously, the extent of short range order.

There are reports of apparently different forms of amorphous pharmaceuticals with different physical and chemical properties. For example, Pikal et al (1977) clearly showed a difference in enthalpy of solution between spray-dried and freeze-dried amorphous samples of the same material. Surana et al. (2004b) prepared amorphous trehalose by freeze-drying, spray-drying, dehydration, and melt-quench. It was reported that the preparation method influenced the water uptake profile, crystallisation behaviour, enthalpy relaxation, and morphologic properties. Amorphous trehalose prepared by dehydration showed the highest enthalpy recovery at T_g and the highest tendency to crystallise. Amorphous trehalose prepared by melt-quench showed the least or no tendency to crystallise. Spray-drying originated the amorphous form with the highest rate of water uptake as compared to other methods.

According to Hancock et al. (2002) these different forms of glassy amorphous pharmaceuticals are most probably the same amorphous form at different extents of relaxation towards the super-cooled liquid state. There are many possible relaxation states of most glassy amorphous pharmaceuticals, which are a continuum of kinetic states differentiated by the extent of departure from the equilibrium super-cooled liquid, rather then distinct thermodynamic phases.

It is clear that differences could be observed in the amorphous state produced by different methods. Such differences should be addressed regarding their pharmaceutical significance. Furthermore, it raises questions about what should be used as an amorphous standard for characterisation and quantification of the range of order in the amorphous state.

1.13.7. ONE-STATE VERSUS TWO-STATE MODEL OF PARTIALLY CRYSTALLINE SYSTEMS

In order to assess partially crystalline systems, two models have been considered: the 'one-state model' and the 'two-state model'.

In the 'two-state model', domains of material are assumed to be either entirely crystalline or entirely amorphous and they co-exist side by side in a physical mixture. Thus, by combining quantities of amorphous and crystalline material, it is possible to prepare physical mixtures of known amorphous content. According to the 'two-state model', the degree of crystallinity depends on the fraction of amorphous material in the mixture (Suryanarayanan, 1985).

The alternative 'one-state model' considers that the degree of crystallinity depends of the state of disorder in the crystal lattice. According to the "one-state" model, the material consists of domains which are truly crystalline and in which the molecules have formed a partially disordered structure as a result of processing (Suryanarayanan, 1985).

Although the 'one-state model' is a better description of the reality, it is not possible to process a sample to achieve an exact amount of amorphous content. Moreover, as it has been shown that the 'two-state model' is a good representation of a 'one-state model' (Saleki-Gerhardt and Zografi, 1994b), the 'two-state model' is more often applied to the study of partially amorphous systems.

1.14. SURFACE OF POWDERS. AMORPHOUS SURFACE AND SURFACE ENERGETICS

The surface of powders is vital in controlling the way the solid interacts with other phases, and hence the ease of production, the stability and the usefulness of drug products. For example, the success or failure of a dry powder inhaler system is dependent upon the nature of the surface of the materials used (Buckton, 1995b).

Powders behave in different manners in products if they have differences in purity, size, crystal habit, polymorphic form, hydrate or solvate form, or degree of crystallinity. These factors are known to alter the surface of the powder to some extent. For instance, the size, crystal habit, polymorphic form or presence of a hydrate may well affect the surface of the powder if the crystals express the various functional groups in different proportions.

The extent of crystallinity at the surface of the powder is considered to be the most important cause of variability in powder properties. Processing is known to alter the crystallinity of the surface to some extent (Section 1.12). In this case not only the chemical groups at the surface of the powder can be affected, but also the

amorphous surface is thermodynamically unstable and thus in a higher energy state (Feeley, et al., 1998; Newell et al., 2001) than its crystalline counterpart.

1.14.1. SURFACE ENERGETICS

Surface energy can be defined as the value of work required per unit area to move molecules to the surface of the liquid (Buckton, 1995b). A solid is a rigid material which is resistant to stress. However, at the surface of a solid there is net imbalance of forces, and so solids will have a surface energy. The surface energy can be divided into two components; the dispersive surface energy, which represents the dispersion forces, and the polar component that can describe the acidic/basic nature of the surface, which can further be divided into an electro donor and an electron acceptor contribution.

This surface energy has a value which is descriptive of the powder surface (Buckton, 1995b). It is a function of its chemical nature and of its previous treatment history. Newell et al. (2001) showed that the surface energy of particles with small degrees of disorder located on the surface is very similar to totally amorphous particles and very different to a physical mixture of the same amorphous content. In the amorphous state the disordered molecules can assume a higher number of orientations on the surface of the particle, and this may as well account for the higher range of surface energies measured for the amorphous state. Additionally, different batches of an amorphous material exhibit different surface energies (Grimsey et al., 2002). The surface energy of amorphous material obtained by different methods can also be different (Ohta and Buckton, 2004b). The energetics of processing and the ability of the material to recover to the initial crystalline state will certainly affect the performance of the material.

Determinations of surface energy successfully distinguished between batches of crystalline salbutamol sulphate (Ticehurst et al., 1994) and α-lactose monohydrate (Ticehurst et al., 1996). It has also been shown that surface energy varies with the shape of the crystals (Grimsey et al., 2002), isomeric form (Grimsey et al., 1999) and processing route (Grimsey et al., 2002).

Surface energy differences in two nominally equivalent batches of salbutamol sulphate, before and after micronisation, were related to powder flow properties (Feeley et al., 1998). Cline and Dalby (2002) correlated the *in vitro* performance of

powder blends for dry powder inhalers to surface energy interactions between a drug and a carrier.

The surface energy of a solid can be determined by contact angle measurements or vapour sorption techniques, which can be gravimetric, microcalorimetric or chromatographic.

1.15. ADVANTAGES AND DISADVANTAGES OF AMORPHOUS MATERIAL

As already mentioned materials can be intentionally or inadvertently rendered partially or fully amorphous during processing. Both advantages and disadvantages of amorphous materials are due to its enhanced molecular mobility, in comparison to the crystalline state.

1.15.1.1. ADVANTAGES

Amorphous materials have several advantages over the crystalline materials.

Several studies report that the solubility advantage of the amorphous forms may be significant, when compared to the correspondent crystalline form of the drug. For example, when the amorphous forms were used an increase of 1.4 fold in the solubilisation of indometacin (Imaizumi, 1980), 2 fold in the solubilisation of cefalexin (Egawa et al., 1992) and 10 fold in the solubilisation of novobiocin (Mullins and Macek, 1960) have been reported. The presence of low levels of amorphous material in milled griseofluvin, which were not detected by differential scanning calorimetry, resulted in a 2 fold or more increase in solubilisation (Elami et al., 1994). The solubility advantage of the amorphous state is related to the fact that the amorphous state can solubilise faster than the crystalline state because it lacks the strong intermolecular forces of the crystalline state (amorphous solids do not exhibit heat of solvation). If sufficient material is added to the dissolution medium, an amorphous form will attain a saturation point faster than the corresponding crystalline counterpart. This is the true solubility advantage of the amorphous state. However, if the solubilised molecules are not removed from the dissolution medium, they might crystallise into the more stable crystalline form and, after some time, the solubility will be that of the crystalline form. In case a mechanism exists that avoids crystallisation from the solution, the apparent solubility of the amorphous form might be higher than the equilibrium solubility of the crystalline solid. This property of the

amorphous state has been explored for formulation of poorly soluble drugs in order to improve their bioavailibility. For example, formulations of cefditoren pivoxil (Spectracef®), rosuvastatin calcium (Crestor®) and cefuroxime axetil (Ceftin®).

Improved tablet strength is another advantage of amorphous material. Sebhatu et al. (1994b, 1997) attributed the improved tablet strength to an increased deformability of the amorphous particles and to the formation of interparticulate bonds, which were favoured by the presence of residual water that caused the material to crystallise during compression. It had previously been observed that milled material exhibited a greater tablets strength due to its enhanced deformability and to bonding within the tablets, what was attributed to the enhanced surface reactivity of the particles (Hüttenrauch, 1983).

The amorphous state plays an important role in the stabilisation of macromolecules by carbohydrates. This stabilisation is thought to be due to the ability of amorphous sugars to hold proteins rigid in their glassy matrix (Green and Angell, 1989). Another possibility is that upon drying sugars are capable of replacing hydrogen bonds which are present in solution between proteins and water (Hanafusa, 1985). An alternative mechanism for stabilisation of proteins by sugars is based on the ability of some sugars to form hydrates upon crystallisation, simultaneously removing water from the remaining amorphous phase (Aldous et al., 1995).

1.15.2. DISADVANTAGES

A first disadvantage of the amorphous state is its tendency to crystallise (Makower and Dye, 1956; Pikal et al., 1978; Kontny et al., 1987), thus altering the physical properties of the product. The crystallisation of amorphous areas within a crystalline particle can be dramatic for formulation and product performance. The reversion of the unstable amorphous material to the lower energy crystalline state can have a dramatic effect due to particle aggregation (Yoshioka et al., 1996; Ward and Schultz, 1995; Duddu et al., 1997) or formation of polymorphs with different properties (Andronis et al., 1997). For example, the agglomeration of micronised albuterol sulphate due to crystallisation of its amorphous surfaces cancelled out the efforts of particle size reduction and can have a detrimental effect on the performance of such material in dry powder inhalers (Ward and Schultz, 1995). Furthermore, Mackin et al., (2002) observed that a milled batch that recrystallised over a short period of time, did not exhibit the same physical properties as the unmilled batch, and this

resulted in the drug product batches failing to meet their pre-lubrification acceptance criteria for blend content uniformity.

The lower chemical stability of the amorphous material in relation to the crystalline state is another undesired property of the amorphous state. For example, the rates of degradation of β-lactam antibiotics (Pikal et al., 1977), cefoxitin sodium (Oberholtzer and Brenner, 1979) and quinapril hydrochoride (Guo et al., 2000) were enhanced for the amorphous forms of these materials. The chemical degradation may be a function of both molecular mobility and relaxation behaviour (Craig et al., 1999). The concept of orientation-specific degradation is related to the fact that solid-state reactivity may be associated to the orientation of the molecules (Craig et al., 1999). A study of the physical characteristics and chemical degradation of amorphous quinapril hydrochloride concluded that the temperature dependence for chemical degradation below T_g correlated very closely with the temperature dependence of molecular mobility. Above T_g, however, the chemical degradation was slower than predicted from molecular mobility (Guo et al., 2000).

A further disadvantage of the amorphous state is its high water affinity. The amorphous regions, of greater molecular disorder and reactivity, should be able to take up more water than would normally be adsorbed on the crystalline portions of the surface of the solid. If the amount of water taken up is sufficient to plasticise the local regions such that T_g drops below T, molecular mobility can be high enough to further enhance chemical reactivity and solid-state phase changes. This effect of water is known as amplification (Hancock and Zografi, 1997). In addition, the absorbed water in the amorphous state can also lead to microbial contamination in the material. Furthermore, the absorbed water can induce collapse of the amorphous regions (Section 1.11). Subsequent drying of the collapsed material will not remove that water, since it may only be removed by slow diffusion from the collapsed material.

It is known that accidentally induced amorphous material varies between batches, which mean that it might not be possible to predict the behaviour of the product due to batch to batch variability.

1.16. MODEL MATERIALS FOR THE STUDY OF CRYSATLLINE AND AMORHOUS PROPERTIES

Two model materials were chosen for the study of the crystalline and amorphous states: lactose and indometacin.

1.16.1. LACTOSE

Lactose is a white to off-white, odourless and slightly sweet-tasting, crystalline powder freely but slowly soluble in water (Rowe et al., 2003). It is a disaccharide of glucose and galactose that exists in two optical isomeric forms: α- (O-β-D-galactopyranosyl-(1→4)-α-D-glucopyranose) and β-lactose (O-β-D-galactopyranosyl-(1→4)-β-D-glucopyranose), which differ in the orientation of the H and OH on the glucose ring (Figure 1.5). There are also reports of crystalline complexes consisting of both α- and β- lactose (Bushill et al., 1965; Buma, 1978; Lerk, et al., 1984a and 1984b)

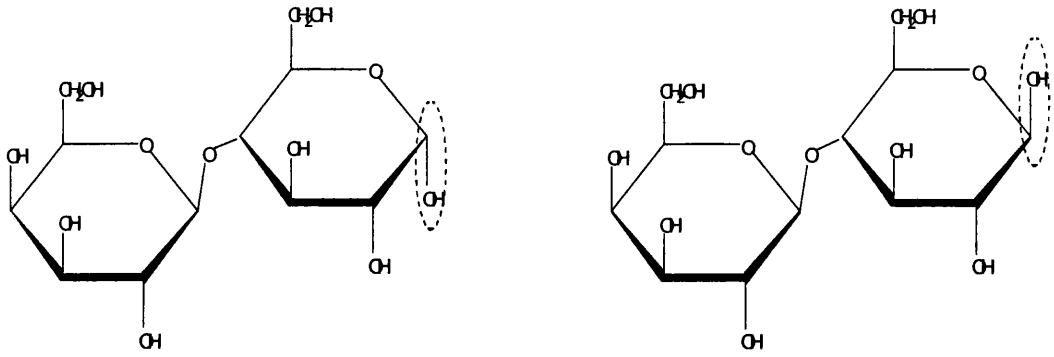

Figure 1.6 *Structural formula of α- and β-lactose showing the different orientation of the –OH group.*

Lactose is naturally present in the milk of most mammals and commercially it is produced from the whey of cow's milk (Rowe et al., 2003). α-lactose is crystallised from a supersaturated whey solution below 93 °C; the β-form is more saturated at this temperature than the α-form. A hygroscopic α-lactose is formed, which absorbs one molecule of water per molecule of lactose forming α-lactose monohydrate (O-β-D-galactopyranosyl-(1→4)-α-D-glucopyranose monohydrate). If the mononhydrate is stored under vacuum between 100-130 °C, the hygroscopic α-form is formed. A non-hygroscopic α-form can be produced by desiccating the monohydrate over dry

methanol, or by thermal treatment of the monohydrate above 110 °C at high relative humidities. The molecular formula of anhydrous lactose is $C_{12}H_{22}O_{11}$, with a molecular weight of 342.30, while the monohydrate form has a molecular weight of 360.31 and exists as $C_{12}H_{22}O_{11}.H_2O$.

Anhydrous β-lactose is produced by precipitation from a saturated whey solution above 93 °C, where the α-form is more soluble. The β-lactose cannot incorporate water into its crystal lattice. This is because of its higher density that requires a greater enthalpy for expansion of the anhydrous lattice (Berlin et al., 1971). Instead water will induce mutarotation to α-lactose that will then incorporate water, especially at high relative humidities (Angberg et al., 1991).

The two anomeric forms of lactose are simultaneously present in aqueous solution at an α/β ratio of 40/60 at room temperature and mutarotate according to temperature. As the solution temperature increases, the α-form is favoured (Dwivedi and Mitchell, 1989). In the solid state, although the crystalline forms are relatively stable, is has been shown that β-lactose undergoes mutarotation to α-lactose under relatively high relative humidities (Angberg et al, 1991). Upon heating, the hydrated α-form can loose its water of crystallisation which can be sufficient to cause α- to β-lactose mutarotation (Olano et al, 1983; Lerk et al., 1984). However, heating can also induce mutarotation in the opposite direction (Olano et al, 1993 and Lerk et al, 1984). The heat that accompanies β- to α-lactose mutarotation was said to be 0.42J/g (Hudson and Brown, 1908).

α-lactose crystals normally exhibit a tomahawk-like habit. The packing is characterised by a complex three-dimensional hydrogen bond network, with each lactose molecule being involved in 14 hydrogen bonds and in the case of the monohydrate, each molecule of water is hydrogen-bonded to four α-lactose molecules.

According to Schmitt et al. (1999) α-lactose monohydrate loses its water of crystallisation at 145 °C. The T_g of amorphous lactose is located at approximately 114 °C and the crystallisation exotherm of lactose is located at 187 °C. The melting point of α-lactose is located at 212 °C and β-lactose melts at 239 °C.

Amorphous lactose is easily produced by spray-drying, remaining amorphous for long periods of time when stored at 0% RH and room temperature. The anomeric

composition of amorphous lactose is influenced by processing (Otsuka et al., 1991; Chidavaenzi et al., 1997). Mutarotation following crystallisation is a consequence of the fact that lactose exists as two anomers and is a characteristic of lactose (Angberg et al., 1991)

Lactose is a commonly used excipient in the pharmaceutical industry (Rowe et al., 2003). It is used and a dilluent and filler in tableting and capsule filling. In dry powder inhalers is used as a carrier to aid processing and uniformity of dosing. Lactose is also used in combination with sucrose to prepare coating solutions. Spray-dried lactose (α-lactose monohydrate with a quantity of amorphous lactose) is used in direct compression for production of tablets with higher breaking strength. Several commercial grades of lactose are available and the grade is chosen according to the type of application.

1.16.2. INDOMETACIN

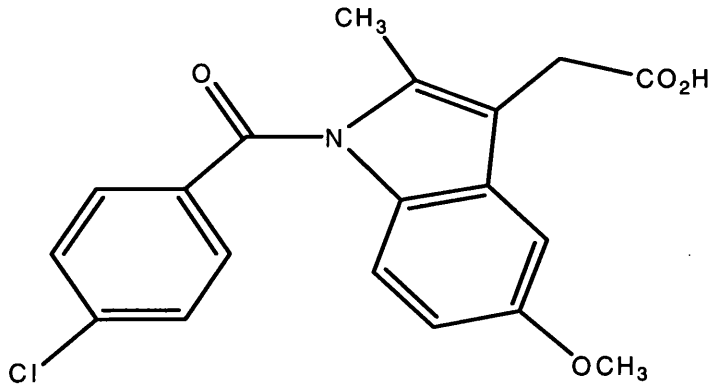

Figure 1.7 *Structural formula of indometacin.*

Indometacin ([1-(4-chlorobenzoyl)-5-methoxy-2-methylindol-3-yl]acetic acid) is a white or yellow, crystalline powder, practically insoluble in water and sparingly soluble in alcohol. Indometacin is used as an anti-inflamatory and analgesic agent. It is commercially available since 1963, being used in the therapy of rheumatic disease. The molecular formula of indometacin is $C_{19}H_{16}ClNO_4$, with a molecular weight of 357.8. Basically, indometacin is a small relatively nonpolar organic carboxilic acid, with the chemical structure shown in Figure 1.6.

Indometacin exhibits a complicated polymorphism consisting of several true polymorphs and a wide range of solvates collectively named Form V (β). Yamamoto (1968) first described three polymorphic forms (α, β and γ) and Borka (1974) identified Forms III, IV and solvate containing form. Form V (β) exists in films grown from the melt and in the presence of co-solvates, and originates Forms I (γ) or II (α) by desolvation. Of the true polymorphs only Forms I (γ) and II (α) are normally obtained. Form III is believed to be a decomposition product of the melt growth process and Forms IV, VI and VII are metastable and rapidly transform to the mostly stable Forms I or II on standing or heating.

Forms I (γ) and II (α) of indometacin are the most stable and consequently the most useful of polymorphs. Forms I (γ) and II (α) exhibit a melting point of approximately 160 °C and 154 °C, respectively (Borka, 1974) and, as implied from its melting point, Forms I (γ) is the most thermodynamically stable of the two. Form II (α), although metastable, has been shown to persist at room temperatures for long periods of time. Form I (γ) shows a well defined rhombic morphology, while Form II (α) exhibits a fibrous/spherulitic structure (Slavin et al., 2002).

The melt of indometacin solidifies as a brittle, glassy amorphous mass (T_g approximately 45 °C) which can remain uncrystallised for at least two months at room temperture (Borka, 1974). However, amorphous indometacin is well plasticised by water and crystallisation can occur below T_g over relatively short time scales (Andronis and Zografi, 1998). Both Forms I (γ) and II (α) can crystallise from the amorphous state, being possible to stimulate the crystallisation into one of the forms or a mixture of both by selecting the temperature and relative humidity of crystallisation. Crystallisation of amorphous indometacin at temperatures close of below T_g favours the formation of the stable Form I (γ), while crystallisation at higher temperatures favours the formation of the metastable Form II (α) (Andronis and Zografi, 2000). Andronis et al. (1997) verified that at 30 °C, below 43% RH only the stable Form I (γ) crystallised, whereas at higher relative humidity, only Form II (α) was detected.

1.17. AIMS OF THIS THESIS

This thesis aimed to investigate the physical properties of the crystalline and amorphous states. It focuses on: 1) the determination of amorphous contents of lactose by isothermal microcalorimetry and on the characterisation of the crystallisation of lactose from the amorphous state, taking into consideration the effect of the variability (anomeric composition) of the crystalline and amorphous portions; 2) the impact of the variability (anomeric composition) of both amorphous and crystalline forms of lactose on the quantification of small levels of the amorphous content by thermal methods; 3) the characterisation of the relaxation behaviour of amorphous lactose and indometacin by isothermal methods (solution calorimetry and inverse phase gas chromatography) in comparison to StepScan differential scanning calorimetry.

CHAPTER TWO

MATERIALS AND METHODS

2.1. MATERIALS

All materials (listed in Table 2.1) were used as received, unless otherwise stated. Purified water was obtained from an Elga DV25 purifier.

Table 2.1 *Materials used and their suppliers and batch numbers.*

Material	Supplier	Batch number
α-lactose Monohydrate	Burculo whey Products	23416
β-lactose	Acros Organics	A010045201
Indomethacin	Sigma	122K0718
Sucrose	Fluka Biochem	453620/1
Potassium Chloride	National Bureau of Standarts	Standard reference material 1655
Magnesium Nitrate	Acros Organics	A018958601
DMSO	Acros Organics	A017283301
Pyridine	Aldrich	06106PA
TMSI	Aldrich	S10146-493
Phosphorous pentoxide	Acros Organics	A016916901
Ethanol	Hayman Ltd	-

2.2. METHODS

2.2.1. SPRAY DRYING

2.2.1.1. INTRODUCTION

Spray drying is a continuous process which involves the transformation of a fluid feed into a particulate dried product by spraying the feed into a hot drying medium, which is normally air. The fluid mixture can be a solution, suspension, dispersion or agglomerate and can only be spray-dried if the final product behaves as a non-sticky, flowing powder.

Aside from the pharmaceutical industry, spray drying is also used in the food industry since products retain nutritive content and are easily reconstituted (Marster, 1991). Pharmaceutically it is a favoured process to optimise particle size, particle shape, size distribution, bulk density, porosity, moisture content, flowability and stability (Corrigan, 1995).

The spray drying process consists of four phases. The first stage is called atomisation, when the feed is pumped into the drying chamber and atomised into a spray. This increases the surface area of the material dramatically, aiding the vaporisation of the droplet, which begins immediately upon contact with the hot air. Moisture evaporation starts to take place from the surface of the droplet. Finally the dried product is recovered from the drying air to a cyclone collection vessel.

The final product can be a powder, granulate or an agglomerate, depending on the physical and chemical properties of the feed, the characteristics of the dryer and the operation parameters such as atomiser pressure, feed rate, air flow rate and inlet and outlet temperatures. Inlet temperature alters the rate at which drying proceeds, as it controls the temperature of the drying air. If too high, this will have a detrimental impact on thermolable substances, although since the evaporation of water is an endothermic process, the actual temperature of the material does not reach the inlet temperature until its surface is dry. The outlet temperature is that of the air as the particulate material enters the collection vessel, although this may not be the temperature of the product since vaporisation removes heat from the product. The larger the temperatures difference between the outlet and inlet temperatures, the larger the amount of residual moisture in the final product. A higher aspirator speed implies a shorter residence time and results in a larger amount of residual moisture, resulting also in a higher degree of separation in the cyclone. It is important to be aware of the impact of any residual moisture content on the glass transition temperature of the product, as it is possible for the amorphous glass to transform into the rubbery phase, facilitating collapse and crystallisation. The flow rate of the compressed air, when increased, will result in reduced particle size. Increasing the concentration of the feed mixture will, however, produce larger and more porous particles.

2.2.1.2. INSTRUMENTATION

A Buchi 191 mini spray-dryer (Buchi, Switzerland) was employed to produce batches of 100% amorphous lactose with different α- and β-lactose proportions and it is schematically represented in Figure 2.1.

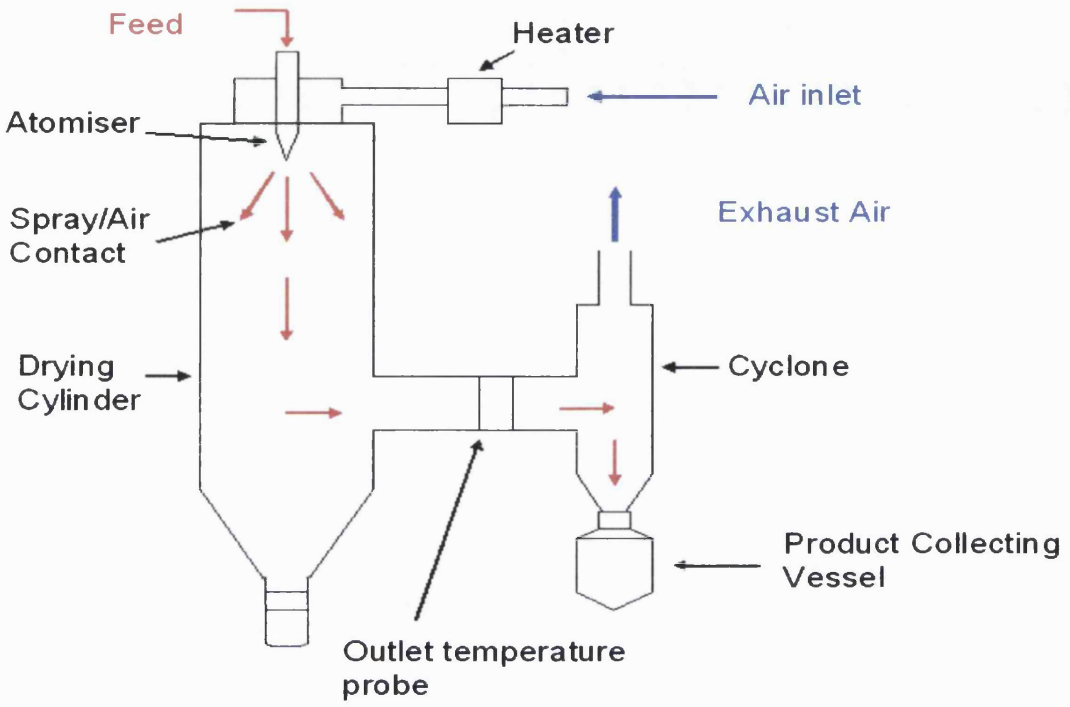

Figure 2.1 *Schematic of the 191-Buchi Mini Spray Dryer, showing the route of the feed (red arrows) and air flow (blue arrows) inside the spray dryer (Adapted from Buchi).*

2.2.1.3. EXPERIMENTAL

Table 2.2 *Operating parameters for the preparation of 100% amorphous lactose.*

Operating parameter	***Settings***
Inlet temperature (ºC)	185 – 190
Outlet temperature (ºC)	98 – 105
Feed rate	15
Aspirator	66
Air flow rate	600
Feed solution concentration (% w/v)	10
Feed solution temperature (ºC)	25
	40
	85

Each batch of amorphous lactose was produced by spray drying 200 mL of feed solution, using the operating parameters described in Table 2.2. In order to obtain amorphous lactose with different anomeric composition, the feed solution was previously equilibrated at 25 ºC, 40 ºC and 85 ºC. A yield of approximately 30% was

achieved and confirmation of its amorphous nature was carried out by batch isothermal microcalorimetry at 53% RH and 25ºC as described in Section 2.2.2.3.1 and X-ray powder diffraction as described in section 2.2.8.3. Samples of each batch were derivatised for chromatographic analysis as described in Section 2.2.7.3. The amorphous product was stored at 0% RH in an evacuated desiccator over phosphorous pentoxide at room temperature.

2.2.2. ISOTHERMAL MICROCALORIMETRY

2.2.2.1. INTRODUCTION

As isothermal microcalorimetry is a technique which measures heat flow, it can be employed to study all the physical and chemical processes which are accompanied by heat changes, be they exothermic or endothermic. The sample is maintained under isothermic conditions and once the reaction occurs, a thermal gradient is generated between the sample and its surroundings. The heat flows associated with all the reactions that occur simultaneously within the sample are recorded as a function of time. This allows one to study complex systems and processes but can cause difficulties in data analysis. Poor sample preparation can also lead to erroneous heat flow signals. Other information that can be obtained includes: rate of basic chemical reactions, extent of basic chemical reactions, changes of phase, changes of structure and metabolism of living systems. In the pharmaceutical industry, isothermal microcalorimetry is generally used in studies of physical and chemical stability, excipient compatibility and physical form characterisation. Buckton and Beezer (1991), Buckton (1995c) and more recently Gaisford and Buckton (2001) reviewed the applications of microcalorimetry to physical pharmacy and pharmaceutics.

2.2.2.2. INSTRUMENTATION

A 2277 Thermal Activity Monitor (TAM) (Thermometric AB, Jarfalla, Sweden) was employed in this study and is represented in Figure 2.2. The TAM is very sensitive and can measure thermal events to fractions of a microwatt. It operates by utilising the basic principle of thermal equilibrium within a system, such that any heat

produced diffuses away in a process termed as "Heat Flow" of "Heat Leakage". This instrument comprises four calorimetric channels, equipped with sample and reference measuring cups. The sample and reference cells are surrounded by a semi-conductor thermopile, which is in contact with a high heat capacity, large mass heat sink (Figure 2.3). This heat sink consists of a 25-litre water thermostat (distilled water) that surrounds the reaction measuring vessel and guarantees optimal thermal stability. The heat sink can be maintained at a temperature ranging from +5 to 80 ºC with a stability of 0.0001 ºC, which is achieved via an external water circulator (2219 MultiTemp, Thermometric AB, Järfalla, Sweden).

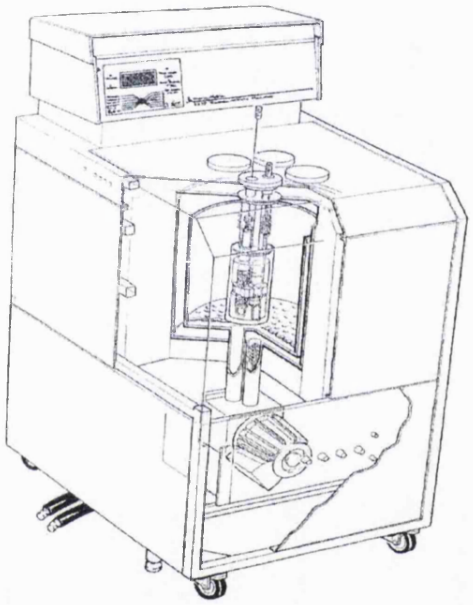

Figure 2.2 *Diagram of the 2277 Thermal Activity Monitor (Thermometric AB).*

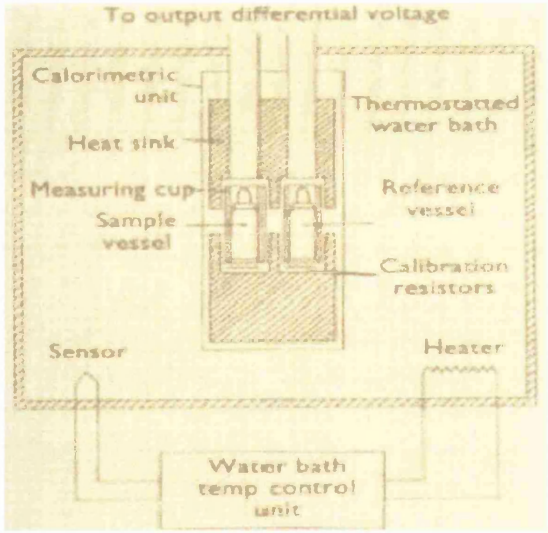

Figure 2.3 *Outline of the functional design of the Thermal Activity Monitor (Thermometric AB).*

Any process occurring within the sample cell results in a change in enthalpy and a heat flow across the thermopiles is generated, in an effort to restore thermal equilibration to its surroundings (Figure 2.4). The heat energy that is generated is channelled through the thermopile before escaping to the heat sink. The thermopiles are extremely sensitive detectors and convert heat energy into a voltage signal proportional to the heat power flowing across them, this signal is amplified, multiplied by the cell constant (determined by electrical calibration) and recorded as power versus time via the dedicated software package Digitam 4.1 (Thermometric AB, Järfalla, Sweden). The output voltage of the sample thermopile is connected in opposition to the thermopile of the reference cell, to eliminate concurrent environmental change effects. The output signal is the rate of change of heat (power) (dq/dt) which is recorded as a function of time. The TAM allows conduction of four types of isothermal microcalorimetry experiments, namely batch isothermal microcalorimetry (ampoules, Section 2.2.2.3.1), RH perfusion isothermal microcalorimetry (Section 2.2.2.3.2), titration isothermal microcalorimetry and solution calorimetry (Section 2.2.3).

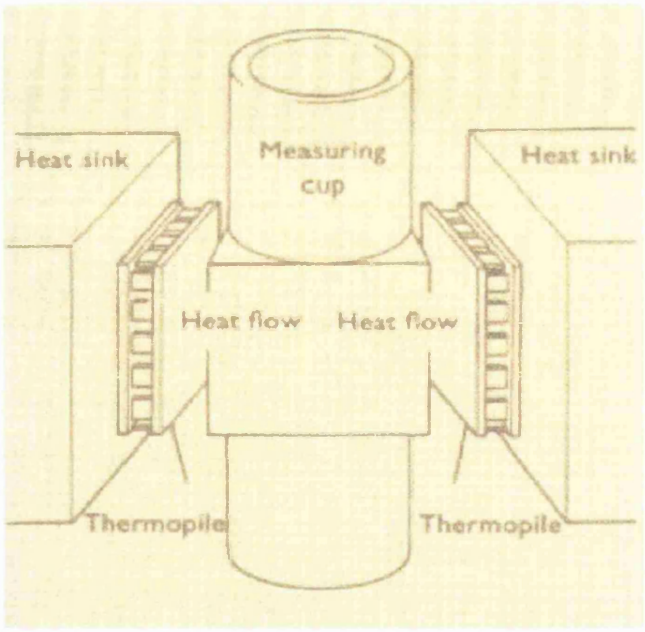

Figure 2.4 *Diagram of the Thermal Activity Monitor detection and measurement unit (Thermometric AB).*

2.2.2.3. EXPERIMENTAL

2.2.2.3.1. BATCH ISOTHERMAL MICROCALORIMETRY

Batch isothermal calorimetry was used to quantify the amorphous content of amorphous lactose samples. Each sample (approximately 30 mg, accurately weighed) was weighed into a 3 ml glass ampoule and exposed to elevated relative humidities, by means of a mini-hygrostat containing a saturated salt solution, which was also placed into the reference ampoule. The ampoules were then sealed with a Teflon seal and aluminium cap and lowered to the temperature equilibration position of the channel and data collection initiated. They were maintained in this position for the minimum time required for the recorded heat flow reach zero, approximately 20 minutes. At this time the ampoules were lowered to the measuring position. All the experiments were carried out at 25°C and in order to reduce thermal equilibration time, all materials were pre-stored at 25°C for at least 30 min. Data were recorded using the dedicated software package Digitam 4.1 (Thermometric AB, Järfalla, Sweden). Data analysis was performed using Origin version 7.0 (Microcal Software Inc., USA) for peak area determination.

2.2.2.3.2. ISOTHERMAL PERFUSION MICROCALORIMETRY

A 2250 Micro Reaction RH Perfusion insertion vessel (Thermometric, Järfalla, Sweden) was employed in all experiments for the determination of the heat of crystallisation of fully amorphous and partially amorphous lactose samples. A solid sample (approximately 50 mg, accurately weighed) was loaded into the 4 mL stainless steel ampoule and the unit sealed and lowered into the measuring site of the calorimetric channel. A flow of nitrogen gas at 120 mL/h, created by a pulse free pump action, was passed over the solid sample. The unit controls the relative humidity (RH) of a carrier gas flowing over the sample by proportional mixing of two gas lines (0% and 100% RH) via a 2281 Precision Flow Switching Valve (Thermometric, Järfälla, Sweden). This allows freshly loaded samples to be held under a dry atmosphere, preventing the onset of crystallisation and allowing the apparatus to reach thermal equilibrium before the commencement of data capture. The Flow Switch Valve was continuously heated at 40 ºC by an incorporated heater in order to prevent condensation from forming in the outlet tube from the RH Perfusion unit, which can happen when high humidities are used.

Following the loading of the samples, lowering of the RH perfusion unit to the measuring position of the calorimetric channel was carried out in stages, using a circular clamp to hold the unit in the three equilibration positions illustrated in Figure 2.5 for the periods of time indicated. An empty stainless steel 2 mL reference ampoule was employed for each unit throughout the studies. Each week the humidifier chambers were charged with distilled water (0.5 mL in each) by means of a syringe. Data were recorded at least in triplicate via the dedicated software package Digitam 4.1 (Thermometric AB, Järfalla, Sweden). Peak analysis was performed using Origin (Microcal Software Inc., USA).

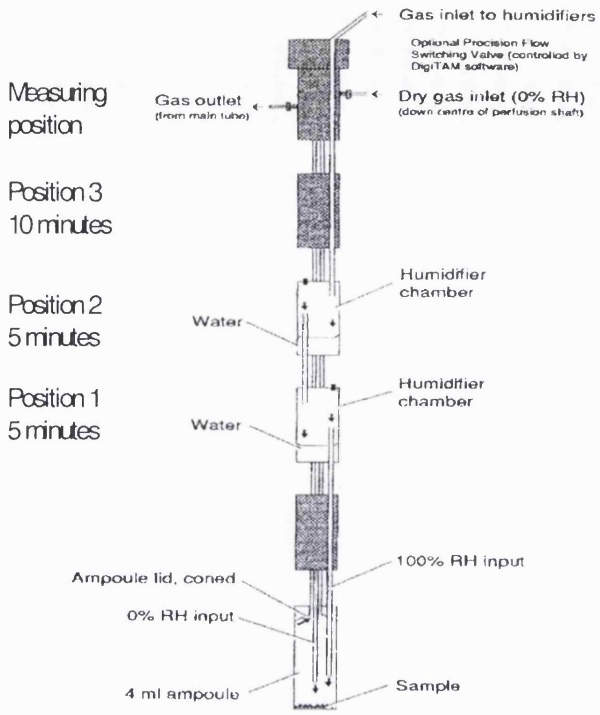

Figure 2.5 *RH Perfusion unit used in the isothermal perfusion microcalorimetry experiments (Thermometric AB).*

2.2.2.4. CALIBRATION

2.2.2.4.1. BATCH ISOTHERMAL MICROCALORIMETRY

A static calibration of each calorimetric channel was carried out each fortnight or whenever the experimental conditions were changed. A static calibration is a calibration where the steady state response in heat flow, when a known electrical calibration power is applied, is adjusted to show the known calibration power by adjusting the Fine knob on the TAM. In order to carry out a static calibration, two sealed glass ampoules containing a mini-hygrostat with the saturated salt solution to be employed in the next set of experiments were used. A range of amplifier settings is available, although in these studies only the 1000 and 3000 μW were used. Both ampoules were lowered into the measuring position of the TAM and data collection initiated. Once a steady baseline was achieved, the signal was adjusted to 0.000 ± 0.100 μW using the zeroing dial. At this point an accurate quantity of heat was supplied to the ampoules by the heater resistor, a power was dissipated and recorded as an exothermic response. This signal was then adjusted to the correct

value (± 0.1 µW) by means of a fine adjusting dial. Once the correct signal was adjusted, the heater was switched off and the signal allowed to return to a baseline. At this point the zero signal was checked and adjusted to 0.000 ± 0.1 µW if necessary using the zeroing dial.

2.2.2.4.2. ISOTHERMAL PERFUSION MICROCALORIMETRY

Calibrations were carried out before each experiment. Once the loaded RH Perfusion unit and reference ampoule had been lowered into the measuring positions of the channel as outlined in Section 2.2.2.3.2 and a baseline was reached, the calibration procedure was carried out exactly as stated in Section 2.2.2.4.1. During calibration RH was maintained at 0%.

2.2.3. SOLUTION CALORIMETRY (AMPOULE BREAKING)

2.2.3.1. INTRODUCTION

The principle of solution calorimetry is to create a liquid system where any small enthalpy change can be detected due to the dispersion or dissolution of a solute as a function of time. The enthalpy of solution of a particular solute, be it liquid or solid, may be affected by minor changes in its physico-chemical properties. The determination of the enthalpy of solution of a certain solute in one of its solvents has been applied pharmaceutically for detection of polymorphism (Souillac et al., 2002), quantification of amorphous content (Hogan and Buckton, 2000; Gao and Rytting, 1997) and to investigate interactions between a drug and a carbohydrate (Chadha et al., 2002), and a protein and a carbohydrate (Souillac et al., 2002).

2.2.3.2. INSTRUMENTATION

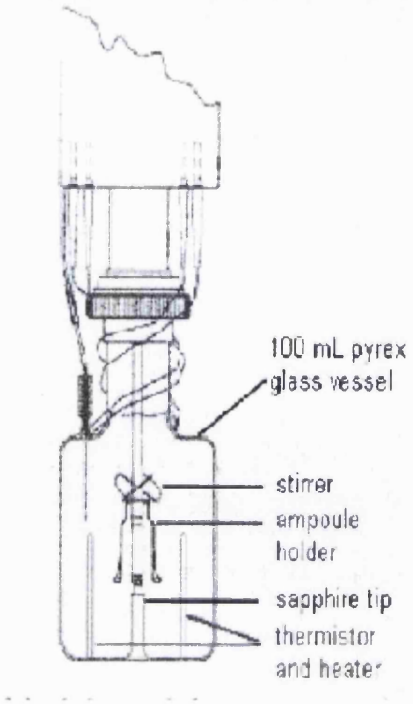

Figure 2.6 *Diagram of the reaction vessel of the Solution Calorimeter, showing the stirrer, ampoule holder, sapphire tip and the thermistor and heater (Thermometric AB).*

A Thermometric 2225 Precision Solution Calorimeter (SolCal) (Thermometric AB, Järfalla, Sweden) was employed throughout this study to determine enthalpies of solution (Figure 2.6). It consists of a calorimetric unit which is connected to a calorimetric cylinder and a Solution Calorimeter Module (Thermometric AB, Järfalla, Sweden) through which communication between the calorimeter and the computer is controlled. The calorimetric unit has two components; a 100 mL thin-walled Pyrex glass reaction vessel and its holder and the stirrer unit. Within the reaction vessel there is a thermistor and a heater, permanently mounted in two pockets descending from the top of the vessel, and a sapphire breaking tip at the bottom of the vessel. The reaction vessel is attached to the holder above it by a large locking nut, which contains the Wheatstone bridge, the electrical component of the calorimeter, which also serves as a thermal insulator. The stirrer system comprises an upper component containing the motor, and the gold stirrer which is also an ampoule holder. The stirrer system is inserted into the reaction vessel during experiments and is mounted on a spring to function as a plugger, the entire system being pushed

down at the point of the experiment where the ampoule is required to be broken in order to initiate the reaction.

The SolCal is a semi-adiabatic calorimeter. In an ideal adiabatic calorimeter there is no heat exchange between the calorimetric vessel and its surroundings (Wadsö and Goldberg, 2001), which is usually attained by placing an adiabatic shield around the vessel. Thus, any change in the heat content of a sample as it reacts causes either a temperature rise (exothermic processes) or fall (endothermic processes) in the vessel. This change in temperature is monitored via a thermistor incorporated in the reaction vessel. The change in heat is, in an ideal case, equal to the product of the temperature change and an experimentally determined proportionality constant (or calibration constant ε, which is the effective heat capacity of the system). The proportionality constant is usually determined by electrical calibration. In practice, true adiabatic conditions are difficult to achieve and there is usually some heat-leak to the surroundings. If this heat-leak is designed into the calorimeter, the system operates under semi-adiabatic (or isoperibol) conditions and corrections must be made in order to return accurate data. Corrections account for the heat generated by stirring the solution, heat generated by the thermistor and heat leakage.

At the start of an experiment the SolCal is held above or below the temperature of its thermostatting bath (typically by up to 200 mK). With time the instrument will approach the temperature of the thermostatting bath; data capture is initiated when this approach becomes exponential (this assumption is a necessary precursor to employing the heat-balance equations used to calculate the heat evolved or absorbed by the system contained within the vessel). Thus, the response due to dissolution, and any electrical calibrations must be performed before the instrument reaches thermal equilibrium with the bath. In practice, this limits the technique to studying events that, ideally, reach completion in less than 30 min. The SolCal typically requires relatively large volumes of sample and solvent (200 mg and 100 mL respectively) because of its measuring sensitivity although, dependent upon the magnitude of the enthalpy change of the system under investigation, some reactions can be investigated with as little as 20 mg of sample.

2.2.3.3. EXPERIMENTAL

All experiments were carried out with the TAM water bath set to 25.00 ± 0.0001 ºC. Samples of 80-120mg were accurately weighted directly into the glass ampoules. Amorphous material was previously desiccated over phosphorous pentoxide until constant weight. The ampoules were then plugged with a silicone bug and double coated with beeswax and inserted into the stirring unit of the instrument. This unit was then inserted into the reaction vessel which had been previously filled with 100 mL of solvent. The two combined units were then plugged to the Solution Calorimeter Module and the Precision Solution Calorimetry software initiated in order to register the initial temperature of the reaction vessel. If this temperature happened to be higher than 25ºC, the vessel was cooled down to a temperature offset of about -1000 µK with an ice box. The combined unit was then lowered into the equilibration position of the solution calorimeter channel of the TAM and heated up to approximately 25 ºC (-200 µK temperature offset). The unit was lowered to the measuring position and allowed to equilibrate further before an electrical calibration was undertaken (parameters were selected in order to mimic the magnitude of the break experiment and to make the calibration signal cross the zero point of the temperature offset scale). Following this, the stirrer unit was lowered in order to break the glass ampoule on the sapphire tip at the bottom of the vessel. Following the break a second temperature calibration was carried out, using the same parameters as the first. Data were collected by the 'Software for Solution Calorimeter' version 1.2 (Thermometric AB, Järfälla, Sweden) in terms of temperature offset from a predefined zero point (actually the temperature of the air bath of the TAM). The same software was used for data analysis and calculation of enthalpy of solution.

2.2.3.4. CALIBRATION AND PERFORMANCE TESTING

Performance of the solution calorimeter was tested by determination of the enthalpy of solution of potassium chloride (sample mass of approximately 100 mg accurately weighted) into 100 mL of purified water. The experiment was carried out as a common break experiment as described in Section 2.2.3.3.1 before each set of experiments.

2.2.4. DIFFERENTIAL SCANNING CALORIMETRY

2.2.4.1. INTRODUCTION

Differential scanning calorimetry (DSC) measures the heat flow into or from a sample as it is heated cooled or maintained at isothermal conditions in relation to an inert reference that is subject to the same thermal treatment. The heat flow is presented in units of watts (W) and is the heat *q* supplied to or given out by the sample per unit time *t*. The heating rate, to which the sample is subjected, is the temperature increase per unit time *t*.

As events that are accompanied by a change in enthalpy or heat capacity can be analysed by DSC, this technique is commonly used to determine enthalpies associated with a transition or reaction, melting and crystallisation temperatures and glass transition temperature. This has been applied for the quantification of amorphous content (Gombás et al., 2002; Saunders et al., 2004; Hurtta and Pitkänen, 2004), detection and characterisation of polymorphs (McGregor et al., 2004) and determination of enthalpy relaxation (Shamblin and Zografi, 1998).

DSCs are generally operated by a controlled programme which changes the temperature on time. These programmes are normally divided according to the heating rate, namely linear heating rate methods (conventional DSC) and those with variable heating rate (periodical or non-periodical) (Sections 2.2.4.1.4. and 2.2.4.1.5). Modulated differential scanning calorimetry is a DSC method that involves the use of a sinusoidal heating signal superimposed on a linear (or isothermal) scan programme.

There are two designs of DSC available, heat flux and power compensated. Both measure the response of a sample to a thermal treatment, but they differ in the way the stimulus is applied and the response measured (Höhne et al., 2003). In a heat flux DSC the sample and reference sides of a single furnace share the same heating and measuring system. The heat flow difference between the sample and the reference sides is proportional to the temperature difference between the sample and the reference. Power compensation DSC involves the application and measurement of power to either the reference or the sample pan in order for the temperature difference between the two to be zero, even when a thermal transition

(a chemical or physical transition that is accompanied of absorption or release of heat) occurs in the sample. The heat flow is given by the following equation:

$$P = I^2 R \qquad \textit{Equation 2.1}$$

where:

- P is the power supplied in order to maintain the pans at the same temperature
- I is the current supplied to the heater of resistance R.

Power compensated instruments use individual reference and sample furnaces of lower mass, which translates into an extremely fast response time (due to less thermal inertia) and the ability to achieve faster heating and cooling rates as compared to the heat flux DSC and provides a much higher resolution (Höhne et al., 2003).

2.2.4.1.1. DETERMINATION OF ENTHALPIES

Integration of the measured curve with the baseline subtracted yields the heat of transition or reaction, however, only if the heat capacity is constant during the transformation, and is given by the following equation:

$$A = k.m.(-\Delta H) \qquad \textit{Equation 2.2}$$

where:

- A is the peak area
- k is the calorimetric sensitivity
- m is the mass of sample
- ΔH is the heat change.

2.2.4.1.2. DETERMINATION OF HEAT CAPACITY

The heat capacity is the amount of heat required to raise the temperature of one gram of material by 1ºC under constant pressure. It can be calculated from the rate of heat input and the resulting heat flow. The following equation can be used to calculate the heat capacity of the sample:

$$Cp = \frac{K\Delta Y}{b} \qquad \text{Equation 2.3}$$

where:

- K is a proportional constant related to the sensitivity of the calorimeter
- ΔY is the difference in baseline
- b is the heating rate.

Basically the heat capacity is given by the heat flow divided by the used heating rate.

2.2.4.1.3. MEASUREMENT OF GLASS TRANSITION

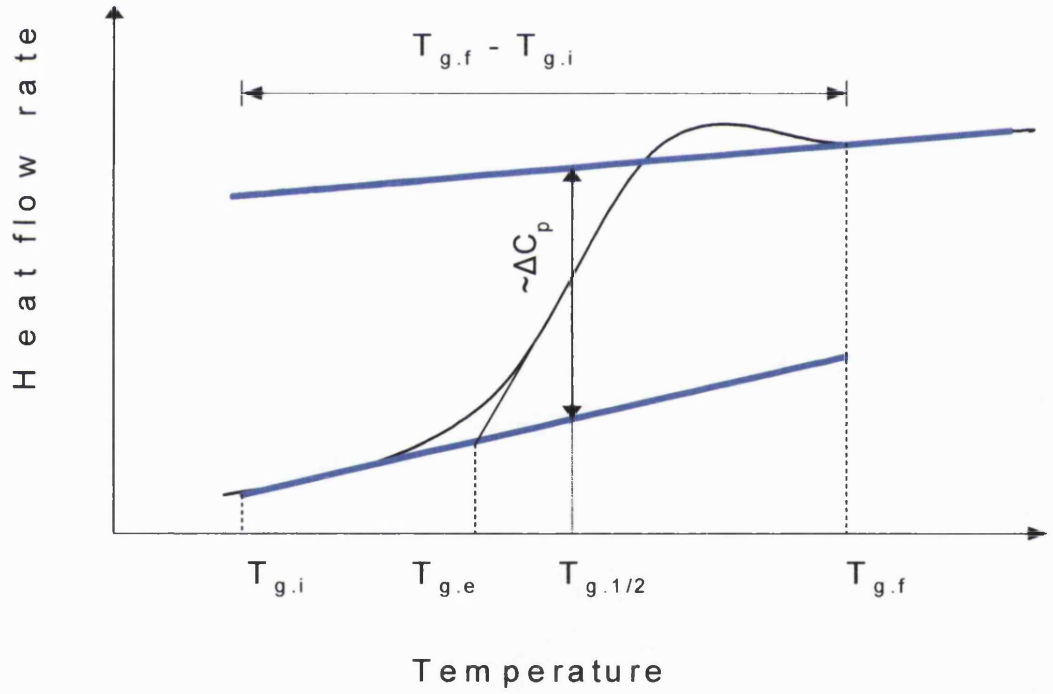

Figure 2.7 *Definition of the most frequently used conventional quantities for characterisation of the glass transition. $T_{g.e}$ is the extrapolated onset temperature, $T_{g1/2}$ is the half-step temperature, ΔC_p is the heat capacity change at the half-step temperature, $T_{g.i}$ and $T_{g.f}$ are the initial and final temperatures of the glass transition, and $T_{g.f}$ - $T_{g.i}$ is the temperature interval of the glass transition. (Adapted from Höhne et al., 2003).*

The glass transition temperature (T_g) value should ideally be specified as the temperature of half vitrification on cooling, which is the temperature at which the heat capacity is halfway between that of the liquid and glassy states (Höhne et al., 2003). On a DSC trace the glass transition is detectable by a step change of the heat capacity on heating or cooling. It is calculated from the extrapolation of the baselines. The T_g is then calculated as the midpoint between the lines. Other parameters can be used to characterise this region. These include $T_{g.i}$, the beginning of the transition; the extrapolated onset $T_{g.e}$; and the endpoint, $T_{g.f}$.

The glass transition is a kinetic event and, consequently, its value depends on the heating and cooling rates; the rate dependence also means that is not possible to compare values obtained by other techniques. However, the true value of the glass transition temperature is only dependent on the conditions of formation, e.g. on the cooling rate of the sample in the case of quenching. Determination of the glass transition on heating will not give the "true" value of the glass transition temperature, which will depend on the underlying heating rate. To overcome this problem, the fictive temperature can be determined, which is independent of the heating rate. The fistive temperature is obtained upon cooling from well above the glass transition region and depend solely on the material. The fictive temperature guives the "true" liquid-glass crossing point (Craig et al, 1999; Yu, 2001).

2.2.4.1.4. HIGH SPEED DIFFERENTIAL SCANNING CALORIMETRY

High Speed DSC consists of the use of linear controlled scan rates at least ten times higher than conventional DSC measurements (10°C/min) up to 500°C/min (cooling or heating) and measuring the real sample temperature (Pijpers et al., 2002). In a High Speed DSC experiment, the heat flow, as a consequence of a thermal event, occurs over a shorter time frame and therefore the thermal event becomes larger. When using conventional DSC, sample changes such as recrystallisation during melting, decomposition after melting or structural changes can occur during the experiment due to the slow heating rate. High Speed DSC can eliminate or reduce these events, allowing an examination of the compound as near to as it already is (snapshot of sample). Other advantages of High Speed DSC include: 1) very high throughput of samples, 2) heat capacity data are more easily obtained since instrument drift is negligible during such rapid measurements, 3) effects of

decomposition are displaced to higher temperature allowing events near to decomposition to be studied more easily, and 4) easier to observe a T_g for a sample as the change of baseline is more pronounced and the duration of T_g is longer. High speed DSC has been recently applied for the detection and quantification of low levels of amorphous content in predominantly crystalline samples (Hurtta and Pitkänen, 2004; Saunders et al., 2004) and to investigate the thermal properties of drug polymorphs (McGregor et al., 2004).

2.2.4.1.5. STEPSCAN DIFFERENTIAL SCANNING CALORIMETRY

StepScan mode of operation is a discontinuous heating or cooling mode. After changing the sample temperature by 1 - 2 K at a certain heating rate (2, 5 or 10 ºC/min, normally) the heat flow rate is allowed to equilibrate again during an isothermal period (20 to 30 s), which results in a sequence of short heat-hold segments over a large temperature range, as represented in (Figure 2.8). This can be done many times in a periodical or non-periodical manner. The StepScan-DSC requires rapid DSC response times, being only feasible with the power compensated DSC, which, as mentioned previously, allows fast heating and thermal equilibration.

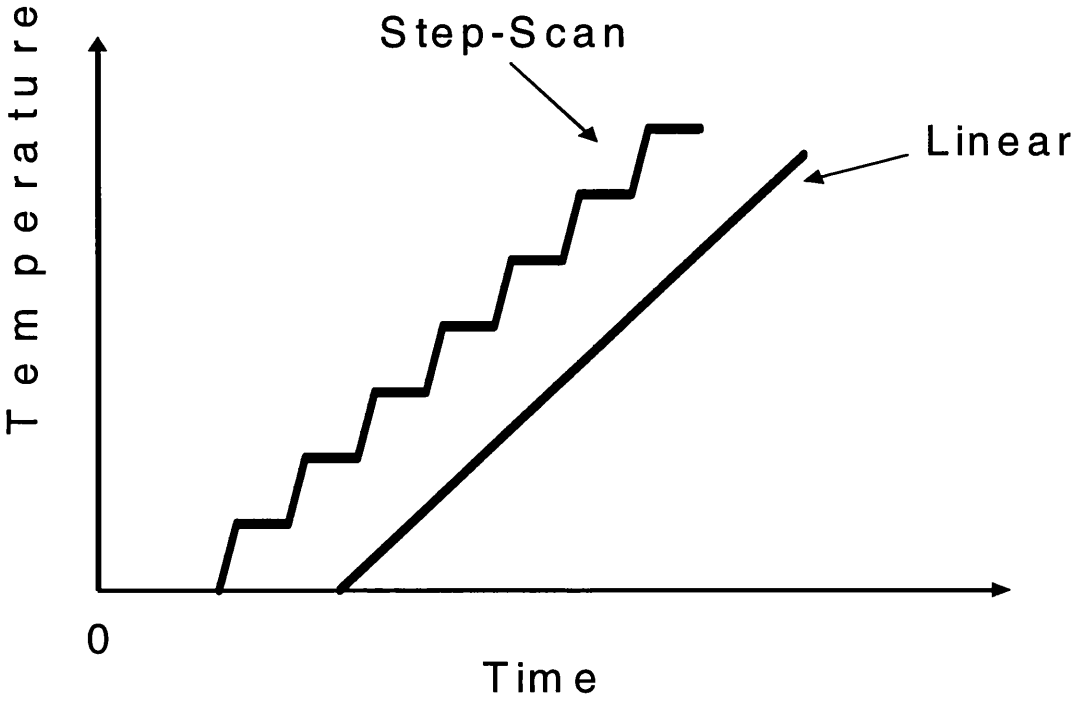

Figure 2.8 *Representation of a StepScan and linear heating mode (Adapted from Höhne et al., 2003).*

Analysis of a StepScan-DSC curve originates two curves, namely the specific heat capacity and the kinetic or isokinetic baseline. The former is simply the interpolated curve through the discrete heat capacity values obtained from the areas A of the peaks caused by the discrete temperature steps ΔT:

$$C_p = \frac{A}{m.\Delta T} \qquad \textit{Equation 2.4}$$

It reflects the sample's vibrational heat capacity, as well as contributions of reactions and transitions like glass transition; the kinetic or irreversible effects are eliminated in this curve.

The isokinetic baseline is the interpolated line through the end point of the isothermals after each temperature step. This equals the zeroline of the DSC but contains all the kinetic or irreversible reaction and transition heat flow rates produced by the sample even in isothermal mode. Within the region of the processes, the shape of this contours curve is highly influenced by the period of time chosen for the equilibration after the temperature step. The longer the isothermal period, the lower is the end value of the heat flow rate caused by reactions or transitions, which usually follow a time law. Thus the great advantage of StepScan DSC is to allow the separation of overlapping events of different nature. For example it allows the separation of T_g from an overlapping event such as enthalpy relaxation, crystallisation or moisture loss.

2.2.4.2. INSTRUMENTATION

A power compensated Pyris 1 DSC (Perkin Elmer Instruments, Beaconsfield, Bucks, UK) fitted with an Intracooler 2P-cooling unit (PerkinElmer Instruments, Beaconsfield, Bucks, UK) was used throughout this study. A schematic representation of a power compensated DSC can be seen in (Figure 2.9). The sample and reference pans are held in a separate, self-contained calorimeter, with its own platinum resistance heater and temperature sensor, which are distributed over the full area of the furnace base and so provide truly distributed heating and temperature monitoring at all points in the furnaces. The micro-furnaces, being made of a platinum alloy, are very inert in order to resist chemical attack. The two calorimeters are mounted on a heat sink, which is kept at a temperature below the

temperature range of the experiment to ensure that the heat could be lost from the calorimeters to the heat sink very quickly.

The power compensated DSC operates in a thermal null state at all times. The thermal-null system works with the aid of two separate control loops that precisely control the temperature of the sample and reference furnaces. The "average temperature control loop" provides power to both furnaces at the pre-determined rate and temperature range, ensuring that both furnaces are always at the same temperature. The "differential temperature control loop" measures any difference in the temperature that occurs between the sample and reference furnaces. In the case of a thermal event occuring in the sample, the temperature of the two furnaces will be different. The platinium resistance thermometer (placed on the base of the furnace, Figure 2.9) sensing any temperature changes retains thermal null, in the form of a power adjustment by the differential temperature control loop to bring the two furnaces back to the same temperature and maintain the temperature at the programmed value. The amount of energy that is provided or removed to maintain the system in equilibrium conditions is directly proportional to the energy changes occurring in the sample. A direct measurement of energy flow is possible with a power compensated DSC. The system is fully controlled by a software that also allows data collection and analysis.

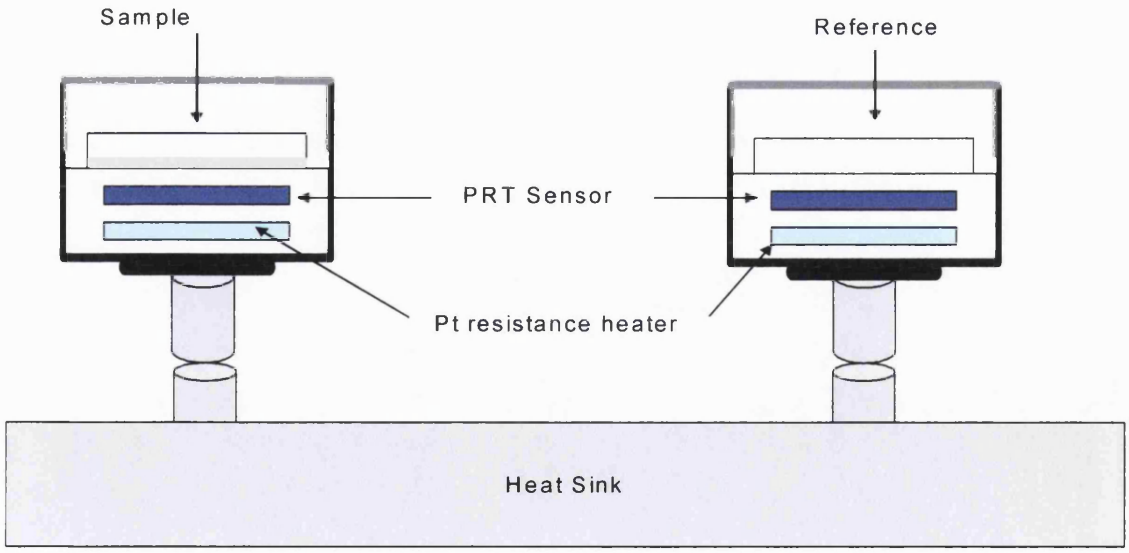

Figure 2.9 *A schematic representation of a power-compensated DSC (Perkin-Elmer), showing the separated sample and reference furnaces, the platinum resistance thermometer (PRT sensor) and the platinum heater.*

2.2.4.3. EXPERIMENTAL

For conventional, High Speed DSC and StepScan samples were accurately weighed on a PerkinElmer autobalance AD-4 (Perkin-Elmer Instruments, Beaconsfield, Bucks, UK) and crimped into non-hermetically sealed aluminium pans (Perkin-Elmer Instruments, Beaconsfield, Bucks, UK). Powder samples were spread in a thin layer on the bottom of the pan, in order to maximise the contact surface between the sample and pan, thus reducing the resistance of sample to heat flow. A blank aluminium pan was used as a reference. A scan of two empty pans was used in order to increase the baseline reproducibility of High Speed DSC experiments. In the High Speed DSC mode, the instrument was used at scanning rates of 200 ºC to scan from 30 ºC to 260 ºC samples (1-2 mg accurately weighted) of pure α-lactose monohydrate and recrystallised 100, 85, 50 and 25 % w/w amorphous lactose. In the SptepScan mode samples of amorphous lactose and indomethacin were analysed using the parameters described in Table 2.3. Data were recorded using the dedicated Pyris software package. Data analysis was performed using the same dedicated Pyris software package and Microcal version 7.0 (Microcal software Inc, USA).

Table 2.3 *Parameters used in the StepScan-DSC method.*

Sample	Initial Temperature (ºC)	Heating Rate (ºC/min)	Step (ºC)	Isothermal (min)	Repeats	Sample mass (mg)
Amorphous lactose	90	2	1	1.0	40	~7
Amorphous Indomethacin	5	5	2	0.5	65	~7

2.2.4.4. CALIBRATION

The instrument was calibrated using high purity standards which have well defined temperature and energy transitions. Indium and lead were the reference materials used to calibrate the instrument. Calibration with both reference materials were carried out before each set of experiments and each time the heating rate was changed or the instrument switched off. The measured temperatures of fusion of both indium and lead and the enthalpy of fusion of indium were recorded and corrected to the literature figures, which are presented in Table 2.4.

Table 2.4 *Temperatures and enthalpy of fusion of the reference materials used to calibrate the Pyris 1 DSC.*

Reference material	Temperature of fusion (Temperature onset ºC)	Enthalpy of fusion (J/g)
Indium	156.6	28.47
Lead	327.46	-

Each calibration was validated by analysing a new scan of a fresh indium sample.

2.2.5. THERMAL GRAVIMETRIC ANALYSIS

2.2.5.1. Introduction

Thermal gravimetric analysis (TGA) is an experimental technique in which the amount and rate of mass change of a substance is measured either as a function of increasing temperature or isothermally as a function of time, in a controlled atmosphere. It can be used to characterize any material that exhibits weight changes when subjected to a certain temperature programme, allowing the detection of decomposition, oxidation, residual solvent and dehydration.

2.2.5.2. Instrumentation

The thermobalance system used in this study was a Thermogravimetric analyser 2950 (TA Instruments, Crawley, UK), which has four major components: 1) the balance, which provides precise measurement of sample weight. 2) the sample platform which loads and unloads the sample to and from the balance. 3) the furnace, which controls the sample atmosphere and temperature. 4) the heat exchanger, which dissipates heat from the furnace

2.2.5.3. Experimental

Recrystallised lactose samples of approximately 8 mg were loaded into tared aluminium open pans (Perkin Elmer Instruments, Beaconsfield, UK). The sample temperature was increased from room temperature to 230 ºC at a heating rate of 10

ºC/min under a nitrogen atmosphere and the weight change with temperature was recorded.

2.2.5.4. Calibration

Two calibration procedures (temperature and weight) were carried out monthly or each time the instrument was switched off. Weight calibrations were performed using 100 mg and 1 g standards. Temperature calibrations were carried out using indium as the reference material.

2.2.6. INVERSE PHASE GAS CHROMATOGRAPHY

2.2.6.1. INTRODUCTION

Inverse gas chromatography (IGC) is a gas phase technique used for the characterisation of powders, fibres and thin films. IGC is the inverse of conventional gas chromatography, in which a series of known solutes in a gas stream (corresponding to the mobile phase) are used to probe a stationary uncharacterised solid phase.

IGC has been used for the assessment of the surface properties of powders. It has been investigated as a means of detecting batch to batch variability (Ticehurst et al., 1996), and ascertaining the effect of milling on the surface energy (Feeley et al., 1998). Newell et al. (2001a) used IGC to investigate the effect of relative humidity on the surface energy of amorphous lactose and the processes of collapse and crystallisation. Recently, Ohta and Buckton (2004a) investigated the effect of relative humidity on the surface energetics of a milled drug.

The characterisation of a material by IGC requires that the material is packed into a glass column. Well-characterised volatile probes pass through the column under the flow of an inert gas; the probes are normally used at low concentration, which is normally referred to as infinite dilution. Under these conditions, minor amounts of gaseous solutes are injected over the material surface, at the limit of detection of the most sensitive detectors. Therefore, the adsorbed probe molecules will be well

The free energy of adsorption (ΔG^0_{ads}), resulting from polar and non-polar interactions, for a gaseous probe molecule under isothermal conditions is given by the following equation:

$$\Delta G^o_{ads} = \Delta G^D_{ads} + \Delta G^{SP}_{ads} \qquad \textit{Equation 2.7}$$

where:

- ΔG^D_{ads} is the non-polar free energy of adsorption
- ΔG^{SP}_{ads} is the acid/base or specific free energy of adsorption.

The free energy of adsorption is related to the retention volume by:

$$\Delta G^0_{ads} = -RT\ln(V_N) + C \qquad \textit{Equation 2.8}$$

where:

- C is a constant that takes into account the weight, surface area and vapour pressure of probes in the gaseous state
- R is the ideal gas constant
- T is absolute temperature.

The free energy of adsorption of an apolar probe can be related to the work of adhesion by:

$$\Delta G^0_{ads} = N.a.W_{ads} \qquad \textit{Equation 2.9}$$

where:

- W_{ads} is the work of adhesion
- N is the Avogadro's number
- a is the surface area of the liquid probe molecules.

Since the work of adhesion (W_{ads}) of an apolar liquid onto a solid can be expressed as the geometric mean of the dispersive components of the solid (γ^d_s) and the liquid (γ^d_1) (Fowkes, 1964):

$$W_{ads} = 2\left(\gamma^d_s . \gamma^d_1\right)^{1/2} \qquad \textit{Equation 2.10}$$

$$W_{ads} = 2\left(\gamma_s^d . \gamma_1^d\right)^{1/2} \qquad \text{Equation 2.10}$$

Combining Equations 2.8, 2.9 and 2.10:

$$RT \ln V_N = 2N.\left(\gamma_s^d\right)^{1/2} .a.\left(\gamma_1^d\right)^{1/2} + C \qquad \text{Equation 2.11}$$

From a plot of the free energy of adsorption of liquid probes onto solids ($RT \ln V_N$) as a function of the product of the alkane surface area and the dispersive component of the alkane surface energy ($a.\left(\gamma_1^d\right)^{1/2}$) a straight line is obtained. The dispersive component of the solid, (γ_s^d) can thus be obtained from the slope of the line. The values of *a* and γ_l^d can be obtained from the literature (Schultz et al, 1987; Nardin and Papirer, 1990).

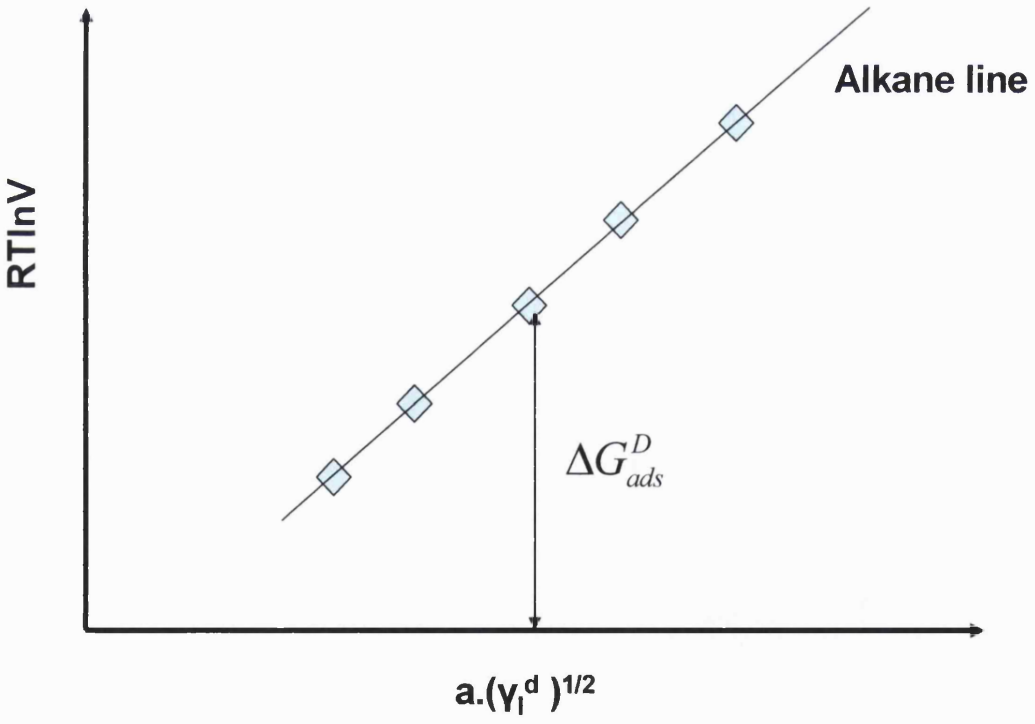

Figure 2.10 *An illustration of the free energy of adsorption of alkanes as a function of* $a.\left(\gamma_1^d\right)^{1/2}$. *The alkanes used were decane (higher* $a.\left(\gamma_1^d\right)^{1/2}$*), nonane, octane, heptane and hexane (lower* $a.\left(\gamma_1^d\right)^{1/2}$*).*

2.2.6.2. INSTRUMENTATION

Experiments were performed using an inverse phase gas chromatograph (Surface Measurement Systems Ltd, London, UK). This system comprises a flow control system, containing a series of mass flow controllers (MKS Instruments, Cheshire, Uk), which prepare a carrier gas stream of mixtures of dry helium and water vapour saturated helium in the required proportions to produce the reference and elutant gas mixtures with the desired relative humidity. For the purpose of performing elution experiments, the system is provided with an automated injection valve capable of injecting 250 µL of the elution mixture (probe) into the gas flow which will transported through the columns to the detectors. A gas chromatography oven (Agilent 6890 series, West Lothian, UK) was used to control the temperature of the liquid probes reservoir, from where the elutant vapours were generated.

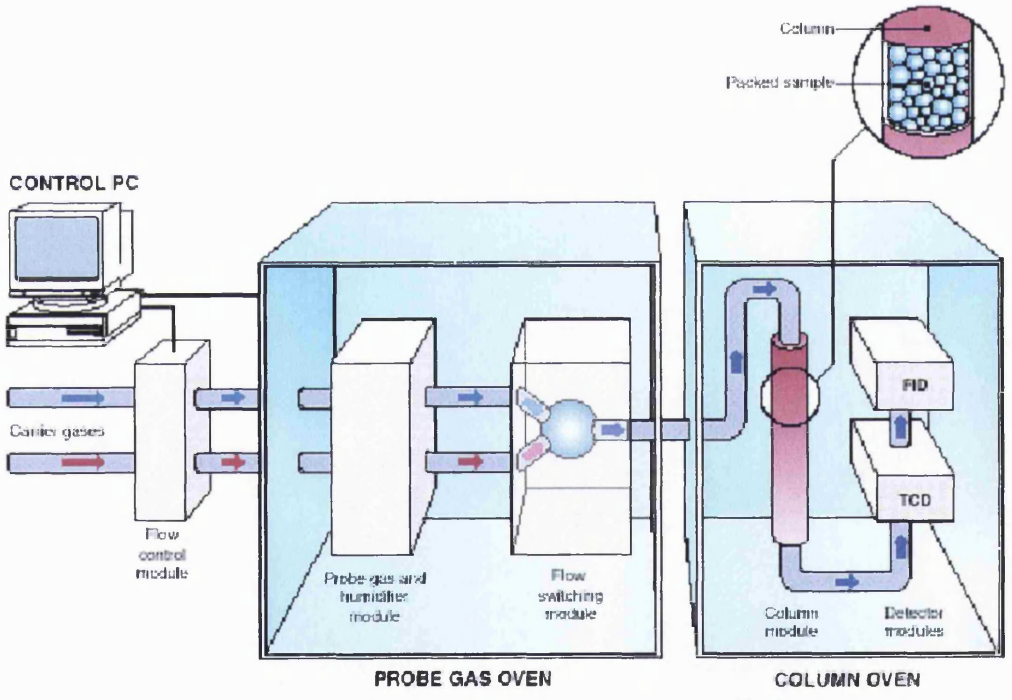

Figure 2.11 *Diagram of the Inverse Gas Chromatograph (Surface Measurement Systems).*

The 6890 GC data acquisition system was used to record data from the flame ionisation detector (FID) and the thermal conductivity detector (TCD) which are positioned in series with the column outlet. The FID allows sensitive analysis of the eluting organic vapours, while the TCD detects the eluting gas humidity levels. Differential pressure transducers (Baratron, MKS, Cheshire, UK) were used to

measure the pressure drop along the column. A separate oven was used to control the sample column temperature, which can be set between room temperature and 390K. Straight glass tube columns employed in this study were 6 mm outer diameter, 3 mm internal diameter and 300 mm long. These columns were treated with dimethyldichlorosilane solution (DMCS, Repelcote®, BDH) and washed thoroughly with absolute alcohol and purified water to passivate the glass surface. DMCS silanised glass wool was used to hold the powdered samples in place.

2.2.6.3. EXPERIMENTAL

Each passivated glass column was packed with 150 – 200 mg of accurately weighed powder sample. For this, a small quantity of silanised glass wool (DMCS) was introduced into one end of the column to plug it. The sample was packed by vertical tapping for at least 15 minutes or until there were no visual cracks, hollows or channels in the body of the powder.

After being inserted into the oven and prior to analysis, the columns were subjected to a conditioning cycle. The column was left under 0% relative humidity and 303 K for a minimum of 5 hours, whilst the detector signals were monitored to ensure that the sample was stable. Vapours (3 % v/v) for retention times analysis and calculations were: decane (Acros Organics, HPLC grade), nonane (Aldrich, HPLC grade), octane (Lancaster, HPLC grade), heptane (Fisher, HPLC grade), hexane (Sigma, HPLC grade). Methane (BOC, research grade) was injected as the non-interacting reference probe. The dispersive surface energy was determined by injecting a series of alkanes, from decane to hexane. The columns were mantained at 303 K and 0 % relative humidity through out the experiments. A helium gas flow was used in all the experiments at 10 mL/min. The entire system was fully automated by the dedicated software SMS iGC Controller v1.5 (Surface Measurment Systems, London, UK) and the data analysed using the SMS iGC Analysis macros version 1.2 (Surface Measurment Systems, London, UK).

2.2.6.4. Calibration

There was no reference material to calibrate the system with. However checks with poly methyl methacrylate (dispersive surface energy of 35-40 mJ/m^2) were

conducted to ensure dispersive surface energy component measured was within that stated by the manufacturer.

2.2.7. GAS CHROMATOGRAPHY

2.2.7.1. INTRODUCTION

Gas chromatography is a separation technique whereby a vaporised sample is carried by a flow stream of an inert gas through a column which is either filled with fine particles or is wall-coated with a low-volatility liquid (Swarbrick et al., 2001). This technique can be used for the analysis of gas, liquid and solid samples, providing that the latter two can be thermally vaporised without decomposition. It has been widely used for identification, separation and quantification of components in a mixture.

2.2.7.2. INSTRUMENTATION

A CP9001 Gas Chromatograph (Varian-Chrompack, Oxford, UK) was used in this study to determine the anomeric composition of different batches of amorphous and crystalline lactose. The instrument was fitted with a CPsil-5CB capillary column (0.25 mm (ID) x 10 m length) (Varian-Chrompack, Oxford, UK) and a flame ionisation detector.

A schematic representation of a gas chromatographer is shown in Figure 2.12, where its basic main components are represented. These consist of the sample injection system, the chromatographic column, the thermal compartment, the detector and a data collector system. A system to control the flow and pressure of the carrier gas is also present in a gas chromatographer.

A stream of carrier gas flows continuously through the column. The sample is injected into the carrier gas through the injection system, where the sample must be instantaneously vaporised and carried into the column by the carrier gas. The chromatography column is housed in an oven, and it can be submitted to a linear or nonlinear temperature program. The sample components are then moved towards

the column outlet by the carrier gas. The separation of the sample components in the chromatography column results from differences in the multiple forces by which the column materials tend to retain each of the components. The retention process is governed by the temperature, gas flow rate and physicochemical properties of the materials being separated and those of the stationary and mobile phase. The separation can occur by adsorption, solubility, chemical bonding or polarity, depending on both component and stationary phase properties. All the sample components pass through the column at varying speeds and emerge in the inverse order of their retention times. After emerging at the column outlet, the gaseous phase reaches the detector. There are a few types of detectors and the choice is determined by the type of column used. The flame ionisation detector (FID) consists of a burner and an electrometer system. As column elluent enters the FID through the burner and it is burned, a current proportional to the number of ions or electrons formed is produced and detected by the electrometer system.

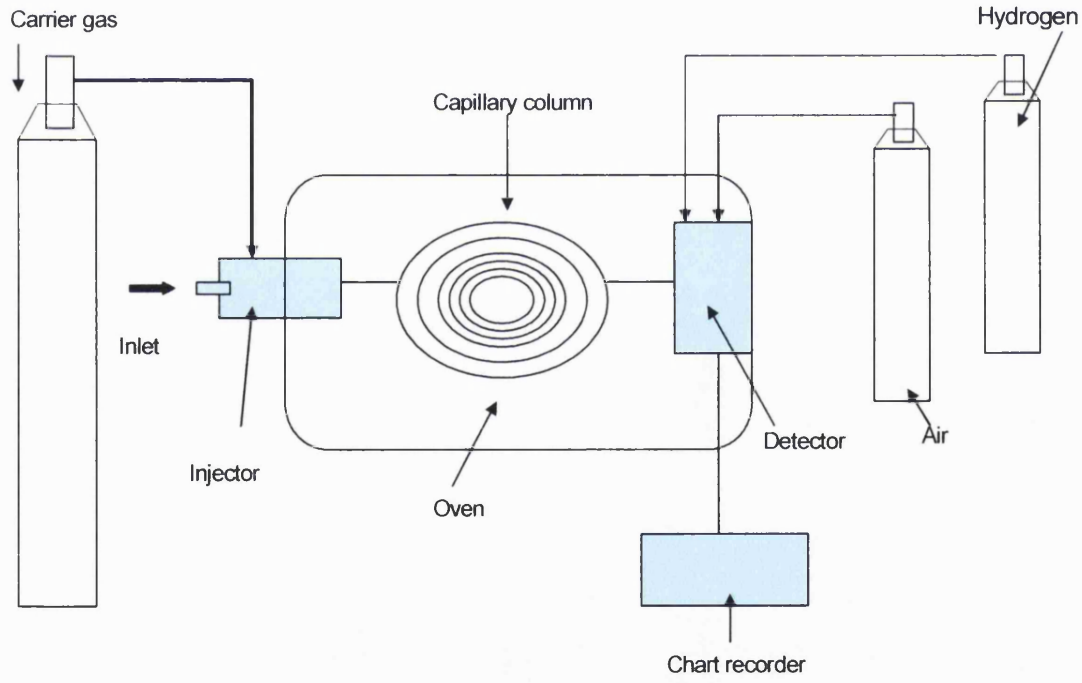

Figure 2.10 *A schematic representation of a Gas Chromatograph (Adapted from Kline and Soine, 1981).*

2.2.7.3. EXPERIMENTAL

2.2.7.3.1. SAMPLE PREPARATION

Amorphous lactose, crystalline β–lactose and α-lactose monohydrate and recrystallised partially amorphous lactose samples were derivatised prior to GC analysis (Dwivedi et al., 1989). Through this reaction, samples were simultaneously solubilised for GC analysis and derivatised in order to maintain their original anomeric composition. The derivatisation mixture consisted of trimethilsilylimidazole (22%), dimethyl sulphoxide (19.5%) and pyridine (58.5%); the dimethyl sulphoxide helps to solubilise the sample and the combination of pyridine and trimethilsilylimidazole guarantees a fast derivatisation without causing further mutarotation of the sample. 1mg of dry sample was dissolved in 2.25 ml of a derivatisation mixture and vortexed for until complete dissolution. The samples were kept at room temperature for 20 minutes before derivatisation was complete.

2.2.7.3.2. METHODOLOGY

The chromatographic measurements were carried out according to the conditions tabulated below (Table 2.5).

Table 2.5 *Operating parameters for the gas chromatographic analysis of lactose samples.*

Injector port temperature (ºC)	Detector temperature (ºC)	Column inlet temperatur e (ºC)	Column outlet temperatur e (ºC)	Column heating rate (ºC/min)	Carrier gas (Heliu m) (KPa)	Sample size (µL)
300	250	150	260	10	55	1

The chromatograms were recorded and analysed for peak area calculation by means of the dedicated software Prime (HPLC Technology Ltd, Herts, UK).

2.2.8. X-Ray Powder Diffraction

2.2.8.1. INTRODUCTION

As each form of a compound has a defined X-ray spectrum, X-ray powder diffraction (XRPD) is recognised as a powerful technique for the identification of crystalline phases, identification and quantification of polymorphs (Haque and Roos, 2005b) and it can assess quantitatively mixtures of different forms through a range of approaches (Stephenson et al., 2001). The relatively random arrangement of molecules in noncrystalline substances makes them poor coherent scatterers of X-rays, resulting in broad, diffuse maxima in diffraction patterns. The X-ray patterns are quite different from crystalline specimens, which give sharply defined diffraction patterns. This makes X-ray a useful technique for detection and quantification of amorphous material (Chen et al., 2001). The limit of quantification of amorphous material by XRPD is approximately 10%. However, it is widely used to confirm the crystalline/amorphous nature of a sample.

2.2.8.2. INSTRUMENTATION

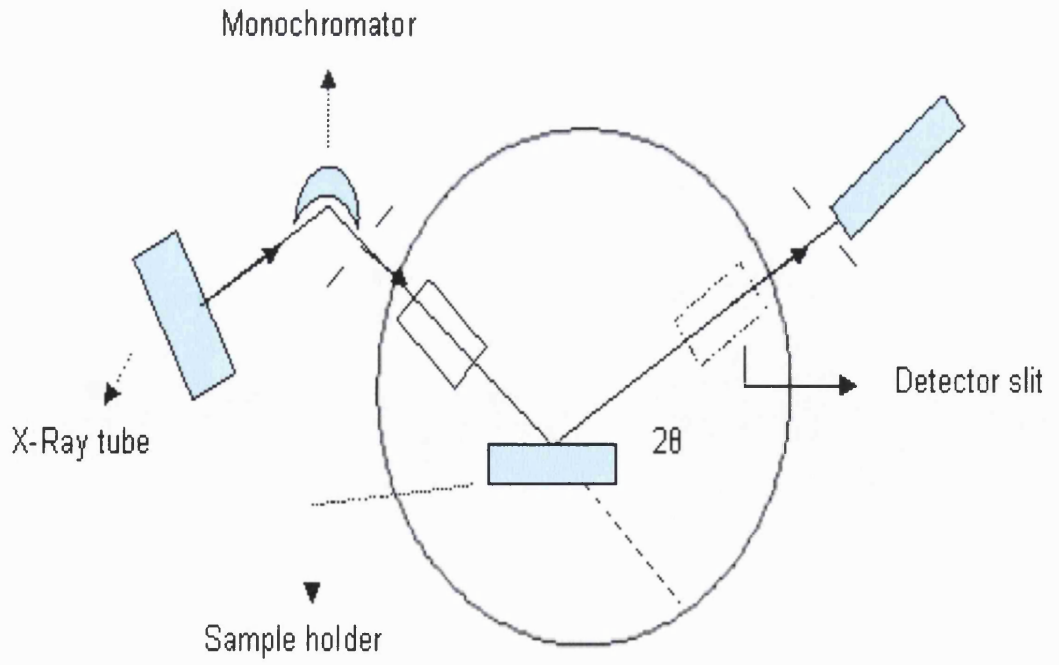

Figure 2.13 *A schematic representation of a x-Ray powder difractometer (Adapted from Byrn et al., 1999).*

X-rays are a type of electromagnetic radiation with a wavelength ranging from about 10^{-5} to 10^{3} Å. They are a by-product of the sudden deceleration of electrons that had previously been accelerated to a high velocity. Within the X-ray tube, electrons emitted by the cathode are accelerated through a high-voltage field and a copper anode is bombarded at high potential. On impact the electrons transfer their kinetic energy to the copper atoms, producing photon X-rays. The x-rays then pass out the tube via a beryllium window and are focused by a series of divergence slits within the goniometer on to the flat surface of the sample. When an X-ray beam encounters a crystal, most of the X-rays will destructively interfere with each other and cancel each other out, but under specific conditions they constructively interfere and reinforce one another. The rays diffracted at Bragg angle 2θ constructively interfere and converge approximated to a single line, where a receiving slit is placed. The X-ray passes through the receiving slit onto a second parallel slit system, a scatter slit and a monochomator. Finally the beam reaches the detector where the signal provides an output of intensity vs scan angle 2θ.

A Philips PW3710 X-ray powder diffractometer (Philips, Cambridge, UK) was used in all studies. The Cu anode tube was operated at 45 kV and 30 mA in combination with a Ni filter to give monochromatic Cu K_{α} X-rays.

2.2.8.3. EXPERIMENTAL

X-ray powder diffraction was used throughout this study to confirm the amorphous nature of spray dried lactose batches and quench-cooled indomethacin. Samples were carefully filled into the 27 mm diameter cavity of the sample holder. The baseplate of the sample holder was gently tapped on the bench top to allow the powder to settle. Excess powder was removed and the surface of the sample levelled and smoothed using a glass block. Any excess of sample surrounding the circular sample holder cavity was removed using a piece of paper. The powder bed achieved a measured depth of approximately 2 mm.

The sample holder was loaded into the diffractometer and samples were scanned at 45 kV and 30 mA. The start angle (2θ) was 5º and end angle 40º. The scan speed was 0.05º 20/s. Method set up and data collection was achieved by means of the dedicated software XPert Data Collector (Pananalytical, Almelo, Netherlands).

2.2.9. PREPARATION OF SATURATED SALT SOLUTIONS

2.2.9.1. INTRODUCTION

Relative humidity may be defined as the percentage of the vapour pressure of water vapour in the air over the vapour pressure of water vapour in air saturated at the same temperature. Saturated salt solutions can be used to maintain a specific relative humidity in closed chambers (Nyqvist, 1983).

2.2.9.2. EXPERIMENTAL

Saturated salt solutions of potassium sulphate (provides a 97% RH at 25 ºC) (Nyqvist, 1983) and magnesium nitrate (provides a 53% RH at 25 ºC) (Nyqvist, 1983) were prepared by dissolving a quantity of salt in distilled water, ensuring that an excess of salt remained at the bottom of the container. The quantity of salt used depended on the solubility of the salt and the volume of water used. The solutions were heated to 45 ºC and the final solution stirred for 20 minutes. They were then slowly cooled whilst continuing to be stirred, making sure that by the time they reached 25 ºC, crystals of the salt were in solution. Storage of these solutions was at the temperature they were to be used, usually 25 ºC.

2.2.10. PREPARATION OF SAMPLES

Amorphous lactose was prepared by spray drying as described in Section 2.2.1.3 and stored in an evacuated desiccator over phosphorous pentoxide at room temperature. The preparation of partially amorphous lactose samples is described in the respective results chapters.

Amorphous indomethacin was prepared by quench-cooling. A quantity of indomethacin was melted in a porcelain pot on the Bunsen flame and once melted, immediately immersed into liquid nitrogen for rapid cooling. Once the liquid nitrogen was evaporated it was stored in an evacuated desiccator over phosphorous pentoxide at room temperature.

CHAPTER THREE

AN INVESTIGATION OF THE USE OF ISOTHERMAL MICALORIMETRY FOR QUANTIFICATION OF AMORPHOUS CONTENT IN LACTOSE

ASSESSMENT OF THE CRYSTALLISATION BEHAVIOUR OF AMORPHOUS LACTOSE, AS IT IS INDUCED DURING AN ISOTHERMAL MICROCALORIMETRY EXPERIMENT

3.1. INTRODUCTION

The impact that the degree of crystallinity of drugs and excipients might have on drug formulations has already been discussed at length (Chapter 1). The presence of amorphous material can affect both the physical-chemical stability (Pikal et al., 1978) and the performance of the system during product manufacture and use (Inghelbrecht and Remon, 1998; Harjunen et al., 2002). Amorphous forms of the drug can intentionally be used to increase the dissolution rate of poorly soluble drugs (Ohara et al., 2005). On the other hand mechanical processing of solid-state pharmaceuticals may cause accidental formation of amorphous regions in what was previously an entirely crystalline material (Ohta and Buckton, 2004a). In this second case, despite the amorphous material occupying only a few percent of the bulk mass, its location on the particle surfaces gives it a disproportionate control over the surface interactions of what is a predominantly crystalline powder (Newell et al., 2001a; Newell et al., 2001b). In both situations, the amorphous content may decrease the physical and chemical stability of the formulation. The reversion of the unstable amorphous material to the lower energy crystalline state (Yoshioka et al., 1994) can have a dramatic effect due to particle aggregation (Yoshioka et al., 1996; Duddu et al., 1997) or formation polymorphs with different properties (Andronis et al., 1997). Furthermore, the Food and Drug Administration's (FDA) drug substance guideline states that "appropriate" analytical procedures should be used to detect polymorphic, hydrated, or amorphous forms of the drug substance (Byrn et al., 1995). Consequently, the detection, quantification, characterisation and management of amorphous contents, particularly small amorphous contents, play a central role in the implementation process control during development and manufacturing stages (Byrn et al., 1995). The development of techniques that allow a quantitative determination of low (~1% w/w) amorphous contents is therefore of considerable importance and have long been investigated.

The transition of a material from the unstable amorphous form to the crystalline form is accompanied by a heat exchange that can be followed by isothermal microcalorimetry. Isothermal Microcalorimetry has long been applied for the quantification of amorphous content of excipients (Briggner et al., 1994; Sebhatu et al., 1994a; Buckton, 1995a; Kawakami et al., 2002; Al-Hadithi et al., 2004; Dilworth et al., 2004) and drugs (Ahmed et al., 1996; Ohta et al., 2000; Kawakami et al., 2002; Mackin et al., 2002; Samra and Buckton, 2004; Verumi et al., 2004). A common approach to crystallise partially amorphous samples in an isothermal

calorimeter is to use an elevated relative humidity (maintained through the use of a mini-hygrostat located in the sample ampoule as described in Section 2.2.2.3.1, a methodology commonly known as batch isothermal microcalorimetry. The sample absorbs moisture, is plasticised and, after a time period that varies in proportion to the amorphous content and RH selected, crystallises. The amorphous content is determined from the linear relation between the heat output of crystallisation and physical mixtures of known amorphous content; the higher the amorphous content, the higher the heat output of crystallisation. In the 1990's a series of studies recognised this methodology appropriate to quantify amorphous content of lactose down to at least 1% (Briggner et al., 1994) or 2% (Sebhatu et al., 1994a). Batch isothermal microcalorimetry also proved useful for the quantification of amorphous content of hydrophobic drugs (Ahmed et al., 1996; Samra and Buckton, 2004). Batch isothermal microcalorimetry can be used for the quantification of amorphous content of both hydrophilic and hydrophobic materials, provided that a vapour phase exists which can induce crystallisation. It was recently demonstrated that batch isothermal microcalorimetry was suitable for the quantification of amorphous content in mixed systems (amorphous trehalose with crystalline lactose) (Al-Hadithi et al., 2004) down to 1% amorphous trehalose. However, difficulties might be found when trying to apply IM for the quantification of amorphous content in a mixed system containing more than one amorphous phase (Al-Hadithi et al., 2004).

3.2. AIMS OF THE STUDY

This study aimed to investigate the use of isothermal microcalorimetry for the quantification of amorphous content in lactose. A further aim of this study was to characterise the crystallisation of amorphous lactose, as induced during an isothermal microcalorimetry experiment.

3.3. EXPERIMENTAL

3.3.1. PREPARATION OF AMORPHOUS LACTOSE

Amorphous lactose was prepared by spray drying from a 10% (w/w) lactose solution, previously equilibrated at 25 °C as described in Section 2.2.1.3.

Confirmation of the amorphous nature was obtained from XRPD as outlined in Section 2.2.8.3.

3.3.2. PREPARATION OF PARTIALLY AMORPHOUS LACTOSE SAMPLES

Partially amorphous samples (5, 10, 25, 50, 75, 80, 90 and 95%) were prepared by weighing proportional quantities of sieved (<425 µm) of amorphous and α-lactose monohydrate (~15 g in a 30 mL amber glass container) and mixing in a Turbula mixer for 20 min at

3.3.3. BATCH ISOTHERMAL MICROCALORIMETRY

Calorimetric data were recorded using a 2277 Thermal Activity Monitor (TAM, Thermometric AB, Järfalla, Sweden); which is described in Section 2.2.2.2. Samples (~30 mg) were weighed into a 3 mL glass ampoule. Both reference and sample ampoules contained a mini-hygrostat containing a 100 µL of saturated salt solution ($Mg(NO_3)_2.6H_2O$ which maintains an RH of 53% at 25 °C. All experiments were carried out at 25 °C as described in Section 2.2.2.3.1. The instrument was calibrated periodically as described in Section 2.2.2.4.1. Data were collected via Digitam 4.1 (Thermometric AB, Järfalla, Sweden) and analysed using Origin 7.0 (Microcal software Inc., USA).

3.3.4. DIFFERENTIAL SCANNING CALORIMETRY

DSC data were recorded using a Pyris 1 (Perkin-Elmer, Beaconsfield, UK) (Section 2.2.4.2). Samples (~1-2 mg) of crystalline α-lactose monohydrate and recrystallised lactose samples were crimped into non-hermetically aluminium pans and subjected to a scanning rate of 200 °C/min as described in Section 2.2.4.3. A blank aluminium pan was used as a reference. Calibrations were carried out using indium and lead as standards as described in Section 2.2.4.4. Data were collected via the dedicated Pyris-1 software (Perkin-Elmer Instruments, Beaconsfield, UK) and analysed using Pyris-1 (Perkin-Elmer Instruments, Beaconsfield, UK) and Origin 7.0 (Microcal software Inc, USA).

3.3.5. THERMAL GRAVIMETRIC ANALYSIS

Thermal gravimetric analysis experiments were carried out using a Thermogravimetric analyser 2950 (TA Instruments, Crawley, UK), which is briefly described in Section 2.2.5.2. Recrystallised amorphous lactose samples (~ 8 mg) were analysed as described in Section 2.2.5.3. The thermogravimetric analyser was periodically calibrated as described in Section 2.2.5.4.

3.4. RESULTS AND DISCUSSION

3.4.1. CRYSTALLISATION OF AMORPHOUS LACTOSE; PROCESSES DESCRIBED IN THE LITERATURE.

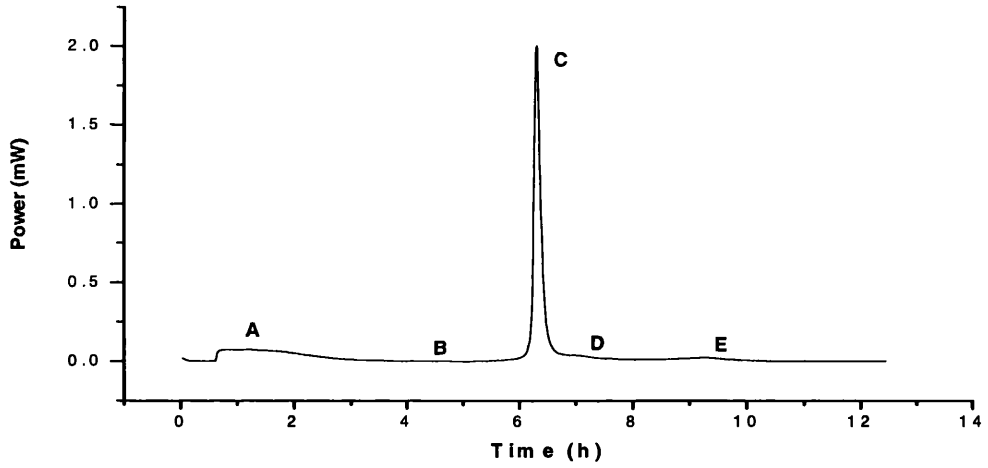

Figure 3.1 *The typical crystallisation response for 30 mg of 100% amorphous lactose at 53% RH and 25 °C, as recorded by isothermal microcalorimetry.*

A typical thermal response generated by amorphous lactose (30 mg) under 53% RH is presented in Figure 4.1. The response is a complex event, comprising a number of exo- and endothermic processes and the microcalorimeter records only the balance of these events, originating several distinct regions denoted A-E. An initial sharp exotherm, which results from the lowering of the ampoules and does not form part of the thermal response of the sample, is followed by a more prolonged exotherm lasting for more than 2h. This results from evaporation of water from the

hydrating reservoir in order for the atmosphere in the ampoule to reach the desired RH (endothermic), wetting of the lactose as it absorbs water (exothermic) (Sebhatu et al., 1994a; Ahmed et al., 1995; Darcy and Buckton, 1998) and possibly structural collapse of the amorphous lactose following absorption of the water (Buckton and Darcy, 1996). It is possible that the rates of water evaporation and water sorption are out of balance which explains the existence of region A, where absorption predominates. The decay of peak A may be attributed to a reduction in the magnitude of the exothermic water sorption, an increase in evaporation from the hygrostat or, most likely, a combination of both. After the exothermic peak A, a flat baseline can be seen (region B). This response can be attributed to endothermic vaporisation of the salt solution and the exothermic vapour sorption by the sample being equal and opposite in magnitude and therefore cancelling each other out (Angberg et al., 1992a). Dilworth et al., (2004) observed an endothermic zone B for the response of amorphous lactose at 75% RH, which was attributed to the predominance of evaporation (endothermic process) over water sorption by the sample (exothermic). The duration of region B has been shown to be related to the mass of amorphous material, the RH generated by the saturated salt solution and the surface area of the mini-hygrostat (Briggner et al., 1994). In the work described here, an equivalent saturated salt solution is placed in the sample and reference of the microcalorimeter. This will blank out some of the response associated with generating water vapour in the sealed ampoules; however, the presence of amorphous lactose will cause a greater generation of water vapour in the test side as the lactose effectively desiccates the air space. It is clear therefore that the "blank" in the reference side is not a complete blank. It is also clear that the data generated using this methodology will differ from those obtained when an empty ampoule is used as the reference. At approximately 6 h the sample crystallises (region C), generating a peak that indicates a cooperative process of high heat output, which has occurred over a short period of time (Briggner et al., 1994). Previous work has shown that samples removed immediately after this exothermic response are crystalline (Briggner et al., 1994) and physical inspection of the sample reveals a hard, fused, solid mass instead of a free-flowing powder. It has been observed that following crystallisation, carbohydrates expel the previously absorbed plasticising water (Makower and Dye, 1956); in the case of lactose, some of the sorbed water will cause some of the sample to crystallise into the monohydrate, the remainder will be desorbed. According to Buckton and Darcy (1995) at high relative humidities, the water vapour starts to be absorbed into the upper layers of the amorphous lactose, and is then transferred away generating a

concentration through the entire sample. As the water content increases in the lower layers, the rate of water absorption at the surface becomes more rapid than the rate of water transfer to the lower layers. Consequently, the surface saturates of water and starts to crystallise and liberates a great amount of water vapour, which is sufficient to saturate the lower layers of sample which will also crystallise. While crystallisation will be an exothermic event, the expulsion of water will be endothermic and the calorimetric data (region C) represents the balance of these heat changes. The crystallisation peak (C) shows a shoulder (D). Sebhatu et al. (1994a) suggested that this shoulder should not be attributed to the expulsion of water following crystallisation since that event should be cancelled out by the exothermic condensation of that water back into the mini-hygrostat. Sebhatu et al. (1994a) suggested that the shoulder represented incorporation of water into the anhydrous α-lactose formed immediately after crystallisation to form α-lactose-monohydrate. This event was also attributed to mutarotation of β- to α-lactose and water incorporation into α-lactose to form α-lactose monohydrate (Briggner et al., 1994); processes that occur simultaneously and are accompanied by a heat loss (exothermic) (Angberg et al., 1992a). Angberg et al. (1991) showed that such mutarotation can occur at humidities lower than 94% RH, although it occurs to a higher extent at relative humidities above 94%, which could possibly be generated as large quantities of water desorbing from the crystallising lactose, subjecting the sample to a high enough relative humidity to cause mutarotation. Finally, a long and slow exothermic process is observed after crystallisation (region E). Dilworth et al. (2004), when exposing amorphous lactose to 75% RH described a similar region which was attributed to water movements within the ampoule, either between the sample and the hydrating reservoir or within the sample itself, and to β- to α-lactose mutarotation and/or water incorporation. While for amorphous lactose at 75% RH such exothermic region appeared coupled together with regions C and D, for lactose exposed to 53% RH such exothermic event occurs later and is separated from regions C and D.

From this description it is clear that the crystallisation of lactose is a complex event, comprising a number of simultaneous exo- and endothermic processes, and that the calorimeter records only the balance of these events. Using the integration methodology proposed by Dilworth et al. (2004) (i.e. integrating the area under the curve between the end of the first exothermic peak to the final baseline from y = 0 using Origin Microcal software), an enthalpy of crystallisation of 57.35 ± 2.4 J/g (n=8) was determined, which is in very good agreement with the enthalpy of

crystallisation of lactose determined by Dilworth et al., (2004) (53.4 J/g). Enthalpies of crystallisation of amorphous lactose ranging from 32 to 57 J/g have been reported in the literature (Sebhatu et al., 1994a; Briggner et al., 1994; Chidavaenzi et al., 1997; Darcy and Buckton, 1998 and Dilworth et al., 2004), most probably as a result of different experimental conditions used and differences in the section of the power-time response that was integrated.

3.4.2. Quantification of the amorphous content in partially crystalline lactose samples by Isothermal Microcalorimetry

Figure 3.2 shows the calorimetric response of 10 and 25% amorphous lactose samples when exposed to 53% RH at 25 °C, and it can clearly be seen that the crystallisation response of partially amorphous samples is much smaller and occurs over a shorter period of time than that of a fully amorphous sample (because less water needs to be absorbed to initiate crystallisation). The multi-peak response observed for the 10% amorphous sample is a characteristic of a lower amorphous content sample (Buckton and Darcy, 1999).

Isothermal microcalorimetry data can be used to quantify amorphous contents because it is assumed that there is a linear relationship between amorphous content and the measured heat of crystallisation. In the present study samples from 10 to 95 % amorphous lactose were crystallised at 53% RH, since previous data have shown that this provides sufficient water to induce crystallisation and generates a sufficiently long lag-time, which avoids the loss of the starting point of the calorimetric response commonly verified when higher RH are used (Briggner et al., 1994).

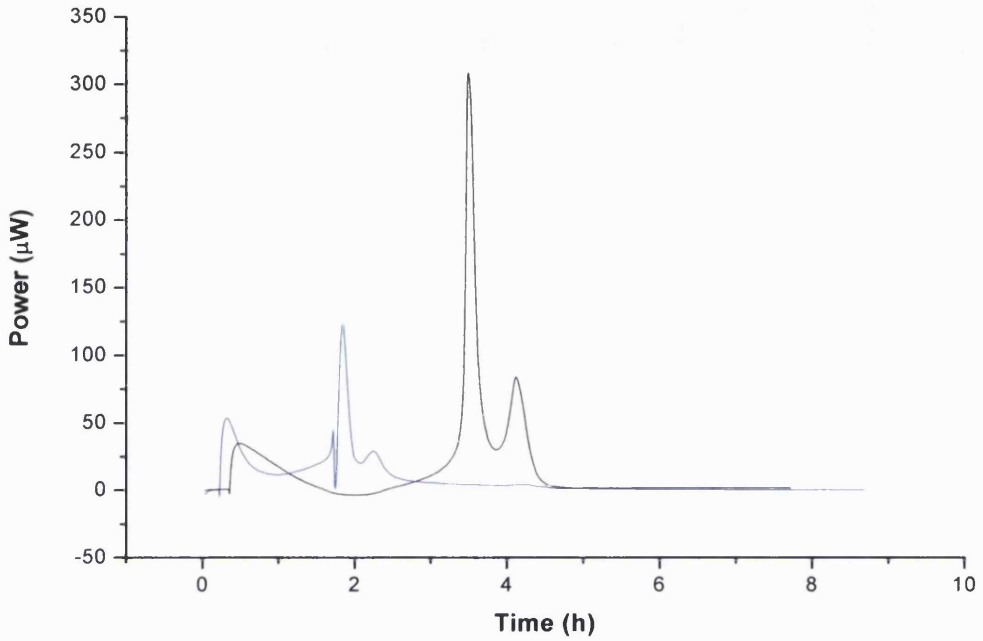

Figure 0.2 *A typical crystallisation response for 30 mg of a 10% (blue) and 25% (black) amorphous lactose sample at 53% RH and 25 °C, as recorded by Isothermal Microcalorimetry.*

Recent studies of lactose crystallisation using electro-chemical atomic force microscope (EC-AFM) have suggested that samples maintained under an RH of 58% do not completely crystallise (Price and Young, 2004) because primary nucleation cannot occur at such low RH; the same study suggested that complete crystallisation requires an RH of 94% or greater. In order to investigate the presence of residual amorphous material in the crystallised samples, all samples removed from the TAM were analysed by Hyper-DSC. Hyper-DSC has proved efficient in detecting small amorphous content by detecting the heat capacity change at T_g of the partially amorphous samples (Gabbott et al., 2003; Saunders et al., 2004). Figure 3.3 represents a typical DSC trace for the crystallised samples, showing the loss of hydrate water (peak A) and the melting peaks of α- and β-lactose (peaks B and C). However, no T_g was onserved for the crystallised samples; the glass transition temperature of lactose is normally located around 114 °C. It is possible that the analysed samples completely crystallised because the presence of crystalline material in the ampoule will promote secondary nucleation, which reduces the activation energy for nucleation and growth, aiding crystallisation (Hammel, 1969); furthermore, it is likely that the expulsion of water following

crystallisation is an extremely rapid process and condensation may be rather slower (Darcy and Buckton, 1998), resulting in the (temporary) formation of a saturated vapour space which will force complete crystallisation of the sample.

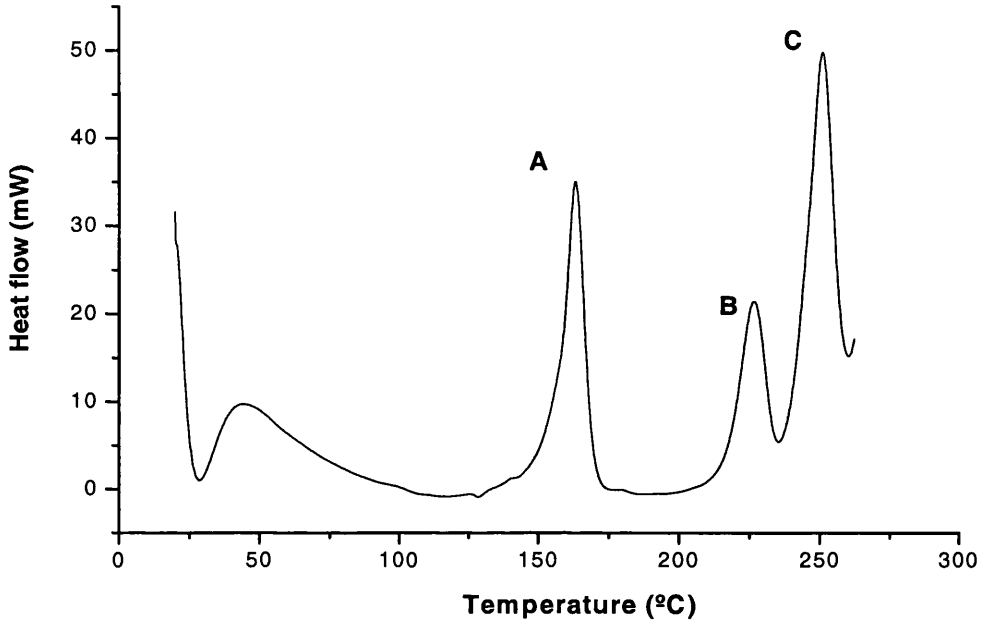

Figure 3.3 *DSC trace for re-crystallised amorphous lactose, after being removed from the TAM, showing the loss of hydration water (A) and the α- (B) and β-lactose (C) melting peaks.*

The enthalpy of crystallisation of fully and partially amorphous samples was determined following the integration methodology recommended by Dilworth et al. (2004), which consists in integrating the calorimetric data from the beginning of region A to the end of region E of Figure 3.1 from y=0. Although this methodology integrates regions that arise from processes other than crystallisation, it was shown to returned the calibration curves with best linear regression fits (Dilworth et al., 2004); furthermore, this methodology avoids problems of identifying starting and ending points of the different, normally overlapped regions, which is particularly useful for low amorphous content samples that exhibit a multi-peak crystallisation. This methodology returned amorphous contents (measured amorphous content) that were consistently lower that the expected, originating a calibration curve with a negative deviation from linearity (Figure 3.4); the measured amorphous contents were determined using the enthalpy of crystallisation of the fully amorphous sample as a reference.

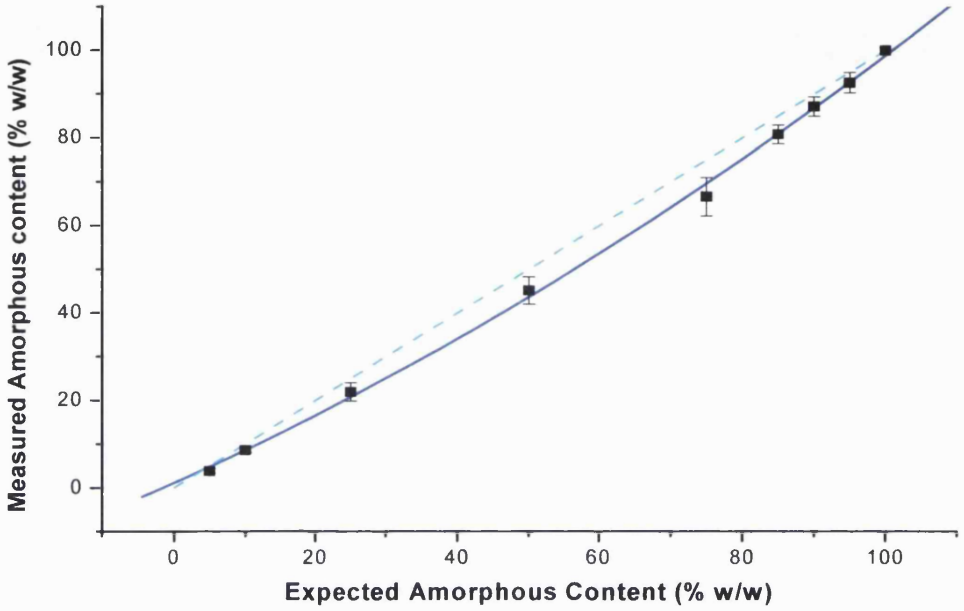

Figure 3.4 *Calibration curve for the quantification of amorphous lactose constructed from enthalpy of crystallisation. Measured amorphous contents were calculated from enthalpy of crystallisation data obtained by crystallising 30mg samples at 53% RH and 25 °C and using the enthalpy of crystallisation of fully amorphous lactose as a reference. ■ Measured amorphous content (Average, n=3) _ _ _ Represents the amorphous content as expected ____ Represents the fitting to the experimentally measured amorphous content.*

As mentioned in the methodology section, the partially amorphous samples were prepared by mixing appropriate quantities of amorphous and crystalline lactose in a glass container; this method was chosen because it is relatively gentle compared with other mixing methodologies (such as blend-sieve-blend for instance) and to be in accordance with the methodology followed by Dilworth et al., (2004), from which the present study followed. There is the possibility that some of the amorphous content could be lost during mixing, either because the forces exerted on the sample during mixing could cause some of the amorphous material to crystallise or because of preferential adsorption to the glass container, thus affecting the magnitude of the subsequently recorded experimental data. Dilworth et al., (2004) verified that a partially amorphous lactose sample prepared directly into the calorimetric ampoule returned a lower amorphous content than expected, indicating that the mixing was unlikely to affect the amorphous nature of the sample.

Interestingly, a close analysis of the published literature revealed results similar to those presented here. A recent study has shown calibration curves for quantification of amorphous content in lactose constructed from enthalpy of crystallisation data obtained by isothermal microcalorimetry exhibit a better fitting for a negative-deviated curve than for a linear curve (Steckel and Bolzen, 2005). Using DSC to determine the enthalpy of crystallisation of partially amorphous lactose samples, a negative-deviated calibration curve was also reported by Fix and Stevens (2004). It is definitely worth investigating the reasons behind such results.

3.4.3. AN INVESTIGATION OF THE FACTORS THAT MIGHT HAVE CAUSED THE NEGATIVE-DEVIATED CALIBRATION CURVE. DETERMINATION OF THE ENTHALPY OF FUSION OF A- AND B-LACTOSE BY HYPER-DIFFERENTIAL SCANNING CALORIMETRY

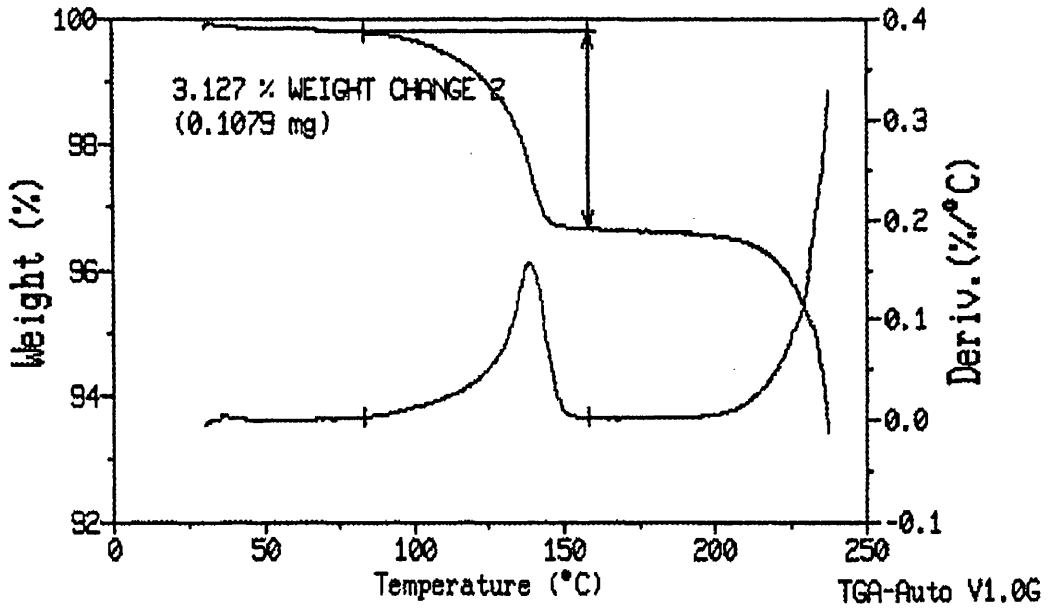

Figure 3.5 *Thermal gravimetric trace for crystallised lactose, showing the weight loss due to loss of the monohydrate water obtained by heating a 8 mg sample at 10 ºC/min to approximately 240ºC.*

Thermal gravimetric data of crystallised lactose showed a loss of the water of crystallisation (between 100 and 150 °C) in the order of 3% (w/w) (Figure 3.5), which is in keeping with gravimetric data presented previously (Hogan, 2001). If the sample crystallised totally to α-lactose monohydrate, a mass increase of 5% (w/w)

would be observed. DSC traces of the samples removed from the TAM (Figure 3.6, top) showed a hydrate water loss peak and α- and β-lactose melting peaks. These data suggest that amorphous lactose is crystallising to a mixture of α-lactose monohydrate and anhydrous α-lactose and/or β-lactose.

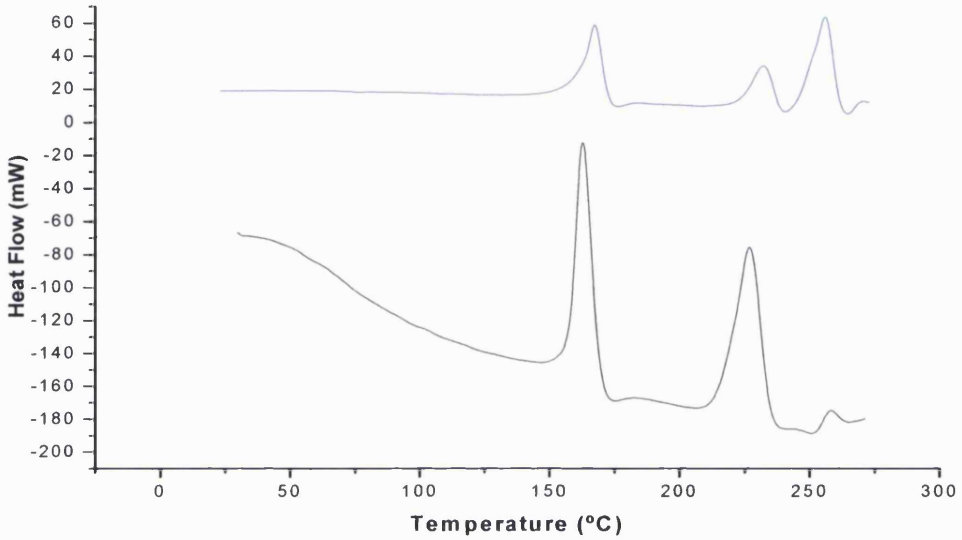

Figure 3.6 *DSC traces of recrystallised 100% amorphous lactose (top) and of pure α-lactose monohydrate (bottom), obtained by heating 1-2 mg samples at 200 °C/min.*

3.4.3.1. DETERMINATION OF THE ENTHALPY OF FUSION OF α- AND β-LACTOSE BY HYPER-DSC

In order to determine the enthalpy of fusion of α- and β-lactose, α-lactose monohydrate and crystallised samples (initially 100% amorphous) were subjected to a Hyper-DSC analysis. Hyper-DSC data for pure α-lactose monohydrate show a dehydration peak centred at 155 °C and a melt centred at 222 °C, which gives an enthalpy of fusion of approximately 169 ± 5.6 J/g (n=4) (Figure 3.6, bottom).

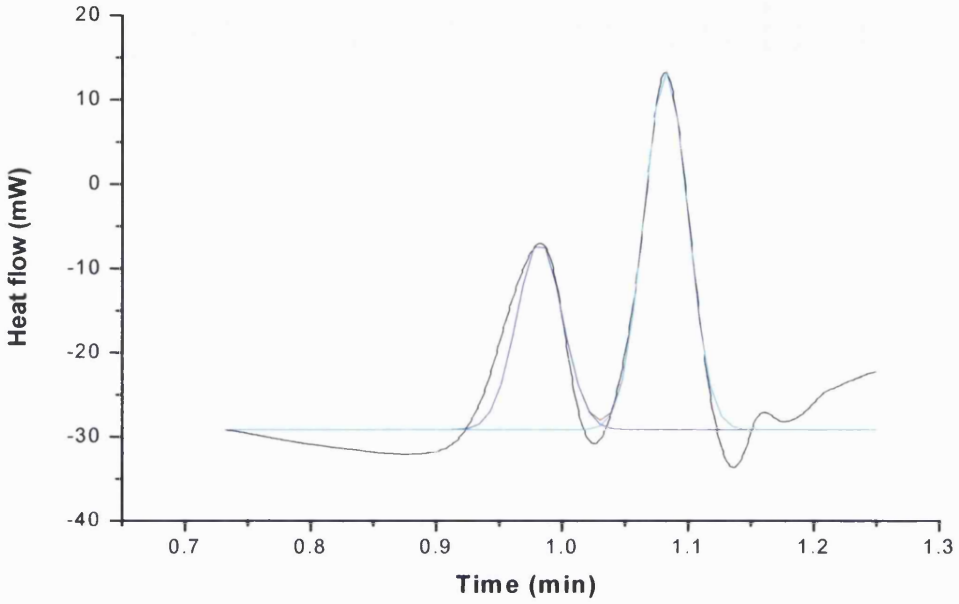

Figure 3.7 *Gaussian fitting of the melting peaks of a crystallised lactose sample; the melting peaks were obtained by heating 1-2 mg of a crystallised lactose sample (initially containing 100% amorphous lactose) at 200 °C/min on a Pyris-1 DSC.*

Pure β-lactose is difficult to prepare, so it was not possible to record a DSC trace for this material directly. However, amorphous lactose crystallises to a mixture of α-lactose monohydrate and anhydrous α- and/or β-lactose (Figure 3.6, top) and from these data it is possible to estimate the enthalpy of fusion for β-lactose. The β-lactose melt is centred at approximately 248 °C. It is difficult to quantify the enthalpy of fusion of β-lactose accurately because it overlaps the α-melt and the subsequent degradation (from 255 °C onwards). In order to ameliorate this, areas for the β-peak were determined by fitting the α- and β-peaks to a double Gaussian model, allowing their separation, as shown in Figure 3.7. Using the previously determined enthalpy of fusion of α-lactose to quantify the amount of α-and β-lactose in the sample and using the area under the melting peak of β-lactose identified by the Gaussian fitting, an enthalpy of fusion of approximately 197 ± 19 (n=4) J/g was determined for β-lactose.

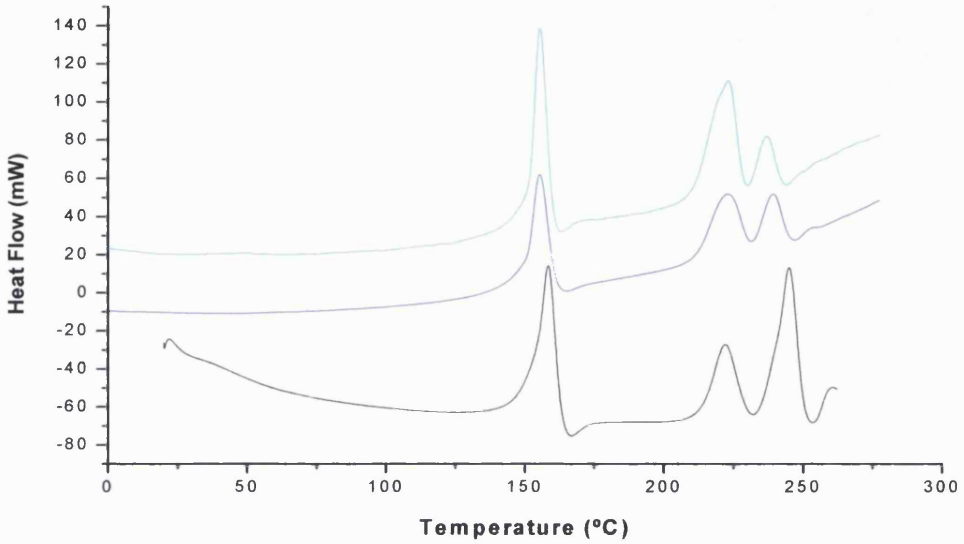

Figure 3.8 *DSC traces of crystallised lactose samples obtained by heating 1-2 mg sample at 200°C/min on a Pyris-1 DSC. Before crystallisation, the samples contained 25% (top), 50% (middle) and 85% (bottom) amorphous lactose .*

The fact that the DSC trace of recrystallised amorphous lactose indicates that it crystallised to a mixture of α- and β-lactose and the distinct enthalpy of fusion determined for the two lactose anomers suggest that the negative-deviated calibration curve obtained (Section 3.4.2) might be a consequence of the fact that amorphous lactose crystallises to a mixture of α- and β-lactose, whose proportions, and consequent measured heat response, depend on the initial amorphous content of the sample. This is further supported by the DSC traces of crystallised lactose samples (initially partially amorphous samples), which clearly show a change in the ratio of α- and β-lactose formed (Figure 3.8); the lower the amorphous content, the smaller the melting peak of β-lactose. However the different proportions of α- and β-lactose seen in the DSC scans might be the result of some artefacts. Firstly, as the amorphous content of the samples decreases, the amount of crystalline α-lactose monohydrate increases in the sample, which might cause the higher α-peak for the 25% (w/w) amorphous lactose sample (Figure 3.8). Secondly, α-lactose is known to mutorotate to β-lactose upon heating (Lerk et al., 1984b) and, although the high scanning rate used in the DSC experiments did not subject the samples to a long thermal treatment, some α- to β-lactose mutarotation could have occurred. The present results alluded to the need to further investigate the crystallisation of

amorphous lactose as it is induced during an isothermal microcalorimetry experiment.

3.4.4. ASSESSMENT OF THE CRYSTALLISATION BEHAVIOUR OF AMORPHOUS LACTOSE AS IT IS INDUCED DURING AN ISOTHERMAL MICROCALORIMETRY EXPERIMENT.

3.4.4.1. INTRODUCTION

Crystallisation of sugars is of a practical importance in pharmaceutical and food industries. Many studies have investigated the crystallisation behaviour of lactose (Bushill et al., 1965; Otsuka et al., 1991 and 1993; Briggner et al., 1994; Sebhatu et al., 1994a; Buckton and Darcy, 1995; Drapier-Beche et al., 1997; Joupilla et al., 1998; Chidavaenzi, 1999; Chidavaenzi et al., 2001 and 2002; Buckton et al., 2002; Berggren et al., 2004; Haque and Roos, 2005a and 2005b; Miao and Roos, 2005; Steckel and Bolzen, 2005; Burnett et al., 2006; Timmermann et al., 2006). Some of these studies focused on investigating the anomeric composition of the recrystallised amorphous lactose (Bushill et al., 1965; Otsuka et al., 1991; Drapier-Beche et al., 1997; Joupilla et al., 1998; Chidavaenzi, 1999; Haque and Roos, 2005a and 2005b; Miao and Roos, 2005; Steckel and Bolzen, 2005; Burnett et al., 2006; Timmermann et al., 2006). Studies have found that amorphous lactose was crystallising to a mixture of α-lactose monohydrate and β-lactose (Bushill et al., 1965; Briggner et al., 1994; Sebhatu et al., 1994a; Drapier-Beche et al., 1997; Chidavaenzi, 1999; Chidavaenzi et al., 2001 and 2002; Buckton et al., 2002). More recent studies have shown that freeze-dried and spray-dried lactose can crystallise to a mixture of α-lactose monohydrate, β-lactose, anhydrous α-lactose and anhydrous forms of crystals with α-lactose and β-lactose (Haque and Roos, 2005a Miao and Roos, 2005;). The presence of crystalline trehalose did not affect the crystalline forms originated during crystallisation of freeze-dried amorphous lactose (Haque and Roos, 2005a). However, the presence of different proteins was seen to affect the final crystalline form of lactose (Haque and Roos, 2005b). Buckton et al. (2002) and Chidavaenzi (1999) investigated the isothermal crystallisation of fully amorphous lactose batches of different anomeric composition prepared by spray-drying; sample mass, relative humidity, time of exposure to a certain relative humidity, and initial anomeric composition were seen to affect the anomeric

composition of recystallised lactose. Preparation method, temperature and time may also affect the type of crystal formed (Drapier-Beche et al., 1997; Joupilla et al., 1997). Otsuka et al. (1991) grinded crystalline α-lactose monohydrate, anhydrous α-lactose, and β-lactose in a centrifugal ball mill generating amorphous lactose, which, upon storage, originated crystalline lactose with different proportions of α- and β-lactose according to the original crystalline form. During the course of the present study Steckel and Bolzen (2005) investigated the influence of the relative humidity and the amount of amorphous material present on the anomeric composition of the recrystallised lactose by crystallising partially amorphous lactose as in a isothermal microcalorimetry experiment and using DSC data to determine the final anomeric composition; both factors were seen to influence the final anomeric composition. Recently, Timmermann et al. (2006) studied the influence of relative humidity, the amount of amorphous lactose and the presence of α-lactose monohydrate and β-lactose on the anomeric composition of recrystallised lactose. Using the desorption isotherm obtained by subjecting partially amorphous samples to high RH in a isothermal perfusion unit, the authors verified that at 60-80% RH amorphous lactose produced a high content of β-lactose, and samples containing crystalline β-lactose produced less β-lactose than the samples containing crystalline α-lactose monohydrate. On the other hand, the authors reported that at 90% RH all samples formed only α-lactose monohydrate.

These studies have definitely contributed to the knowledge of the crystallisation of lactose; however, this is not a fully understood process. The results presented in the previous section suggest that the anomeric composition of the recrystallised lactose is affected by the initial amorphous content of the sample, which motivated a deeper investigation into the isothermal crystallisation of amorphous lactose.

3.4.4.2. AIMS OF THE STUDY

The present study aims to investigate the effect of the amorphous:crystalline proportion and of the anomeric composition of crystalline and amorphous lactose on the final anomeric composition of recrystallised lactose. Crystallisation was induced as for an isothermal microcalorimetry experiment, in order to better understand the results presented in the previous section.

3.4.4.3. EXPERIMENTAL

3.4.4.3.1. PREPARATION OF AMORPHOUS SAMPLES

Amorphous lactose was prepared by spray drying as described in Section 2.2.1.3. Commercial α-lactose monohydrate (consisting of 94% (w/w) α-lactose and 6% (w/w) β-lactose) and commercial β-lactose (consisting of 14% (w/w) α-lactose and 86% (w/w) β-lactose) were used to prepare 10% (w/w) lactose solutions. These were equilibrated at 25 °C and 85 °C and spray dried to produce amorphous lactose batches of different anomeric composition (Figure 3.9). Confirmation of the amorphous nature was obtained from XRPD as outlined in Section 2.2.8.3. Anomeric composition was determined by gas chromatography according to the method described in Section 2.2.7.3.

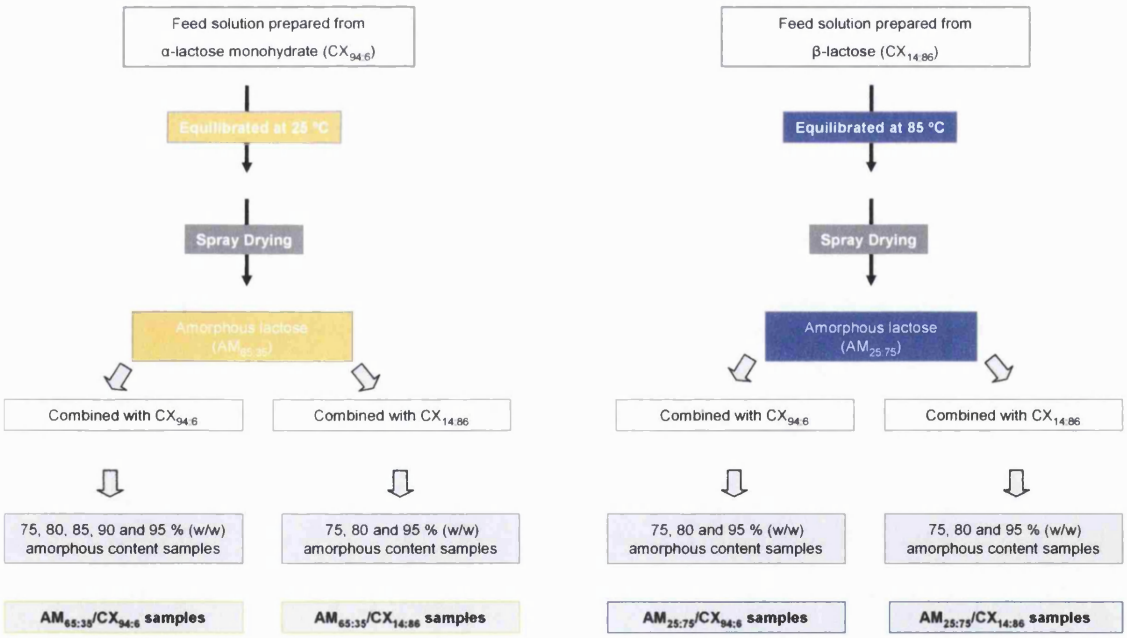

Figure 3.9 *Schematic representation of the preparation of the amorphous lactose batches and partially amorphous lactose samples used throughout the present study. CX represents the crystalline material, AM represents amorphous material and AM/CX represents partially amorphous samples. The anomeric composition of each crystalline, amorphous and partially amorphous (both amorphous and crystalline portions) sample is given by the subscript numbers as α:β.*

3.4.4.3.2. Preparation of partially amorphous samples

Partially amorphous samples (75, 80, 90 and 95%) were prepared by weighing proportional quantities of appropriate amorphous and crystalline lactose (a total weight of 15g into 30 mL amber glass container) and mixing in a Turbula mixer for 20 min. Each amorphous batch was mixed with α-lactose monohydrate and β-lactose according to Figure 3.10.

3.4.4.3.3. CRYSTALLISATION

The four groups of samples represented in Figure 3.10 were induce to crystallise at 25 °C by exposure to a 53% RH atmosphere (maintained by 100 mL of saturated salt solution of $Mg(NO_3)_2.6H_2O$ contained in a mini-hygrostat housed into the 3 mL glass ampoule) and to a 97% RH atmosphere (maintained by 100 mL of saturated salt solution of K_2SO_4 contained in a mini-hygrostat housed into the ampoule into the 3 mL glass ampoule). Samples were crystallised at least in triplicate. In order identify the endpoint of crystallisation, samples were crystallised in the TAM as described in Section 2.2.2.3.1.

3.4.4.3.4. GAS CHROMATOGRAPHY ANALYSIS

A basic description of the technique and gas chromatograph can be found in Sections 2.2.7.1 and 2.2.7.2. Samples (amorphous lactose, α-lactose monohydrate, β-lactose and crystallised 100, 95, 80 and 75 % amorphous samples, and hydrated crystalline α-lactose monohydrate, β-lactose) were derivatised as described in Section 2.2.3.7.1 prior to being analysed in a CP9001 Gas Chromatograph (Varian-Chrompack, Oxford, UK) following the methodology described in 2.2.7.3.2. Areas under the peaks corresponding to α- and β-lactose were used to determine their percentage in each sample. The chromatograms were recorded and anlysed for peak area calculation by means of the dedicated software Prime (HPLC Technologies Ltd, Herts, UK).

3.4.4.4. RESULTS AND DISCUSSION

In order to investigate the crystallisation behaviour of amorphous lactose, fully and partially amorphous lactose samples were crystallised and analysed by gas chromatography for anomeric composition determination. The anomeric composition of amorphous and crystalline lactose batches used during this study is presented in Table 3.1.

Table 3.1 *The anomeric composition of the crystalline and amorphous batches used for preparation of partially amorphous samples, as determined by Gas Chromatography (n=3). A summary of the preparation of the amorphous batches and partially amorphous samples is schematically represented in Figure 3.9.*

Material		**Anomeric composition (% w/w)**	
		α-lactose	**β-lactose**
Crystalline	α-lactose monohydrate ($CX_{94:6}$)	94.4 ± 1.2	5.6 ± 1.2
	β-lactose ($CX_{14:86}$)	14.0 ± 0.9	86.0 ± 0.9
Amorphous	Prepared from solution at 25 °C $AM_{65:35}$	65.1 ± 1.0	34.9 ± 1.0
	Prepared from solution at 85 °C $AM_{25:75}$	25.1 ± 2.7	74.9 ± 2.7

The α-lactose content (including both α-lactose monohydrate and anhydrous α-lactose) of the crystallised lactose samples is represented in Figures 3.10 and 3.11 according to the initial amorphous content; the α-lactose content of recrystallised 75, 80 and 90% amorphous content sample is given by the coloured bars. The α-lactose content of recrystallised 100% amorphous sample is given by the empty bar located at 100% amorphous content. Assuming that each partially amorphous sample would crystallise to the same proportion of α- and β-lactose as the fully amorphous sample, the expected α-lactose content was determined for each amorphous content; this expected α-lactose content is represented by the empty bars for each amorphous content. Comparison of the actual α-lactose content with the theoretical α-lactose content will aid the discussion and allow to identify the cases in which mutarotation occurred.

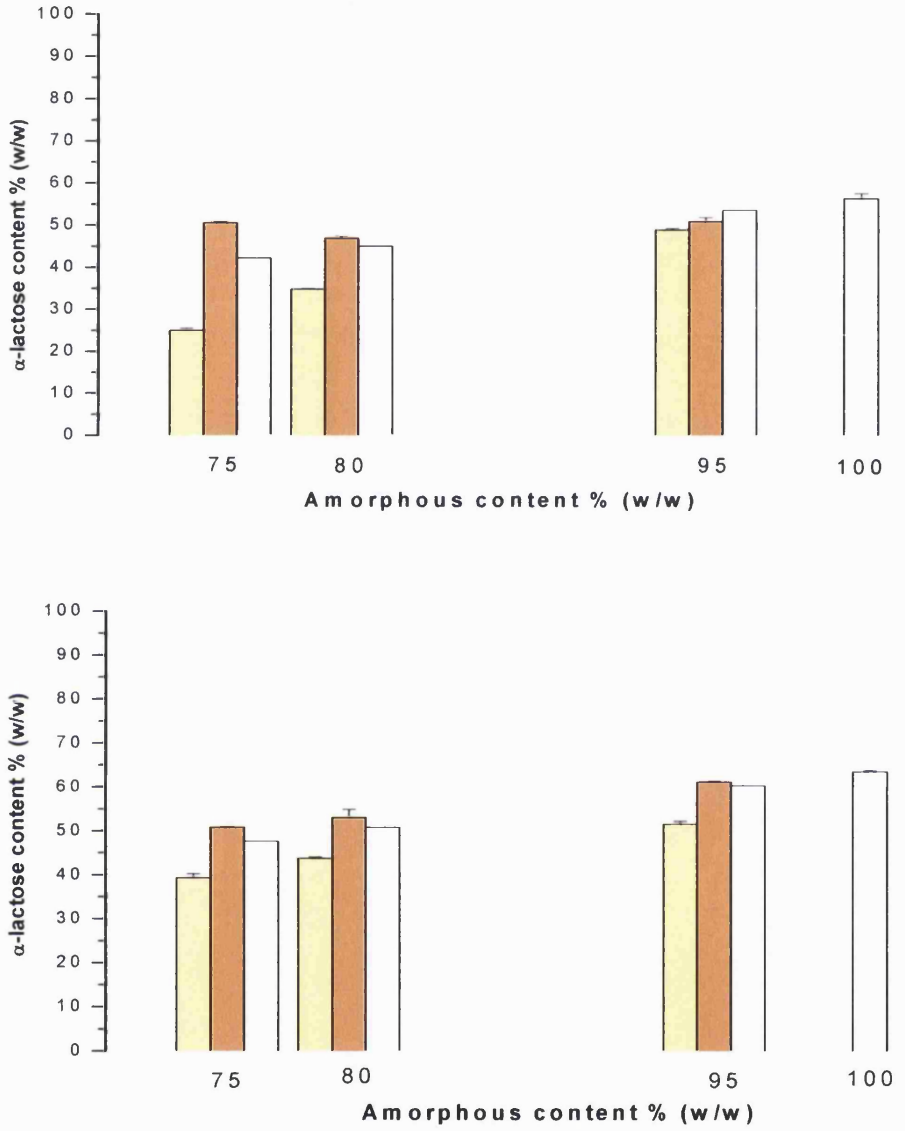

Figure 3.10 *Final α-lactose content (% w/w) of partially and fully $AM_{65:35}$ amorphous lactose samples (amorphous lactose containing 65% α-lactose and 35% β-lactose) crystallised at 53% RH and 25°C (top) and 95% RH and 25 °C (bottom), according to initial amorphous content.* □ *$AM_{65:35}$ and as if partially amorphous samples crystallised as 100% amorphous lactose does* ■ *$AM_{65:35}/CX_{94:6}$ samples* ■ *$AM_{65:35}/CX_{14:86}$ samples.*

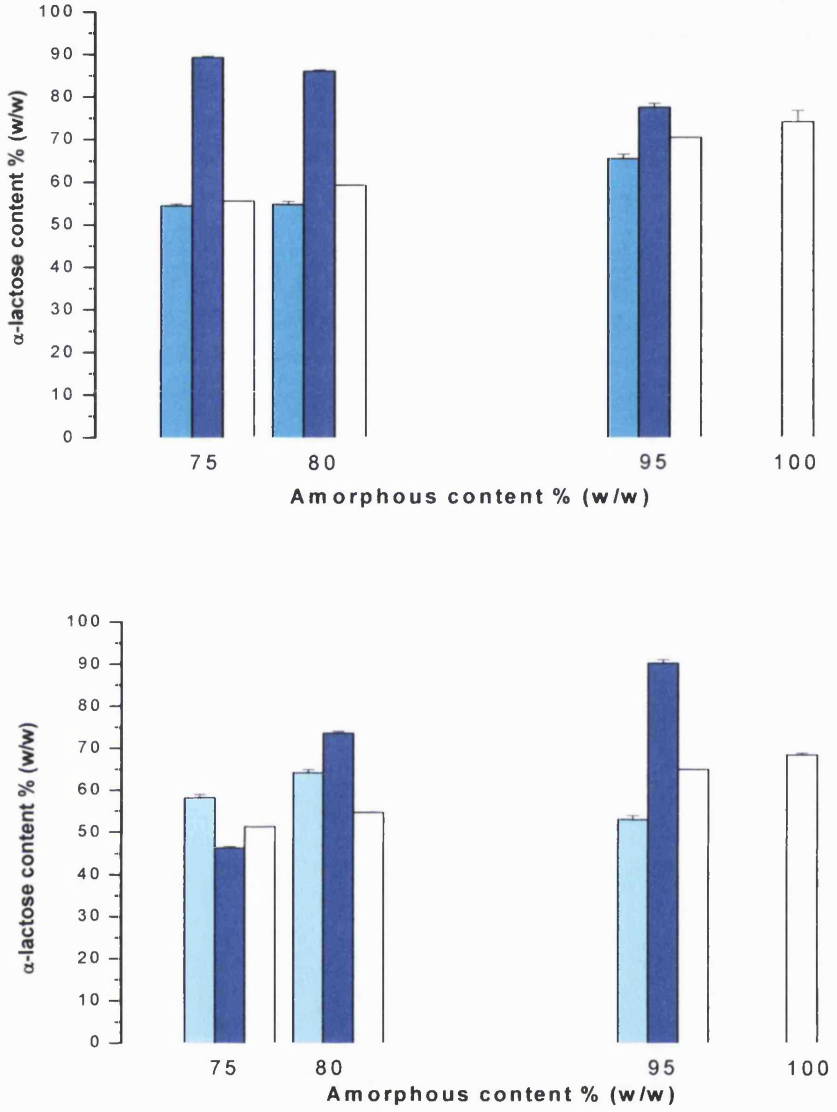

Figure 3.11 *Final α-lactose content (% w/w) of partially and fully $AM_{25:75}$ amorphous lactose samples (amorphous lactose containing 25% α-lactose and 75% β-lactose) crystallised at 53% RH and 25°C (top) and 95% RH and 25 °C (bottom), according to initial amorphous content.* □ *$AM_{25:75}$ and as if partially amorphous samples crystallised as 100% amorphous lactose does* ■ *$AM_{25:75}/CX_{94:6}$ samples* ■ *$AM_{25:75}/CX_{14:86}$ samples.*

When analysing the crystallisation behaviour of partially amorphous lactose samples, it has to be considered that both amorphous and crystalline lactose can mutorotate. Crystalline lactose is known to mutorotate from β- to α-lactose when exposed to high relative humidites (Angberg et al., 1991). At relative humidities

higher than 94% RH, mutarotation is known to progress easily. At lower relative humidities mutarotation was seen to occur, specially is the crystalline lactose contained a high content of anhydrous α-lactose (Angberg et al., 1991). According to Jouppila et al. (1998), mutarotation in the amorphous state may occur before crystallisation, and that the nuclei of crystals formed initially are probably the determinants of the ratio of the various crystal forms. Chidavaenzi (1999) and Buckton et al. (2002) had reported that amorphous lactose was crystallising to a different anomeric composition than that of the amorphous sample. Consequently, differences in the final anomeric content of crystallised lactose might be caused by mutarotation of the amorphous lactose, crystallisation and mutarotation of the original and newly formed crystalline lactose.

3.4.4.4.1. EFFECT OF THE AMORPHOUS CONTENT ON THE FINAL ANOMERIC COMPOSITION OF RECRYSTALLISED LACTOSE

As mentioned, the empty columns at 75, 80 and 95% amorphous content represent the expected α-content. The expected α-content was calculated using the final anomeric composition of 100% amorphous sample and assuming that the partially amorphous sample was crystallising exactly as the correspondent fully amorphous lactose. When comparing the actual α-content for each partially amorphous sample (given by the coloured bars) with the expected amorphous content (empty bars), it is clear that crystallisation is not originating a final product with the same anomeric composition as expected from the 100% amorphous sample.

Considering samples containing $CX_{94:6}$ crystallised at 53% RH and 25 °C, namely $AM_{65:35}/CX_{94:6}$ samples (Figure 3.10 top) and $AM_{25:75}/CX_{94:6}$ samples (Figure 3.11 top), the crystalline lactose contained higher α-content than expected; the difference in α-content increased with decreasing amorphous content of the original sample. On the other hand, samples containing $CX_{14:86}$ crystallised at 53% RH 25 °C, namely $AM_{65:35}/CX_{14:86}$, (Figure 3.10 top) and $AM_{25:75}/CX_{14:86}$ (Figure 3.11 top), produced crystalline lactose containing lower α-content than expected; for $AM_{25:75}/CX_{14:86}$ samples the difference in α-content decreased with decreasing amorphous content, while for $AM_{65:35}/CX_{14:86}$ no relationship between amorphous content and final anomeric composition could be established.

$AM_{65:35}/CX_{94:6}$ samples have the same anomeric composition as the samples used to construct the calibration curve for quantification of amorphous content by isothermal microcalorimetry (Figure 3.4). As can be seen for the $AM_{65:35}/CX_{94:6}$ samples crystallised at 53% RH and 25 °C (represented by the orange columns in Figure 3.10 top), the lower the amorphous content, the bigger the difference in α-content between the α-lactose samples and the expected α-content (given by the empty column for each amorphous content). This means that, for the analysed samples, the lower the amorphous content, the more α-lactose was formed. The hypothesis raised in Section 3.4.3 to explain the negative-deviated calibration curve is supported by such results; the samples used to construct the calibration curve for quantification of amorphous content of lactose by isothermal microcalorimetry were actually crystallising to different proportions of α- and β-lactose according to their amorphous content.

The negative-deviated calibration curve for quantification of amorphous content from isothermal microcalorimetry data exhibits the most negative-deviated point at ~50% amorphous content. From the shape of the calibration curve and the final anomeric composition of α-lactose samples, it is possible that from 50 to 100% amorphous contents the higher the amorphous content is, the higher the final β-lactose, while for amorphous contents lower than 50%, the final β-lactose increases with decreasing amorphous content. Steckel and Bolzen (2005) determined the anomeric composition of 1 to 100% amorphous lactose samples previously recrystallised at 58% RH by DSC and their results contrast with those presented here. The authors observed that from 1 to 100% amorphous content, the final β-lactose content increased. However, it should be noted that DSC is not the best method to determine the anomeric composition of lactose because the heating programme can cause α- to β-lactose mutarotation (Lerk et al., 1984b). In addition to that, the lower amorphous content samples contain more crystalline α-lactose monohydrate, and it can be this that is being detected on the DSC and not the one formed during crystallisation. Only by comparison with the expected anomeric composition, conclusions could be made.

For samples crystallised at 97% RH the influence of the initial amorphous content on the final anomeric composition is not as clear as for samples crystallised at 53% RH. At this higher relative humidity, mutarotation and water incorporation can take place in a greater extent (Anberg et al., 1991) and these processes are most probably affecting the crystallisation. This will be further explained in Section 3.4.4.4.2.

3.4.4.4.2. EFFECT OF THE INITIAL ANOMERIC COMPOSITION ON THE FINAL ANOMERIC COMPOSITION OF RECRYSTALLISED LACTOSE

3.4.4.4.2.1. EFFECT OF THE ANOMERIC COMPOSITION OF THE AMORPHOUS PORTION ON THE FINAL ANOMERIC COMPOSITION OF THE CRYSTALLISED LACTOSE

In order to evaluate the effect of the anomeric composition of the amorphous portion on the final anomeric composition of crystallised lactose samples, two amorphous lactose batches were analysed, namely $AM_{65:35}$ (containing 65% w/w α-lactose and 35% w/w β-lactose) and $AM_{25:75}$ (containing 25% w/w α-lactose and 75% w/w β-lactose). $AM_{65:35}$ and $AM_{25:75}$ were crystallised at 53 and 97% RH and their anomeric composition determined.

At 53% RH $AM_{65:35}$ crystallised to a lower α-content than $AM_{25:75}$, as expected from a previous study (Chidavaenzi, 1999). $AM_{65:35}$ crystallised to 63.5% α-lactose and $AM_{25:75}$ crystallised to 74.1% α-lactose. This clearly indicates that while $AM_{65:35}$ crystallises, 1.6% of α-lactose mutarotated to β-lactose. On the other hand, $AM_{25:75}$ exhibited 49.0% β- to α-lactose mutarotation. Chidavaenzi (1999) observed that amorphous lactose containing higher content of β-lactose underwent significant β- to α-lactose mutarotation, while amorphous lactose of lower β-lactose content would exhibit a less significant α- to β-lactose mutarotation. Crystallisation at 97% RH differed from that at 53%RH; $AM_{65:35}$ crystallised to 56.3% α-lactose and $AM_{25:75}$ crystallised to 68.4% α-lactose. At 97% RH, during the crystallisation of $AM_{65:35}$ 8.8% of α-lactose mutarotated to β-lactose, while during the crystallisation of $AM_{25:75}$ 43.3% of β-lactose mutarotated to α-lactose.

By comparing the final anomeric composition of partially amorphous samples containing the same crystalline portion and different amorphous portion, it is possible to evaluate the impact of the anomeric composition of the amorphous portion on the anomeric composition of the crystallised samples. At 53%, $AM_{25:75}/CX_{94:6}$ samples and $AM_{25:75}/CX_{14:86}$ samples originated more final α-lactose than $AM_{65:25}/CX_{94:6}$ samples and $AM_{65:35}/CX_{14:86}$ samples, respectively. As already seen, $AM_{25:75}$ undergoes a higher degree of β- to α-lactose mutarotation during crystallisation, which most probably is contributing to the higher α-lactose content of the recrystallised $AM_{25:75}/CX_{94:6}$ samples and $AM_{25:75}/CX_{14:86}$ samples in relation to

the recrystallised $AM_{65:25}/CX_{94:6}$ samples and $AM_{65:35}/CX_{14:86}$ samples, respectively. At 97% RH a similar crystallisation pattern was observed, with the exception of the 75% $AM_{25:75}/CX_{94:6}$; 95% and 80% $AM_{25:75}/CX_{94:6}$ samples crystallised to higher α-lactose content than 95% and 80% $AM_{65:35}/CX_{94:6}$ samples but 75% $AM_{25:75}/CX_{94:6}$ sample crystallised to lower α-lactose content than 75% $AM_{65:35}/CX_{94:6}$. As already mentioned, it has been suggested that in the crystallisation of lactose from the amorphous state, the nuclei of crystals formed initially are probably the determinants of the ratio of the various crystal forms and that mutarotation before crystallisation may occur (Jouppila et al., 1998).

3.4.4.4.2.2. EFFECT OF THE ANOMERIC COMPOSITION OF THE CRYSTALLINE PORTION ON THE FINAL ANOMERIC COMPOSITION OF THE CRYSTALLISED LACTOSE

The transition form the amorphous to the crystalline state occurs as a result of sufficient molecular mobility for nucleation and crystal growth. In a partially amorphous lactose system, the presence of a seed crystal, such requirements are removed and the molecular motion need only be sufficient for molecular reordering for secondary nucleation and growth. The presence of the seed material is expected to reduce the activation energy for nucleation and growth (Hammel, 1969). Both amorphous batches ($AM_{65:35}$ and $AM_{25:75}$, Figure 3.9) were crystallised in presence of crystalline $CX_{94:6}$ (commercial α-lactose monohydrate containing 94% w/w α-lactose and 6% β-lactose) and $CX_{14:86}$ (commercial β-lactose containing 84% w/w α-lactose and 16% β-lactose). It is expected that the presence of $CX_{94:6}$, richer in α-lactose, will favour crystallisation to α-lactose and the presence of $CX_{14:86}$, richer in β-lactose, will favour the crystallisation to β-lactose, as this would be the most energetically favourable option.

By comparing the final anomeric composition of partially amorphous samples containing the same amorphous portion and different crystalline portion ($AM_{65:35}/CX_{94:6}$ compared with $AM_{65:35}/CX_{14:86}$ and $AM_{25:75}/CX_{94:6}$ compared $AM_{25:75}/CX_{14:86}$), it is possible to evaluate the impact of the anomeric composition of the crystalline portion on the anomeric composition of the crystallised samples. As supposed, for samples recrystallised at 53% and 97% RH, when $CX_{94:6}$ was the crystalline material, the final α-lactose was higher than when $CX_{14:86}$ was present, with the exception of the 75% $AM_{25:75}/CX_{94:6}$ sample crystallised at 97% RH.

At 53% RH, both sets of amorphous samples containing $CX_{94:6}$ ($AM_{65:35}/CX_{94:6}$ and $AM_{25:75}/CX_{94:6}$) originated a higher final α-content than expected (Figures 3.10 and 3.11 top). At the same relative humidity, samples containing $CX_{14:86}$ ($AM_{65:35}/CX_{14:86}$ and $AM_{25:75}/CX_{14:86}$) originated a smaller final α-content (higher β-lactose content) than the expected (Figures 3.10 and 3.11 top). This is in keeping with the fact that the presence of a seed material will induce crystallisation to the crystalline material of the same type as the seed.

At 97% RH, the effect of the anomeric composition of the crystalline portion on the final anomeric composition seems more complex than at 53% RH. At 53%RH, samples containing $CX_{94:6}$ originated higher α-content than expected and samples containing $CX_{14:86}$ originated lower α-content than expected. At 97% RH was not observed for all sets of samples. To analyse the effect of the anomeric composition of the crystalline portion on the final anomeric composition of samples crystallised at 97% RH, the final anomeric composition of samples containing the same amorphous portion and different crystalline portions was compared among them and with the correspondent expected α-content.

When considering the crystallisation in presence of $CX_{94:6}$ ($AM_{65:35}/CX_{94:6}$ and $AM_{25:75}/ CX_{94:6}$ samples) at 97% RH, the 75 and 80% $AM_{65:35}/CX_{94:6}$ samples originated higher α-lactose content than the expected (Figure 3. 10 bottom). β- to α-lactose mutarotation took place in the order of 1.9 and 8.4% for 75% and 80% $AM_{65:35}/CX_{94:6}$, respectively. 95% $AM_{65:35}/CX_{94:6}$ originated lower α-lactose content than expected and mutarotation of α- to β-lactose occurred (2.6 %). $AM_{25:75}/CX_{94:6}$ samples crystallised at 97% RH did not exhibit a crystallisation trend. 95 and 80% amorphous $AM_{25:75}/CX_{94:6}$ samples crystallised to more α-lactose than expected (Figure 3.11 bottom); there was a β- to α-lactose mutarotation of 25.2. and 18.9 respectively. Unexpectedly, 75% amorphous $AM_{25:75}/CX_{94:6}$ samples crystallised to less α-lactose than expected (Figure 3.11 bottom); a 5 % α- to β-lactose was observed. Because $CX_{94:6}$ is in principle, stable to mutarotation, the observed mutarotation is most probably originated in the amorphous portion of the sample and induced by the presence of the $CX_{94:6}$.

$AM_{65:35}/CX_{84:16}$ exhibited a final α-lactose content lower than expected (Figure 3.10 bottom). By comparing the final α-content with the expected α-content (Figure 3.10 bottom), a 4.7, 10.2 and 17.2 % α- to β-lactose mutarotation was observed for the 95, 80 and 75% $AM_{65:35}/CX_{84:16}$ samples, respectively. At 97% RH, the lower the

amorphous content, the higher is the crystalline β-lactose present after crystallisation. Consequently, the higher presence of $CX_{14:86}$ might induce a higher degree of mutarotation during crystallisation of the amorphous portion.

$AM_{25:75}/CX_{14:86}$ samples did not exhibit a crystallisation trend at 97% RH. The 95% amorphous sample crystallised to less α-lactose than expected (Figure 3.11 bottom), exhibiting a 12% α- to β-lactose mutarotation. On the other hand, 80 and 75% $AM_{25:75}/CX_{14:86}$ samples crystallised to more α-lactose than expected (Figure 3.11 bottom), exhibiting a 9.5 and 6.9% β- to α-lactose mutarotation, respectively. When considering the crystallisation of samples containing $CX_{14:86}$, it should be noted that this crystalline lactose contains 86% β-lactose, which at high RH can mutorotate to α-lactose. It is possible that for 75% and 80% $AM_{25:75}/CX_{14:86}$ samples, the β-lactose portion of the crystalline lactose is mutarotating to α-lactose.

Figure 3.12 summarises the crystallisation behaviour of amorphous lactose. The crystallisation of lactose from the amorphous state is a complex event. When amorphous lactose crystallises in presence of crystalline lactose, the process is clearly more complex. The present crystallisation study showed that the anomeric composition of the recrystallised lactose is affected by the initial anomeric composition, relative humidity and initial amorphous content. The results of the present study are useful for modelling and prediction of lactose crystallisation from the amorphous state.

Timmermann et al. (2006) investigated the crystallisation of amorphous lactose at various relative humidites by isothermal perfusion microcalorimetry and used the enthalpies of desorption after crystallisation to characterise the anomeric composition of the recrystallised lactose. At 60 to 80% RH the amorphous lactose and partially amorphous lactose containing crystalline α-lactose monohydrate were seen to crystallise to a mixture containing more β-lactose than α-lactose, whereas at 90% RH all samples completely crystallised to α-lactose monohydrate. Samples containing crystalline β-lactose completely crystallised to α-lactose monohydrate at 90% RH and formed a equally proportion mixture of β-lactose and α-lactose when crystallisation took place at 60-80% RH. Steckel and Bolzen (2005) had also verified that amorphous lactose crystallised at 100% RH produced α-lactose monohydrate only. These results contradict those obtained in the present study, in which the crystallisation of fully of partially amorphous lactose, always lead to a mixture of both anomers. Bushill et al. (1965), Drapier-Beche et al. (1997), Briggner et al. (1994),

Sebhatu et al. (1994a), Jouppila et al (1998), Chidavaenzin (1999), Schmitt et al. (1999), Buckton et al. (2002), Haque and Roos (2005a) and Miao and Roos (2005) all reported that the crystallisation of amorphous lactose was leading to a mixture of crystalline forms. However, it should be noted that the conditions used in the different studies might influence the final crystallisation result.

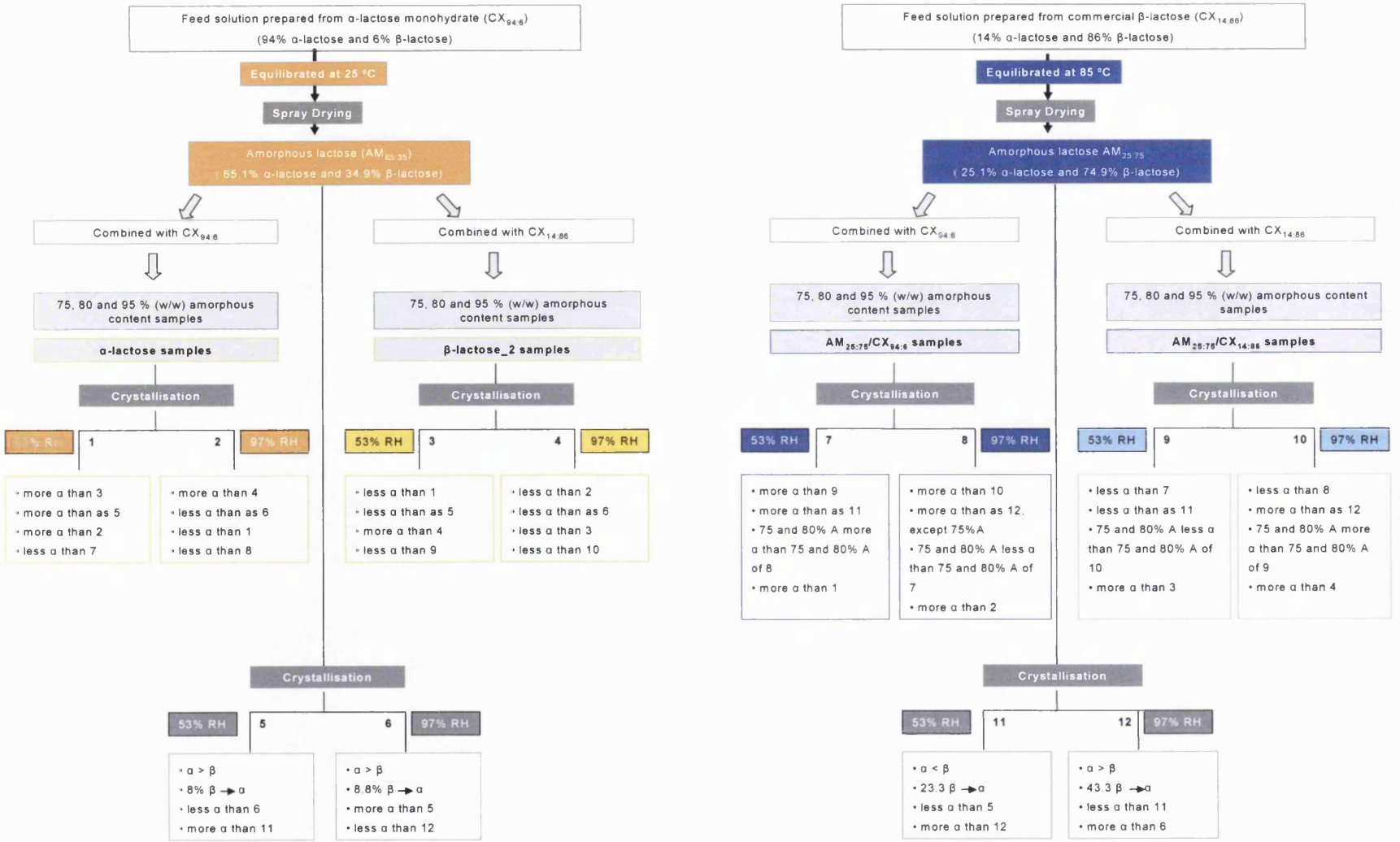

Figure 3.12 *A summary of the recrystallisation behaviour of amorphous lactose according to the initial anomeric composition of amorphous and crystalline material at the two relative humidities investigated. α means α-lactose content, β means β-lactose content and → represents the direction of mutarotation.*

3.5. CONCLUSION

The results presented in this chapter have highlighted the complexity of lactose crystallisation as well as the number of potential processes involved in it. It was possible to construct a calibration curve for quantification of amorphous content in lactose from TAM data, but this curve was not linear. However, the enthalpies measured in the calorimeter, at any particular amorphous content, were reproducible.

The causes of the non-linear calibration curve were investigated. It was seen that α- and β-lactose exhibit different enthalpies of fusion, and, consequently different enthalpies of crystallisation.

The study of the crystallisation of amorphous lactose investigated the effect of the anomeric composition, amorphous content and relative humidity on the final anomeric composition of the recrystallised lactose. The results presented clearly show that the crystallisation of lactose from the amorphous state is a complex process.

The anomeric composition of the recrystallised lactose was seen to be affected by the initial anomeric composition, relative humidity and initial amorphous content. These data are important for modelling of the crystallisation phenomena in materials containing amorphous lactose and, consequently, for prediction of the performance and stability of lactose-containing food and pharmaceutical materials. The crystalline forms of lactose are known to have different properties, which might influence the product stability and performance. For example, dehydration of α-lactose monohydrate affects the binding properties of the solid; the more dehydrated the higher the binding properties (Lerk et al., 1983a).

The outcome of the crystallisation of amorphous lactose will most certainly impact on the measured heat output during crystallisation of amorphous lactose in an isothermal microcalorimetry experiment, and consequently, on the quantification of amorphous contents by determination of the enthalpy of crystallisation by a calorimetric method. However, the use of such methods is not invalidated by the present results; these only demonstrate that when planning the experimental design, effort must be taken to ensure that the test and standard partially

amorphous lactose samples are crystallising to lactose of the same anomeric composition. In addition to that, the crystallisation and the isothermal microcalorimetry data discussed in this chapter raise the need to investigate the effect of the crystallisation of lactose, and, ultimately of the anomeric composition, on the quantification of small amorphous contents of lactose. Such subject will be further investigated in Chapter 4.

In this chapter…

…a previously recommended integration method for determination of the enthalpy of crystallisation from isothermal microcalorimetry data was applied to partially amorphous lactose samples;

…reproducible heats of crystallisation could be determined at any particular amorphous content;

… a calibration curve for quantification of amorphous content in lactose could be plotted, but this was not linear;

… different enthalpies of fusion for α- and β-lactose were determined from differential scanning calorimetry data, and such difference was considered to contribute to the non-linearity of the calibration curve;

… the crysatllisation behaviour of amorphous lactose as induced during a isothermal microcalorimetry experiment was investigated;

…initial anomeric composition, relative humidity and amorphous content were seen to affect the final anomeric composition, and consequently the quantification of amorphous content of lactose by determination of the enthalpy of crystallisation;

CHAPTER FOUR

EFFECT OF THE ANOMERIC COMPOSITION OF CRYSTALLINE AND AMORPHOUS LACTOSE ON THE QUANTIFICATION OF SMALL AMORPHOUS CONTENT IN LACTOSE BY ISOTHERMAL PERFUSION MICORCALORIMETRY AND SOLUTION CALORIMETRY

4.1. INTRODUCTION

The presence of amorphous material in a pharmaceutical system can affect both the physical and chemical stability and the performance of the system during product manufacture and use, a subject previously discussed in Chapter 1. Consequently, the quantification of amorphous content and its stability are vital to control steps during development and manufacture, in order to ensure stability and continued efficacy of the drug products upon storage. The development of techniques that allow a quantitative determination of low (~1% w/w) amorphous contents is therefore of considerable importance and have long been investigated.

As already mentioned (Section 1.16.1), crystalline lactose can exist as α-lactose monohydrate and anhydrous β- and α-lactose. In reality, any of the commercially available crystalline forms of lactose are normally contaminated by the two others to some extent. In addition, amorphous lactose exists as a mixture of the two anomers, α- and β-lactose (Chidavaenzi et al., 2002), whose proportions vary according to processing conditions. Amorphous lactose crystallises to a mixture of β - and α-lactose and α-lactose monohydrate (Chidavaenzi et al., 2002). In Chapter 3 it was demonstrated that the anomeric composition of the final crystallised lactose varies according to the relative humidity, type of crystalline and amorphous materials, and even according to the amorphous content that undergoes crystallisation. Another recent study (Steckel and Bolzen, 2005) has reached similar conclusions. As α- and β-lactose exhibit different enthalpies of crystallisation (Chapter 3), the quantification of small amorphous contents by a method based on the determination of enthalpies of crystallisation, such as isothermal microcalorimetry methods, might be affected by the factors that influence the final anomeric composition of lactose. In this chapter, the effect of the anomeric composition of amorphous and crystalline lactose on the quantification of amorphous content by isothermal microcalorimetry is investigated.

A methodology for quantification of amorphous content of lactose by solution calorimetry has been developed and is based on the fact that amorphous and crystalline lactose exhibit different enthalpies of solution (Hogan and Buckton ,2000; Harjunen et al., 2004). However, as the three crystalline forms of lactose exhibit different enthalpies of solution (Hudson and Brown, 1908), the impact of the anomeric composition of the crystalline and amorphous lactose on the quantification

of small amounts of amorphous content in lactose is also investigated in the present chapter.

4.2. EFFECT OF THE ANOMERIC COMPOSITION OF BOTH CRYSTALLINE AND AMORPHOUS LACTOSE ON THE QUANTIFICATION OF AMORPHOUS CONTENT IN LACTOSE BY ISOTHERMAL RELATIVE HUMIDITY PERFUSION MICROCALORIMETRY

4.2.1. INTRODUCTION

The transition of a material from the unstable amorphous form to the crystalline form is accompanied by a heat exchange that can be followed by isothermal microcalorimetry. Isothermal Microcalorimetry has long been applied for the quantification of amorphous content of excipients (Sebhatu et al., 1994; Briggner et al., 1994b; Buckton et al., 1995a; Kawakami et al., 2002; Al-Hadithi et al., 2004; Dilworth et al., 2004) and drugs (Ahmed et al., 1996; Ohta et al., 2000b; Kawakami et al., 2002; Mackin et al., 2002a; Samra and Buckton, 2004). A common approach to crystallise partially amorphous samples in an isothermal calorimeter is to use an elevated relative humidity (maintained through the use of a mini-hygrostat located in the sample ampoule and reference as described in Section 2.2.2.3.1), a methodology commonly known as batch isothermal microcalorimetry, which was described in Chapter 3 as a method to induce crystallisation of amorphous lactose.

While a batch isothermal microcalorimetry experiment is simple to run, when lactose is the sample the data are complex and contain (usually) up to 5 phases (Section 3.4.1), which can make data analysis complicated. It has also been reported that at very low amorphous contents, the crystallisation response of the samples is less reproducible (Buckton et al., 1995c; Sebhatu et al., 1994a). Two of the principal problems of the batch isothermal microcalorimetry method are that hydration is initiated externally from the calorimeter and, hence, the initial wetting, and possibly some crystallisation, data are lost, and that there are imbalances in the rate of water evaporation and condensation. These problems make it difficult to obtain reproducible data, an essential prerequisite for a calibration study, and are particularly critical when quantifying small amounts of amorphous material. In order to overcome such problems, a gas-flow set up has been devised which allows for a

dynamic system to be used, providing external control of the relative humidity to which the sample is exposed. This facilitates the alteration of relative humidity throughout the duration of the experiment, providing control over the behaviour of the sample. Such a set-up allows for the establishment of a steady baseline whilst the sample is exposed to 0% RH, so that the amorphous material may be dried prior to the crystallisation step and the effects of lowering the apparatus into the channel can dissipate without any risk of crystallisation in the sample. Once a baseline has been achieved, the sample may then be exposed to elevated RH in order to induce crystallisation, and the heat flow generated recorded simultaneously.

In comparison with batch isothermal microcalorimetry, little work has been published on the use of the RH perfusion unit. One of the earliest studies (Bhatt and Rubenstein, 1983) used the system to measure the heats of adsorption and desorption of water vapour at various crystalline and amorphous solids surfaces. This work showed that isothermal RH perfusion microcalorimetry is capable of detecting very small quantities of contaminants in a crystalline material. This early work relied on the use of saturated solution to generate the required RH, and from it, the current gas flow system was developed, where the vapour pressure (relative humidity) of the solvent is controlled through accurate mixing of two different gas flows (0% and 100% RH, respectively) (Section 2.2.2.3.2). This system was employed to probe the powder surface energetics of α-lactose monohydrate obtained from three suppliers in order to differentiate between them when contact angle measurements could not (Sheridan et al., 1995); the calorimetric data obtained in this study showed that one supplier's product had different surface energy. The RH perfusion system has also been successfully used to determine the hygroscopicity of drug substances (Jakobsen et al., 1997); the authors reported isothermal microcalorimetry as a useful tool for determining the storage conditions of drug substances. Isothermal RH Perfusion microcalorimetry has also been employed for characterisation of adsorption properties of sodium benzoate (Pudipeddi et al., 1996). Using a similar experimental set up, et al. (2000) were able to characterise the adsorption properties of amorphous cefditoren pivoxil.

Isothermal RH perfusion microcalorimetry has also been used to investigate the crystallisation of a micronised drug substance. Using a ramping method (whereby the sample is exposed to continually changing RH at a defined rate), Briggner (1993) showed that the heat flow curve recorded could be divided into three distinct

regions; the first region (exothermic) represented wetting of the drug substance, which was followed by a further exothermic response due to crystallisation itself, before a final endothermic region attributed to the evaporation of excess moisture from the sample following structural collapse and subsequent crystallisation. The author suggested that integrating between any two RH values, it would be possible to obtain a precise value for the heat evolved or absorbed during the process, showing that the RH perfusion technique could be suitable for the quantification of amorphous content by determination of the enthalpy of crystallisation. More recently, isothermal RH perfusion microcalorimetry was successfully used to quantify low levels of amorphous content in micronised active batches (Mackin et al., 2002a 2002b), being able to detect a 0.5 % amorphous content. The use of this technique in early stages of the active development program allowed the authors to assess fully the impact of so small amorphous quantities on the quality attribute of the formulation.

4.2.2. AIMS OF THE STUDY

This study aimed to investigate the effect of the anomeric composition of both crystalline and amorphous lactose on the quantification of small amorphous contents by Isothermal Relative Humidity Perfusion Microcalorimetry. The crystallisation response of amorphous lactose of different anomeric composition as induced by Isothermal Perfusion Microcalorimetry was also evaluated. This study also aimed to establish the best methodology for quantification of amorphous content by Isothermal Relative Humidity Perfusion Microcalorimetry.

4.2.3. EXPERIMENTAL

4.2.3.1. PREPARATION OF AMORPHOUS LACTOSE

Amorphous lactose was prepared by spray drying as described in Section 2.2.1.3. Commercial α-lactose monohydrate (consisting of 94% (w/w) α-lactose and 6% (w/w) β-lactose) and commercial β-lactose (consisting of 84% (w/w) α-lactose and 6% (w/w) β-lactose) were used to prepare 10% (w/w) lactose solutions. These were equilibrated at 25 °C and 85 °C and spray dried to produce amorphous lactose batches of different anomeric composition (Figure 4.1). Confirmation of the amorphous nature was obtained from XRPD as outlined in Section 2.2.6.3. Anomeric composition was determined by gas chromatography according to the method described in Section 2.2.7.3.

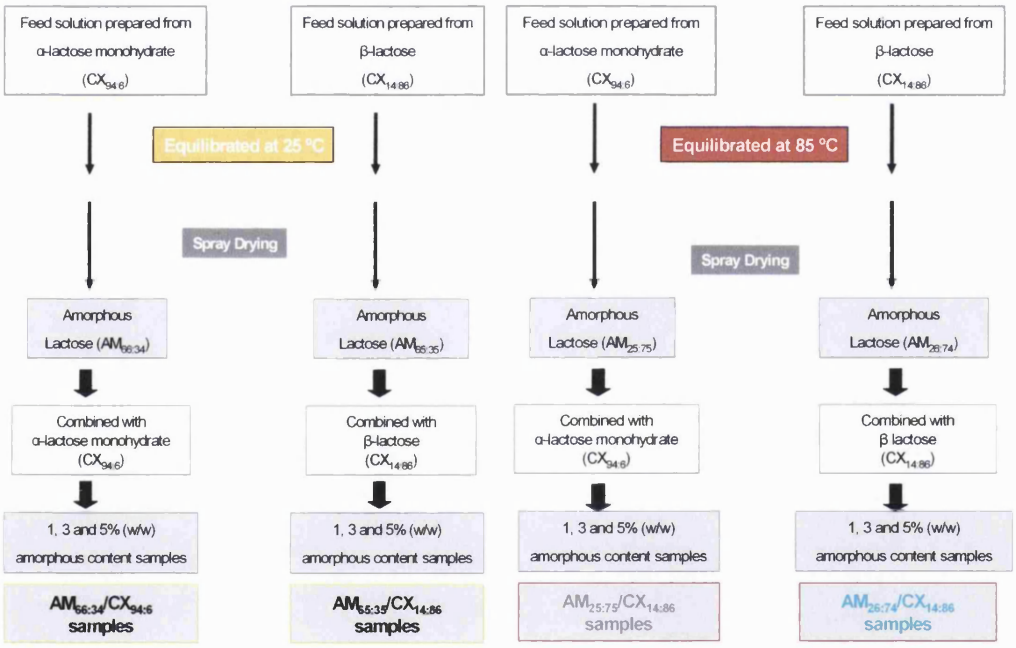

Figure 4.1 Schematic representation of the preparation of the amorphous lactose batches and partially amorphous lactose samples used throughout the present study. CX represents the crystalline material, AM the amorphous material and AM/CX the partially amorphous samples. The anomeric composition (α-lactose and β-lactose content as % w/w) of each crystalline, amorphous and partially amorphous (both amorphous and crystalline portions) sample is given by the subscript numbers as α:β.

4.2.3.2. PREPARATION OF PARTIALLY AMORPHOUS LACTOSE SAMPLES

Partially amorphous samples were prepared by directly weighing proportional masses of appropriate amorphous and crystalline lactose (Figure 4.1) into the 4 mL stainless steel relative humidity perfusion sample ampoule. Each amorphous batch was mixed with α-lactose monohydrate or β-lactose, according to which crystalline material had been used in its preparation (Figure 4.1). The mass of the crystalline component was kept constant in all mixtures (50 ± 0.01 mg) and an appropriate amount of amorphous material was added to make 1, 3 and 5% amorphous samples. Both crystalline and amorphous materials were passed through a sieve stack prior to weighing and only the <425 μm fraction was used. Samples were made homogeneous by rotating and tapping the ampoule. An alternative approach would have been to sample from a larger batch that had been mixed in a turbula mixer. This method might reduce the weighing error but there is the possibility of amorphous material adhering to the mixing vessel walls, which at such amorphous content introduces a greater error.

4.2.3.3. PREPARATION OF CRYSTALLINE SAMPLES

Prior to analysis of their wetting response by isothermal relative humidity perfusion calorimetry, crystalline α-lactose monohydrate and -lactose were passed through a sieve stack and only the <425 μm fraction was used.

4.2.3.4. ISOTHERMAL RELATIVE HUMIDITY PERFUSION MICROCALORIMETRY

Details of the experimental set up can be found in Section 2.2.2.3.2. A 2250 Micro Reaction RH Perfusion Insertion Vessel (Thermometric AB, Järfälla, Sweden), designed to use in conjunction with the air and water bath of the Thermometric Thermal Activity Monitor (TAM, Thermometric AB, Järfälla, Sweden), was used throughout this study. The samples were prepared directly into the 4 mL stainless steel sample ampoule as described above. The reference used was an identical 4 mL stainless steel ampoule, held on an ampoule lifter. The humidifier chambers were filled with 0.5 mL of purified water. The flow switch heater was set to 40 °C to prevent condensation of water within the unit. A nitrogen gas flow of 120 mL/h was directed down either the wet line (to become 100% RH) or dry line (0% RH) in varying proportions in order to achieve the desired RH. Samples were kept at 0% RH until dry (5h), which was achieved when the power-time signal reached a steady baseline. The drying step was followed by exposure to 90% RH for a period of time long enough to allow crystallisation to reach completion, which was verified when the power-time signal reached a steady baseline. Partially amorphous samples were subjected 90% RH for 10 h and amorphous lactose samples were subjected to 90% RH for 34 hours. After exposure to high relative humidity, partially amorphous samples were subjected to a final drying step of 5 hours at 0% RH and amorphous samples were dried for 10h at 0% RH, which was long enough to allow complete desorption. Crystalline samples were subjected to the same RH programme as partially amorphous samples. Calibrations were carried out before each experiment as described in Section 2.2.2.4.2. Data was collected via Digitam 4.1 (Thermometric AB, Järfälla, Sweden) and analysed using Origin 7.0 (Microcal software Inc., USA).

4.2.3.5. GAS CHROMATOGRAPHY

Amorphous and crystalline lactose samples were prepared for gas chromatography analysis as outlined in Section 2.2.7.3.1 and analysed in a CP9001 Gas Chromatograph (Varian-Chrompack, Oxford, UK) as described in Section 2.2.7.3.2 for quantification of their anomeric composition. Data were collected and analysed for peak area calculation by means of the dedicated Prime software (HPLC Technology Ltd, Herts, UK).

4.2.4. RESULTS AND DISCUSSION

4.2.4.1. APPROACHES TO DETERMINE THE AMORPHOUS CONTENT BASED ON THE DETERMINATION OF THE ENTHALPY OF CRYSTALLISATION FROM RELATIVE HUMIDITY PERFUSION DATA

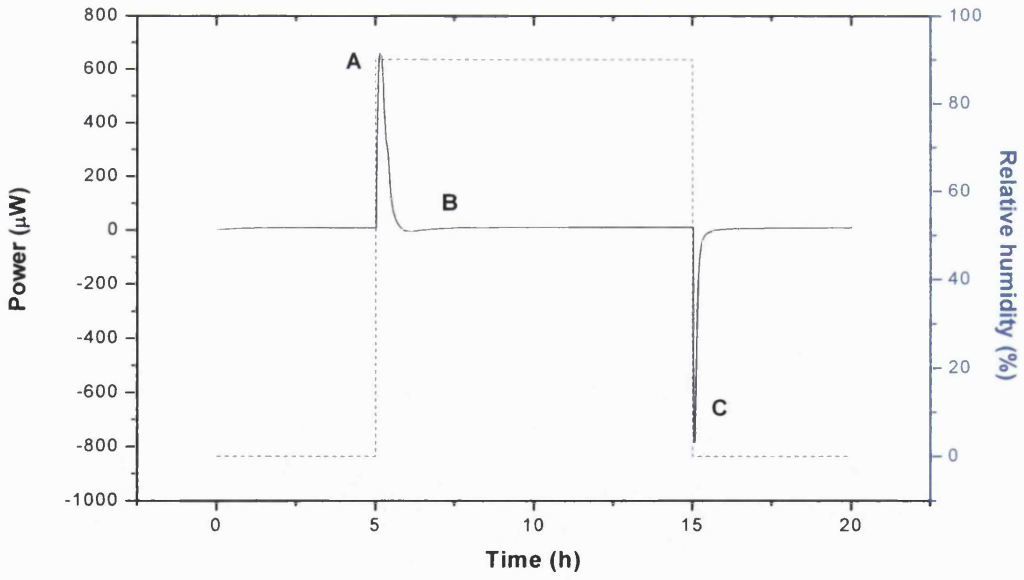

Figure 4.2 *Power time data of the wetting+crystallisation (A) and drying (C) of 50 mg of a 3% (w/w) amorphous $AM_{66:34}/CX_{94:6}$ sample exposed to 5h at 0% RH, 10h at 90% RH and 5h at 0%RH, at 25 °C.*

In this study we opted to use an isothermal relative humidity perfusion unit to initiate crystallisation of amorphous and partially amorphous lactose samples because it allows external control of the relative humidity to which the sample is exposed, obviating problems of data loss of the initial wetting and crystallisation. However, it also requires a different approach to data analysis. This is because, once the RH has been elevated, all the internal surfaces of the ampoule, as well as the sample, are wetted, which produces a large exothermic heat signal that often occurs over a time-period that is longer than the time required for the sample to crystallise. In effect, the crystallisation signal can be obscured by the wetting response; an example of this is shown by the response of a 3% w/w $AM_{66:34}/CX_{94:6}$ sample (containing amorphous lactose with 66% w/w α-lactose and crystalline lactose containing 94% w/w α-lactose) which is represented in Figure 4.2 (the wetting and crystallisation peak is denoted A). There are four ways of resolving this issue in order to determine the crystallisation signal;

i) Assume that the wetting response is uniform in all samples and measure the total heat released once the RH is increased.
ii) Determine the wetting response of the empty ampoule in a separate experiment and subtract this value from the experimental data.
iii) Determine the wetting response of an equivalent mass of the crystalline material in a separate experiment and subtract it from the experimental data.
iv) Return the system to 0% RH after crystallisation and subtract the drying response from the wetting and crystallisation response.

Method (i) does not allow a quantitative assessment of the enthalpy of crystallisation while method (ii) does not compensate for the wetting response of the sample, which may become significant with larger sample masses; these methods were therefore discarded. Method (iii) compensates for the wetting response of the crystalline component of the sample (and ignores the wetting of the amorphous material) while method (iv) compensates for the wetting response of the entire sample (although it is noted that the sample that wets, partially amorphous, differs slightly from that dries, crystalline); in both cases it is assumed that the errors are negligible which is reasonable for the standards used to prepare the calibration plots

but may be an issue for processed samples. Accordingly, calibration curves were prepared using methods (iii) (Section 4.2.4.2) and (iv) (Section 4.2.4.3).

4.2.4.2. QUANTIFICATION OF THE AMORPHOUS CONTENT BASED ON THE DETERMINATION OF THE ENTHALPY OF CRYSTALLISATION BY DETERMINING THE WETTING RESPONSE OF AN EQUIVALENT MASS OF CRYSTALLINE MATERIAL AND SUBTRACTING IT FROM THE EXPERIMENTAL DATA (METHOD III)

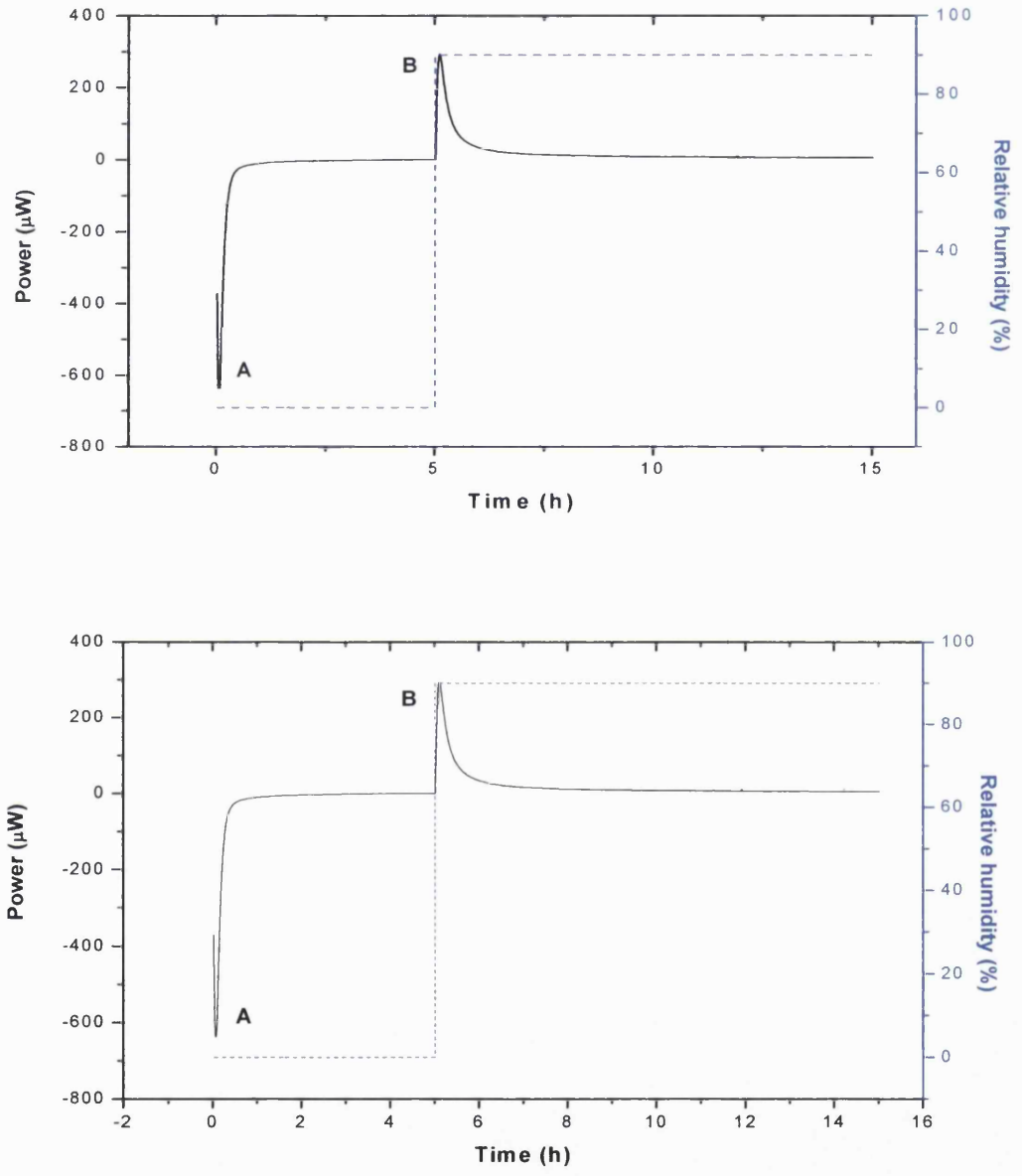

Figure 4.3 *Power-time data for the wetting response of a 50 mg sample of $CX_{94:6}$ (containing 94% α-lactose, top) and $CX_{14:86}$ (containing 14% w/w of α-lactose, bottom) as recorded by drying the samples at 0% RH for 5h and exposing to 90% RH for 10h at 25 °C. _____ Sample response _ _ _ _ RH Change.*

In order to quantify amorphous content in lactose samples using the described method (iii), two sets of partially amorphous lactose samples were induced to crystallise by isothermal RH perfusion ampoule; namely the two sets of samples described as $AM_{66:34}/CX_{94:6}$ (composed of amorphous lactose containing 66% w/w α-lactose ($AM_{66:34}$) and crystalline lactose containing 94% w/w α-lactose ($CX_{94:6}$), Figure 4.1) and $AM_{65:35}/CX_{14:86}$ (composed of amorphous lactose containing 65% w/w α-lactose ($AM_{65:35}$) and crystalline lactose containing 14% w/w α-lactose ($CX_{14:86}$), Figure 4.1). The exothermic peak denoted A in Figure 4.2 represents the wetting, water absorption into the amorphous portion and crystallisation of a 3% (w/w) $AM_{66:34}/CX_{94:6}$ sample. In addition to that, the wetting of both crystalline lactoses, $CX_{94:6}$ and $CX_{14:86}$, was also determined; Figure 4.3 represents a typical wetting response of both crystalline lactoses.

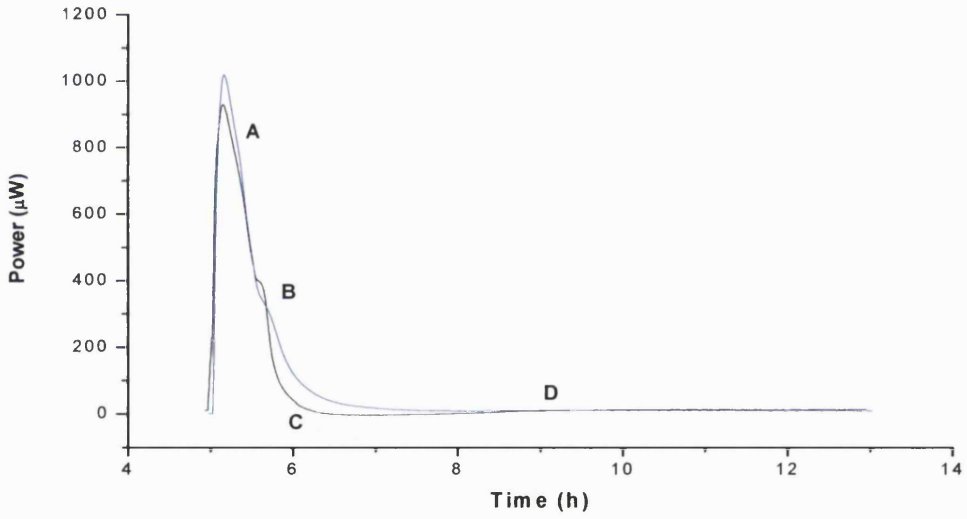

Figure 4.4 *Power-time data obtained via method iii (subtraction of the crystalline wetting response from the experimental data) for 5% (w/w) amorphous lactose samples. _____ $AM_{66:34}/CX_{94:6}$ _____ $AM_{65:35}/CX_{14:86}$ A represents the main crystallisation peak with the shoulder B. C is an endothermic region seen only for $AM_{66:34}/CX_{94:6}$ samples and D indicates the point when the power signal achieved baseline again.*

Subtraction of the wetting response of the correspondent crystalline material (denoted B in Figure 4.3) from the wetting and crystallisation response of each sample (denoted A in Figure 4.2) resulted in a peak as the one shown in Figure 4.4; it should be noted that for $AM_{66:34}/CX_{94:6}$ and $AM_{65:35}/CX_{14:86}$ samples, the wetting of $CX_{94:6}$ and $CX_{14:86}$ were used, respectively.

From Figure 4.4 it can be seen that the crystallisation response shows a sequence of areas; a main peak (A) followed by a shoulder (B) and, in the case of $AM_{66:34}/CX_{94:6}$ sample a final endothermic peak (C) can be seen before the signal returns to baseline (D). The endothermic region C was observed for all $AM_{66:34}/CX_{94:6}$ samples. The peaks are most certainly the result of simultaneous processes. The first main peak (A) can be the result of water absorption into the sample and crystallisation. It is known that the crystallisation of lactose can be accompanied by a number of events such as mutarotation (Angberg et al., 1991) and/or water incorporation into the crystal lattice (Angberg et al., 1991) which might explain the shoulder (B). Using batch isothermal microcalorimetry, Dilworth et al (2004) showed that the best approach for determination of the enthalpy of crystallisation consisted in including all the endothermic and exothermic phases of the crystallisation response in the integration methodology. Despite the fact that the crystallisation response obtained by isothermal RH perfusion microcalorimetry differs from that obtained by batch isothermal microcalorimetry, in this study it was chosen to integrate the area under the curve from the initial baseline until the power signal returned to a baseline after crystallisation (marked by letter D in Figure 4.4). This integration methodology includes all the events accompanying crystallisation and avoids problems of identifying the endpoint of the different phases.

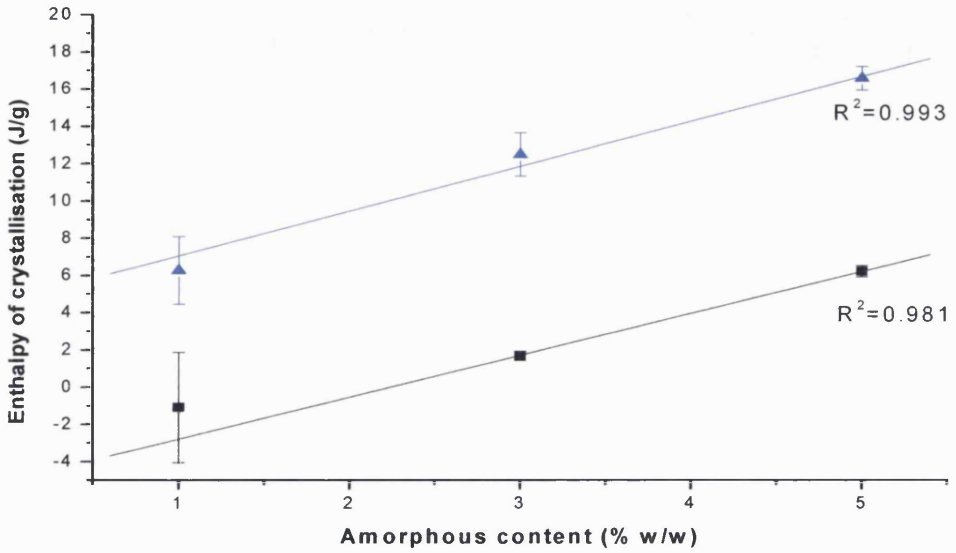

Figure 4.5 *Calibration curves for quantification of amorphous content prepared using method iii. The lines are linear regression fits.* ■ *$AM_{66:34}/CX_{94:6}$ samples* ▲ *$AM_{65:35}/CX_{14:86}$ samples*

Based on the fact that the energy released during crystallisation is proportional to the amorphous content, the enthalpy of crystallisation was used for construction of the calibration curve for $AM_{66:34}/CX_{94:6}$ and $AM_{65:35}/CX_{14:86}$ samples by plotting the determined enthalpy of crystallisation versus the known amorphous content for each set of samples. Two clearly distinct calibration curves were obtained (Figure 4.5); a discussion of the impact of this on the quantification of amorphous content is given in Section 4.2.4.6.

A few issues can be discussed from the observation of the calibration curves constructed using method (iii) (Figure 4.5). The enthalpy of crystallisation (average, n=3) of 1% $AM_{66:34}/CX_{94:6}$ sample was calculated as -1.1 J/g ($\forall$ 3.0), which causes the calibration curve to intercept the y axes below zero. This value was obtained by subtracting the enthalpy of wetting of the crystalline $CX_{94:6}$ from the experimental data. The enthalpy of wetting of crystalline $CX_{94:6}$ was determined as 12.7 $\pm$ 0.08 J/g (n=3). However, the enthalpy of wetting of the $AM_{66:34}/CX_{94:6}$ samples, determined as enthalpy of desorption by drying the sample after crystallisation (Section 4.2.4.3) was 8.7 $\pm$ 1.6 J/g. The difference in enthalpy of wetting of crystalline $CX_{94:6}$ and

$AM_{66:34}/CX_{94:6}$ samples suggests that the wetting of the crystalline $CX_{94:6}$ does not represent the wetting of the partially amorphous sample.

The calibration curve constructed from the $AM_{65:35}/CX_{14:86}$ samples does not tend to a y-intercept value of zero with no amorphous material present; this effect was more dramatic when using method (iv) (Section 4.2.4.3). Although this observation initially seems counter-intuitive, one explanation for this discrepancy may be the fact that β-lactose is known to mutorotate to α-lactose under elevated RH conditions and original and newly formed α-lactose can incorporate water into its crystal lattice to form α-lactose monohydrate, processes that occur simultaneously and are accompanied by a heat loss (exothermic) (Angberg et al., 1992a). These being so, mutarotation and water incorporation in both crystalline and amorphous portions of the partially amorphous samples during crystallisation and of the crystalline standard during wetting may well differ. In this case, the mutarotation and water incorporation in the sample might have happened in a greater extent than that of the wetted crystalline material, which might be because of the faster water uptake by the amorphous material. This resulted in a net exothermic addition to the measured response during wetting and crystallisation of the sample that is only partially compensated for using method (iii). In addition to that, as it has previously been shown (Chapter 3), amorphous lactose can crystallise to a higher amount of β-lactose when in the presence of crystalline $CX_{14:86}$. This might also account for the higher enthalpy of crystallisation observed for $AM_{65:35}/CX_{14:86}$ samples, because of the higher enthalpy of crystallisation of β-lactose (enthalpy of fusion of β-lactose is ~197 J/g, while the enthalpy of fusion of α-lactose is ~169 J/g; both estimated by DSC, Section 3.4.3). The enthalpy of wetting of crystalline $CX_{14:86}$ (12.9 ± 0.32 J/g, n=3) more closely resembles the enthalpy of wetting of $AM_{65:35}/CX_{14:86}$ samples (11.3 ± 2.1 J/g, determined as enthalpy of desorption by drying the sample after crystallisation). Consequently, the enthalpy of wetting of crystalline $CX_{14:86}$ does not seem to contribute to the higher enthalpy of crystallisation observed for $AM_{65:35}/CX_{14:86}$ samples.

A further reason for the lower enthalpies of crystallisation observed for $AM_{66:34}/CX_{94:6}$ samples is the fact that the power-time curve of these samples shows an endothermic region (denoted C in Figure 4.4) that was included in the determination of the heat-output associated with crystallisation, resulting in a net endothermic addition to the measured response during crystallisation. This endothermic region is

normally attributed to the expulsion of plasticising water. In a recent study, Timmermann et al. (2006) attributed the existence of such an endothermic region to the fact that the sample was crystallising to an anhydrate, and not using the plasticising water to form the monohydrate. Such an endothermic region was not observed for $AM_{65:35}/CX_{14:86}$ samples, which contain a higher percentage of crystalline β-lactose. It is possible that mutarotation of β- to α-lactose and/or water incorporation into the crystal lattice of newly formed and original α-lactose (simultaneous processes with an overall exothermic heat output) and crystallisation to β-lactose compensate for the endothermic water expulsion (crystallisation to β-lactose is a more exothermic process than crystallisation to α-lactose and was seen to proceed to a higher extent in $AM_{65:35}/CX_{14:86}$ samples). On the other hand, as discussed in Chapter 3, $AM_{66:34}/CX_{94:6}$ samples are preferentially crystallising to α-lactose, which is a less exothermic process than crystallisation to β-lactose. Consequently, in the $AM_{66:34}/CX_{94:6}$ samples crystallisation and the water incorporation into the crystal lattice of α-lactose do not compensate for the endothermic water expulsion.

4.2.4.3. QUANTIFICATION OF THE AMORPHOUS CONTENT BASED ON THE DETERMINATION OF THE ENTHALPY OF CRYSTALLISATION BY RETURNING THE SYSTEM TO 0% RH AFTER CRYSTALLISATION AND SUBTRACTING THE DRYING RESPONSE FROM THE WETTING/CRYSTALLISATION RESPONSE (METHOD IV)

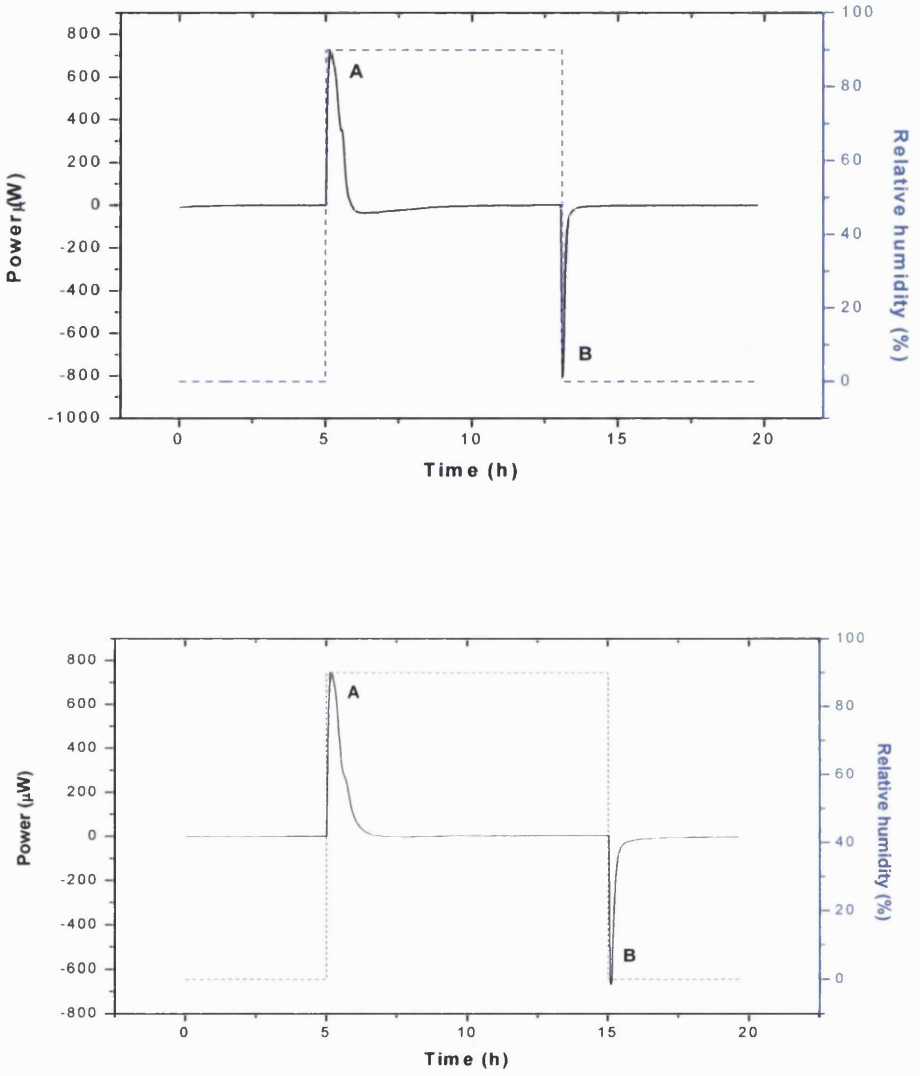

Figure 4.6 *Power time data of the wetting+crystallisation (A) and drying (B) of a 50 mg 5% (w/w) amorphous* $AM_{66:34}/CX_{94:6}$ *(top) and of a 50mg 5% (w/w) amorphous* $AM_{65:35}/CX_{14:86}$ *sample (bottom), as recorded by exposing the samples to 0% RH for 5h, 90% RH for 10h and 0% RH for 5h at 25 °C. _____ Sample response _ _ _ _ RH change.*

In order to quantify the amorphous content in lactose samples using the described method (iv), two sets of partially amorphous lactose samples were induced to crystallise by exposure to elevated RH in a isothermal RH perfusion ampoule; namely the two sets of samples described as $AM_{66:34}/CX_{94:6}$ and $AM_{65:35}/CX_{14:86}$. The exothermic peaks denoted A in Figure 4.6 represent wetting, water absorption into the amorphous portion and crystallisation of a 5% (w/w) amorphous $AM_{66:34}/CX_{94:6}$ sample (top) and a 5% (w/w) $AM_{65:35}/CX_{14:86}$ sample (bottom). After the period at elevated RH, long enough for crystallisation of the sample, confirmed by the achievement of a baseline during this period, the crystallised sample was exposed to 0% RH. At these conditions, the sample dried and all the remaining free sorbed water was released, producing an endothermic peak (denoted B in Figure 4.6). The enthalpy of desorption can be determined from peak B. The use of method (iv) for the determination of the crystallisation response is based on the fact that desorption (drying) generates a heat flow which is equal but opposite to that of the wetting response.

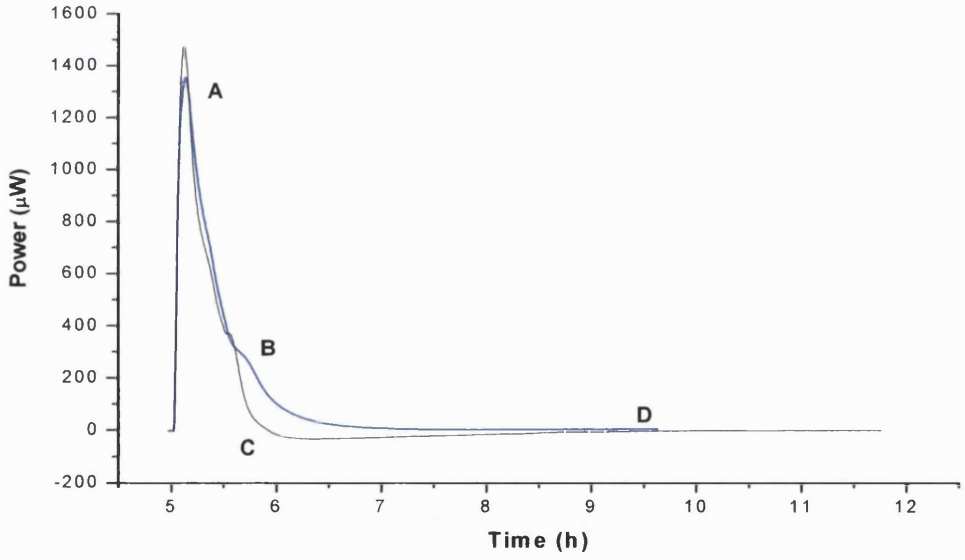

Figure 4.7 *Power-time data obtained via method iv (subtraction of the drying response from the wetting response of the partially amorphous sample) for a 50mg 5% (w/w) amorphous lactose sample at 25 °C.* _____ *$AM_{66:34}/CX_{94:6}$ sample* _____ *$AM_{65:35}/CX_{14:86}$ sample. A represents the main crystallisation peak with the shoulder B. C is an endothermic region only seen for $AM_{66:34}/CX_{94:6}$ samples and D indicates the point when the power signal returned to baseline.*

Subtraction of the drying response of each sample (denoted B in Figure 4.6) from the wetting and crystallisation response of each sample (denoted A in Figure 4.6) resulted in a peak as the one shown in Figure 4.7. Once again, it can be seen that the crystallisation response shows a sequence of areas; a main peak (A) followed by a shoulder (B) and, in the case of α-lactose samples a final endothermic peak (C) can be seen before the signal returns to baseline (D). As already mentioned, these areas are most certainly the result of simultaneous processes. The first main peak (A) can be the result of water absorption into the sample and crystallisation, while shoulder (B) can be due to mutarotation and/or water incorporation into the crystal lattice (Angberg et al., 1991). As for method (iii), it was chosen to integrate the area under the curve from the initial baseline until the power signal returned to a baseline after crystallisation (marked by letter D in Figure 4.7). This integration methodology includes all the events accompanying crystallisation and avoids problems of identifying the endpoint of the different phases.

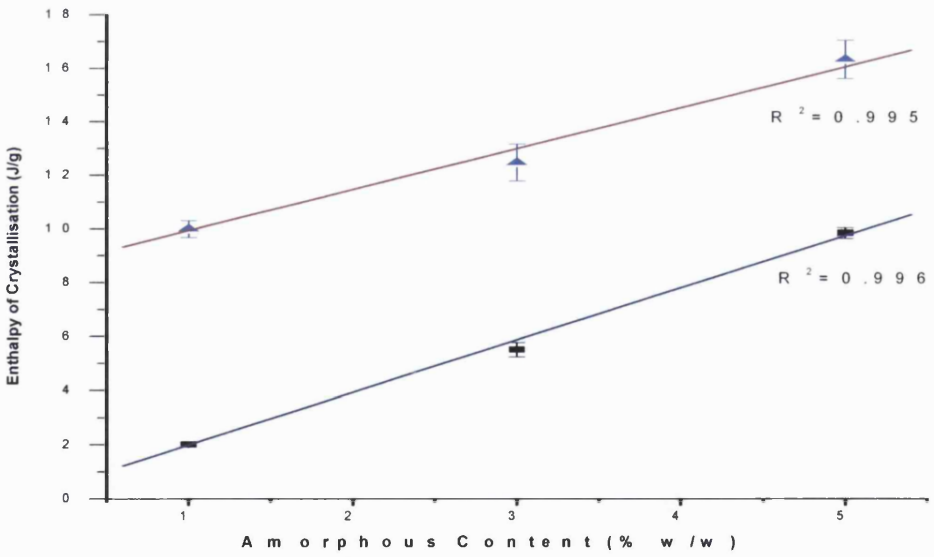

Figure 4.8 *Calibration curves for the two lactose batches prepared using method iv. The lines shown are linear regression fits.* ■ $AM_{66:34}/CX_{94:6}$ *samples* ▲ $AM_{65:35}/CX_{14:86}$ *samples.*

Based upon the fact that the energy released during crystallisation is proportional to the amorphous content, the enthalpy of crystallisation was used for construction of

the calibration curve for $AM_{66:34}/CX_{94:6}$ and $AM_{65:35}/CX_{14:86}$ samples by plotting the determined enthalpy of crystallisation versus the known amorphous content for each set of samples. Once again, two clearly distinct calibration curves were obtained (Figure 4.8); a discussion of the impact of this on the quantification of amorphous content is given in Section 4.2.4.6.

As before, Figure 4.8 brings out a few points for consideration. Once again the calibration curve obtained from $AM_{65:35}/CX_{14:86}$ samples does not tend to a y-intercept value when no amorphous content is present. In addition, the calibration curve constructed from $AM_{66:34}/CX_{94:6}$ samples more closely approaches the zero y-intercept value when no amorphous content is present, although it does not exactly do so; for zero amorphous content, the calibration curve would return an enthalpy of crystallisation of 0.05 J/g. The α-lactose monohydrate ($CX_{94:6}$) used as the crystalline portion of $AM_{66:34}/CX_{94:6}$ samples is the most stable form of lactose. However it contains around 6% of β-lactose that can indeed mutorotate to α-lactose, which can incorporate water into its crystal lattice to form the monohydrate (Angberg et al., 1991); these are simultaneous processes that are accompanied by a heat loss (exothermic) (Angberg et al., 1991). The smaller deviation from zero enthalpy at zero amorphous content verified for the $AM_{66:34}/CX_{94:6}$ samples might be explained by the less mutarotation and water incorporation in these samples, when compared with samples containing $CX_{14:86}$. The mutarotation and water incorporation events are not cancelled out at all when using method (iv) of data manipulation. This is because during the drying of the sample mutarotation does not take place, as β- to α-lactose mutarotation and water incorporation are known to occur at elevated RH. In addition to that, as already mentioned, amorphous lactose crystallises to a higher amount of β-lactose when in presence of crystalline lactose containing a higher percentage of β-lactose ($CX_{14:86}$, which contains 86% β-lactose) (Chapter 3). Thus, because of the higher enthalpy of crystallisation of β-lactose might account for the higher enthalpy of crystallisation observed for $AM_{65:35}/CX_{14:86}$ samples, whose crystalline portion consists of crystalline lactose containing 86% (w/w) β-lactose.

As previously mentioned and discussed in Section 4.2.4.2, a further reason for the lower enthalpies of crystallisation observed for $AM_{66:34}/CX_{94:6}$ samples is the fact that the power-time curve of these samples shows an endothermic region (denoted C in Figure 4.7).

4.2.4.4. COMPARISON OF METHODS (III) AND (IV). LIMITATIONS OF ISOTHERMAL CALORIMETRY METHODS

As already mentioned, the fact that during the period at elevated RH both wetting and crystallisation responses will take place, requires the subtraction of the wetting response so that the enthalpy of crystallisation can be determined. Two methods of data analysis were investigated, namely method (iii) that consisted in determining the wetting response of an equivalent mass of the crystalline material in a separate experiment and subtract it from the experimental data and method (iv) that consisted in returning the system to 0% RH after crystallisation and subtracting the drying response from the wetting response.

As discussed, none of the methods accounts for all the events occurring during wetting. Method (iii) compensates for the wetting response of the crystalline component of the sample but ignores the wetting of the amorphous material. Method (iv) compensates for the wetting response of the entire sample, although it should be noted that the sample that wets, partially amorphous, differs slightly from that which dries, crystalline. In the case of lactose, mutarotation can happen when both crystalline and amorphous materials are exposed to elevated RH. Method (iii) can partially account for the mutarotation of the crystalline portion of the sample, while method (iv) does not account for mutarotation at all.

Although method (iv) does not account for all the events taking place during wetting, mutarotation and/or water incorporation, comparison of the standard deviations listed in Table 4.1 reveals that method (iv) returned the lowest standard deviation values, and would thus be recommended for future studies of quantification of amorphous content by isothermal RH perfusion microcalorimetry.

Table 4.1 *Enthalpy of crystallisation data (∀S.D.) for the two sets of samples determined using methods (iii) and (iv) (n=3) using the two methods of data analysis..*

Samples n=3	Amorphous content % (w/w)	H_{cryst}(J/g)	
		Method (iii)	Method (iv)
$AM_{66:34}/CX_{94:6}$	1	-1.1 ± 3.0	2.0 ± 0.1
	3	1.7 ± 0.2	5.5 ± 0.3
	5	6.2 ± 0.3	9.8 ± 0.2
$AM_{65:35}/CX_{14:86}$	1	6.3 ± 1.8	10.0 ± 0.3
	3	12.5 ± 1.2	12.5 ± 0.7
	5	6.2 ± 0.3	16.3 ± 0.7

An additional problem with isothermal calorimetry methodologies is that the nature of the amorphous standards used to prepare the calibration curves do not mimic the physical nature of processed materials (i.e. the standards comprise particles that are either wholly amorphous or wholly crystalline while a processed material is likely to comprise smaller particles (and hence have greater surface area) consisting of crystalline cores with an outer corona of amorphous material. This raises a number of concerns. Firstly, the difference in surface area mean that the rate of water absorption will be different in a processed material than the calibration standards; necessarily, this will manifest itself as a change in the kinetic response of the sample during analysis although, as net areas are measured, should not affect the enthalpy obtained.

Secondly, a greater problem is likely to be that the wetting response of a processed sample will (in effect) be that of a wholly amorphous material while that of a standard approximates to the wetting response of a crystalline material (especially at lower amorphous contents). This is important because, using method (iv), the drying response (of the now crystalline material) is subtracted from the wetting and crystallisation response (of the processed material). Thus, if the wetting enthalpies of the amorphous and crystalline forms are different, it is likely that the amorphous content predicted from the calibration plot will be affected by a systematic error.

Finally, the amorphous material in a processed material is sited directly on top of a crystalline substrate, which acts as a seed, which means that secondary nucleation predominates. In the material used for calibration, the amorphous and crystalline particles are discreet entities, which means that primary nucleation may occur. This

requires an almost saturated vapour space, presumably because more water needs to be absorbed to plasticise the sample sufficiently to induce nucleation and crystallisation. To a large degree, the data presented above and in Chapter 3 suggest that the crystalline particles do act as a seed, allowing secondary nucleation, because at such low amorphous contents, they considerably outnumber the amorphous particles; this effect will, however, diminish as the proportion of amorphous material increases.

4.2.4.5. DETERMINATION OF ENTHALPY OF CRYSTALLISATION OF FULLY AMORPHOUS LACTOSE WITH DIFFERENT ANOMERIC COMPOSITION

Amorphous lactose batches (n=3), $AM_{65:35}$ and $AM_{25:75}$ were dried at 0% RH for 5 hours and then induced to crystallise by exposure to 90% RH and, once crystallisation was complete, dried at 0%RH. The enthalpy of crystallisation was determined in triplicate for each batch. Upon exposure to elevated RH, an exothermic process began (peaks A in Figure 4.9) which represents the wetting and water absorption into the amorphous sample. The very sharp peak is due to the fact that the sample had previously been held at 0% RH and was therefore very dry.

Following approximately 5 hours, a second exothermic event was observed (represented by peak B in Figure 4.9), which is due to the crystallisation of the sample. In opposition to partially amorphous samples, fully amorphous samples exhibit a clear separated peak for crystallisation, which is, however, very short (approximately 1h). This exothermic peak was followed by a 19h long endothermic signal (represented by C in Figure 4.9), which was caused by the expulsion of plasticising water by the sample. After crystallisation and water expulsion, the RH was returned to zero in order to allow the crystallised sample to dry, which is an endothermic event denoted D in Figure 4.9.

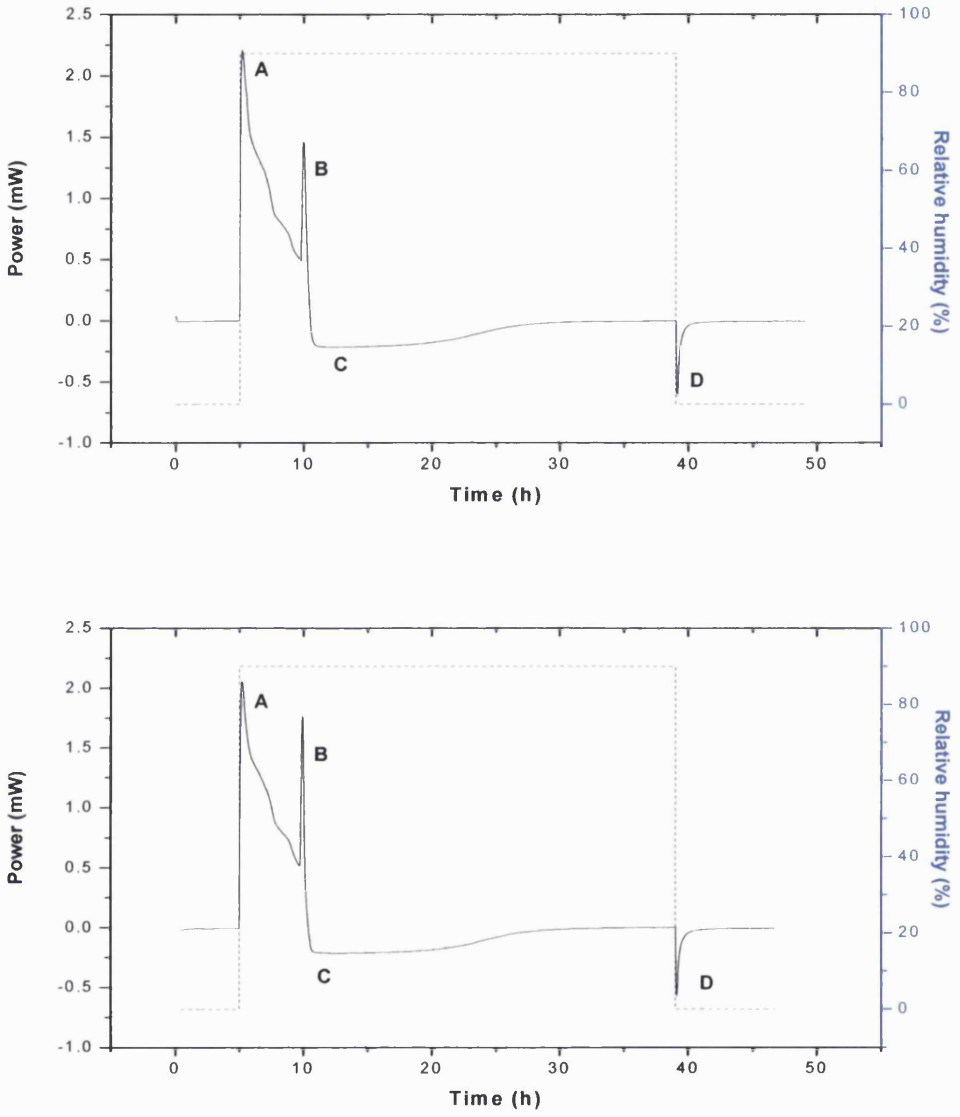

Figure 4.9 *The drying, wetting and crystallisation and final drying calorimetric response of fully amorphous lactose* $AM_{65:35}$ (top) and $AM_{25:75}$ (bottom), as recorded by exposing the samples to 0% RH for 5h, 90% RH for 34h and 0%RH for 10h *at 25 °C. _____Sample response. _ _ _ _RH change. A represents wetting, B represents crystallisation, C represents water expulsion and D represents drying.*

In order to determine the enthalpy of crystallisation of $AM_{65:35}$ and $AM_{25:75}$ batches, the drying response of each sample (denoted D in Figure 4.9) was subtracted from the wetting and crystallisation response (denoted A and B in Figure 4.9), following method (iv) of data analysis. This resulted in the response shown in Figure 4.10.

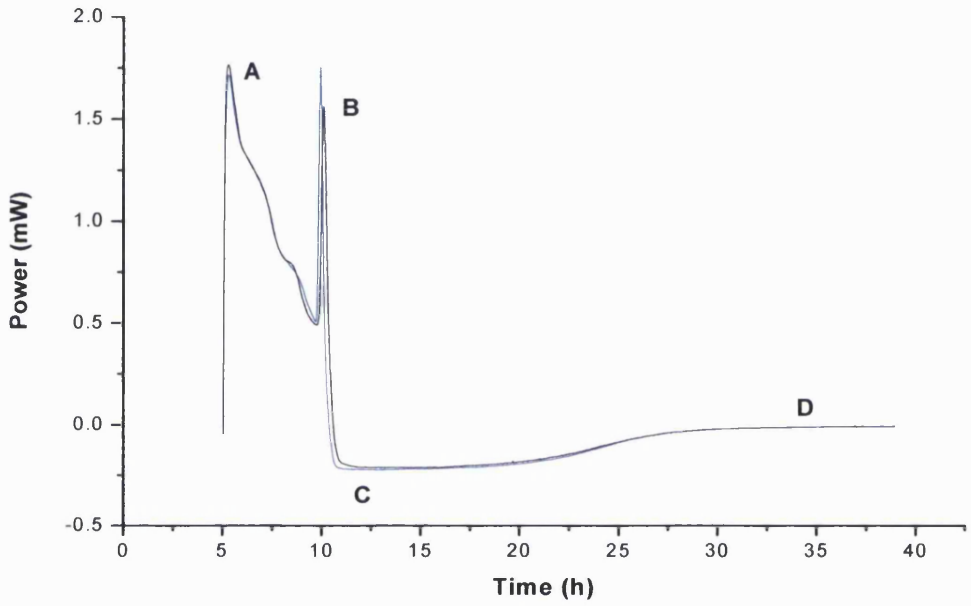

Figure 4.10 *Power-time data obtained via method iv (subtraction of the drying response from the wetting response of the fully amorphous lactose samples).* _____ $AM_{65:35}$ *batch* _____ $AM_{25:7}$ *batch. Peak A represents water absorption, B is the main crystallisation peak, C is an endothermic region caused by water expulsion and D indicates the point when the power signal returned to baseline.*

The peaks represented in Figure 4.10 correspond now to slightly different processes than those represented in Figure 4.9. Peak A results from the subtraction of the drying response from the wetting and crystalline response, and it now represents the water absorption into the amorphous sample. In partially amorphous samples, peaks A and B are overlapped, making it difficult to identify the crystallisation peak. However, for these fully amorphous samples, a water absorption and crystallisation peaks are only partially overlapped, and an exothermic crystallisation peak could be

identified (peak B). As before, endothermic area C represents water expulsion from the crystallised sample.

If no water is incorporated into the crystal lattice during crystallisation, water expulsion by the crystalline sample should be equal but opposite to water absorption by the initial amorphous sample, and consequently, water absorption and expulsion should cancel each other out. However, water incorporation into the crystal lattice of α-lactose does take place during crystallisation from the amorphous state; fully amorphous lactose crystallises to approximately 3% (w/w) α-lactose monohydrate. As such, the total energy resulting from the integration of the all areas of Figure 4.10 corresponds to crystallisation and any other simultaneous processes to crystallisation such as mutarotation and/or water incorporation. This integration methodology can be considered a valid approach because of the impossibility of clearly ascertaining the beginning and end of the crystallisation signal.

The $AM_{65:35}$ batches exhibited an enthalpy of crystallisation of 211.3 ± 1.9 J/g (n=3) and the $AM_{25:75}$ amorphous batches exhibited an enthalpy of crystallisation of 200.6 ± 1.3 J/g (n=3). Partially, the difference observed might be because the $AM_{25:75}$ batches (richer in β-lactose) is crystallising to a higher content of α-lactose, as previously seen in Chapter 3. Enthalpy of crystallisation of α-lactose (~169 J/g) is lower than the enthalpy of crystallisation of β-lactose (~197 J/g), as already reported in Chapter 3. It should be noted that the determined enthalpies of crystallisation are a sum of many simultaneous endo- and exothermic processes, and any conclusion on the recrystallisation behaviour of fully or partially amorphous lactose should be carefully drawn.

It is important to note that the crystallisation response as determined by isothermal perfusion microcalorimetry differs from that obtained by batch isothermal microcalorimetry. This is for a number of reasons. Firstly, in the isothermal perfusion microcalorimetry ampoule, the solvent vapour is generated outside the sample ampoule, and, consequently, the wetting and sorption by the sample can be detected in an isothermal perfusion microcalorimetry experiment. It has been suggested (Angberg et al., 1991 and 1992a) that in the batch isothermal microcalorimetry set up this is not seen, or is at least diminished, due to the fact that the generation of solvent vapour (*i.e.* evaporation from the salt solution reservoir within the ampoule) generates a heat flow which is equal but opposite of that of the

wetting response. It is also possible that the constant availability of humidified gas flow facilitates further reactions in the sample, such as mutarotation and water incorporation. In addition, since there is a constant flow of gas through the isothermal perfusion microcalorimetry ampoule, once expelled, the plasticising water is removed from the ampoule and therefore a condensation response does not contribute to the overall response detected. The constant flow of gas through the isothermal perfusion microcalorimetry ampoule facilitates wetting and crystallisation and, consequently, the time necessary to the onset of crystallisation is shorter than that observed in a batch calorimetric experiment at the same relative humidity.

4.2.4.6. Effect of anomeric composition of both crystalline and amorphous lactose, on the quantification of amorphous content of partially amorphous lactose samples

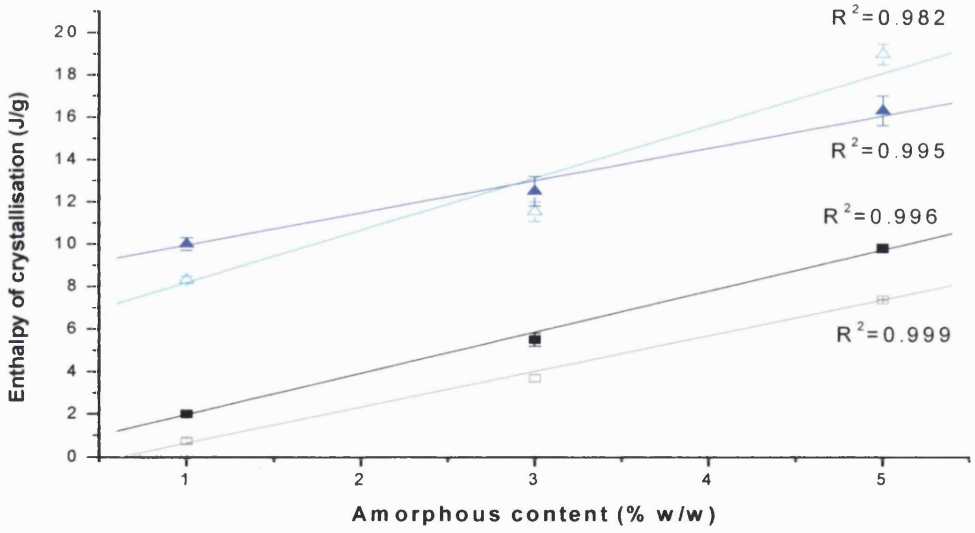

Figure 4.11 *Calibration curves of the four sets of data prepared using method iv. Lines represent linear regression fits.* ■ $AM_{66:34}/CX_{94:6}$, ▲ $AM_{65:35}/CX_{14:86}$, □ $AM_{25:75}/CX_{94:6}$, △ $AM_{26:74}/CX_{14:86}$. *A clear difference between the values of the enthalpy of crystallisation of the four sets of samples is evident, indicating that the crystallisation response is not identical.*

Partially amorphous samples, namely $AM_{66:34}/CX_{94:6}$, $AM_{65:35}/CX_{14:86}$, $AM_{26:74}/CX_{14:86}$ and $AM_{25:75}/CX_{94:6}$ were induced to crystallise and the enthalpy of crystallisation determined using method (iv), already seen as the more accurate method of data analysis (Section 4.2.4.4).

As expected, the enthalpies of crystallisation of samples containing initial crystalline and amorphous lactoses of different anomeric composition are clearly different and gave rise to different calibration plots (Figure 4.11). A few reasons might explain such results. Firstly, as already mentioned (Sections 4.2.4.2 and 4.2.4.3) β-lactose, in both amorphous and crystalline forms, is able to mutorotate to α-lactose when exposed to elevated RH (Angberg et al., 1991; Chidavaenzi et al., 2002), and as verified in Chapter 3. Mutarotation is normally accompanied by water incorporation into the crystal lattice of α-lactose, processes that occur simultaneously and are accompanied by an overall heat loss (exothermic) (Angberg et al., 1991). This might well account for the higher enthalpies of crystallisation verified for the sets of samples containing $CX_{14:86}$ as the crystalline material, namely $AM_{65:35}/CX_{14:86}$ and $AM_{26:76}/CX_{14:86}$. $CX_{14:86}$ contains 14% (w/w) α-lactose and 86% (w/w) β-lactose which can mutorotate to α-lactose, which, in turn, together with the original 14% (w/w) α-lactose can incorporate water into the crystal lattice and form α-lactose monohydrate.

In addition to that, amorphous lactose is known to crystallise to a final product whose anomeric composition is affected, among other factors, by the anomeric composition of the initial crystalline material (Chapter 3). In a general way, in Chapter 3 it was shown that the same amorphous material crystallised in presence of crystalline $CX_{14:86}$, richer in β-lactose, originated crystalline lactose with higher β-lactose content, than when that same amorphous lactose crystallised in presence of $CX_{94:6}$ (poorer in β-lactose). Because α- and β–lactose were seen to exhibit distinct enthalpies of crystallisation (Chapter 3) (enthalpies of fusion of ~169 J/g for α-lactose and ~197 J/g for β-lactose), these differences in crystallisation outcome might also account for the difference in enthalpies of crystallisation of partially amorphous samples and, consequently, partially explain the differences in the calibration curves of the same amorphous lactose in presence of different crystalline lactose. In fact, samples prepared with different crystalline material but with amorphous material with similar anomeric composition exhibited different enthalpies

of crystallisation; $AM_{66:34}/CX_{94:6}$ exhibited lower enthalpy of crystallisation than $AM_{65:35}/CX_{14:86}$ and $AM_{25:75}/CX_{94:6}$ exhibited lower enthalpy of crystallisation than $AM_{26:74}/CX_{14:86}$.

A further factor affecting the measured enthalpies of crystallisation might be the anomeric composition of the amorphous lactose. This is because the anomeric composition of the amorphous material affects the anomeric composition of the final product (Chapter 3), *i.e.* it might affect the amount of α- and β-lactose formed during crystallisation. Such an effect is not significant for the samples containing crystalline $CX_{14:86}$ ($AM_{65:35}/CX_{14:86}$ and $AM_{26:76}/CX_{14:86}$), while for samples containing crystalline $CX_{94:6}$ is clearly more evident; calibration curves for samples containing crystalline $CX_{94:6}$ are clearly more separated than those prepared from samples containing crystalline $CX_{14:86}$. Considering the two sets of partially amorphous samples crystallised in presence of crystalline $CX_{94:6}$, $AM_{25:75}/CX_{94:6}$ samples gave lower enthalpies of crystallisation than $AM_{66:34}/CX_{94:6}$ samples. This is in agreement with the fact that the $AM_{25:75}$ amorphous batch crystallises to a final higher α-lactose content of the $AM_{25:75}$ amorphous batch (the enthalpy of crystallisation of α-lactose is lower than the enthalpy of crystallisation of β-lactose, Chapter 3).

It should be noted that the impact of the anomeric composition of the crystalline portion on the measured heat output is more significant for low amorphous contents, while the impact of the anomeric composition of the amorphous material would be prevalent at higher amorphous contents.

Independently of the reason behind the differences in the obtained calibration curves, the important fact is that they are clearly different. An important consequence of this is that quantification of the amorphous content of a partially amorphous lactose sample of unknown anomeric composition from its enthalpy of crystallisation would give different results from the four calibration curves presented. The best way to overcome this problem, therefore, is to ensure that the crystalline and amorphous standards used have the same anomeric composition as that of the test samples and that both standard and test samples crystallise to a final product with the same anomeric composition. However, while for standard samples, consisting of fully amorphous and fully crystalline particles, it is possible to determine the anomeric composition of the crystalline and amorphous portions, the

same is not so straightforward for processed samples, where a particle has got a crystalline core and an external amorphous corona.

The use of isothermal microcalorimetry for the quantification of amorphous content in lactose (and of any other material) is not invalidated by the findings discussed above. However, in case a material exhibits anomers or polymorphs with different enthalpy of crystallisation, care must be taken to ensure that crystallisation is leading to a final material of the same anomeric or polymorphic composition of the one formed by the samples used to construct the calibration curves.

4.3. EFFECT OF THE ANOMERIC COMPOSITION OF BOTH CRYSTALLINE AND AMORPHOUS LACTOSE ON THE QUANTIFICATION OF AMORPHOUS CONTENT IN LACTOSE BY SOLUTION CALORIMETRY

4.3.1. INTRODUCTION

The goal of solution calorimetry is to create a liquid system where any small enthalpy change due to the dispersion or dissolution of a solute in one of its solvents can be detected (either directly or as a temperature change that is subsequently converted to a heat change) as a function of time. A common experiment consists of a two component system; the solute sealed in a glass ampoule that is housed within a reaction vessel containing the solvent. This prevents dissolution until thermal equilibration is achieved, when the ampoule is broken and the reaction initiated. The measured heat response might be influenced by contributing heat sources other than the reaction of interest; these include the effects of breaking the ampoule, stirring, changes in solvent activity because of solute dissolution, evaporation of solvent, and change in volume upon dissolution of the solute. All these effects, if present, should be accounted for.

The enthalpy of solution of a particular solute, being it liquid or solid, may be affected by minor changes in its physico-chemical properties. Consequently, the determination of the enthalpy of solution of a certain solute in one of its solvents has been applied pharmaceutically for detection and characterisation of polymorphism (Ip et al., 1986; Gerber et al., 1991; Souillac et al., 2002), investigate the extent of crystallinity of drugs and excipients (Gao and Rytting, 1997; Hogan and Buckton, 2000; Harjunen et al., 2004; Katainen et al., 2005) and to characterise interactions between a drug and a carbohydrate (Chadha et al., 2002), and a protein and a carbohydrate (Souillac et al., 2002). Royall and Gaisford (2005) have recently reviewed the applications of solution calorimetry in pharmaceutics.

The principle of solution calorimetry is to create an isothermal system within which very small enthalpy changes due to physical (e.g dispersion or dissolution) or chemical interactions during mixing of two solutions, or a solid and a liquid, may be recorded as a function of time. According to Gao and Ritting (1997), isoperibol solution calorimetry is based on the following equation:

$$S + L \leftrightarrow SL_1 \qquad \text{Equation 4.1}$$

where:

- S is the substract
- L is the ligand.

In an equilibrium system, the total heat evolved (Q) is related to the enthalpy change (ΔH^0) and to the number of moles of SL_1 by:

$$Q = SL_1 \times \Delta H^0 \qquad \text{Equation 4.2}$$

During a solution calorimetry experiment, the heat generated during substrate dissolution is measured, and it is assumed that SL_1 is the total amount of sample and that ΔH^0 is the heat of solution to infinite dilution of any fixed solvent L. The heat of solution can be calculated through the measurement of the total heat generated/absorbed during the process. In a non-interacting binary system, the total heat of solution (ΔH^0_t) is the weight sum of the specific heats of the individual components (Craig and Newton, 1991) according to the following relationship:

$$\Delta H^0_t = X_a \Delta H^0_a + X_b \Delta H^0_b \qquad \text{Equation 4.3}$$

where

- X_a and X_b are the weight fractions of two non-interacting substances
- ΔH^0 are the heats of solution of two non-interacting substances.

The heat of solution method for the quantification of amorphous content is based on the energy difference between the amorphous and crystalline forms of the same substance; in fact, the energy of the amorphous form is, for many solids, significantly higher than that of the crystalline form. When applying Equation 4.3 for the quantification of amorphous content, X_a and X_b are the fractions of the amorphous and crystalline portions and ΔH_a and ΔH_b are the enthalpies of solution of the amorphous and crystalline forms of the same material. In practice, the amorphous content is determined from the linear relation between the enthalpy of solution and physical mixtures of known amorphous content (Gao and Rytting, 1997; Hogan and Buckton, 2000; Harjunen et al., 2002b; Harjunen et al., 2004; Katainen

et al., 2005). According to Hogan and Buckton (2000) the use of solution calorimetry for the quantification of amorphous lactose between 0 and 10% amorphous content proved to be good to ± 0.5%. Using solution calorimetry a limit of detection and quantification of amorphous lactose of 1.8% and 6.0% respectively were recently determined (Harjunen et al., 2004).

The use of solution calorimetry for quantification of amorphous content requires the determination of the enthalpy of solution of 100% amorphous and crystalline standards. Materials from different sources or produced in a different way might well exhibit different enthalpies of solution. Equally produced batches of the same crystalline material might well exhibit different enthalpies of solution (Pikal et al., 1978). α-lactose monohydrate is a commonly used excipient in pharmaceutics. The commercial forms of α-lactose monohydrate (the most commonly used form of lactose) are always "contaminated" by β-lactose to some extent and vice-versa.

4.3.2. AIMS OF THE STUDY

This study aimed to investigate the effect of anomeric composition of crystalline and amorphous lactose on the quantification of amorphous content by solution calorimetry.

4.3.3. EXPERIMENTAL

4.3.3.1. PREPARATION OF AMORPHOUS LACTOSE

Commercial α-lactose monohydrate, consisting of 94% (w/w) α-lactose and 6% (w/w) β-lactose were used to prepare 10% (w/w) lactose solutions. These were equilibrated at 25 °C, 40 °C and 85 °C and spray dried to produce amorphous lactose batches of different anomeric composition (Figure 4.12). Confirmation of the amorphous nature was obtained from XRPD as outlined in Section 2.2.8.3. Anomeric composition was determined by gas chromatography according to the method described in Section 2.2.7.3.

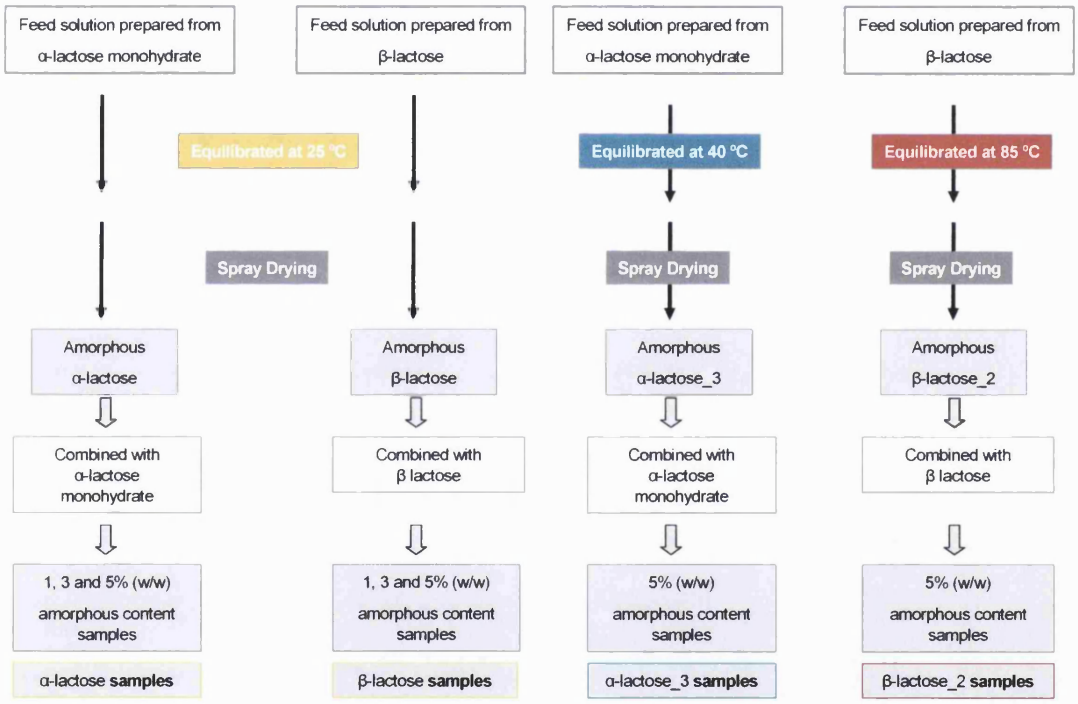

Figure 4.12 *Schematic representation of the preparation of the amorphous lactose batches and partially amorphous lactose samples used throughout the present study. CX represents the crystalline material, AM the amorphous material and AM/CX the partially amorphous samples. The anomeric composition (α-lactose and β-lactose content as % w/w) of each crystalline, amorphous and partially amorphous (both amorphous and crystalline portions) sample is given by the subscript numbers as α□β.*

4.3.3.2. PREPARATION OF PARTIALLY AMORPHOUS LACTOSE SAMPLES

Partially amorphous samples were prepared by directly weighing proportional masses of appropriate amorphous lactose ($AM_{65:35}$, $AM_{65:35}$, $AM_{43:57}$ and $AM_{26:74}$), and crystalline α-lactose monohydrate ($CX_{94:6}$) and β-lactose ($CX_{14:86}$) as summarised in Figure 4.12 into the glass crushing ampoule. The mass of the crystalline component was kept constant in all the mixtures (200 ± 0.01 mg) and an appropriate amount of spray-dried material was added to make 1, 3 and 5% amorphous samples respectively. Both crystalline and amorphous materials were passed through a sieve stack prior to weighing and only the <425 μm fraction was used.

4.3.3.3. PREPARATION OF CRYSTALLINE MIXTURES

Mixtures of α-lactose monohydrate ($CX_{94:6}$) and β-lactose ($CX_{14:86}$) (85:15, 50:50 and 30:70) were prepared by accurately weighing portions of each. The samples were subsequently mixed in a Turbula mixer for twenty minutes to ensure a homogeneous content. Anomeric composition was determined by gas chromatography according to the method described in Section 2.2.7.3.

4.3.3.4. SOLUTION CALORIMETRY

Enthalpies of solution of crystalline α-lactose monohydrate ($CX_{94:6}$), β-lactose ($CX_{14:86}$) and mixtures of both, amorphous and partially amorphous lactose were determined using the Thermometric 2225 Precision Solution Calorimeter (Thermometric AB, Järfälla, Sweden), an instrument designed to use in conjunction with the air and water bath of a Thermometric 2277 Thermal Activity Monitor (TAM, Thermometric AB, Järfälla, Sweden) as described in Section 2.2.3.2. Samples (approximately 200 ± 0.01 mg) were sealed into the glass breaking ampoule and loaded into the solution calorimeter. The combined unit was then lowered into the TAM. The data were collected by measuring the temperature offset from the temperature of the air bath of the TAM (25 °C). In each experiment an electrical calibration was performed before and after the break (Figure 4.13).

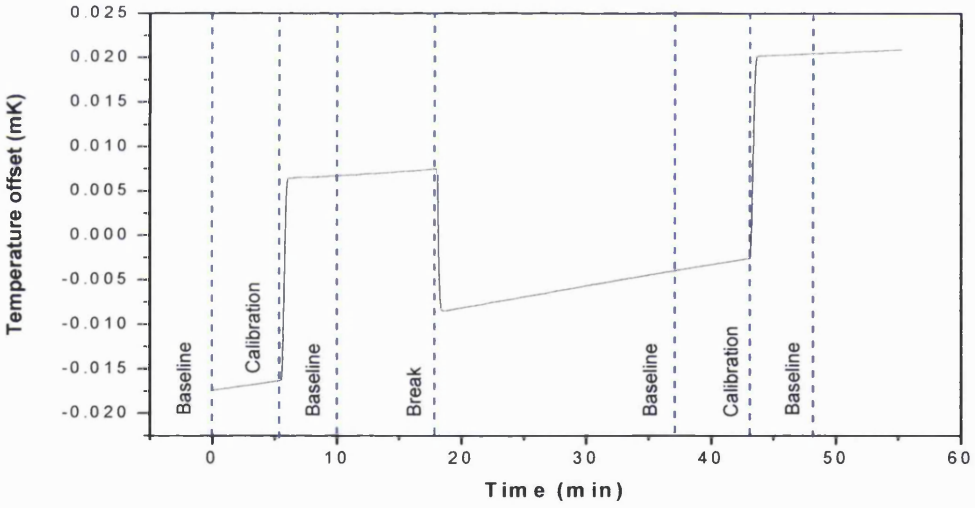

Figure 4.13 *Plot of temperature against time for a 5% (w/w) amorphous lactose sample, with a stirring rate of 600 rpm. This trace shows the calibration sections of the experiment, which take place before and after the ampoule is broken, as well as the baseline periods, which aid calculations to adjust for heat exchange between the solution calorimeter and the environment, as well as the heat generated by the stirrer. Following the breaking of the ampoule, a drop in temperature is seen, implying that the response in this case is endothermic.*

4.3.3.5. DETERMINATION OF ENTHALPY OF SOLUTION

Data were collected via the dedicated Software for Solution Calorimeter System version 1.2 (Thermometric AB, Järfälla, Sweden). All data reported in this study are based upon the calculations performed using the calibration carried out after the breaking of the ampoule. The software allows the conversion of the measured temperature offset to power (Figure 4.14), which makes it possible to clearly see the end of each thermal event and place the event markers at the immediate end of the thermal event so that only that portion of the data is considered in the enthalpy of solution calculation.

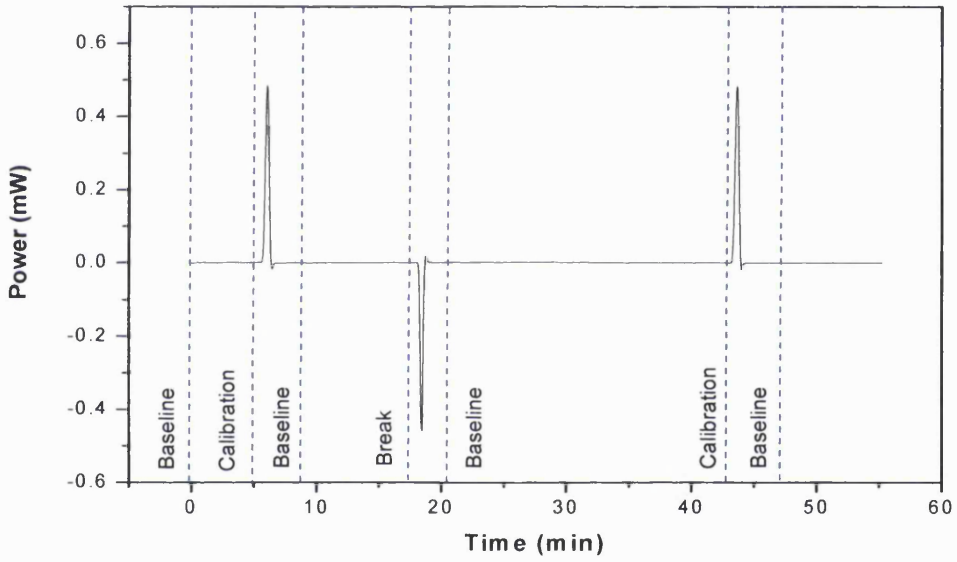

Figure 4.14 *Plot of power (heat flow) against time for a 5% (w/w) amorphous lactose sample. It is possible to move the event marker (shown in blue) to that point where the heat response due to the break event ends. In this way it is possible to aid the software in calculating the enthalpy of solution by including only the data which is directly associated with the dissolution event itself.*

4.3.3.6. GAS CHROMATOGRAPHY

Amorphous and crystalline lactose samples were prepared for gas chromatography analysis as outlined in Section 2.2.7.3.1 and analysed in a CP9001 gas chromatograph (Varian-Chrompack, Oxford, UK) as described in Section 2.2.7.3.2 for quantification of their anomeric composition. Data was collected and analysed for peak area calculation via the dedicated Prime software (HPLC Technology Ltd, Herts, UK).

4.3.4. RESULTS AND DISCUSSION

4.3.4.1. DETERMINATION OF THE ENTHALPY OF SOLUTION OF AMORPHOUS LACTOSE WITH DIFFERENT ANOMERIC COMPOSITION AND OF CRYSTALLINE α-LACTOSE MONOHYDRATE AND β-LACTOSE AND THEIR MIXTURES

The enthalpies of solution of both crystalline and amorphous standards will affect the quantification of amorphous contents from enthalpy of solution data; from Equation 4.3 it can be seen that the enthalpy of solution of partially amorphous standards will result from the enthalpies of solution of the crystalline and amorphous standards and their weight fractions in the sample. As such it is important to analyse the enthalpies of solution of crystalline and amorphous lactose. The net measured enthalpy of solution is a summation of numerous different processes. Firstly, the powder is wetted (exothermic), followed by dissolution that involves breaking of the crystal lattice (endothermic) and formation of bonds between the newly isolated molecules of solute and the solvent (exothermic). There will also be some rearrangement of bonding within the solvent in order to accommodate the solute. Depending on the relative magnitudes of the processes involved, in particular of the magnitude of the enthalpy associated with the crystal lattice breaking and enthalpy of solvation, the net measured enthalpy of solution will be endo- or exothermic. The dissolution of the amorphous form of a material is, in general, more exothermic than the dissolution of its crystalline counterpart, as the former does not involve the breaking of the crystal lattice (Pikal et al., 1978).

The area under the dissolution signal (Figure 4.14) was used to determine the enthalpy of solution of both amorphous and crystalline samples. The enthalpy of solution of the three amorphous batches tested varied between -65.7 ± 0.4 J/g for the amorphous batch with 43.1% α-lactose ($AM_{43:57}$) and -68.9 ± 0.9 J/g for the amorphous batch with 25% α-lactose ($AM_{25:75}$) (Figure 4.15). Although the difference in enthalpy of solution of each batch does not seem to be significantly different because the standard deviations overlap, the small differences observed will most certainly impact on the quantification of amorphous content.

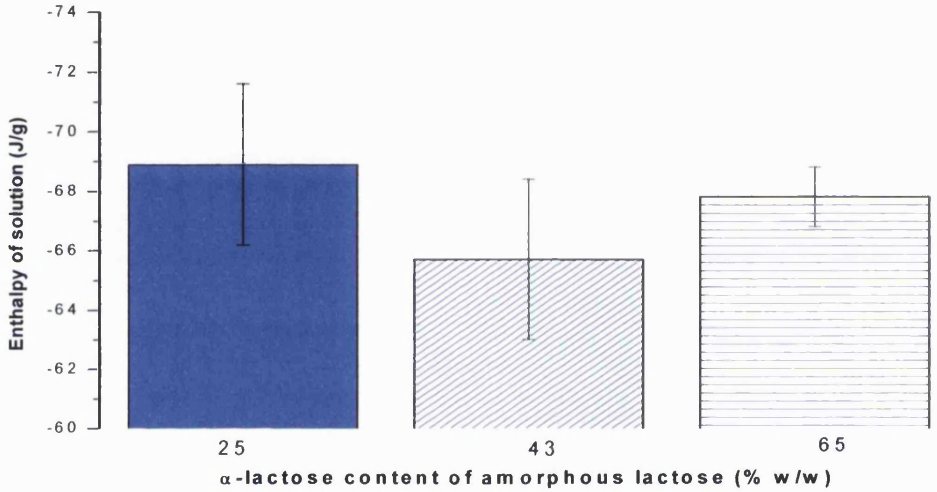

Figure 4.15 *Enthalpy of solution of amorphous lactose batches with different anomeric composition. Amorphous lactose containing 25% α-lactose is $AM_{25:75}$, sample containing 43% α-lactose is $AM_{43:57}$ and amorphous lactose containing 65% α-lactose is $AM_{65:35}$.*

One limitation of the determination of enthalpy of solution for quantification of amorphous content is that the samples need to be completely dry. The higher the amount of water in the sample, the lower the wetting response (exothermic) and consequently the enthalpy of solution will be less exothermic (Pikal et al., 1978; Hogan and Buckton, 2000). This is more important for amorphous and partially amorphous samples, as amorphous material tend to sorb more water then its crystalline counterpart. Although the three amorphous batches were dried until constant weight, variations in residual moisture might also account for the differences in enthalpy of solution observed. Drying and protection of samples from atmospheric moisture is essential, however a long drying period might lead to aging of the amorphous material; Pikal et al. (1978) showed that the enthalpy of solution of

∃-lactam antibiotics becomes more endothermic upon aging, which was attributed to the decomposition of the sample as well as to annealing of the amorphous antibiotics. As it is discussed in Chapter 5, aged amorphous lactose exhibited a clearly distinct enthalpy of solution from the freshly prepared amorphous material.

Amorphous forms of the same material, produced by different methods, may exhibit different enthalpies of solution. Pikal et al. (1978) clearly showed a difference in the enthalpy of solution between spray-dried and freeze-dried amorphous samples of the same material. Although, the three amorphous lactose batches were all produced by spray-drying, the feed solutions were equilibrated at different temperatures (Figure 4.12), and so, consequently, the three batches were subjected to a slightly different processing. This could have lead to differences in the spray dried material.

It should be stated that if the standard and test amorphous material have different enthalpies of solution, the quantification of amorphous content can be erroneously affected. In this case, the higher the amorphous content, the bigger the impact on quantification.

As already mentioned, the enthalpy of solution of the crystalline standard also affects the quantification of amorphous content from enthalpy of solution data, according to Equation 4.3. Any of the crystalline forms of lactose is normally contaminated by the other forms to some extent, and as the three crystalline forms of lactose exhibit different enthalpies of solution (Hudson and Brown, 1908), the enthalpy of solution of a crystalline lactose batch will depend on its anomeric composition. In fact, crystalline $CX_{94:6}$ exhibited an enthalpy of solution of 57.1 ± 0.2 J/g, while the enthalpy of solution of crystalline $CX_{14:86}$ is 6.5 ± 0.2 J/g (Table 4.3). Mixtures of crystalline $CX_{94:6}$ and $CX_{14:86}$ exhibited an intermediate enthalpy of solution according to their anomeric composition as seen in Figure 4.16. In addition to that, crystalline materials from different sources or produced in different ways may well exhibit different enthalpies of solution; Pikal et al. (1978) reported that the enthalpy of solution of fully crystalline batches of cephalothin sodium differed, which the authors attributed to differences in crystal perfection.

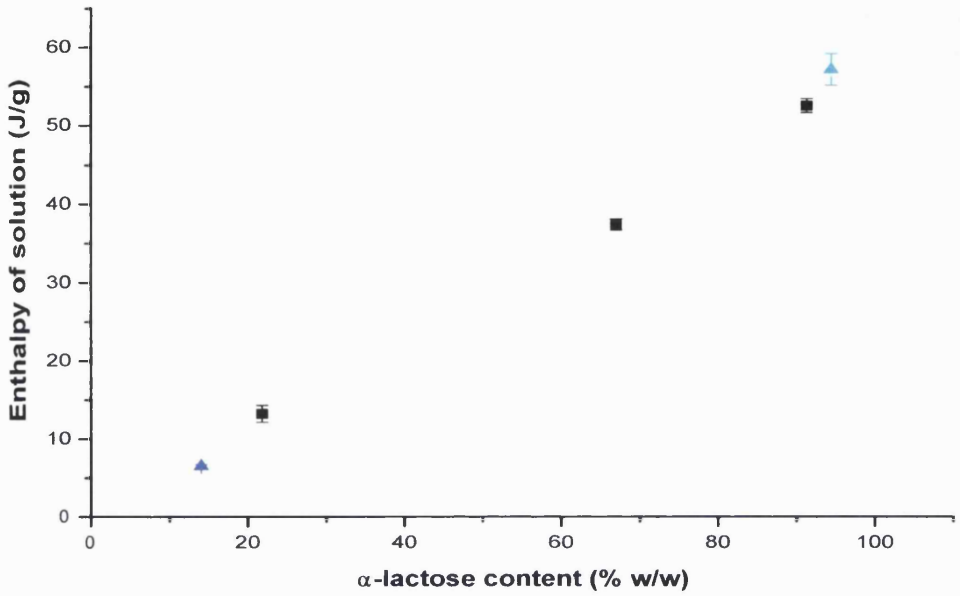

Figure 4.16 *Enthalpies of solution of $CX_{94:6}$ (▲), $CX_{14:86}$ (▲) and mixtures of both (■) according to α-lactose content.*

If the crystalline portion of the standard and test samples exhibit different enthalpy of solution, the quantification of amorphous content from enthalpy of solution data can be erroneously affected. In this case, the lower the amorphous content, the bigger the impact on quantification

4.3.4.2. QUANTIFICATION OF AMORPHOUS CONTENT OF LOW CONTENT PARTIALLY AMORPHOUS LACTOSE SAMPLES WITH DIFFERENT ANOMERIC COMPOSITION BY SOLUTION CALORIMETRY

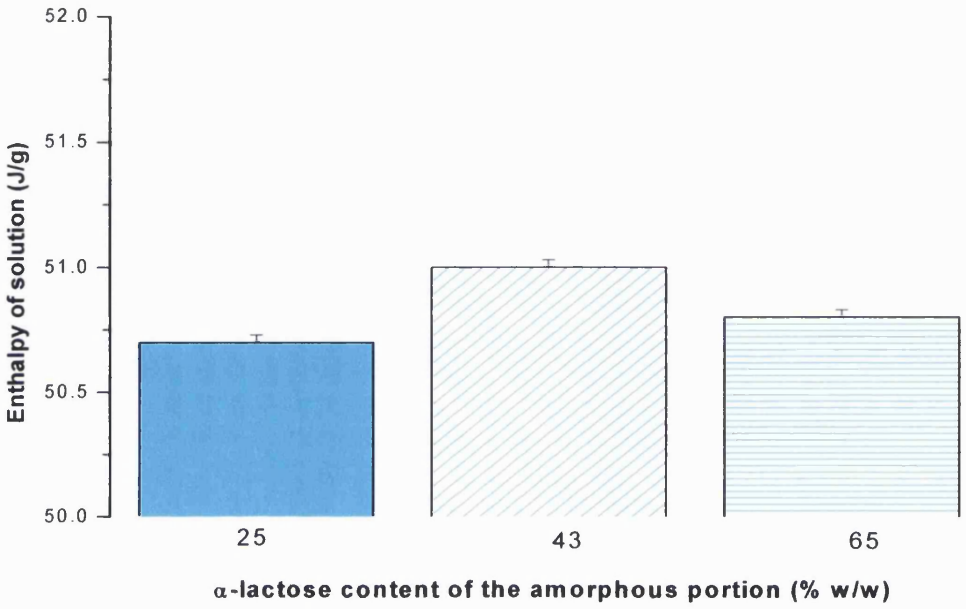

Figure 4.17 *Enthalpy of solution of 5% amorphous lactose samples prepared with amorphous lactose of different anomeric composition, using $CX_{94:6}$ as the crystalline material. Sample containing 25% α-lactose is $AM_{25:75}/CX_{94:6}$, sample containing 43% α-lactose is $AM_{43:57}/CX_{94:6}$ and sample containing 65% α-lactose is $AM_{65:35}/CX_{94:6}$.*

As already mentioned, the enthalpy of solution of a partially amorphous sample will be the result of the enthalpies of solution of the amorphous and crystalline portions and their weight fractions (Equation 4.3). In order to evaluate the impact of the enthalpy of solution of the amorphous portion on the enthalpy of solution of partially amorphous samples, and consequently in the quantification of amorphous content from enthalpy of solution data, 5% amorphous samples were prepared from crystalline $CX_{94:6}$ and amorphous batches that exhibited different enthalpy of solution (Figure 4.15). As all three samples contain the same crystalline material, any difference in their enthalpy of solution is because of the different enthalpies of solution of the amorphous batches used in their preparation. In fact, the enthalpy of solution of the 5% amorphous samples (Figure 4.17) varied in agreement with the

enthalpy of solution of the correspondent amorphous batch; the sample prepared from amorphous lactose containing 25% α-lactose ($AM_{25:75}/CX_{94:6}$) exhibited the less endothermic enthalpy of solution, which is in agreement with the more exothermic enthalpy of solution of the correspondent amorphous batch (Figure 4.15). The sample prepared from amorphous lactose containing 43% α-lactose ($AM_{43:57}/CX_{94:6}$) exhibited the more endothermic enthalpy of solution, which is a consequence of the less exothermic enthalpy of solution of the correspondent amorphous batch (Figure 4.15).

The construction of calibration curves for the three different amorphous batches would return different calibration curves. As such, quantification of amorphous content of samples containing an amorphous material prepared in a different way, or containing different anomeric composition, of the standard batch used for the construction of the calibration curves would be associated with an error. A possible way to avoid such problems is to guarantee that both standard and test amorphous materials were produced in the same way, and that exhibit the same enthalpy of solution. However, processed samples normally consist of particles that exhibit a crystalline core surrounded by an amorphous corona, which makes it impossible to only determine the enthalpy of solution of the amorphous portion of the processed sample, and consequently there is no guarantee that the amorphous material of the standard and test samples exhibit the same enthalpy of solution.

In order to investigate the impact of the anomeric composition of crystalline lactose on the quantification of amorphous contents from enthalpy of solution data, two batches of partially amorphous lactose samples were prepared; $AM_{65:35}/CX_{94:6}$ and $AM_{65:35}/CX_{14:86}$ samples. Figure 4.18 shows the calibration curves constructed for $AM_{65:35}/CX_{94:6}$ and $AM_{65:35}/CX_{14:86}$ samples using the enthalpy of solution data. It is immediately evident that there are significant differences between the two batches. As already mentioned, using entirely crystalline samples, the enthalpy of solution of $CX_{94:6}$ was determined to be 57.1 ± 0.2 J/g while that of $CX_{14:86}$ was 6.5 ± 0.2 J/g, corresponding to the y-intercepts of the two calibration plots. For both batches, the measured heats of solution decrease as the amorphous content increases, reflecting the fact that the endothermic contribution from breaking the crystal lattice is decreasing.

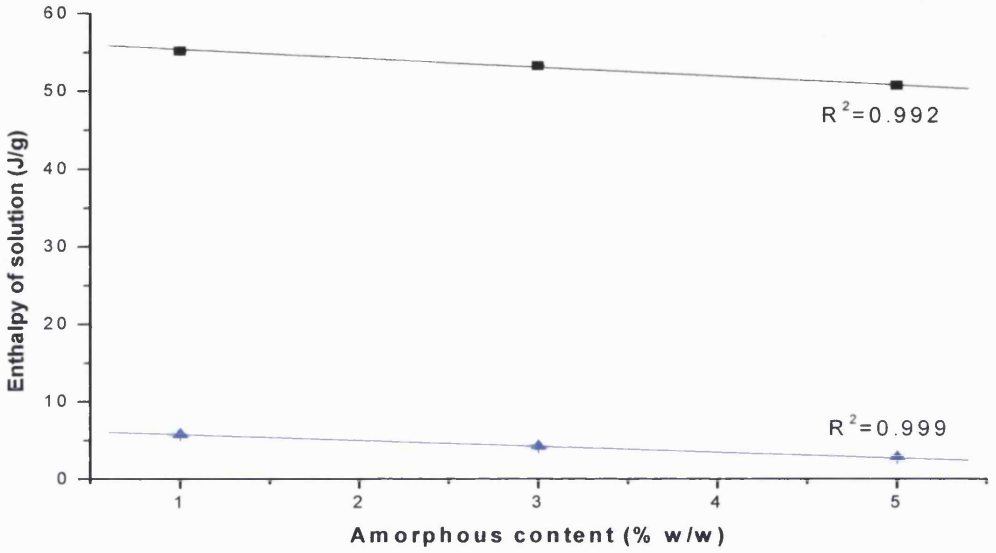

Figure 4.18 *Calibration curves for the two batches of amorphous lactose prepared from enthalpy of solution data.* ▲ *$AM_{65:35}/CX_{14:86}$ samples* ■ *$AM_{65:35}/CX_{14:86}$* sample, a *clear difference in the enthalpy of solution of the two sets of samples is evident.*

The standard deviations associated with the data shown in Figure 4.18 are very small, which is mainly a consequence of the weighing methodology chosen to prepare the samples; both crystalline and amorphous portions were directly weighted into the glass ampoule. For each set of samples, the three amorphous percentages used for the construction of the calibration curves show clearly different enthalpies of solution. This might not be the same for other materials, as the sensitivity will depend upon the difference in enthalpy of solution between the amorphous and crystalline forms, which for lactose are quite different. Obviously the larger the difference the greater will be the sensitivity for quantification and vice versa.

One of the major concerns regarding the preparation of calibration curves for amorphous content determination is now clear; measurement of the enthalpy of solution of a sample of lactose that is partially amorphous would result in two different estimates of amorphous content and, without prior knowledge of its isomeric composition, it would be impossible to know which was the correct value. The impact of these observations will surely depend on how different the enthalpies

of solution of the two or more crystalline anomers/polymorphs are. In addition to that, the lower the amorphous content of the sample, the higher is the contribution of the crystalline portion of the sample to the measured enthalpy of solution.

The problem of the effect of the anomeric composition on the measured enthalpy of solution can be overcame for partially amorphous samples made of entirely amorphous particles mixed with totally crystalline particles. It is only necessary to ensure that the standards and test samples have the same anomeric composition. However, in reality most amorphous pharmaceuticals will be processed materials consisting of crystalline cores with an outer corona of amorphous material, being more complex to quantify the anomeric composition of each fraction. Moreover, it is likely that the interactions in a particle that is partially crystalline and partially amorphous differ from those of wholly amorphous and wholly crystalline particles, which certainly calls into question the use of such calibration curves for quantification of amorphous content of processed materials.

4.4. CONCLUSION

From the investigations carried out using isothermal RH perfusion microcalorimetry, it was possible to demonstrate that the anomeric composition of amorphous and crystalline lactose does affect the quantification of small amorphous content in lactose. Although these findings do not invalidate the use of isothermal RH perfusion microcalorimetry for quantification of small amorphous contents, care must be taken to ensure that standards and test samples exhibit the same anomeric composition, and that crystallisation leads to a final lactose with the same anomeric composition. This work also highlighted the best methodology for determination of the enthalpy of crystallisation. The crystallisation response of amorphous lactose with different anomeric composition was also described, and the differences to the crystallisation of lactose as followed by batch isothermal microcalorimetry were also discussed.

From the solution calorimetry study it was possible to demonstrate that the anomeric composition of the crystalline portion of partially amorphous lactose samples does affect the quantification of amorphous contents in lactose because of the dependence of the enthalpy of solution of crystalline lactose on its anomeric composition. Furthermore, the technique was able to distinguish between partially

amorphous samples consisting of the same crystalline lactose and amorphous lactoses of different anomeric composition. This demonstrates that the anomeric composition of amorphous lactose affects the quantification of amorphous contents. It should be noted that these findings do not invalidate the use of solution calorimetry for the quantification of amorphous contents in lactose. However, it has to be ensured that the amorphous and crystalline standards and test sample are of the same anomeric nature.

At this point, a discussion of the impact of the "quality" of the amorphous material on its quantification is relevant. The anomeric composition of an amorphous material can be considered as an example of variability of that amorphous material. As the anomeric composition affected the quantification of amorphous contents in lactose, other factors of variability in the amorphous form, such as method of preparation, aging, etc might as well have an impact onto the quantification methods. Although one becomes more aware that the importance of the "quality" of an amorphous material on its detection and quantification, more research into such matters is definitely necessary. Furthermore, an investigation of the variability or "quality" of the amorphous material onto product manufacturing and performance is equally essential.

In this chapter…

- ***…from the Isothermal Relative Humidity Perfusion Microcalorimetry study:***

  - *two methods for data analysis for quantification of amorphous content from Isothermal Perfusion data were discussed;*

  - *the most appropriate method for data analysis for quantification of amorphous content from isothermal perfusion data was recommended;*

  - *the crystallisation of amorphous lactose with different anomeric composition was discussed as followed by Isothermal RH Perfusion Microcalorimetry;*

  - *it was demonstrated that the anomeric composition of both amorphous and crystalline lactose affect the quantification of amorphous lactose by. Care must be taken to ensure the crystalline and amorphous lactose standard used to construct the calibration curves are of the same anomeric nature as the test samples.*

- ***…from the Solution Calorimetry study:***

  - *it was shown that the enthalpy of solution of amorphous lactose with different anomeric composition did not differ significantly;*

  - *it was shown that enthalpy of solution of crystalline lactose with different anomeric composition differs greatly;*

  - *it was demonstrated that the differences in enthalpy of solution of amorphous and crystalline lactose affect the quantification of amorphous lactose by this method. Care must be taken to ensure the crystalline and amorphous lactose standards used to construct the calibration curves are of the same anomeric nature as the test samples.*

CHAPTER FIVE

CHARACTERISATION OF AGING OF AMORPHOUS LACTOSE AND AMORPHOUS INDOMETHACIN BY STEPSCAN DIFFERENTIAL SCANNING CALORIMETRY, SOLUTION CALORIMETRY AND INVERSE PHASE GAS CHROMATOGRPAHY

5.1. INTRODUCTION

Amorphous systems are a versatile option in pharmaceutics because of their improved dissolution rate and bioavailability, and performance characteristics of drugs and excipients, as previously discussed in Section 1.15.1. These advantages are a consequence of its excess properties, as the higher enthalpy, free volume and entropy of the amorphous systems. However, these high energy systems are highly unstable and will tend to revert to the thermodynamically stable crystalline state. Such changes can also occur in crystalline systems which contain amorphous regions induced by processing. This metastability is caused by the high degree of molecular motion existing in the amorphous state; molecular motion also exists below the glass transition temperature, as discussed in Sections 1.7 to 1.9. Even if crystallisation does not take place on the experimental time scales, the amorphous system will tend to lose its excess enthalpy or free volume and become denser with time. This process is known as structural relaxation and has strong temperature dependence, as discussed in Section 1.9.

Relaxation of an amorphous material can occur during pharmaceutical unit operations involving thermal or mechanical stresses. Time-dependent changes in physical and mechanical properties of glassy pharmaceuticals have been attributed to relaxation. For example, aging of amorphous trehalose below the glass transition temperature caused nucleation leading to a decrease in the crystallisation temperature and a decrease in the rate and extent of water sorption at low relative humidities (Surana et al., 2004). Aso et al. (2000) investigated the relationship between the crystallisation rates of amorphous nifedipine, phenobarbital and flopropione and their molecular mobility; the authors partially ascribed the faster crystallisation of nifedipine than that of phenobarbital and flopropione observed at temperatures below the glass transition temperature to its higher molecular mobility at those temperatures. Yoshioka et al. (1997a, 1997b, and 1998) verified that the stability of γ-globulin formulations was closely related to the molecular mobility. Protein aggregation and molecular mobility of lyophilised formulations containing antibody were found to be related to enthalpy relaxation time below their glass transition temperature (Duddu et al., 1997). Because structural relaxation is an indicator of molecular mobility, physical/chemical stability and structural relaxation may well be closely related and a full characterisation and understanding of the relaxation process is necessary in order to ameliorate those problems in the amorphous state. In fact, in pharmaceutical systems, aging studies have focussed

on the measurement of structural relaxation times, in an effort to correlate molecular mobility with the shelf-live of a material (Shamblin et al., 1999 and 2000).

A variety of techniques have been used for the characterisation of molecular motions in amorphous materials, such as dielectric relaxation (Andronis and Zografi, 1998), dynamic mechanical analysis (Andronis and Zografi, 1997), nuclear magnetic resonance (Aso et al., 2000) and thermal methods (Kawakami and Pikal, 2005; Liu et al., 2002; Aso et al., 1995). Of these, differential scanning calorimetry is frequently used (Kawai et al., 2005; Surana et al., 2004; Kakumanu and Bansal, 2002) because of ease of analysis and small sample requirement.

Solution calorimetry is commonly used for the characterisation and quantification of amorphous content of pharmaceuticals, as previously discussed in Chapter 4. Pikal et al. (1978) reported differences in the enthalpy of solution between freeze-dried and spray-dried amorphous samples of the same compound. The enthalpy of solution of amorphous freeze-dried cefamandole sodium and cemandole nafate became more endothermic upon aging. Such differences were attributed to "some type" of annealing phenomenon in the amorphous forms. In another study, poly(ethylene)glycols of different molecular weights were prepared with different thermal histories (by quench-cooling from the melt, slow cooling form the melt, and left untreated) and their enthalpy of solution was determined. It was found that the enthalpy of solution varied as a function of molecular weight and thermal history of the sample (Craig and Newton, 1991). Because of the wide use of the determination of enthalpies of solution for the characterisation and quantification of the amorphous state (Royall and Gaisford, 2005), it is of great importance to investigate the effect of structural relaxation of amorphous pharmaceuticals on their enthalpy of solution.

Determination of powder surface energetics has been carried out for characterisation of pharmaceutical and non-pharmaceutical material, as discussed in Section 1.14.1. Some studies tried to correlate the determined surface energies with the product performance (Cline and Dalby, 2002). Others investigated the use of inverse gas chromatography to detect batch to batch variability (Ticehurst et al., 1994 and 1996) and the effect of processing on the surface energy of a material (Feeley et al., 1998). Using Inverse phase gas chromatography, Ambarkhane et al. (2005) were able to identify the temperature below the glass transition temperature where molecular mobility of amorphous lactose becomes insignificant by analysis of changes in the retention time of decane probe. The effect of annealing on the

dispersive surface energy and acid-base properties of polymers has also been ascertained (Andrzejewska et al., 1996; Voelkel et al., 1996); it was observed that both dispersive surface energy and acid-base properties of the polymers investigated were affected by the annealing process. Because of the wide use of the determination of surface energies for the characterisation of pharmaceutical materials, it is of great importance to investigate the effect of structural relaxation of amorphous pharmaceuticals on their surface energy.

5.2. AIMS OF THIS STUDY

This study aimed to characterise the aging of amorphous lactose and indometacin by StepScan differential scanning calorimetry. This study aimed to investigate the effect of aging of amorphous lactose and indometacin on its enthalpy of solution and dispersive surface energy. A further aim of the present study was to investigate the use of solution calorimetry and inverse phase gas chromatography to characterise the aging of amorphous lactose and indometacin, in comparison to StepScan differential scanning calorimetry.

5.3. EXPERIMENTAL

5.3.1. PREPARATION OF AMORPHOUS LACTOSE AND INDOMETACIN SAMPLES

Amorphous lactose was prepared by spray-drying from a 10% (w/w) solution equilibrated at 25 ºC as described in Section 2.2.1.3. Amorphous indometacin was prepared by quench-cooling as described in Section 2.2.10. Amorphous nature was confirmed by XRPD as described in Section 2.2.8.3. Amorphous batches were dried in an evacuated desiccator over phosphorous pentoxide.

5.3.2. AGING OF AMORPHOUS SAMPLES

Dry amorphous lactose was sieved and the fraction < 425 µm was aged at 50, 65 and 100ºC and 0% RH (maintained in an evacuated desiccator containing phosphorous pentoxide). Amorphous lactose samples aged at 50 ºC ($T_g - T_a$ = 64 ºC) were collected for StepScan DSC, solution calorimetry and inverse gas chromatography analysis after 1, 2, 3 7, 11 and 17 days. Amorphous lactose samples aged at 65 ºC ($T_g - T_a$ = 49 ºC) were collected after 3, 7, 11 and 17 days.

Amorphous lactose samples aged at 100 ºC ($T_g - T_a$ = 16 ºC) were collected after 1, 2, 3, 7, 9 and 11 days.

Dry amorphous indometacin was aged at 25 ($T_g - T_a$ = 21 ºC) and 37 ºC ($T_g - T_a$ = 9 ºC) and 0% RH (maintained in an evacuated desiccator containing phosphorous pentoxide). Amorphous indometacin samples aged at 25 ºC ($T_g - T_a$ = 21 ºC) were collected after 1, 2, 3 4, 7, 11, 14 and 18 days. Amorphous indometacin samples aged at 37 ºC ($T_g - T_a$ = 9 ºC) were collected after 1, 2, 3, 4, 7, 11 and 14 days. The particle size of amorphous indometacin was gently reduced by means of a mortar and pestle and sieved after aging and the fraction < 425 µm used for solution calorimetry and StepScan DSC analysis.

5.3.3. STEPSCAN DIFFERENTIAL SCANNING CALORIMETRY

Fresh and aged amorphous lactose and indometacin were analysed by StepScan DSC for determination of the glass transition, heat capacity change at glass transition and enthalpy recovery. Samples were crimped into non-hermetically sealed pans and analysed in a Pyris-1 (Perkin-Elmer Instruments, Beaconsfield, Bucks, UK) DSC using the experimental parameters described in Section 2.2.4.3. Data were collected and analysed using the dedicated Pyris software package (Perkin-Elmer Instruments, Beaconsfield, Bucks, UK). The glass transition response was recorded from the thermodynamic C_p line (as a reversible transition). The enthalpy recovery was calculated by integrating the area under the peak of the IsoK baseline corresponding to the glass transition temperature range.

5.3.4. SOLUTION CALORIMETRY

Enthalpy of solution of fresh and aged amorphous samples and crystalline α-lactose monohydrate and indometacin were determined in a Thermometric 2225 Precision Solution Calorimeter (Thermometric AB, Järfalla, Sweden) according to the methodology described in Section 2.2.3.3. Enthalpy of solution of accurately weighed lactose samples (~0.2 g) was determined in 100 mL of water and enthalpies of solution of indometacin samples (~ 0.1 g) were determined using 100 mL of ethanol as a solvent. Data was collected and analysed via the dedicated software for solution calorimeter (Thermometric AB, Järfalla, Sweden) and Origin 7.0 (Microcal Software Inc., Northampton, USA).

5.3.5. INVERSE PHASE GAS CHROMATOGRAPHY

The dispersive surface energy of fresh and aged amorphous lactose samples and crystalline α-lactose monohydrate was determined by inverse phase gas chromatography (Surface Measurements Systems Ltd, London, UK) by packing approximately 0.2 g of amorphous material and 0.150 of crystalline material into a passivated glass column as described in Section 2.2.6.3 and using the elution method described in Section 2.2.6.3. Data was collected via the SMS iGC Controller v1.5 (Surface Measurements Systems, London, UK) and analysed using the SMS iGC Analysis macros version 1.2 (Surface Measurements Systems, London, UK) and Origin 7.0 (Microcal Software Inc., Northampton, USA).

5.3.6. DATA ANALYSIS

In order to determine relaxation time constants, the extent of relaxation data (calculated using Equation 1.8) obtained from StepScan DSC, solution calorimetry and inverse gas chromatography was fitted to the KWW equation (Equation 1.7) by least-squares non-linear regression using Origin 7.0 (Microcal Software Inc., Northampton, USA). Extent of relaxation data with negative values was not included in the fitting. The glass transition and heat capacity change at the glass transition of a fresh amorphous sample were used to determine the maximum enthalpy relaxation according to Equation 1.9.

5.4. RESULTS AND DISCUSSION

5.4.1. DETERMINATION OF ENTHALPY RECOVERY BY STEPSCAN DSC

Differential scanning calorimetry is perhaps the most common technique used for investigating the relaxation of pharmaceutical amorphous solids. With DSC techniques, aged amorphous samples are heated through the glass transition and the enthalpy lost during relaxation is measured as an enthalpy recovery endotherm that is superimposed on the heat capacity change at the glass transition, as described in Section 1.8. Analysis of a StepScan DSC scan allows the separation of the glass transition temperature from the superimposed enthalpy recovery endotherm, facilitating measurement of the enthalpy recovery. The results obtained for amorphous lactose are exemplified in Figure 5.1. The glass transition being the reversible response was observed along the Thermodynamic C_p line (as a step

change in the specific heat line) and the enthalpy recovery processes (non-reversible) were seen along the IsoK baseline (as an endothermic peak).

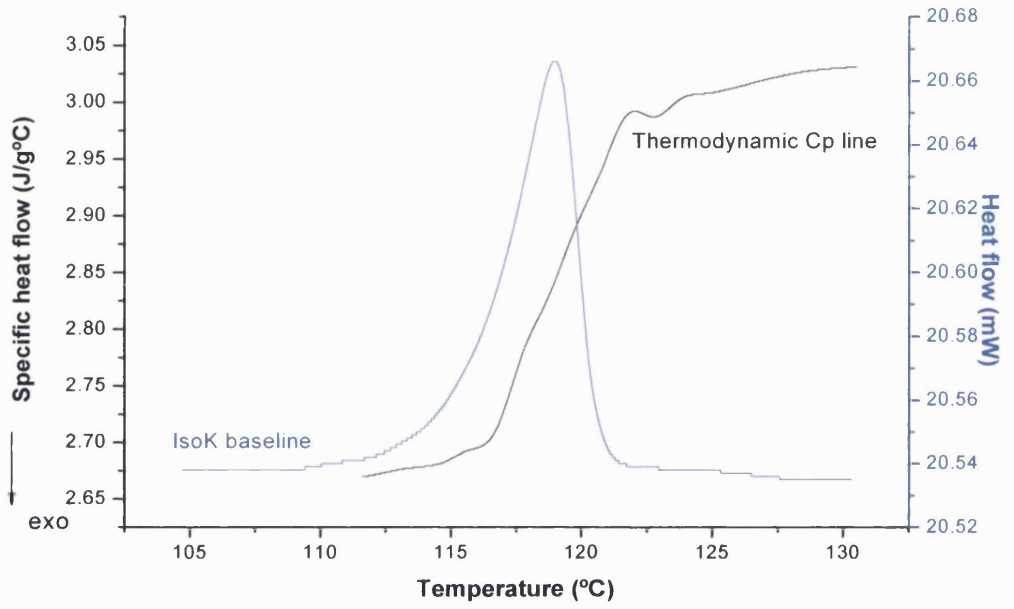

Figure 5.1 *The differentiation of the total heat flow thermodynamic signal (includes the reversing events, represented by the Thermodynamic C_p line) and kinetic component (includes the non-reversing events, represented by the IsoK baseline line) DSC for amorphous lactose aged at 100 °C ($T_g - T_a$ = 16 °C).*

From the thermodynamic C_p line the glass transition temperature and heat capacity change at T_g were determined for amorphous lactose and indometacin before aging. The obtained results are presented in Table 5.1, and matched with the respective values reported in the literature (Craig et al., 2000; Shamblin et al., 1999).

Table 5.1 *Initial parameters of glass transition obtained using StepScanDSC.*

Samples	$T_{g\ ½\ Cp\ extra}$ (°C)	ΔC_p (J/g°C)
Lactose (batch aged at 100 °C, $T_g - T_a$ = 16 °C)	116.3 ± 0.17	0.47 ± 0.08
Lactose (batch aged at 50 °C, $T_g - T_a$ = 64 °C, and 65 °C, $T_g - T_a$ = 49 °C)	114.0 ± 0.2	0.52 ± 0.03
Indometacin	45.9 ± 0.23	0.36 ± 0.01

The area under the endothermic peak observed along the IsoK baseline was calculated to give an estimate of the enthalpy relaxation process. The use of differential scanning calorimetry for the determination of enthalpy relaxation assumes that the measured enthalpy recovery is the same as the enthalpy relaxation.

5.4.2. EFFECT OF AGING ON THE ENTHALPY RECOVERY

The enthalpy lost upon structural relaxation can be measured at different aging times. Figures 5.2 to 5.6 show the enthalpy recovery endotherm of aged amorphous lactose and amorphous indometacin at increasing aging times, as obtained from StepScan data. The height and ultimately the area under the peak of the enthalpy recovery endotherm increased with increasing aging time. This reflects an increase in structural relaxation of the glass towards the supercooled liquid.

For both amorphous lactose and indometacin, an apparent recovery endotherm was seen for non aged amorphous samples, represented in Figures 5.2 to 5.6 as the endotherm at day zero. This most probably results from the experimental procedure and from relaxation during the experiment. This effect is important for StepScan analysis because of the slow heating rates employed. According to Kawakami and Pikal (2005) the best approach for correcting the raw endotherm area data is simply to subtract the apparent enthalpy recovery value obtained with zero annealing time from the values obtained at nonzero annealing times.

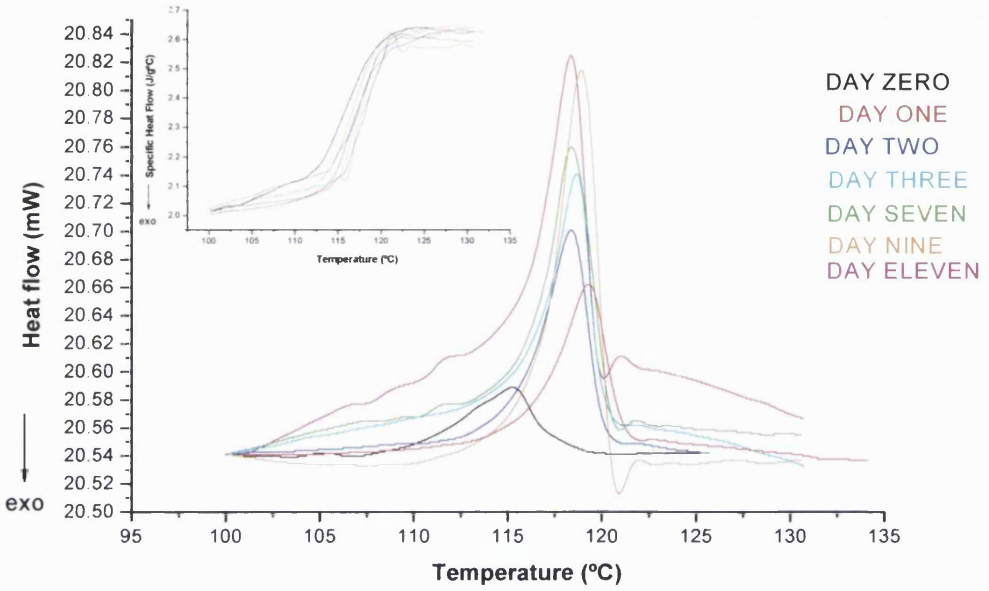

Figure 5.2 *The effect of aging at 100 °C (T_g–T_a=16 °C) on the enthalpy recovery of amorphous lactose. T_g can be seen in the inset graph.*

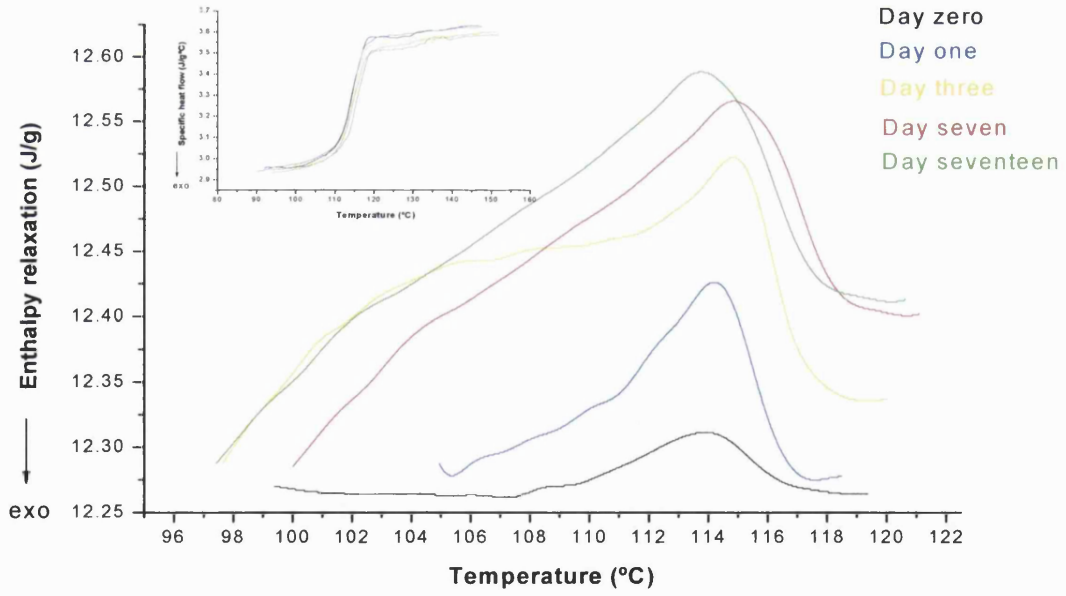

Figure 5.3 *The effect of aging at 65 °C (T_g–T_a=49 °C) on the enthalpy recovery of amorphous lactose; T_g can be seen in the inset graph.*

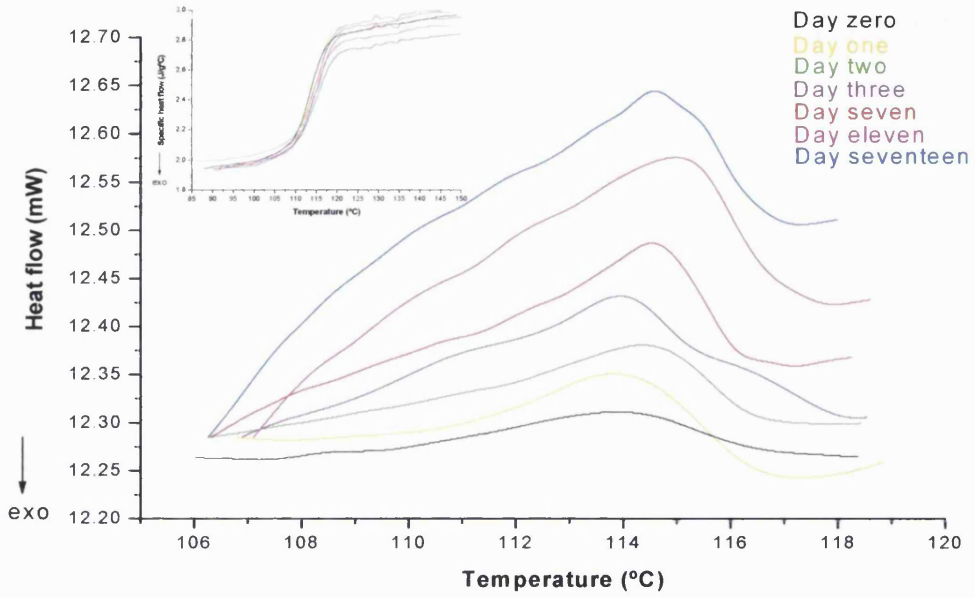

Figure 5.4 *The effect of aging at 50 °C (T_g–T_a=64 °C) on the enthalpy recovery of amorphous lactose; T_g can be seen on the inset graph.*

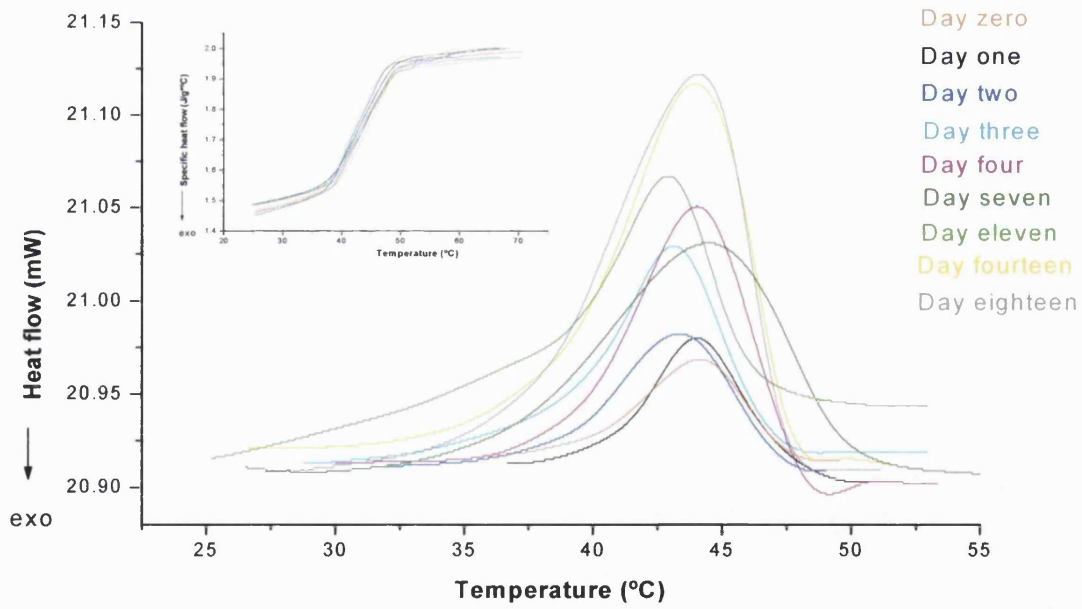

Figure 5.5 *The effect of aging at 25 °C (T_g–T_a=21 °C) on the enthalpy recovery of amorphous indometacin; T_g can be seen in the inset graph.*

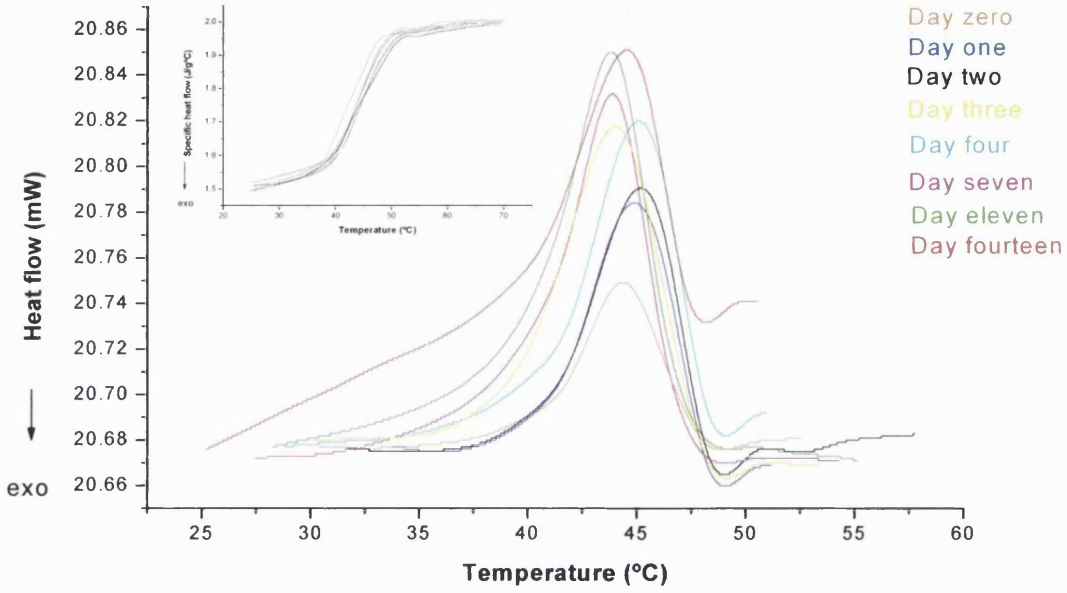

Figure 5.6 *The effect of aging at 37 °C (T_g–T_a=9 °C) on the enthalpy recovery of amorphous indometacin; T_g can be seen in the inset graph.*

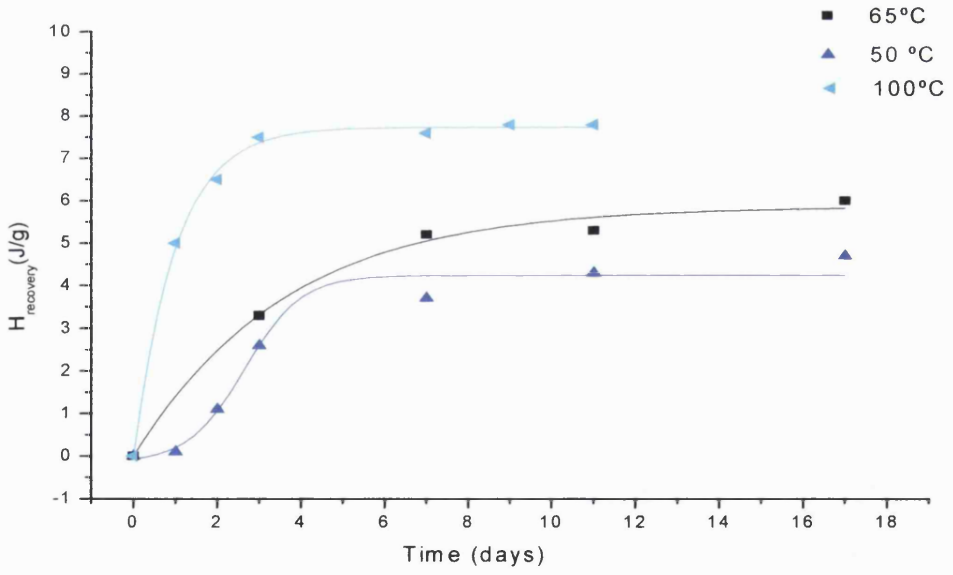

Figure 5.7 *The enthalpy recovery as a function of time obtained for amorphous lactose at different aging temperatures.*

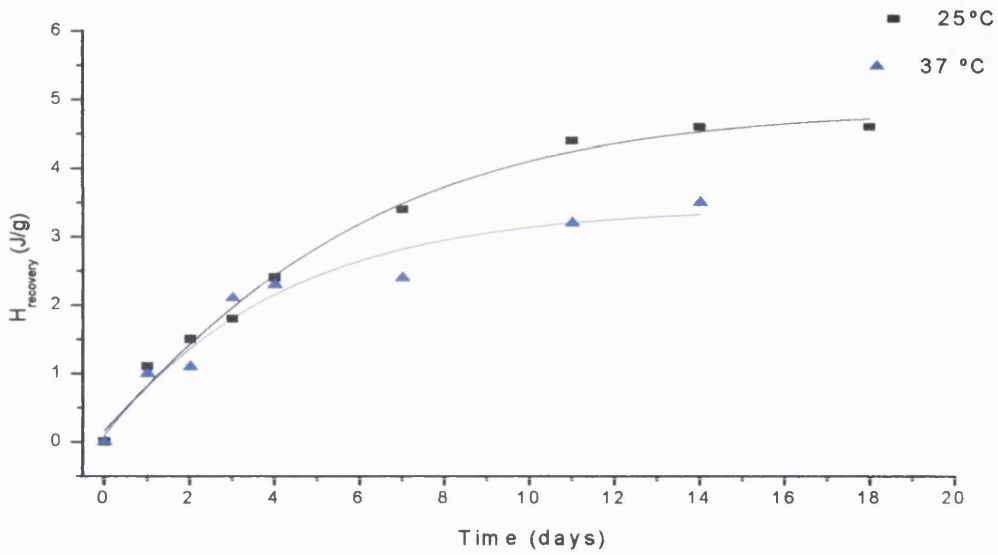

Figure 5.8 *The enthalpy recovery as a function of time obtained for amorphous indometacin at different aging temperatures.*

The enthalpy recovery of amorphous lactose was determined for aging temperatures of 50, 65 and 100 °C, as seen in Figures 5.2 to 5.4. The enthalpy recovery of amorphous indometacin was determined for aging temperatures of 25 and 37 °C, as represented in Figures 5.5 and 5.6. The subtracted enthalpies are plotted according to aging time in Figure 5.7 for amorphous lactose and in Figure 5.8 for amorphous indometacin. It can be seen that for amorphous lactose, for each aging time, the enthalpy recovery increased with increasing aging temperature; amorphous lactose aged at 100 °C exhibited a markedly higher enthalpy relaxation than amorphous lactose aged at 65 and 50 °C. In the case of amorphous indomethacin aged at 25 and 37 °C, the enthalpy recovery increased with increasing aging time. For days 7 to 14 the enthalpy recovery measured for amorphous indomethacin aged at 37 °C was lower than enthalpy recovery measured for amorphous indomethacin aged at 25 °C, while from days 0 to 4 no clear trend could be established.

The enthalpy change necessary for a glass to reach a supercooled state depends on thermal history (preparation process, for example) (Liu et al., 2002) of the amorphous material and the degree of undercooling or aging temperature below the glass transition temperature. According to Equation 1.9, it would be expect that enthalpy relaxation would increase with decreasing aging temperature; the distance in enthalpy between the glass and the supercooled liquid increases with decreasing

temperature. Kawakami and Pikal (2005) compared the enthalpy relaxation of amorphous indometacin and maltose aged for 1 hour according to aging temperature. For amorphous indometacin aging at 37 ºC (T_g-T_a=9ºC) showed a lower enthalpy relaxation than that aged at 25ºC (T_g-T_a=21ºC). On the other hand, amorphous maltose aged at T_g-T_a=11 ˚C exhibited a higher enthalpy relaxation than amorphous maltose aged at approximately T_g-T_a=16 ˚C. Maximum values of enthalpy relaxation were observed in a temperature range 10 to 20 ºC below the glass transition temperature (Kawakami and Pikal, 2005). Thus, there is an aging temperature that gives maximum enthalpy relaxation. The molecular mobility decreases with decreasing temperature, which could explain the presence of an optimum temperature at which the enthalpy relaxation is maximum. Liu et al. (2002) reported that the rank order of relaxation of four sugars aged at the same aging temperature was not the same as their glass transition temperature. This supports the hypothesis that molecular mobility does not solely depend on the $T_a - T_g$.

5.4.2.1. ESTIMATION OF MOLECULAR MOBILITY FROM STEPSCAN DSC DATA

From the maximum enthalpy recovery (calculated using Equation 1.9) the extent to which the glass relaxes can be calculated for each aging time and temperature using Equation 1.8. This normalises the enthalpy recovery values, enabling comparison of the rate of structural relaxation. The extent of relaxation values at different temperatures were plotted against aging time and are represented in 5.9 for lactose and Figure 5.10 for indometacin. The greater the value of the extent of relaxation, the lesser is the relaxation of glass to the equilibrium glass.

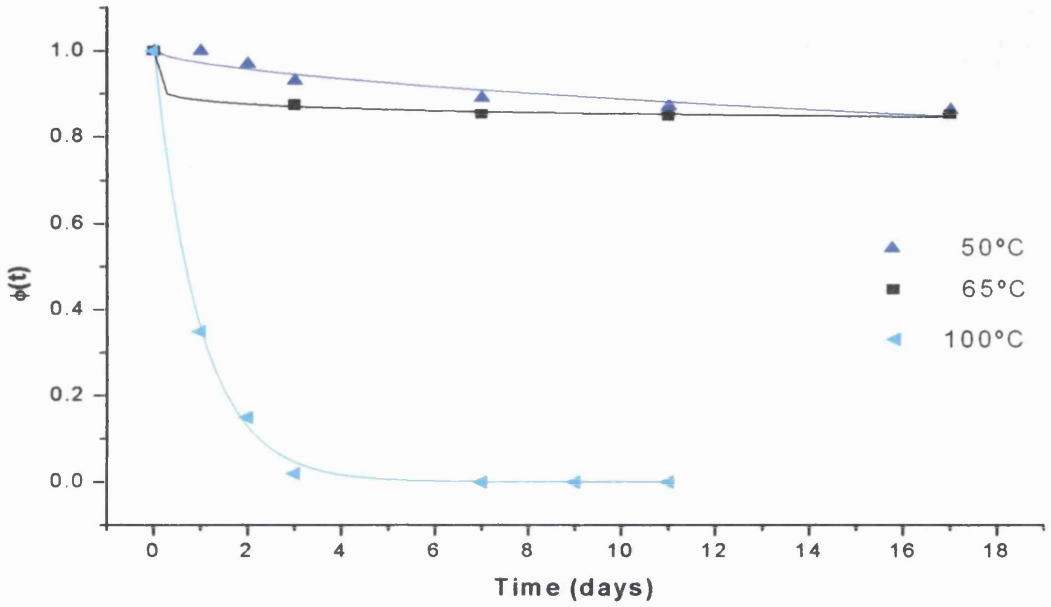

Figure 5.9 *The extent of relaxation as a function of time for amorphous lactose aged at different temperatures as determined from enthalpy recovery data; solid lines are the curves of best fit in the KWW equation.*

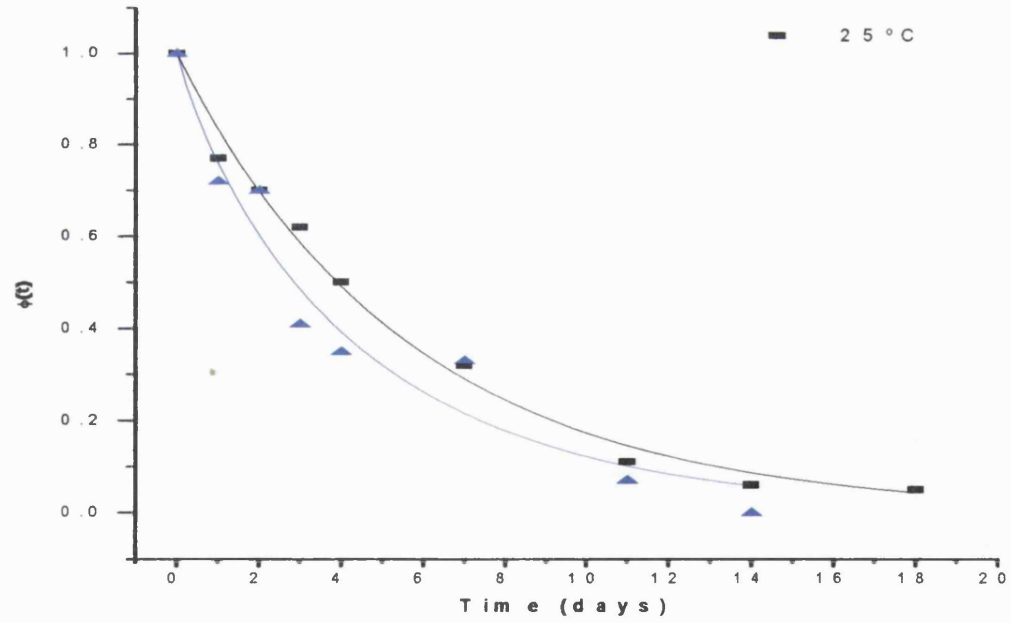

Figure 5.10 *The extent of relaxation as a function of time for amorphous indometacin aged at different temperatures as determined from enthalpy recovery data; solid lines are the curves of best fit in the KWW equation.*

The extent of relaxation values at each temperature were fitted to the KWW equation (Equation 1.7) using τ and β as variables. This provided the values of τ and β for lactose and indometacin for each aging temperature, which are shown in Table 5.2.

Table 5.2 *Average relaxation time (τ), distribution of relaxation times (β) and relaxation time constant on the stretched time scale (τ^{β}) for amorphous lactose and amorphous indometacin aged at different temperatures as determined from enthalpy recovery data.*

Lactose				Indometacin			
Aging temperature (ºC)	**τ (days)**	**β**	**τ^{β}**	**Aging temperature (ºC)**	**τ (days)**	**β**	**τ^{β}**
100 (T_g-T_a=16 °C)	0.97 ± 0.04	0.9 ± 0.08	0.97	**37** (T_g-T_a=8.9 °C)	2 ± 0.4	0.9 ± 0.3	1.9
65 (T_g-T_a=49°C)	62170139 ± 26298921	0.1 ± 0.03	8.17	**25** (T_g-T_a=20.9 °C)	12.5 ± 0.9	0.7 ± 0.06	6.4
50 (T_g-T_a=64 °C)	283.4 ± 209.8	0.6 ± 0.1	35.5				

As expected, for both materials, τ values increased as the aging temperature decreased. This means that as temperature decreases, the time molecules take to complete a certain motion increases. In other words, molecular mobility decreases with decreasing temperature. τ values should be seen as an average relaxation time; some molecular motions may have τ values that are much shorter (and others much longer) than the mean τ value (Shamblin et al., 1999).

According to Kawakami and Pikal (2005) the relaxation time constant, τ^{β}, is a more powerful method for comparison of the data, by which the effect of the maximum annealing time on τ is reduced. For both amorphous lactose and indometacin, τ^{β} values increased with decreasing aging temperature. This is in agreement with the fact that at lower temperatures, molecular mobility is reduced. From Table 5.2 it can also be seen that τ^{β} values are smaller than τ, particularly for amorphous lactose aged at 65 and 50 ºC.

5.4.3. EFFECT OF AGING ON THE ENTHALPY OF SOLUTION OF AMORPHOUS LACTOSE AND AMORPHOUS INDOMETACIN

In order to investigate the effect of aging on the enthalpy of solution of amorphous lactose and amorphous indometacin, amorphous lactose and amorphous indometacin were aged at temperatures below their glass transition temperatures and the enthalpy of solution determined after increasing aging time periods. Figures 5.11 and 5.12 show the enthalpy of solution of aged amorphous lactose and indometacin, respectively, according to aging time and temperature. The enthalpy of solution of crystalline α-lactose monohydrate and crystalline γ-indometacin are presented for reference.

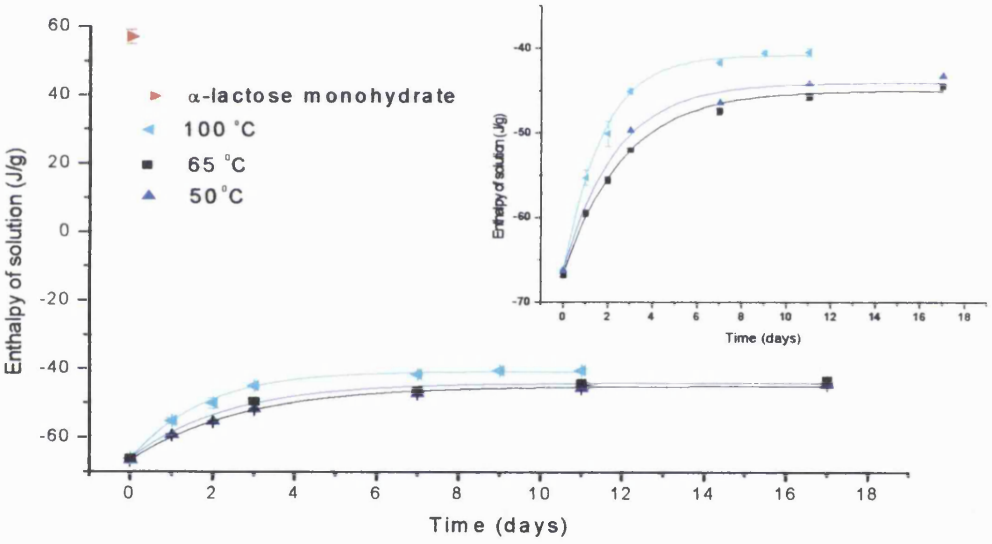

Figure 5.11 *Enthalpy of solution of amorphous lactose according to aging time and temperature, in comparison to the enthalpy of solution of the crystalline α-lactose monohydrate. The inset graph shows the enthalpy of solution of the amorphous lactose in more detail.*

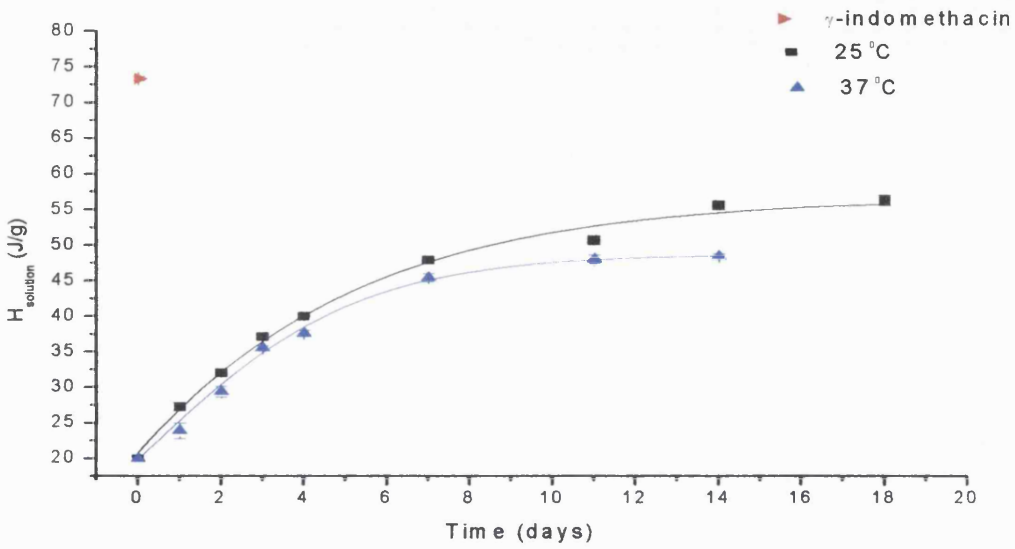

Figure 5.12 *Enthalpy of solution of amorphous indometacin according to aging time and temperature, in comparison to the enthalpy of solution of crystalline indometacin.*

Heat was released by the dissolution of amorphous lactose and absorbed by the dissolution of amorphous indometacin. However, as expected, the enthalpy of solution of the fresh amorphous material was more exothermic than the enthalpy of solution of the correspondent crystalline material. From Figures 5.11 it can be seen that the enthalpy of solution of the amorphous lactose become less exothermic upon aging. In other words, aging of amorphous lactose decreased the amount of heat released. In the case of amorphous indometacin (Figure 5.12), aging increased the amount of heat absorbed.

The effect of structural relaxation on the enthalpy of solution of amorphous material can be explained as follows (Johari, 1995). The difference between the enthalpies (or energy at one atmospheric condition under which pressure and volume variations are negligible) of two forms of the same material is known as excess enthalpy (H_{exc}) and can be written as:

$$H_{exc} = (E^0 + \sum E^i)_{form1} - (E^0 + \sum E^i)_{form2} \quad \textit{Equation 5.1}$$

where:

- E^0 is the sum of the lattice and vibrational energies
- $\sum E^i$ is the sum of the internal energy associated with vibrational, cohesive Van der Waals, covalent and hydrogen bond energy terms, and rotational transitions of molecular segments in the structure.

The enthalpy of solution can be written as:

$$H^s = \left(E^0 + \sum E^i\right)_{solution} + \left[\left(E^0 + \sum E^i\right)_{solvent} + \left(E^0 + \sum E^i\right)_{solute}\right] \quad \textit{Equation 5.2}$$

where E^0 and $\sum E^i$ are as defined for Equation 5.1.

When the solvent is the same for the dissolution of the two different phases of the same material at a certain temperature, $\left(E^0 + \sum E^i\right)_{solution}$ is the same for each, as is $\left(E^0 + \sum E^i\right)_{solvent}$. Thus, these two terms cancel each other out and the excess enthalpy is given by:

$$H_{exc} = -(H_1 - H_2) \quad \textit{Equation 5.3}$$

where:

- H_1 and H_2 are the enthalpies of solution of the two forms in a solvent at a fixed temperature.

Basically, if two forms of a material are dissolved in the same solvent at the same temperature, the difference in the enthalpy of solution will be equal to the difference between the energies of their initial states at that temperature (excess energy), because the final states of two forms of the same material dissolved in a given solvent are the same. Consequently, the enthalpy of solution yields the enthalpy difference between two different structures of the same material.

During structural relaxation the amorphous form decreases in molecular mobility, and consequently, in internal energy (or enthalpy at constant P and V). Progressively, the aged amorphous material approaches the pseudo equilibrium supercooled liquid state. This means that the energy difference between the aged amorphous and the crystalline forms of the material will decrease upon structural relaxation. Consequently, the exothermic enthalpy of solution will decrease (as seen for amorphous lactose) and the endothermic enthalpy of solution will increase (as seen for amorphous indometacin) during structural relaxation of an amorphous material.

The decrease in the exothermic enthalpy of solution of amorphous lactose is greater for the higher aging temperature. On the other hand, the increase in the endothermic enthalphy of solution of amorphous indometacin is greater for the lower aging temperature. This is in keeping with the determined enthalpy recovery for amorphous lactose and amorphous indometacin (Section 5.4.2).

5.4.3.1. ESTIMATION OF MOLECULAR MOBILITY FROM ENTHALPY OF SOLUTION DATA

In order to estimate the molecular mobility of amorphous lactose from enthalpy of solution data, the energy difference between the enthalpy of solution at each time point and the enthalpy of solution of the fresh amorphous lactose (t=0) was considered as the enthalpy relaxation for that time point. Figures 5.13 and 5.14 represent show the enthalpy relaxation values for each time point according to the aging temperature used for amorphous lactose and indometacin, respectively. It is clear that for each aging temperature, the enthalpy relaxation increased with increasing aging time until it reached a plateau. This is because, for a certain aging temperature, as the glass relaxes, its enthalpy progressively decreases with time, and consequently the energy difference between the fresh and the aged amorphous material increases with time.

It can be seen that for amorphous lactose, for each aging time, the enthalpy recovery increased with increasing aging temperature. However, for each aging time the enthalpy recovery determined for amorphous indometacin decreased with increasing aging temperature. This agrees with the enthalpy recovery data obtained by StepScan differential scanning calorimetry (Section 5.4.2). As already discussed,

such difference can be explained by the fact that there might be an aging temperature that gives maximum enthalpy relaxation (Kawakami and Pikal, 2005). Amorphous indometacin aging at 37 °C (T_g-T_a=6°C) resulted in lower enthalpy relaxation than aging at 25°C (T_g-T_a=18°C). The molecular mobility may decrease with decreasing temperature, which could explain the presence of an optimum temperature at which the enthalpy relaxation is maximum.

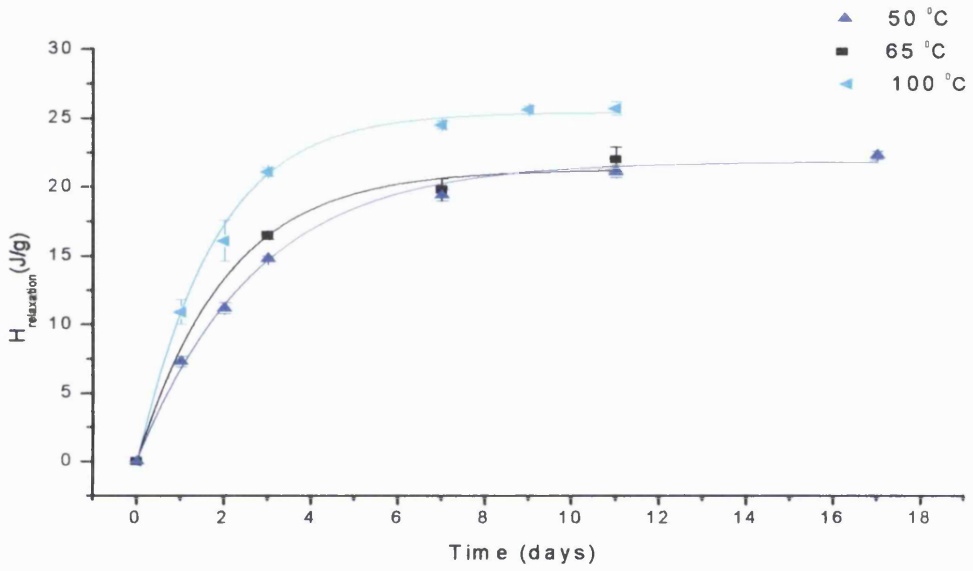

Figure 5.13 *Enthalpy relaxation as a function of time for amorphous lactose aged at different temperatures, as determined from enthalpy of solution data.*

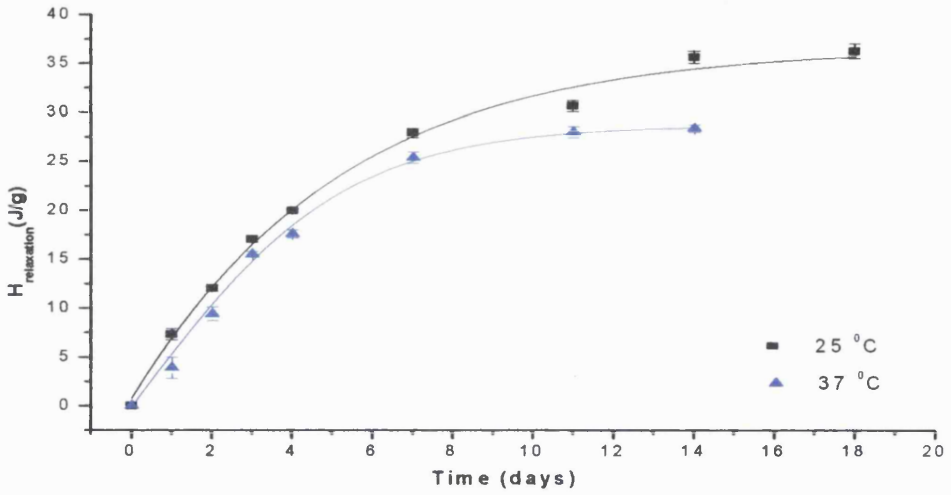

Figure 5.14 *Enthalpy relaxation as a function of time for amorphous indometacin aged at different temperatures, as determined from enthalpy of solution data.*

For both lactose and indometacin, the enthalpy relaxation values obtained from enthalpy of solution data are greater than the enthalpy recovery data presented in Section 5.4.2. It is possible that the higher enthalpy relaxation determined from solution calorimetry data results from a contribution to the thermal power detected by solution calorimetry from a relaxation other than α-relaxation. A similar observation had previously been reported by Liu et al. (2002) enthalpy relaxation data of freeze-dried samples obtained by isothermal microcalorimetry were slightly higher than the enthalpy recovery determined by differential scanning calorimetry.

In order to estimate the molecular mobility of amorphous lactose, the calculated enthalpy relaxation was used to determine the extent of relaxation for each aging time point, according to Equation 1.8. The last enthalpy relaxation value for each aging temperature was considered as the maximum possible enthalpy relaxation ($\Delta H_{(\infty)}$) value; this can be considered a valid approach as the enthalpy relaxation reached a plateau.

This calculation of the extent of relaxation normalises the enthalpy relaxation values, enabling comparison of the rate of structural relaxation. Figure 5.15 shows the extent of relaxation of amorphous lactose aged at different temperatures, as determined from enthalpy of solution data. Figure 5.16 shows the extent of

relaxation of amorphous indometacin aged at 25 and 37°C as determined from enthalpy of solution data. The greater the value of the extent of relaxation, the less is the relaxation of glass to the pseudo equilibrium supercooled liquid. As previously observed for amorphous lactose and indometacin (Section 5.4.2, StepScan DSC data), the higher the aging temperature, the more relaxed the amorphous material was.

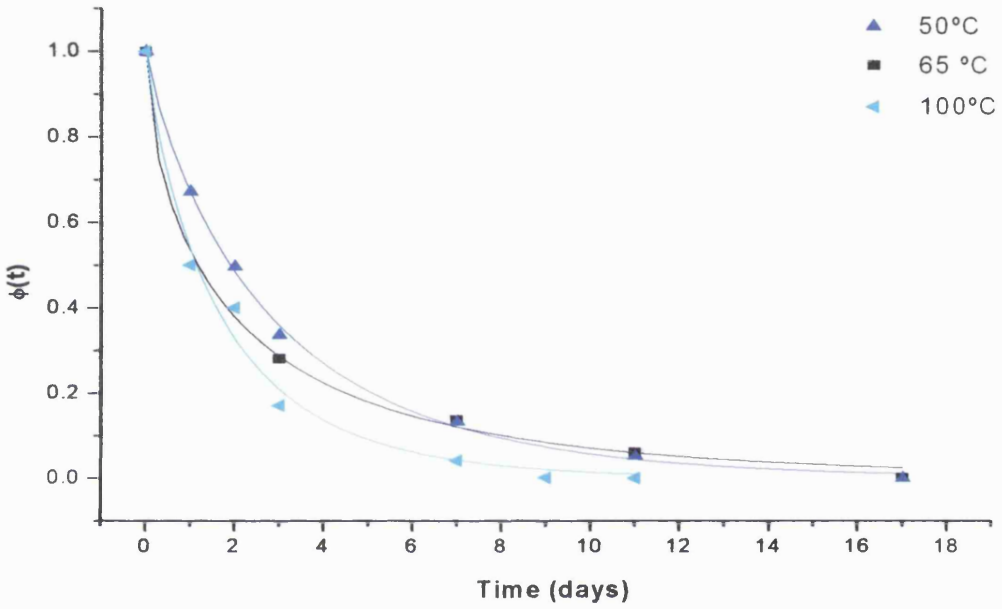

Figure 5.15 *The extent of relaxation as a function of time for amorphous indometacin aged at different temperatures as determined from enthalpy of solution data; solid lines are the curves of best fit in the KWW equation.*

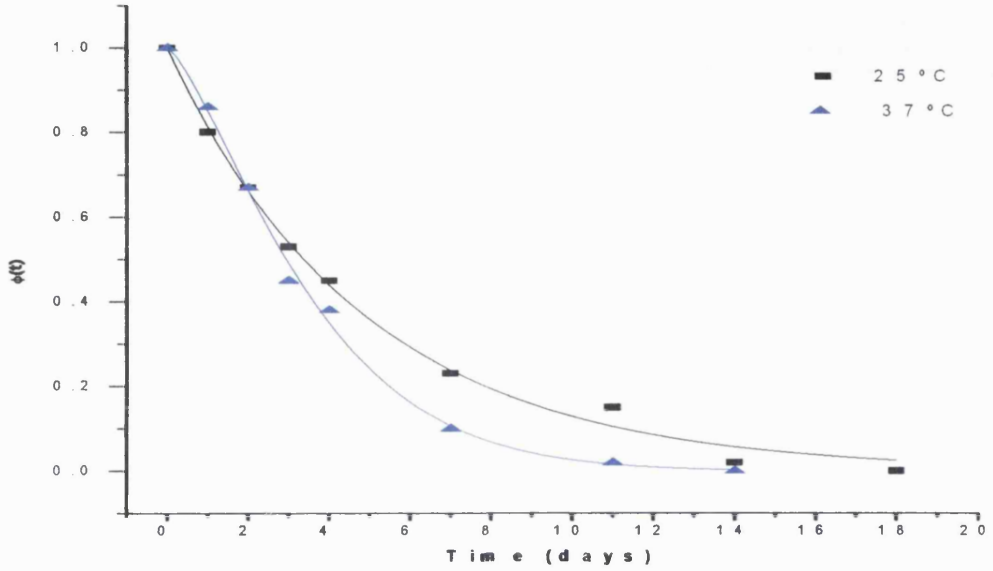

Figure 5.16 *The extent of relaxation as a function of time for amorphous indometacin aged at different temperatures as determined from enthalpy of solution data; solid lines are the curves of best fit in the KWW equation.*

Table 5.3 *Average relaxation time (τ), distribution of relaxation times (β) and relaxation time constant on the stretched time scale (τ^{β}) for amorphous lactose and amorphous indometacin aged at different temperatures as determined from enthalpy of solution data.*

Lactose				Indometacin			
Aging temperature (°C)	**τ (days)**	**β**	**τ^{β}**	**Aging temperature (°C)**	**τ (days)**	**β**	**τ^{β}**
100 (T_g-T_a=16 °C)	1.7 ± 0.1	0.8 ± 0.09	1.5	**37** (T_g-T_a=8.9 °C)	3.8 ± 0.1	0.99 ± 0.06	3.8
65 (T_g-T_a=49 °C)	2.1 ± 0.2	0.6 ± 0.06	1.6	**25** (T_g-T_a=20.9 °C)	4.9 ± 0.17	0.99 ± 0.05	4.8
50 (T_g-T_a=64 °C)	2.9 ± 0.09	0.9 ± 0.04	2.5				

The extent of relaxation values at each temperature were fitted to the KWW equation (Equation 1.7) using τ and β as variables. This provided the values of τ and β for lactose and indometacin for each aging temperature, which are shown in Table 5.3. τ and τ^{β} values decreased with increasing aging temperature. This means that as the temperature increases, molecular motion increases. This is in keeping with

the results obtained from StepScan DSC. These data will be compared to those obtained from StepScan DSC and literature values in Section 5.4.5.

5.4.4. EFFECT OF AGING ON THE DISPERSIVE SURFACE ENERGY OF AMORPHOUS LACTOSE

In order to investigate the effect of structural relaxation of amorphous lactose on its dispersive surface energy, aged amorphous lactose was analysed by inverse phase gas chromatography. The dispersive surface energy of aged amorphous lactose is represented in Figure 5.17 according to the aging temperature and time. The dispersive surface energy of crystalline α-lactose monohydrate is also represented in Figure 5.17 for reference.

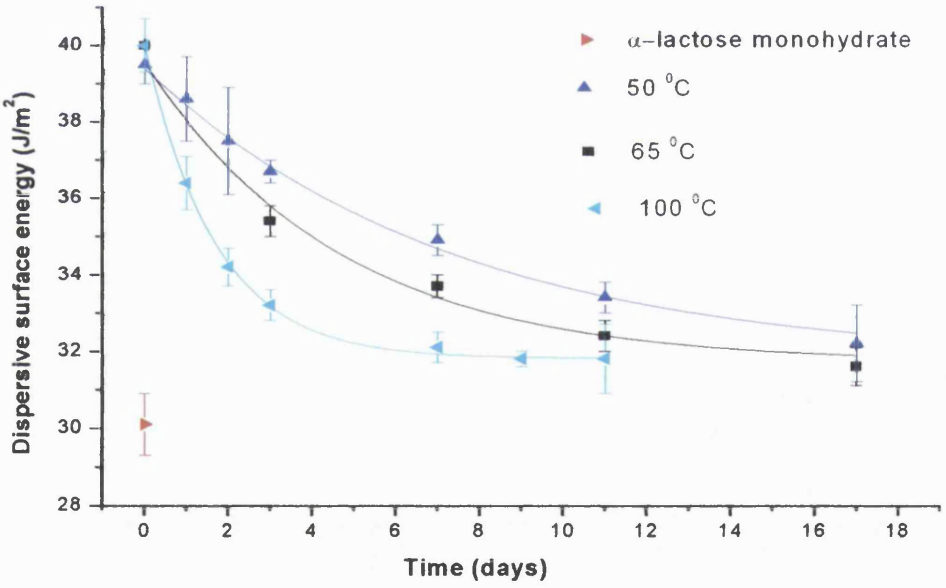

Figure 5.17 *Dispersive surface energy of amorphous lactose according to aging time and temperature.*

As expected, the dispersive surface energy of the amorphous lactose is higher than that of the crystalline α-lactose monohydrate. This can be for a number of reasons. Firstly, in the amorphous state the disordered molecules can assume more random orientations on the surface of the particle, exposing higher energy groups at the surface of the particle. Secondly, the chemical groups at the surface of the powder

can differ from the amorphous to the crystalline form (Grimsey et al., 2002). Finally, the amorphous surface is thermodynamically unstable and thus in a higher energy state (Feeley et al., 1998; Newell et al., 2001b) than its crystalline counterpart.

For all three aging temperatures used in the present study, the dispersive surface energy of aged amorphous lactose decreased with the time the sample had been exposed to that aging temperature. The surface gained sufficient mobility to repack and this was seen as a decrease in the dispersive surface energy. Newell et al. (2001a) have shown that the surface energy of an amorphous material changes and approximates the surface of the crystalline material, prior to crystallisation. In this same work it was shown that the dispersive surface energy of a milled amorphous sample (the amorphous material is located at the surface of the particles) was 40.8 mJ/m^2 at 0% RH, dropping to 34.2 mJ/m^2 after exposure to 30% RH for 30h (conditions that did not lead to crystallisation), and after returning the RH to 0% the surface energy was 38.2 mj/m^2. This demonstrates that the increased molecular mobility at 30% RH originated a different conformation at the surface. Hogan and Buckton (2001) showed that spherical spray-dried amorphous particles of raffinose develop the external shape of crystals prior to crystallisation. Changes of the surface of the particles can alter the proportion of functional groups present at the surface. Consequently, it is clear that relaxation processes within the amorphous state will result in changes in the physico-chemical properties of the amorphous form prior to crystallisation. It is possible that as relaxation proceeds and the amorphous form reduces in volume, the molecules come together. This can result in a progressive change of the groups at the surface of the particles, which, consequently, is reflected in a change in the dispersive surface energy.

The decrease in dispersive surface energy is higher for the higher aging temperature. This is in keeping with the decrease in enthalpy recovery for aged amorphous lactose, as determined by StepScan DSC.

5.4.4.1. ESTIMATION OF MOLECULAR MOBILITY FROM INVERSE PHASE GAS CHROMATOGRAPHY DATA

In order to estimate the molecular mobility of amorphous lactose from inverse phase gas chromatography data, the energy distance between the dispersive surface

energy at each time point and the dispersive surface energy of the fresh amorphous lactose (t=0) was considered as the enthalpy relaxation for that time point. The enthalpy relaxation values for each time point are represented in Figure 5.18 according to the aging temperature used. It is clear that for each time point, the enthalpy relaxation increased with increasing aging temperature until it reached a plateau. This agrees with the enthalpy recovery data obtained by StepScan DSC and enthalpy relaxation data obtained by solution calorimetry for amorphous lactose. Unlike the enthalpy of solution data, the enthalpy relaxation values obtained from dispersive surface energy data more closely resemble the enthalpy of recovery obtained by StepScan DSC.

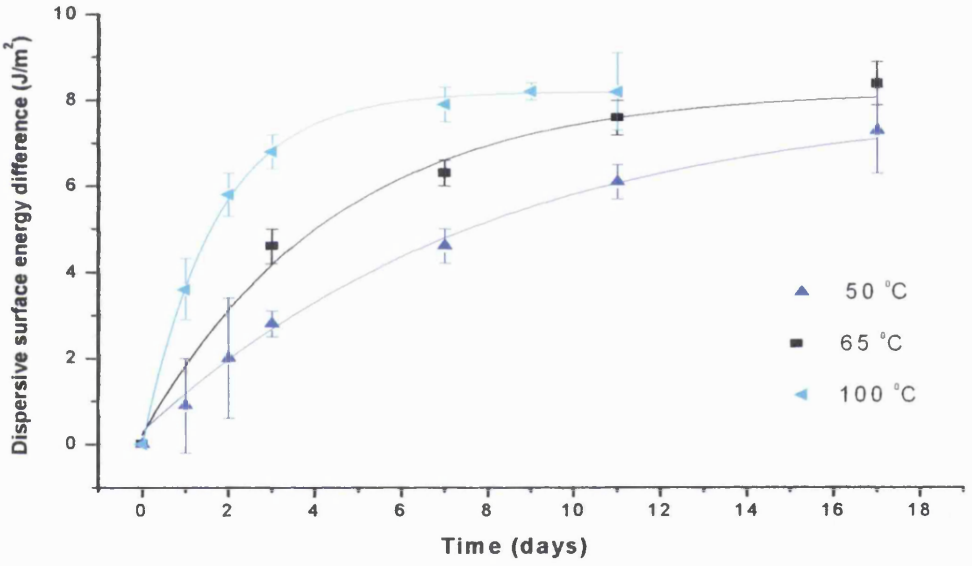

Figure 5.18 *Dispersive surface energy difference value as a function of time for amorphous lactose aged at different temperatures, as determined from dispersive surface energy data.*

As for analysis of enthalpy of solution data (Section 5.4.3.1), the last dispersive surface energy difference value for each aging temperature was considered as the maximum possible enthalpy relaxation ($\Delta H_{(\infty)}$) value.

In order to estimate the molecular mobility of amorphous lactose, the calculated dispersive surface energy difference was used to determine the extent of relaxation for each aging time point, according to Equation 1.8. This normalises the dispersive surface energy difference values, enabling comparison of the rate of structural

relaxation. Figure 5.19 shows the extent of relaxation of amorphous lactose aged at different temperatures, as determined from dispersive surface energy data. The greater the value of the extent of relaxation, the lesser is the relaxation of glass to the pseudo equilibrium supercooled liquid. As previously observed for amorphous lactose, the higher the aging temperature, the more relaxed the amorphous lactose was.

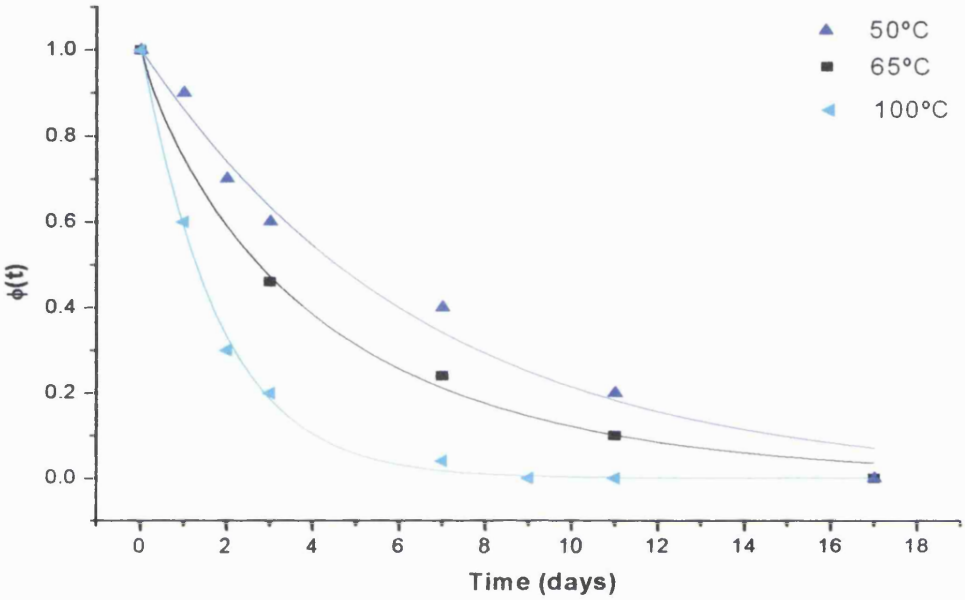

Figure 5.19 *The extent of relaxation as a function of time for amorphous lactose aged at different temperatures as determined from dispersive surface energy data; solid lines are the curves of best fit in the KWW equation.*

The extent of relaxation values at each temperature were fitted to the KWW equation (Equation 1.7) using τ and β as variables. This provided the values of τ and β for lactose for each aging temperature, which are shown in Table 5.4.

Table 5.4 *Average relaxation time (τ), distribution of relaxation times (β) and relaxation time constant on the stretched time scale (τ^{β}) for amorphous lactose aged at different temperatures as determined from dispersive surface energy data.*

Lactose			
Aging temperature (ºC)	**τ (days)**	**β**	**τ^{β}**
100 (T_g-T_a=16 °C)	1.81 ± 0.06	1.0 ± 0.07	1.9
65 (T_g-T_a=49 °C)	4.2 ± 0.3	0.9 ± 0.09	3.4
50 (T_g-T_a=64 °C)	6.5 ± 0.5	0.99 ± 0.1	6.7

As expected, for both materials, τ and τ^{β} values increased as the aging temperature decreased. As already mentioned, this means that as temperature decreases, the time molecules take to complete a certain motion increases. In other words, molecular mobility decreases with decreasing temperature. A comparison with the results obtained from solution calorimetry and StepScan DSC and literature values is given in Section 5.4.5.

5.4.5. COMPARISON OF THE THREE METHODS FOR ESTIMATION OF MOLECULAR MOBILITY

Table 5.5 shows compiles the τ, β and τ^{β} values obtained from StepScan DSC, solution calorimetry and inverse phase gas chromatography following the methodologies described in the previous sections.

Table 5.5 *Average relaxation time (τ), distribution of relaxation times (β) and relaxation time constant on the stretched time scale (τ^{β}) for amorphous lactose and amorphous indometacin aged at different temperatures obtained by the three methods.*

Sample	StepScan DSC			SolCal			iGC		
	τ (days)	β	τ^{β}	τ (days)	β	τ^{β}	τ (days)	β	τ^{β}
Lactose aged at 100 ºC (T_g-T_a=16 °C)	0.97 ± 0.04	0.99 ± 0.08	0.97	1.7 ± 0.1	0.8 ± 0.09	1.5	1.8 ± 0.06	1.0 ± 0.07	1.9
Lactose aged at 65 ºC (T_g-T_a=49 °C)	62170139 ± 262989219	0.1 ± 0.03	8.17	2.1 ± 0.2	0.6 ± 0.06	1.6	4.2 ± 0.3	0.9 ± 0.09	3.4
Lactose aged at 50 ºC (T_g-T_a=64 °C)	283.4 ± 209.8	0.6 ± 0.1	35.5	2.9 ± 0.09	0.9 ± 0.04	2.5	6.5 ± 0.5	0.99 ± 0.1	6.7
Indometacin aged at 37 ºC (T_g-T_a=8.9 °C)	2 ± 0.4	0.9 ± 0.3	1.9	3.8 ± 0.1	0.99 ± 0.06	3.8			
Indometacin aged at 25 ºC (T_g-T_a=20.9 °C)	12.5 ± 0.9	0.7 ± 0.06	6.4	4.9 ± 0.17	0.99 ± 0.05	4.8			

τ values obtained by StepScan DSC for amorphous lactose are in reasonable agreement with the literature. Lactose aged at 100ºC for 16 h showed a τ of approximately 12 hours (0.5 days) determined from enthalpy recovery collected by modulated DSC (Craig et al., 2000). The higher τ values obtained in this study might be caused by the different experimental conditions used during the relaxation experiments, namely the maximum aging time. This produces errors in the τ and β values; τ values become too high and β values too low. Kawakami and Pikal (2005) show the impact of experimental periods (maximum aging time) on the τ and β values of amorphous indometacin, nifedipine and maltose. For the three materials, an increase in τ values was observed with increasing maximum aging times. A comparison of τ^{β} would be preferable.

In the same way, τ values determined by StepScan DSC for amorphous indometacin agree with those reported in the literature; relaxation time for dry amorphous indometacin at 30ºC aged was approximately 4 days (Andronis et al., 1997). However, indometacin aged at 30 ºC for 2 to 16 h exhibited relaxation times between 7.6 and approximately 40 h (Kawakami and Pikal, 2005). Such differences in relaxation times might be caused by the different experimental conditions used during the relaxation experiments, namely the maximum aging time.

In the case of amorphous lactose at lower temperatures, long relaxation times with large error values were obtained from StepScan DSC data. Large error values were previously reported for lactose aged at 80 ºC by Craig et al. (2000) and for amorphous sodium indometacin aged at 5ºC (Tong and Zografi, 1999). These large error values could mean the insensitivity of the KWW model to predict the extremely slow relaxation motions. On the other hand, the very large relaxation times could also be regarded as absent or very slow molecular mobility at a particular aging temperature. The long maximum aging time used during the experiment might also contribute to the very long relaxation times obtained for amorphous lactose aged at 50 and 65ºC.

Solution calorimetry and inverse phase gas chromatography returned τ and τ^{β} values that did not exactly match those obtained by StepScan DSC. This might be a consequence of the fact that solution calorimetry and inverse phase gas chromatography might be able to detect other relaxations than α-relaxation. The methodology used to determine the extent of relaxation from enthalpy of solution and dispersive surface energy might also account for the differences observed. Such methodology used the last data point of enthalpy of solution and dispersive surface energy data as the maximum possible enthalpy relaxation for those aging conditions. This affected the curve of the extent of relaxation against time, particularly for the samples aged at temperatures well below the glass transition temperature; extents of relaxation of amorphous lactose aged at 50 and 65ºC determined from enthalpy of solution and dispersive surface energy approached zero, while those determined from StepScan DSC were well above zero. This might influence the τ and β values obtained by fitting the extent of relaxation according to time to the KWW equation. The τ and β values obtained for samples aged at temperatures close to the glass transition temperature more closely agree between the three methods.

The experimental procedures of StepScan DSC, solution calorimetry and inverse phase gas chromatography are obviously different. The equilibration time on a solution calorimetry experiment and the conditioning step on an inverse phase gas chromatography experiment might have induced some relaxation of the samples and consequently affect the obtained τ and β values. Relaxation might also occur during a StepScan experiment. As such, comparison of the τ^{β} might be a better way of comparing the three techniques. In fact, τ^{β} are closer than τ values.

5.5. CONCLUSION

StepScan DSC proved successful for the characterisation of the aging of amorphous lactose and indometacin. By determination of the enthalpy recovery by StepScan DSC it was seen that enthalpy recovery of amorphous lactose increased with aging temperature and time exposed to that temperature, while enthalpy recovery of amorphous indometacin was seen to increase with aging time.The relaxation time parameters were in good agreement with those reported in the literature, considering the longer maximum aging time used in the present study.

The aging of both amorphous lactose and indometacin affected the enthalpy of solution as measured by solution calorimetry. Enthalpy of solution of amorphous lactose became less exothermic upon aging and enthalpy of solution of amorphous indometacin became more endothermic upon aging. A methodology was proposed in order to determine the enthalpy relaxation from enthalpy of solution data. The enthalpy relaxation values determined from enthalpy of solution data showed the same trend as the enthalpy recovery values, but were higher than enthalpy recovery values. This suggests that there might be a contribution to the thermal power detected by solution calorimetry from a relaxation mode other than α-relaxation. An investigation into this matter is clearly necessary. τ^{β} values determined from enthalpy of solution data exhibited the same trend as those obtained from StepScan DSC data.

At this point, the consequences of the effect of aging on the enthalpy of solution of an amorphous material in the use of solution calorimetry for characterisation and quantification of amorphous contents should be pointed out. As already mentioned, the use of solution calorimetry for quantification of amorphous content requires the determination of the enthalpy of solution of 100% amorphous and crystalline

standards. If the enthalpy of solution of the amorphous form changes upon aging, care must be taken to ensure that standard and test amorphous samples were subjected to the same conditions before enthalpy of solution determination.

The aging of amorphous lactose affected its dispersive surface energy; dispersive surface energy of amorphous lactose decreased with increasing aging temperature and time. The enthalpy relaxation values determined from dispersive surface energy data showed the same trend as those obtained from solution calorimetry data and enthalpy recovery values. Unlikely the enthalpy of solution data, the enthalpy relaxation values obtained from dispersive surface energy data more closely resemble the enthalpy of recovery obtained by StepScan DSC

The determination of surface energy is normally carried out to access the effect of processing on the surface of the material, to predict the processing attributes of a material, and the performance of a drug delivery system. Consequently, in order for the surface energy determination by inverse phase gas chromatography to be valid and meaningful, it is important to take into account any possible effect of aging on the surface energy. An investigation on the effect of aging on the polar component of the surface energy should also be carried out. In addition, if aging affects the surface energy of a material, it can, consequently, affect the processing attributes of such material. This is clearly an important area for further investigation.

In this Chapter…

… StepScan DSC was used to determine the enthalpy recovery of aged amorphous lactose and indometacin because it allows the separation of the glass transition from the enthalpy recovery endotherm;

… it was seen that enthalpy recovery of amorphous lactose increased with aging temperature and time exposed to that temperature, while enthalpy recovery of amorphous indometacin was seen to increase with aging time but was lower for the higher aging temperature;

… it was seen that enthalpy of solution of amorphous lactose and indometacin was affected by the aging of the amorphous material; enthalpy of solution of amorphous lactose became less exothermic upon aging and enthalpy of solution of amorphous indometacin became more endothermic upon aging.

… the difference in enthalpy of solution of the aged amorphous and the fresh amorphous sample, was used to calculate the enthalpy relaxation for that aged sample. Enthalpy relaxation of amorphous lactose increased with aging temperature and time exposed to that temperature, while enthalpy relaxation of amorphous indometacin was seen to increase with aging time but was lower for the higher aging temperature.

… it was seen that the dispersive surface energy of amorphous lactose decreased with increasing aging temperature and time;

… the difference in dispersive surface energy of the aged sample and the freshly prepared sample was used to determine the enthalpy relaxation. Enthalpy relaxation of amorphous lactose increased with aging temperature and time exposed to that temperature.

… enthalpy recovery, enthalpy relaxation obtained from enthalpy of solution data and enthalpy relaxation obtained from dispersive surface energy data were used to calculate the extent of relaxation for each aging condition.

... for each aging condition, the extent of relaxation according to time was fitted to the KWW equation in order to characterise the molecular mobility in terms of τ, β and τ^{β}.

... τ^{β} values obtained by the three techniques showed the same trend; the higher the aging temperature, the lower is τ^{β} value, i.e. the higher is the molecular mobility. The differences were greater for aging temperatures well below the glass transition temperature. This might be caused by differences in the molecular mobility that is being accessed. A further investigation in to this matter is clearly necessary.

CHAPTER SIX

SUMMARY AND FUTURE WORK

Batch isothermal microcalorimetry was used to determine the amorphous content of lactose at 25 ˚C and 53% RH, by determining the enthalpy of crystallisation relating to the amorphous portion of each sample. The crystallisation response of fully and partially amorphous lactose samples can be varied in shape. The changes in the shape of the crystallisation peak can make it difficult to achieve a consistent enthalpy determination. In order to overcome this, an integration methodology which consisted of integrating the calorimetric data from the end of region A to region E of Figure 3.1 from y=0 was used to determine the enthalpy of crystallisation. It was possible to construct a calibration curve for quantification of amorphous content in lactose but this was not linear. However, the heats measured in the calorimeter, at any particular amorphous content, were reproducible.

In order to investigate the possible causes of the non-linearity of the calibration curve, samples removed from the TAM were analysed by thermal gravimetric analyisis and differential scanning calorimetry. It was observed that amorphous samples were crystallising to a mixture of α-lactose monohydrate, β-lactose and anhydrous α-lactose. The final proportion of each anomer seemed to vary with the initial amorphous content. DSC data also indicated that β-lactose and α-lactose exhibit different enthalpy of fusion (and consequently different enthalpy of crystallisation). Such differences in crystallisation and enthalpy of crystallisation probably accounted for the negative-deviated calibration curve obtained by batch isothermal microcalorimetry.

The fact that the anomeric composition of the recrystallised lactose seemed to be affected by the initial amorphous content of the sample motivated a deeper investigation into the isothermal crystallisation of amorphous lactose. Two batches of amorphous lactose with different anomeric composition were crystallised at 53% RH and 97% RH, 25 ºC in the TAM. Both amorphous batches were combined with crystalline lactose with different anomeric composition to prepare partially amorphous samples, which were also recrystallised at 53% RH and 97% RH, 25 ºC in the TAM and the final anoemric composition determined by gas chromatography. The anomeric composition of the recrystallised lactose was seen to be affected by the initial anomeric composition, relative humidity and initial amorphous content. The crystalline forms of lactose are known to have different properties, which might influence the product stability and performance. The results of the crysatllisation study are important for modelling the crystallisation of amorphous lactose and, consequently, for prediction of the performance and stability of lactose-containing

food and pharmaceutical materials. On the other hand, the outcome of the crystallisation of amorphous lactose will most certainly impact on the measured heat output during crystallisation in an isothermal Microcalorimetry experiment, and consequently, on the quantification of amorphous contents by determination of the enthalpy of crystallisation by a calorimetric method.

Isothermal RH perfusion Microcalorimetry was used to investigate the anomeric composition of lactose on the quantification of low amorphous contents. The main advantage of the RH perfusion unit is the control over the RH environment of the sample. This enables the drying of the samples to 0% RH prior and after crystallisation, and it also ensures that the experiment commences from a steady baseline. Two batches of amorphous lactose containing different anomeric composition were combined with commercial crystalline α-lactose monohydrate and β-lactose in order to prepare samples of 1, 3 and 5% (w/w) amorphous content. Samples were dried at 0% RH, crystallised at 90% RH and dried after crystallisation at 0% RH. Two methods for determining the enthalpy of crystallisation were studied. The method consisting of subtracting the drying response of the crystallised sample from the crystallisation response returned the most reproducible enthalpies of crystallisation and was applied to determine the enthalpy of crystallisation of allsets of partially amorphous samples.

It was found that anomeric composition of amorphous and crystalline lactose does affect the quantification of small amorphous content in lactose. This does not invalidate the use of Isothermal RH Perfusion Microcalorimetry for quantification os small amorphous contents. However, care must be taken to ensure that standards and test samples exhibit the same anomeric composition, and that crystallisation leads to a final lactose with the same anomeric composition. For processed samples, consisting of crystalline cores with an outer corona of amorphous material, it can be complex to quantify the anomeric composition of each fraction.

The impact of the anomeric composition of the crystalline portion on the measured heat output is more significant for low amorphous contents. The impact of the anomeric composition of amorphous material with different anomeric composition is expected to be prevalent at higher amorphous contents. Further work is required to investigate this; it would be interesting to construct calibration curves for determination of amorphous content of high amorphous content samples.

A main disadvantage of Isothermal Microcalorimetry is the fact that no chemical data is provided. As such, the crystallisation process is not fully understood, and future work is necessary in order to aid the understanding of the many events that comprise a crystallisation response in the calorimeter.

The effect of the anomeric composition of lactose on the quantification of amorphous content by Solution Calorimetry was also investigated. The enthalpy of solution of crystalline lactose with different anomeric composition, amorphous lactose with different anomeric composition and partially amorphous samples was determined from dissolving the samples in 100 mL of water at 25 °C. The anomeric composition of the crystalline portion of partially amorphous lactose samples does affect the quantification of amorphous content in lactose because of the dependence of the enthalpy of solution of crystalline lactose on its anomeric composition; different calibration curves were obtained for samples containing different lactose crystalline forms. Partially amorphous samples containing the same crystalline lactose and amorphous lactose of different anomeric composition exhibited different enthalpy of solution. It should be noted that these findings do not invalidate the use of solution calorimetry for the quantification of amorphous content in lactose. However, it has to be ensured that the amorphous and crystalline standards and test samples are of the same anomeric nature. The determination of processed samples, consisting of amorphous corona and a crystalline core, might not be so straightforward. Moreover, it is likely that the interactions in processed samples differ from those of wholly amorphous and wholly crystalline particles. Future work is necessary to investigate the use of solution calorimetry for quantification of amorphous content of processed materials, which should be linked with an investigation of the type of interactions in a processed material and how these differ from two component samples.

It is important to note that the ability of solution calorimetry to quantify amorphous ocntent relies upon the difference between the enthalpy of solution of the amorphous and crystalline forms, which differ with each material. If these values are similar for a given material, the quantification accuracy will be compromised. Future work is required to determine the applicability of solution calorimetry for quantification in other materials. The applicability of solution calorimetry for quantification of amorphous content in multi-component systems should also be accessed as these might better represent the real systems.

The relaxation behaviour of amorphous lactose and amorphous indometacin was characterised by isothermal methods, namely solution calorimetry, inverse phase gas chromatography, and stepscan differential scanning calorimetry.

StepScan DSC allowed the separation of the glass transition temperature from the superimposed enthalpy recovery endotherm, facilitating measurement of the enthalpy recovery. The use of DSC for the determination of the enthalpy relaxation assumes that the measured enthalpy recovery has the same magnitude as the enthalpy relaxation. The enthalpy recovery of amorphous lactose aged at 50, 65 and 100 °C was determined at different times. The enthalpy recovery of amorphous indometacin aged at 25 and 37 °C was determined at different times. The enthalpy recovery of amorphous lactose increased with aging temperature and time exposed to that temperature, while enthalpy recovery of amorphous indometacin was seen to increase with aging time. This suggested that there is an optimum aging temperature that gives maximum enthalpy relaxation.

Enthalpy of solution of amorphous lactose aged at 50, 65 and 100 °C and amorphous indometacin aged at 25 and 37 °C was determined at the same time points as for StepScan DSC. The enthalpy of solution of amorphous lactose and indometacin was affected by the aging of the amorphous material; enthalpy of solution of amorphous lactose became less endothermic upon aging and enthalpy of solution of amorphous indometacin became more endothermic upon aging. The difference in enthalpy of solution of the aged amorphous and fresh amorphous sample was used to calculate the enthalpy relaxation for that aged sample. Enthalpy relaxation of amorphous lactose increased with aging temperature and time exposed to that temperature, while enthalpy relaxation of amorphous indometacin was seen to increase with aging time but was lower for higher aging temperature. For both lactose and indometacin, the enthalpy relaxation values obtained from enthalpy of solution data are greater than the enthalpy recovery data obtained from StepScan DSC.

Dispersive surface energy of amorphous lactose aged at 50, 65 and 100 °C was determined at the same time points as for StepScan DSC and Solution Calorimetry. The dispersive surface energy of amorphous lactose decreased with increasing aging temperature and time. The difference in dispersive surface energy of the aged sample and the freshly prepared sample was calculated and was seen to increase with aging temperature and time exposed to that aging temperature.

In order to normalise the enthalpy recovery values, enabling comparison of the rate of structural relaxation, the extent of relaxation was determined from enthalpy recovery, relaxation and dispersive surface energy difference for each aging temperature. The extent of relaxation values at each temperature were fitted to the KWW equation in order to characterise the molecular mobility in terms of τ, β and τ^{β}. For both amorphous lactose and indometacin, τ^{β} values increased with decreasing aging temperature, which is in agreement with the fact that at lower temperatures, molecular mobility is reduced. Solution Calorimetry and inverse phase gas chromatography returned τ and τ^{β} values that did not exactly match those obtained by StepScan DSC. The difference in τ^{β} value for the three techniques were greater for aging temperatures well below the glass transition temperature. This might be caused by differences in the molecular mobility that is being accessed. The methodology used to determine the extent of relaxation from enthalpy of solution and dispersive surface energy might also account for the differences observed.

When using Solution Calorimetry, it should be verified if the enthalpy of solution of the amorphous form changes upon aging. In case it does, care must be taken to ensure that standard and test amorphous samples were subjected to the same conditions before enthalpy of solution determination.

It should be noted that in order for a surface energy determination by Inverse Phase Gas Chromatography to be valid and meaningful, it is important to take into account any possible effect of aging on the surface energy. An investigation of the effect of aging on the polar component of the surface energy should also be carried out. In addition, if aging affects the surface energy of a material, it can, consequently, affect the processing and quality attributes of such material. This is clearly an important subject for further investigation.

The work presented shows that it is essential to investigate the effect of structural relaxation on the various properties of an amorphous material prior to its characterisation. Future work should also try to ascertain which characterisation methodologies are not affected by structural relaxation of the amorphous material.

At this point, a discussion of the impact of the variability or "quality" of the amorphous material on its quantification and characterisation is relevant. The anomeric composition of an amorphous material can be considered as an example of variability of that amorphous material. Upon structural relaxation, the amorphous

material does also change in its properties. This work highlighted the importance of the "quality" of an amorphous material on its detection, quantification, and characterisation. More research into such matters is definetly necessary. Furthermore, an investigation of the impact of the variability or "quality" of the amorphous material onto product manufacturing and performance is equally essential.

REFERENCES

Ahmed, H., Buckton, G., Rawlins, D.A., 1996. The use of isothermal microcalorimetry in the study of small degrees of amorphous content of a hydrophobic powder. International Journal of Pharmaceutics, 130, 195-201.

Al-Hadithi, D., Buckton, G., Brocchini, S., 2004. Quantification of amorphous content in mixed systems: amorphous trehalose with lactose. Thermochimica Acta, 417, 193-199.

Aldous, B.J., Auffret, A.D., Franks, F., 1995. The crystallisation of hydrates from amorphous carbohydrates. Cryo-Letters, 16, 181-186.

Alnheck, C., Zografi, G., 1990. The molecular basis of moisture effects on the physical and chemical stability of drugs in the solid state. International Journal of Pharmaceutics, 62, 87-95.

Ambarkhane, A.V., Pincott, K., Buckton, G., 2005. The use of inverse gas chromatography and gravimetric vapour sorption to study transitions in amorphous lactose. International Journal of Pharmaceutics, 294, 129-135.

Andronis, V., Yoshioka, M., Zografi, G., 1997. Effects of sorbed water on the crystallisation of indometacin from the amorphous state. Journal of Pharmaceutical Sciences, 86, 346-351.

Andronis, V., Zografi, G., 1997. Molecular mobility of supercooled amorphous indometacin, determined by dynamic mechanical analysis. Pharmaceutical Research, 14, 410-414.

Andronis, V., Zografi, G., 1998. The molecular mobility of supercooled amorphous indometacin as a function of temperature and relative humidity. Pharmaceutical Research, 15, 835-842.

Andronis, V., Zografi, G., 2000. Crystal nucleation and growth of indometacin polymorphs from the amorphous sate. Journal of Non-Crystalline Solids, 271, 236-248.

Andrzejewska, E., Voelkel, A., Andrezejewski, M., Maga, R., 1996. Examination of surfaces of solid polymers by inverse phase gas chromatography: 2. Acid-base properties. Polymer, 37, 4333-4344.

Angberg, M., Nyström, C., Castensson, S., 1991. Evaluation of heat-conduction microcalorimetry in pharmaceutical stability studies. III. Crystallographic changes due to water vapour uptake in anhydrous lactose powder. International Journal of Pharmaceutics, 73, 209-220.

Angberg, M., Nyström, C.S., 1992a. Evaluation of heat-conduction microcalorimetry in pharmaceutical stability studies. V. A new approach for continuous measurments in abundant water vapour. International Journal of Pharmaceutics, 81, 153-167.

Angberg, M., Nyström, C., Carstensen, J.T., 1992b. Evaluation of heat-conduction microcalorimetry in pharmaceutical stability studies. VI. Continuous monitoring of the interaction of water vapour with powders and powder mixtures at various relative humidities. International Journal of Pharmaceutics, 83, 11-23.

Angell, C.A., 1991. Relaxation in liquids, polymers and plastic crystals - strong/fragile patterns and problems. Journal of Non-Crystalline Solids, 131-133, 13-31.

Aso, Y., Yoshioka, S., Kojma, S., 2000. Relationship between the crystallsation rates of amorphous nifedipine, phenobarbital, and flopropione, and their molecular mobility as measured by their enthalpy relaxation and ^{1}H NMR relaxaion times. Journal of Pharmaceutical Sciences, 89, 408-416.

Berggren, J., Frenning, G., Alderborn, G., 2004. Compression behaviour and tablet-forming ability of spray-dried amorphous composite particles. European Journal of Pharmaceutical Sciences, 22, 191-200.

Berlin, E., Klima, P.G., Andersen, B.A., Pallansch, M.J., 1971. Calorimetric measurment of the heat of desorption of water vapour from amorphous and crystalline lactose. Thermochimica Acta, 2, 143-152.

Bhatt, B., Rubinstein, M.H., 1983. The use of a flow microcalorimeter to characterise powder surfaces. Drug Development and Industrial Pharmacy, 9, 215-222.

Bolhuis, G.K., Chowhan, Z.T., 1996. Materials for direct compaction. In: Alderborn,G., Nyström,C. (Eds.), Pharmaceutical Powder Compaction Technology, 1st Ed., Marcel Dekker, New York, 419-500.

Borka, L., 1974. The polymorphism of indometacin. New modifications, their melting behaviour and solubility. Acta Pharmaceutica Suecica, 11, 295-303.

Briggner, L.-E. Microcalorimetric Characterisation of physical changes in solid state drugs - Thermometric Application note 22022. 1993.

Briggner, L.-E., Buckton, G., Bystrom, K., Darcy, P., 1994. The use of isothermal microcalorimetry in the study of changes in crystallinity induced during the processing of powders. International Journal of Pharmaceutics, 105, 125-135.

Buckton, G., Beezer, A.E., 1991. The applications of microcalorimetry in the field of physical pharmacy. International Journal of Pharmaceutics, 72, 181-191.

Buckton, G., 1995a. Surface characterization: Understanding sources of variability in the production and use of pharmaceuticals. Journal of Pharmacy and Pharmacology, 47, 265-275.

Buckton, G., 1995b. Interfacial phenomena in drug delivery and targeting. 1st Ed., Hartwood Academic Publishers, Amsterdam.

Buckton, G., 1995c. Applications of isothermal microcalorimetry in the pharmaceutical sciences. Thermochimica Acta, 248, 117-129.

Buckton, G., Darcy, P., Mackellar, A.J., 1995. The use of isothermal microcalorimetry in the study of small degrees of amorphous content of powders. International Journal of Pharmaceutics, 117, 253-256.

Buckton, G., Darcy, P., 1995. The influence of additives in the crystallisation of amorphous spray dried lactose. International Journal of Pharmaceutics, 121, 81-87.

Buckton, G., Darcy, P., 1996. Water mobility in amorphous lactose below and close to the glass transition temperature. International Journal of Pharmaceutics, 136, 141-146.

Buckton, G., Yonemochi, E., Hammond, J., Moffat, A., 1998. The use of near infra-red spectroscopy to detect changes in the form of amorphous and crystalline lactose. International Journal of Pharmaceutics, 168, 231-241.

Buckton, G., Darcy, P., 1999. Assessment of disorder in crystalline powders - a review of analytical techniques and their application. International Journal of Pharmaceutics, 179, 141-158.

Buckton, G., Chidavaenzi, O.C., Koosha, F., 2002. The effect of spray-drying feed temperature and subsequent crystallisation conditions on the physical form of lactose. AAPS PharmaSciTech Technical, 3, 1-6.

Buma, T.J., Wiegers, G.A., 1967. X-Ray powder patterns of lactose and unit cell dimensions of b-lactose. Netherlands Milk and Dairy Journal, 21, 208-213.

Burnett, D.J., Thielmann, F., Sokoloski, T., Brum, J., 2006. Investigating the moisture-induced crystallisation kinetics of spray-dried lactose. International Journal of Pharmaceutics, 313, 23-28.

Bushill, J.H., Wright, W.B., Fuller, C.H.F., Bell, A.V., 1965. The crystallisation of lactose with particular reference to its occurrence in milk powder. Journal of Science Food and Angriculture, 16, 622-628.

Byrn, S.R., Pfeiffer, R.R., Stowell, J.G., 1999. Solid-state chemistry of drugs. 2nd Ed., Academic Press, New York.

Casrtensen, J.T., 1993. Pharmaceutical principles of solid dosage forms. Termochimic publication, Lancaster.

Chadha, R., Kashid, N., Kumar, A., Jain, D.V.S., 2002. Calorimetric studies of diclofenac sodium in aqueous solution of cyclodextrin and water-ethanol mixtures. Journal of Pharmacy and Pharmacology, 54, 481-486.

Chen, X., Bates, S., Morris, K.R., 2001. Quantifying amorphous content of lactose using parallel beam X-ray powder diffraction and whole pattern fitting. Journal of Pharmaceutical and Biomedical Analysis, 26, 63-72.

Chidavaenzi, O.C., Buckton, G., Koosha, F., Pathak, R., 1997. The use of thermal techniques to assess the impact of feed concentration on the amorphous content and polymorphic forms present in spray dried lactose. International Journal of Pharmaceutics, 159, 67-74.

Chidavaenzi, O. C. The effect of spray drying on the physicochemical properties of products. 1999. University of London.

Chidavaenzi, O.C., Buckton, G., Koosha, F., 2001. The effect of co-spray drying with polyethylene glycol 4000 on the crystallinity and physical form of lactose. International Journal of Pharmaceutics, 216, 43-49.

Chidavaenzi, O.C., Buckton, G., Koosha, F., 2002. The effect of spray drying feed temperature and subsequent crystallisation conditions on the physical form of lactose. AAPS PharmaSciTech Technical note 1, 3, 1-6.

Cline, D., Dalby, R., 2002. Predicting the quality of powders for inhalation from surface energy and area. Pharmaceutical Research, 19, 1274-1277.

Corrigan, O.I., 1995. Thermal analysis of spray dried product. Thermochimica Acta, 248, 245-258.

Craig, D.Q.M., Newton, J.M., 1991. Characterisation of polyethylene glycol solid dispersions using differential scanning calorimetry and solution calorimetry. International Journal of Pharmaceutics, 76, 17-24.

Craig, D.Q.M., Royall, P.G., Kett, V.L., Hopton, M.L., 1999. The relevance of the amorphous state to pharmaceutical dosage forms: glassy drugs and freeze dried systems. International Journal of Pharmaceutics, 179, 179-207.

Craig, D.Q.M., Barsnes, M., Royall, P.G., Kett, V.L., 2000. An evaluation of the use of modulated temperature DSC as a means of assessing the relaxation behaviour of amorphous lactose. Pharmaceutical Research, 17, 696-700.

Darcy, P., Buckton, G., 1998. Quantitative assessment of powder crystallinity: Estimates of heat and mass transfer to interpret isothermal microcalorimetry data. Thermochimica Acta, 316, 29-36.

Dilworth, S.E., Buckton, G., Gaisford, S., Ramos, R., 2004. Approaches to determine the enthalpy of crystallisation, and amorphous content, of lactose from isothermal calorimetric data. International Journal of Pharmaceutics, 284, 83-94.

Ding, S.-P., Fan, J., Green, J.L., Lu, Q., Sanchez, E., Angell, C.A., 1996. Vitrification of trehalose by water loss from its crystalline dihydrate. Journal of Thermal Analysis, 47, 1391-1405.

Drapier-Beche, N., Fanni, J., Parmentier, M., Vilas, M., 1997. Evaluation of lactose crystalline forms by nondestructive analysis. Journal of dairy science, 80, 457-463.

Duddu, S.P., Zhang, G., Dul Monte, P.R., 1997. The relationship between protein aggregation and molecular mobility below the glass transition temperature of lyophilised formulations containing a monoclonal antibody. Pharmaceutical Research, 14, 596-600.

Dwivedi, S.K., Mitchell, A.G., 1989. Gas chromatographic analysis of anomeric composition of lactose. Journal of Pharmaceutical Sciences, 78, 1055-1056.

Ediger, M.D., Angell, C.A., Nagel, S.R., 1996. Supercooled liquids and glasses. Journal of Physical Chemistry, 100, 13200-13212.

Egawa, H., Maeda, S., Yonemochi, E., Oguchi, T., Yamamoto, K., Nakai, Y., 1992. Solubility parameter and dissolution behaviour of celefaxin powders with different crystallinity. Chemical and Pharmaceutical Bulletin, 40, 819-820.

Elamin, A.A., Ahlneck, C., Alderborn, G., Nyström, C., 1994. Increased metastable solubility of milled griseofluvin, depending on the formation of a disordered surface structure. International Journal of Pharmaceutics, 111, 159-170.

Feeley, J.C., York, P., Sumby, B.S., Dicks, H., 1998. Determination of surface properties and flow characteristics of salbutamol sulphate, before and after micronisation. International Journal of Pharmaceutics, 217, 45-56.

Ferry, J.D., 1980. Viscoelastic properties of polymers. 3rd Ed., John Wiley and Sons, New York.

Fix, I., Steffens, K.-J., 2004. Quantifying low amorphous or crystalline amounts of alpha-lactose-monohydrate using X-Ray Powder Diffraction, Near-Infrared Spectroscopy, and Differential Scanning Calorimetry. Drug Development and Industrial Pharmacy, 30, 513-523.

Flink, J.M., 1983. Structure and structure transitions in dried carbohydrate materials. In: Peleg,M., Bagley,E.B. (Eds.), AVI Publishing Company, Westport, 473-521.

Florence, A.T., Salole, E.G., 1976. Changes in crystallinity and solubility on comminution of digoxin and observations on spironolactose and oestradiol. Journal of Pharmacy and Pharmacology, 28, 637-642.

Ford, J.L., Timmins, P., 1989. Pharmaceutical thermal analysis. Techniques and applications. 1st Ed., John Willey and Sons, Chichester.

Franks, F., 1992. The properties of aqueous solutions at subzero temperatures. In: Franks,F. (Ed.), Plenum Press, New York, 215-338.

Gaisford, S., Buckton, G., 2001. Potencial applications of microcalorimetry for the study of physical processes in pharmaceutics. Thermochimica Acta, 380, 185-198.

Gao, D., Rytting, J.H., 1997. Use of solution calorimetry to determine the extent of crystallinity of drugs and excipients. International Journal of Pharmaceutics, 151, 183-192.

Gerber, J.J., vanderWatt, J.G., Lötter, A.P., 1991. Physical characterisation of solid forms of cyclopenthiazide. International Journal of Pharmaceutics, 73, 137-145.

Gombás, Á., Szabó-Révész, P., Kata, M., Regdon, G.J., Eros, I., 2002. Quantitative determination of crystallinity of a -lactose monohydrate by DSC. Journal of Thermal Analysis and Calorimetry, 68, 503-510.

Gordon, M., Taylor, J.S., 1952. Ideal co-polymers and the second-order transitions of synthetic rubbers. I. Non-crystaline co-polymers. Journal of Applied Chemistry, 2, 493-500.

Green, J.L., Angell, C.A., 1989. Phase relations and vitrification in saccharide/water solutions and the trehalose anomaly. Journal of Physical Chemistry, 93, 2880-2882.

Grimsey, I.M., Sunkersett, M.R., Osborn, J.C., York, P., Rowe, R.C., 1999. Interpretation of the differences in the surface energetics of two optical forms of mannitol by inverse gas chromatography and molecular modelling. International Journal of Pharmaceutics, 191, 43-50.

Grimsey, I.M., Feeley, J.C., York, P., 2002. Analysis of the surface energy of pharmaceutical powders by inverse phase gas chromatography. Journal of Pharmaceutical Sciences, 91, 571-583.

Guillory, J.K., 1999. Generation of polymorphs, hydrates, solvates and amorphous solids. In: Brittain,H.G. (Ed.), Polymorphism in Pharmaceutical Solids, 1st Ed., Marcel Dekker, New York, 183-225.

Guo, Y., Byrn, S.R., Zografi, G., 2000. Phydical characteristics and chemical degradation of amorphous quinapril hydrochloride. Journal of Pharmaceutical Sciences, 89, 128-143.

Hammel, J.J., 1969. Nucleation in glass forming materials. In: Zettlemoyer,A.C. (Ed.), Marcel Dekker, New York, 489-525.

Hanafusa, N., 1985. The interaction of hydration water and protein with cryoprotectant. Fundamentals and applications of freeze-drying to biological materials, drugs and foodstuffs, 1, 59-64.

Hancock, B.C., Zografi, G., 1994. The relatioship between the glass transition temperature and the water content of amorphous pharmaceutical solids. Pharmaceutical Research, 11, 471-477.

Hancock, B.C., Shamblin, S.L., Zografi, G., 1995. Molecular mobility of amorphous pharmaceutical solids below their glass transition temperatues. Pharmaceutical Research, 12, 799-805.

Hancock, B.C., Zografi, G., 1997. Characteristics and Significance of the Amorphous state in Pharmaceutical Systems. Journal of Pharmaceutical Sciences, 86, 1-12.

Hancock, B.C., Shalaev, E.Y., Shamblin, S.L., 2002. Polyamorphism: a pharmaceutical science prespective. Journal of Pharmacy and Pharmacology, 54, 1151-1152.

Haque, Md.K., Roos, Y.H., 2005a. Crystallisation and X-ray diffraction of spray-dried and freeze-dried amorphous lactose. Carbohydrate Research, 340, 293-301.

Haque, Md.K., Roos, Y.H., 2005b. Crystallisation and X-ray diffraction of crystals formed in water plasticised amorphous spray-dried and freeze-dried lactose/protein mixtures. Journal of Food Science, 70, E359-E366.

Harjunen, P., Lemmo, V.P., Välisaari, J., Lankinen, T., Paronen, P., Järvinen, K., 2002. Effects of ethanol to water ratio in feed solution on the crystallinity of spray-dried lactose. Drug Development and Industrial Pharmacy, 28, 949-955.

Harjunen, P., Lehto, V.-P., Martimo, K., Suihko, E., Lankinen, T., Paronen, P., Järvinen, K., 2002. Lactose modifications enhance its drug performance in novel multiple dose Taifun DPI. European Journal of Pharmaceutical Sciences, 16, 313-321.

Harjunen, P., Vesa-Pekka, L., Koivisto, M., Levonen, E., Paronen, P., Jarvinen, K., 2004. Determination of Amorphous Content of Lactose by Solution Calorimetry. Drug Development and Industrial Pharmacy, 30, 809-815.

Hogan, S.E., Buckton, G., 2000. The quantification of small degrees of disorder in lactose using solution calorimetry. International Journal of Pharmaceutics, 207, 57-64.

Hogan, S. E. Investigation of the amorphous and crystalline properties of lactose and raffinose. 2001. University of London.

Höhne, G.W.H., Hemminger, W.F., Flammersheim, H.-J., 2003. Differential Scanning Calorimetry. Second Ed., Springer, Berlin.

Hudson, C.S., Brown, F.C., 1908. The heats of solution of the three forms of milk-sugar. Journal of the American Chemical Society, 30, 960-971.

Hurtta, M., Pitkänen, I., 2004. Quantification of low levels of amorphous content in maltilol. Thermochimica Acta, 419, 19-29.

Hüttenrauch, R., Keiner, I., 1979. Producing lattice defects drying processes. International Journal of Pharmaceutics, 2, 59-60.

Imaizumi, H., Nambu, N., Nagai, T., 1980. Stability and several physical properties of amorphous and crystalline forms of indometacin. Chemical and Pharmaceutical Bulletin, 28, 2565-2569.

Inghelbrecht, S., Remon, J.P., 1998. The roller compaction of different types of lactose. International Journal of Pharmaceutics, 166, 135-144.

Ip, D.P., Brenner, G.S., Stevenson, J.M., Lindenbaum, S., Douglas, A.W., Klein, S.D., McCauley, J.A., 1986. High resolution spectroscopic evidence and solution calorimetry studies of the polymorphs of enalapril maleate. International Journal of Pharmaceutics, 28, 183-191.

Jakobsen, D.F., Frokjaer, S., Larsen, C., Niemann, H., Buur, A., 1997. Application of isothermal microcalorimetry in preformulation. I. Hygroscopicity of drug substances. International Journal of Pharmaceutics, 156, 67-77.

Johari, G.P., 1995. Obtaining further information from calorimetry. Thermochimica Acta, 266, 31-47.

Jouppila, K., Kansikas, J., Roos, Y.J., 1998. Crystallisation and X-ray diffraction of crystals formed in water-plasticised amorphous lactose. Biothecnology Progress, 14, 347-350.

Kakumanu, K., Bansal, A.K., 2002. Enthalpy relaxation studies of celecoxib amorphous mixtures. Pharmaceutical Research, 19, 1872-1878.

Katainen, E., Niemelä, P., Harjunen, P., Suhonen, J., Järvinen, K., 2005. Evaluation of the amorphous content of lactose by solution calorimetry and Raman spectroscopy. Talanta, 68, 1-5.

Kauzmann, W., 1948. The nature of the glassy state and the behaviour of liquids at low temperatures. Chemical Reviews, 43, 219-256.

Kawai, K., Hagimara, T., Takai, R., Suzuki, T., 2004. Comparative investigation by two analytical approaches of enthalpy relaxation for glassy glucose, sucrose, maltose and trehalose. Pharmaceutical Research, 22, 490-495.

Kawakami, K., Numa, T., Ida, Y., 2002. Assessment of Amorphous content by Microcalorimetry. Journal of Pharmaceutical Sciences, 91, 417-423.

Kawakami, K., Pikal, M.J., 2005. Calorimetric investigation of the structural relaxation of amorphous materials: evaluating validity of the methodologies. Journal of Pharmaceutical Sciences, 94, 948-965.

Knotny, M.J., Grandolfi, G.P., Zografi, G., 1987. Water vapour sorption of water-soluble substances: studies of crystalline solids below their critical relative humidities. Pharmaceutical Research, 4, 104-111.

Konno, T., 1990. Physical and chemical changes in mixtures with adsorbents in the solid state. IV. Study on reduced-pressure mixing for practical use of amorphous mixtures of flufenamic acid. Chemical and Pharmaceutical Bulletin, 38, 2003-2007.

Lerk, C.F., Andreac, A.C., Boer, A.H., Hoog, P., Kussendrager, K., Leverink, J., 1984a. Transitions of lactoses by Mechanical and Thermal Treatment. Journal of Pharmaceutical Sciences, 73, 857-859.

Lerk, C.F., Andreae, A.C., Boer, A.H., 1984b. Alterations of α-lactose during differential scanning calorimetry. Journal of Pharmaceutical Sciences, 73, 856-857.

Levine, H., Slade, L., 1986. A polymer physico-chemical approach to the study of commercial starch hydrolysis products. Carbohydrate Polymers, 6, 213-244.

Levine, H., Slade, L., 1988. "Collapse" phenomena - a unifying concept for interpreting the behaviour of low moisture foods. In: Blanshard,J., Mitchell,J. (Eds.), Food structure - its creation and evaluation, 1st ED., Butterworths, London, 149-180.

Levine, H., Slade, L., 1989. Response to a letter by Simatos, Blond and Le Monde on the relation between glass transition and stability of a frozen product. Cryo-Letters, 10, 347-370.

Liu, J., Rigsbee, D.R., Stotz, C., Pikal, M.J., 2005. Dynamics of pharmaceutical amorphous solids: The study of enthalpy relaxation by isothermal microcalorimetry. Journal of Pharmaceutical Sciences, 91, 1853-1862.

Mackin, L., Zamon, R., Park, J.M., Foster, K., Opalenik, H., Demonte, M., 2002a. Quantification of low levels (< 10%) of amorphous content in micronised active batches using dynamic vapour sorption and isothermal microcalorimetry. International Journal of Pharmaceutics, 231, 227-236.

Mackin, L., Sautnurak, S., Thomas, I., Moore, S., 2002b. The impact of low levels of amorphous material (<5%) on the blending characteristics of a direct compression formulation. International Journal of Pharmaceutics, 231, 213-226.

Makower, B., Dye, W.B., 1956. Equilibrium moisture content and crystallisation of amorphous sucrose and glucose. Journal of Agricultural and food chemistry, 4, 72-77.

Manning, M.C., Paterl, K., Borchardt, T., 1989. Stability of protein pharmaceuticals. Pharmaceutical Research, 6, 903-918.

Matsuda, Y., Otsuka, K., Onoe, M., Tatsumi, E., 1992. Amorphism and physicochemical stability of spray dried frusemide. Journal of Pharmacy and Pharmacology, 44, 627-633.

McGregor, C., Saunders, M., Buckton, G., Saklatvala, R.D., 2004. The use of high-speed differential scanning calorimetry (Hyper-DSC™) to study the thermal properties of carbamazepine polymorphs. Thermochimica Acta, 417, 231-237.

Miao, S., Roos, Y.H., 2005. Crystallisation kinetics and X-ray diffraction of crystals formed in amorphous lactose, trehalose, and lactose/trehalose mixtures. Journal of Food Science, 70, E350-E358.

Miyata, K., Kakizawa, Y., Nishiyama, N., Yamasaki, Y., Watanabe, T., Kohara, M., Kataoka, K., 2005. Freeze-dried formulation for in vivo gene delivery of PEGylated polyplex micelles with disulfide cross linked cores to the liver. Journal of Controlled Release, 109, 15-23.

Mullins, J.D., Macek, T.J., 1960. Some pharmaceutical properties of novobiocin. Journal of Pharmaceutical Sciences, 49, 245-248.

Newell, H.E., Buckton, G., Butler, D.A., Thielmann, F., Williams, D.R., 2001a. The use of inverse phase gas chromatography to study the change of surface energy of amorphous lactose as a function of relative humidity and the process of collapse and crystallisation. International Journal of Pharmaceutics, 217, 45-56.

Newell, H.E., Buckton, G., Butler, D.A., Thielmann, F., Williams, D.R., 2001b. The use of inverse phase gas chromatography to measure the surface energy of crystalline, amorphous and milled lactose. Pharmaceutical Research, 18, 662-666.

Nyqvist, H., 1983. Saturated salt solutions for mantaining specified relative humidities. International Journal of Pharmaceutical Technology and Product Manufacture. 4, 47-48.

Oberholtzer, E.R., Brenner, G.S., 1979. Cefoxitin sodium: solution and solid-state chemical stability studies. Journal of Pharmaceutical Sciences, 68, 863-866.

Ohara, T., Kitamura, S., Kitagawa, T., Katsuhide, T., 2005. Dissolution of poorly water-soluble drug from extended release solid dispersion system with ethylcellulose and hydroxypropylmethylcellulose. International Journal of Pharmaceutics, 302, 95-102.

Ohta, M., Tozuka, Y., Oguchi, T., Yamamoto, K., 2000. Water vapor adsorption properties of amorphous cefditoren pivoxil evaluated by adsorption isotherms and microcalorimetry. Drug Development and Industrial Pharmacy, 26, 643-649.

Ohta, M., Buckton, G., 2004a. Determination of the changes in surface energetics of cefditoren pivoxil as a consequence of processing induced disorder and equilibration to different relative humidities. International Journal of Pharmaceutics, 269, 81-88.

Ohta, M., Buckton, G., 2004b. A study of the differences between two amorphous spray-dried samples of cefditoren pivoxil which exhibited different physical stabilities. International Journal of Pharmaceutics, 289, 31-38.

Oksaken, C.A., Zografi, G., 1990. The relationship between the glass transition temperature and water vapour absorption by poly(vinylpyrrolidone). Pharmaceutical Research, 7, 654-657.

Otsuka, M., Kaneniwa, N., 1990. Effect of grinding on the crystallinity and chemical stability in the solid state of cephalothin sodium. International Journal of Pharmaceutics, 62, 65-73.

Otsuka, M., Ohtani, H., Kaneniwa, N., Higuchi, S., 1991. Isomerization of lactose in solid state by mechanical stress during grinding. Journal of Pharmacy and Pharmacology, 43, 148-153.

Otsuka, M., Ohtani, H., Otsuka, K., Nobuyoshi, K., 1993. Effect of Humidity on Solid-State Isomerization of Various Kinds of Lactose during Griding. Journal of Pharmacy and Pharmacology, 45, 2-5.

Österberg, T., Wadsten, T., 1999. Physical state of L-histidine after freeze-drying and long-term storage. European Journal of Pharmaceutical Sciences, 8, 301-308.

Passot, S., Fonseca, F., Alarcon-Lorca, M., Rolland, D., Marin, M., 2005. Physical characterisation of formulations for the development of two stable freeze-dried protein during both dried and liquid storage. European Journal of Pharmaceutical and Biopharmaceutics, 60, 335-348.

Pikal, M.J., Lukes, A.L., Lang, J.E., 1977. Thermal decomposition of amorphous β-lactam antibacterials. Journal of Pharmaceutical Sciences, 66, 1312-1316.

Pikal, M.J., Lukes, A.L., Lang. J.E., Gaines, K., 1978. Quantitative Crystallinity determinations for β-Lactam antibiotics by solution calorimetry: correlations with stability. Journal of Pharmaceutical Sciences, 67, 767-772.

Pikal, M.J., 1990. Freeze-drying of protein. Part I: Process design. BioPharm, 3, 18-27.

Price, R., Young, P.M., 2004. Visualization of the crystallisation of lactose from the amorphous state. Journal of Pharmaceutical Sciences, 93, 155-164.

Pudipeddi, M., Sokoloski, D., Duddu, S.P., Carstensen, J.T., 1996. Quantitative characterisation of adsoption isotherms using isothermal microcalorimetry. Journal of Pharmaceutical Sciences, 85, 381-386.

Rowe, R.C., Sheskey, P.J., Weller, P.J., 2003. Handbook of pharmaceutical excipients. 4th Ed., Pharmaceutical Press, London.

Royall, P.G., Gaisford, S., 2005. Application of solution calorimetry in pharmaceutical and biopharmaceutical research. Current Pharmaceutical Biotechnology, 6, 215-222.

Saleki-Gerhardt, A., Zografi, G., 1994. Non-isothermal and isothermal crystallisation of sucrose from the amorphous state. Pharmaceutical Research, 11, 1166-1173.

Saleki-Gerhardt, A., Ahlneck, C., Zografi, G., 1994. Assessment of disorder in crystalline solids. International Journal of Pharmaceutics, 101, 237-247.

Saleki-Gerhardt, A., Stowell, J.G., Byrn, S.R., Zografi, G., 1995. Hydration and dehydration of crystalline and amorphous forms of raffinose. Journal of Pharmaceutical Sciences, 84, 318-323.

Samra, R.M., Buckton, G., 2004. The crysatllisation of a model hydrophobic drug (terfenadine) following exposure to humidity and organic vapours. International Journal of Pharmaceutics, 284, 53-60.

Saunders, M., Podluii, K., Shergill, S., Buckton, G., Royall, P., 2004. The potencial of high speed DSC (Hyper-DSC) for the detction and quantification of small amounts of amorphous content in predominantly crysatlline samples. International Journal of Pharmaceutics, 274, 35-40.

Schmitt, E.A., Law, D., Zhang, G.G.Z., 1999. Nucleation and Crystallisation Kinetics of Hydrated Amorphous Lactose above the Glass Transition Temperature. Journal of Pharmaceutical Sciences, 88, 291-296.

Sebhatu, T., Angberg, M., Ahlneck, C., 1994a. Assesment of the degree of disorder in crystalline solids by isothermal microcalorimetry. International Journal of Pharmaceutics, 104, 135-144.

Sebhatu, T., Elamin, A.A., Ahlneck, C., 1994b. Effect of moisture sorption on tabletting characteristics of spray dried (15% amorphous) lactose. Pharmaceutical Research, 11, 1233-1238.

Sebhatu, T., Ahlneck, C., Alderborn, G., 1997. The effect of moisture content on the compression and bon-formation properties of amorphous lactose particles. International Journal of Pharmaceutics, 146, 101-114.

Shamblin, S.L., Zografi, G., 1998. Enthalpy relaxation in binary amorphous mixtures containing sucrose. Pharmaceutical Research, 15, 1828-1834.

Shamblin, S.L., Tang, X., Chang, L., Hancock, B.C., Pikal, M.J., 1999. Characterisation of the timescales of molecular motion in pharmaceutically important glasses. Journal of Physical Chemistry, 103, 4113-4121.

Sheridan, P.L., Buckton, G., Storey, D.E., 1995. Development of a flow microcalorimetry method for the assessment of surface properties of powders. Pharmaceutical Research, 12, 1025-1030.

Slavin, P.A., Sheen, D.B., Shepherd, E.E.A., Sherwood, J.N., Feeder, N., Docherty, R., Milojevic, S., 2002. Morphological evaluation of the g-polymorph of indometacin. Journal of Non-Crystalline Solids, 237-239, 300-305.

Souillac, P.O., Dave, P., Rytting, J.H., 2002. The use of solution calorimetry with micellar solvent systems for the detection of polymorphism. International Journal of Pharmaceutics, 231, 185-196.

Steckel, H., Bolzen, N., 2005. Calorimetric study on amorphous lactose during and after re-crystallisation at different relative humidities. Pharmaceutical Industry, 67, 709-712.

Stephenson, G.A., Forbes, R.A., Reutzel-Edens, S.M., 2001. Characterisation of the solid state: quantitative issues. Advanced Drug Delivery Reviews, 48, 67-90.

Sugisaki, M., Suga, H., Seki, S., 1968. Calorimetric study of the glassy state. IV. Heat capacities of glassy water and ice cubes. Bulletin of the Chemical Society of Japan, 41, 2591-2599.

Surana, R., Pyne, A., Suryanarayanan, R., 2004a. Effect of aging on the physical properties of amorphous trehalose. Pharmaceutical Research, 21, 867-873.

Surana, R., Pyne, A., Suryanarayanan, R., 2004b. Effect of preparation method on physical properties of amorphous trehalose. Pharmaceutical Research, 21, 1167-1176.

Suryanarayanan, R., Mitchell, A.G., 1985. Evaluation of two concepts of crystallinity using calcium gluceptate as a model compound. International Journal of Pharmaceutics, 24, 1-17.

Swarbrick, J., 2001. Encyclopedia of Pharmaceutical Technology. Marcel Dekker, New York.

Talsma, H., Cherng, J.-Y., Lehrmann, H., Kursa, M., Ogris, M., Hennink, W.E., Cotten, M., Wagner, E., 1997. Stabilization of gene delivery systems by freeze-drying. International Journal of Pharmaceutics, 157, 233-238.

Ticehurst, M.D., Rowe, R.C., York, P., 1994. Determination of the surface properties of two batches of salbutamol sulphate by inverse gas chromatography. International Journal of Pharmaceutics, 111, 241-249.

Ticehurst, M.D., York, P., Rowe, R.C., Dwivedi, S.K., 1996. Characterisation of the surface properties of a-lactose monohydrate with inverse gas chromatography, used to detect batch variation. International Journal of Pharmaceutics, 141, 93-99.

Timmermann, I.-L., Steckel, H., Trunk, M., 2006. Assessing the re-crystallisation behaviour of amorphous lactose using the RH-perfusion cell. European Journal of Pharmaceutical and Biopharmaceutics, 64, 107-114.

Tong, P., Zografi, G., 1999. Solid-State characteristics of amorphous sodium indometacin relative to its free acid. Pharmaceutical Research, 18, 1186-1192.

Tsourouflis, S., Flink, .M., Karel, ., 1976. Lost structure in freeze/dried carbohydrates solutions: effect of temperature, moisture content and composition. Journal of Science Food and Agriculture, 27, 509-519.

Voelkel, A., Andrzejewska, E., Maga, R., Andrezejewski, M., 1996. Examination of surface of solid polymers by inverse phase gas chromatogrpahy:1. Dispersive properties. Polymer, 37, 455-462.

Wadsö, I., Goldberg, R.N., 2001. Standards in Isothermal Microcalorimetry. Pure Applied Chemistry, 73, 1625-1639.

Ward, G.H., Schultz, R.K., 1995. Process-induced crystallinity changes in albuterol sulfate and its effect on powder physical stability. Pharmaceutical Research, 12, 773-779.

White, G.W., Cakebread, S.H., 1966. The glassy state in certain sugar-containing food products. Journal of food technology, 1, 73-82.

Williams, G., Watts, D.C., 1970. Non-symmetrical dielectric relaxation behaviour arising from a simple empirical decay function. Transmitions of the faraday society, 66, 80-85.

Woldt, E., 1992. The relationship between isothermal and non-isothermal description of Johnson-Nehl-Avrami-Kolmogorov kinetics. Journal of Physical Chemistry of solids, 53, 521-527.

Yamamoto, H., 1968. 1-Acyl-indoles. II. A new syntheses of 1-(p-chrorobenzoyl)-5-methoxy-3-indolylacetic acid and its polymorphism. Chemical and Pharmaceutical Bulletin, 16, 17-19.

Yamamoto, K., Nakano, M., Arita, T., Takayama, Y., Nakai, Y., 1976. Dissolution behavior and bioavailibility of phenytoin from a ground mixture with microcrystalline cellulose. Journal of Pharmaceutical Sciences, 65, 1484-1488.

Yoshioka, M., Hancock, B.C., Zografi, G., 1994. Crystallisation of indometacin for amorphous state below and above its glass transition temperature. Journal of Pharmaceutical Sciences, 83, 1700-1705.

Yoshioka, S., Aso, Y., Kojma, S., 1996. Determination of molecular mobility of lyophilised bovine serum albumine and gamma globulin by solid/state H-1NMR and relation to aggregation susceptibility. Pharmaceutical Research, 13, 926-930.

Yoshioka, S., Aso, Y., Kojma, S., 1997a. Softening temperature of lyophilised bovine serum albumin and g-globulin as measured by spin-spin relaxation time of protein protons. Journal of Pharmaceutical Sciences, 86, 470-474.

Yoshioka, S., Aso, Y., Kojma, S., 1997b. Dependence of the molecular mobility and protein stability of freeze-dried g-globulin formulations on the molecular weight of dextran. Pharmaceutical Research, 14, 736-741.

Yoshioka, S., Aso, Y., Nakai, Y., Kojma, S., 1998. Effect of high molecular mobility of Poly(vinyl alcohol) on protein stability of lyophilised g-globulin formulations. Journal of Pharmaceutical Sciences, 87, 147-151.

Yu, L., Reutzel-Edens, S.M., Mitchell, A.G., 2000. Crystallisation and polymorphism of conformationally flexible molecules: problems, patterns, and strategies. Organic Process Research and Development, 4, 396-402.

Yu, L., 2001. Amorphous pharmaceutical solids: preparation, characterization and stabilization. Advanced Drug Delivery Reviews, 48, 27-42.

LIST OF PUBLICATIONS

THE WORK DESCRIBED IN THIS THESIS IS PARTIALLY PUBLISHED IN THE FOLLOWING PUBLICATIONS:

Rita Ramos, Simon Gaisford and Graham Buckton, Aug 2005. Calorimetric determination of amorphous content in lactose: A note on the preparation of calibration curves, International Journal of Pharmaceutics, 300, 13-21.

Sarah E. Dilworth, Graham Buckton, Simon Gaisford and Rita Ramos, Oct 2004. Approaches to determine the enthalpy of crystallisation, and amorphous content, of lactose from isothermal calorimetric data, International Journal of Pharmaceutics, 284, 83-94.

RESEARCH WORK CARRIED OUT DURING MY PHD AND NOT PRESENTED IN THIS THESIS IS PUBLISHED AS:

Rita Ramos, Simon Gaisford, Graham Buckton, Paul G. Royall, Barbara T.S. Yff, Michael A.A. O'Neill, A, Aug 2005. Comparison of chemical reference materials for solution calorimeters, International Journal of Pharmaceutics, 299, 73-83.